

https://dspace.org/

Evaluation of transgenic cassava expressing mismatch and non-mismatch hpRNA constructs derived from African cassava mosaic virus and South African cassava mosaic virus open reading frames

Moralo, Maabo

2015
http://hdl.handle.net/10539/19289

Downloaded from a DSpace repository. https://dspace.org/

Evaluation of transgenic cassava expressing mismatch and non-mismatch hpRNA constructs derived from *African cassava mosaic virus* and *South African cassava mosaic virus* open reading frames

Maabo Moralo

A dissertation submitted to the Faculty of Science, University of the Witwatersrand, in fulfilment of the requirements for the degree of Doctor of Philosophy in the School of Molecular and Cell Biology.

Johannesburg, 2015

Declaration

I, Maabo Moralo (0316002e), am a student registered for the degree of Doctor of Philosophy (MCBG 9002) in the academic year 2015. I hereby declare the following:

I hereby declare the following:

- I am aware that plagiarism (the use of someone else's work without their permission and/or without acknowledging the original source) is wrong.
- I confirm that the work submitted for assessment for the above degree is my own unaided work except where explicitly indicated otherwise and acknowledged.
- I have not submitted this work before for any other degree or examination at this or any other University.
- The information used in the Thesis HAS NOT been obtained by me while employed by, or working under the aegis of, any person or organisation other than the University.
- I have followed the required conventions in referencing the thoughts and ideas of others.
- I understand that the University of the Witwatersrand may take disciplinary action against me if there is a belief that this is not my own unaided work or that I have failed to acknowledge the source of the ideas or words in my writing.

Signature  4th day of November 2015

Acknowledgements

- I would like to thank my supervisor, Professor Chrissie Rey for the opportunity to work in her lab and allowing me the chance to be a proficient and confident researcher. I am grateful for her support and enthusiasm.

- I would like to thank the National research foundation (NRF), University of the Witwatersrand for the Postgraduate merit award and scholarship, Technology innovation agency (TIA) and Gauteng Province Agricultural and Rural and development (GDARD) for financial support.

- To my colleagues (past and current) in the Cassava biotechnology lab for their support, assistance, advice, endless fun moments and the saneness they brought into my life through their own 'special insane' methods.

- Thanks to the MCB fellow students and staff members, especially the Support staff for their constant words of encouragement and support.

- My parents, siblings and family (ba ga Moralo and Moemise), for their endless support, patience and encouragement. I am grateful for their love, presence, and unwavering belief in me and for their ongoing prayers of intercession throughout this very challenging academic journey.

- To my friends and Vegas family for the encouragement, strength and courage to pursue postgraduate studies. My Warrup family for their love, friendship, support and patience when research dictated and limited our contact time.

- Last but not least, my God, for making all things possible and seeing me through. (Deutronomy 31:8; Phillipians 4:6)

Dedication

This thesis is **dedicated to the memory of my aunt Martina Veronica Moemise**. Described as "an adventurous dreamer, an organic intellect, an endless flowing river of knowledge", with an ability "to flow with the highs and lows of any conversation, even flowing upstream with the greatest of ease" (Motshabi Moemise, 2013).
Robala ka kgotso Mokgatla, Kgabo!

I hope your fearlessness, intelligence, love and thirst for knowledge will continue to live through this thesis and inspire future generations of the Moralo and Moemise family to achieve only the best that life has to offer.

"In life you will meet challenges and near impossible people. Stand firm, don't be shaken and don't be anxious about anything and most of all don't let anyone or anything kill your spirit"

Research outputs

Rey M.E.C, Mvududu D. and Moralo M (2015). Screening C-MM6 transgenic lines for resistance to African cassava mosaic disease. 8th Annual Agriculture research symposium.

Rey M.E.C., Moralo M., Taylor S.H. Eni A. and Mundembe R (2014). Improved virus-resistant cassava for small-scale and commercial farmers. 4 June 2014. Roodevallei Conference and Meetings Hotel, Roodeplaat.

M.Moralo and M.E.C. Rey (2013). Screening of transgenic cassava expressing mismatched *African cassava mosaic virus* AC1/4:AC2/3 for virus resistance. *The South African Society for Microbiology (SASM)*, 24-27 November 2013. Forever Resorts Warmbaths, Bela-Bela.

M.Moralo and M.E.C. Rey (2013). Stacked mismatched ACMV AC1/4:AC2/3 hairpin RNA silencing construct for resistance against African cassava mosaic virus. *7th International Geminivirus Symposium & 5th International ssDNA Comparative Virology Workshop*, Qizhen Hotel" in Zhejiang University, Zijingang Campus, Hangzhou, 1 November-10 November 2013 China.

M. Moralo and M.E.C. Rey (2012). Genetic transformation of cassava (*Mannihot esculenta* Crantz) for resistance to cassava begomoviruses *Wits 4th cross faculty research symposium.* Wits University, Johannesburg.

M. Moralo and M.E.C. Rey (2012). Genetic Transformation of Cassava (***Manihot esculenta*** Crantz) for resistance to cassava begomoviruses. *Second Scientific conference of the Global Cassava Partnership for the 21st Century (GCP21-II) Cassava : Overcoming challenges of climate chang.* 18-23 June 2012, Kampal*a*, Uganda.

M.E.C. Rey, C. Chetty, C. Rossin, M. Moralo, M. Weinberg and S. Rogans (2011). Small RNAs: Developing resistance to geminiviruses. *Virology Africa 2011*. 29 November – 2 December, 2011, Cape Town.

M.E.C. Rey, C Chetty, C Rossin, M. Moralo, M. Weinberg and S. Rogans (2011). RNA silencing: A tool for engineering resistance to geminiviruses *SA Society for Microbiology Conference*. 6-9 November, 2011, Cape Town, South Africa.

C. Chetty, M. Moralo, R. Mundembe, E.J. Pierce, S. Rogans, F. Van Schalk, H. Vanderschuren and M.E.C. Rey (2011). Biotechnological solutions for engineering virus resistant cassava. *Agricultural Biotechnology for economic Development: moving towards a Bioeconomy.* 6-9 September, Sandton Convention Centre, Johannesburg, South Africa.

M. Moralo and M.E.C. Rey (2011). Genetic transformation of cassava (*Mannihot esculenta* Crantz) for resistance to cassava begomoviruses. *Southern African Society for Plant Pathology 47th Congress*, 23-26th January, Kruger National Park, South Africa.

Abstract

With rising global food prices, growing populations, climate change and future demand for tuber crops for feed and potential energy source, cassava is well positioned to meet the needs of many countries in the SADC region, including South Africa. However a major constraint to cassava cultivation is cassava infecting begomoviruses (CBVs), including *African cassava mosaic virus* (ACMV) and *South African cassava mosaic virus* (SACMV). ACMV and SACMV belong to the family *Geminiviridae*, comprising of circular single-stranded bipartite. Symptoms associated with CBVs infection include yellow and/or green mosaic, leaf deformation, leaf curling and stunted plant growth. Since no chemical control of virus diseases of plants is possible, one approach to develop virus resistance is via biotechnology, through genetic engineering (GE) of cassava to express hairpin RNA (hpRNA) silencing constructs against CBV. However cassava is recalcitrant and difficult to transform and regenerate. The aim of this study was to produce hpRNA/inverted repeat (IR) hpRNA constructs targeting ACMV AC1/4:AC2/3 open reading frames (ORF) and hpRNA targeting SACMV BC1 ORF to engineer hpRNA expressing transgenic cassava resistant to ACMV and SACMV. Furthermore, the approach was to stack two ACMV contiguous overlapping reading frames (AC1/4) and (AC2/3) in an attempt to improve resistance to CBV. However IR sequences are prone to unfavourable tight secondary structure formation known as cruciform structures. To circumvent this, one set of constructs (mutated sense-arm: mismatch constructs) were designed to contain sodium bisulfite deamination-induced mutations in the hairpin sense-arm making it less complementary to the antisense arm and therefore enhancing IR stability and cruciform junction formation. MM2hp (mismatch construct targeting ACMV AC1/4:AC2/3) and MM4hp (mismatch construct targeting SACMV BC1) were generated. The second construct set, non-mismatch: gateway, was designed based on the most currently used Gateway construct system. Gateway constructs contained an intron positioned between the IR fragments. MM6hp (non-mismatch construct targeting ACMV AC1/4:AC2/3) and MM6hp (non-mismatch construct targeting SACMV BC1) were generated. Similar to the deamination-induced mutations, the intron assisted with IR stability. ACMV- or SACMV-derived hpRNA constructs were transformed into model cassava cultivar cv.60444. Additionally, since few farmer-preferred cultivars or landraces have been transformed for resistance, South African high starch landrace T200 was also transformed with the hpRNA constructs. *Agrobacterium*-mediated transformation of friable embryogenic callus (FEC) was used and

plants regenerated. Several transgenic cv.60444 and T200 lines were regenerated. Cassava landraces are generally less amenable to transformation however were able to report 79 % and 76 % for model cv.60444 and landrace T200, respectively. T200 transformation efficiency reported in this study is 43% higher than previously reported. This is also the first report of South African cassava landrace T200 transformation with ACMV and SACMV-derived hpRNA constructs. Transgenic lines were selected and infected with ACMV and SACMV infectious virus clones. Lines were then monitored at 12, 32 and 67 days post infection (dpi) for symptom development, plant growth and SACMV and ACMV viral load. At 67 dpi, a more significant difference between transgenic lines and untransformed infected cv.60444 was observed. At 67 dpi, 69 % and 75% of ACMV AC1/4:AC2/3 and SACMV BC1 transgenic lines, respectively, showed lower symptoms and reduced viral load compared to control susceptible wild-type cv.60444, but comparable to virus-challenged non-transgenic tolerant landrace control TME3. Notably, a lack of correlation between viral load and symptoms was not always observed. Plant to plant variation was observed between individual transgenic lines generated from each construct (MM2hp; MM4hp; MM6hp and MM8hp) transformation events (A-MM2, A-MM4, C-MM6 and C-MM8). However, overall a positive correlation between symptoms and viral load was observed for virus challenge trials of transgenic lines generated from A-MM4, C-MM6 and C-MM8 transformation events, this overall positive correlation was observed at all 3 dpi (12, 32 and 67 dpi). A number of ACMV and SACMV tolerant transgenic lines were obtained for both mismatch and non-mismatch hpRNA expressing transgenic lines, where virus replication persisted, but symptoms were lower at 67 dpi compared to non-transgenic plants. CBV tolerance levels observed in transgenic lines expressing mismatch technology hpRNA was not significantly different to CBV tolerance levels observed in transgenic lines expressing non-mismatch hpRNA. Expression of ACMV and SACMV- derived constructs generated tolerant cassava lines, where tolerance is defined as plants displaying virus replication but lower to no symptoms. In addition to this, a recovery phenotype was observed in five MM2hp (ACMV AC1/4:AC2/4)- derived hp expressing transgenic lines at 365 dpi, where recovery is defined as no to mild symptoms after an initial period of symptoms, and a reduction in or no viral load. In five MM4hp (SACMV BC1)-derived hpRNA expressing transgenic lines, complete recovery was observed at 365 dpi; no symptoms and no detectable virus. From this study we propose that expression of CBV-derived hpRNA targeting ACMV AC1/4:AC2/4 and SACMV BC1 in CBV susceptible cv.60444

enhances cv.60444 ACMV and SACMV tolerance. Mismatch (mutated sense-arm) construct technology offered tolerance levels comparable to the more conventional and more expensive non-mismatch (Gateway) technology. We therefore also propose that the use of mismatch hpRNA technology in cassava genetic engineering can be used as an alternative approach to transgenic crop production. Promising transgenic lines, showing moderate SACMV and ACMV resistance, were identified and these will be used in further trials as they could be considered favourable to farmers.

Table of contents

Evaluation of transgenic cassava expressing mismatch and non-mismatch hpRNA constructs derived from *African cassava mosaic virus* and *South African cassava mosaic virus* open reading frames i

Declaration ii

Acknowledgements iii

Dedication iv

Research Outputs v

Abstract vii

List of Figures xii

List of Tables xxiv

List of Appendices Tables xxvi

List of Abbreviations xxvii

Chapter: 1 Literature review

1.1 Cassava crop 1

1.2 Cassava mosaic disease (CMD) 1

1.3 Geminiviruses 2

1.4 RNA silencing 6

1.5 Geminiviruses as RNA silencing inducers and targets 12

1.6 Viral RNA silencing suppressors 15

1.7 Application of RNA silencing to combat plant disease 19

1.8 hpRNA construct design requirements 22

1.9 Defective interfering molecule-mediated resistance 24

1.10 Protein-mediated resistance 25

1.11 Genetic engineering 26

1.12 Cassava genetic engineering 29

Rationale and Motivation for the study 32

General Objective 33

General Aims 34

Chapter 2Construction of the mutated sense-arm hairpin RNA silencing constructs and Gateway RNA silencing constructs against African cassava mosaic virus, East African cassava mosaic virus and south african cassava mosaic virus 35

2.1 Introduction 36

2.2 Specific Aims 38

Steps for construction of mutated sense-arm hybrid RNA silencing hairpins 38

Steps for Gateway RNA silencing hairpins 39

2.3 Outline of Methodology 40

2.4 Materials and Methods 44

2.5 Results 65

Chapter 3 *Agrobacterium*-mediated transformation of CV.60444 and T200 FEC with mutated AND NON-MUTATED RNA silencing hairpin constructs and regeneration of transformed FRIABLE EMBRYOGENIC CALLUS 91

3.1 Introduction 92

3.2 Specific Aims 96

3.3 Methodology flow chart 97

3.4 Materials and Methods 98

3.5 Results 105

3.6 Discussion 139

Chapter 4 Screening of transgenic plants for SACMV and ACMV resistance 149

4.1 Introduction 150

4.2 Specific Aims 154

4.3 Methodology flow chart 155

4.4 Materials and Methods 156

4.5 Results 162

4.6 Discussion 183

Chapter 5: Summary and Conclusions 196

References 200

Appendices 238

List of figures

Figure 1. 1 (a) Healthy wildtype cassava plant. (b) and (c) CBV infected cassava plant showing CMD symptoms. 2

Figure 1. 2 CBV genome organisation, DNA-A and DNA-B (Gutierrez, 2000) 4

Figure 1. 3 Overview of steps involved in RNA silencing mechanism involving processing of dsRNA intermediates by Dicer into primary siRNA production. Primary siRNA are then used for secondary siRNA production which then enter the RISC complex for sequence-specific degradation of complementary mRNA (Parisi *et al.*, 2009). 10

Figure 1. 4 A model depicting formation of dsRNA intermediates for siRNA induced gene silencing of homologous mRNA . (a) dsRNA generated from complementary viral RNA strands. (b) Imperfect dsRNA-like structures generated from secondary RNA structures. (c) dsRNA generated from aberrant RNA with homologous regions folding on itself or those formed by RDR-mediated amplification forming. (d) Bidirectional promoter transcribed 3' overlapping RNA transcripts forming perfectly paired dsRNA molecules which can become RDR templates (Shimura & Pantaleo, 2011). 14

Figure 1. 5 Different 4-way junctions that can be formed by IR sequences; (a) Open extended-X conformation and (b) compact stacked conformation (Eichman *et al.,* 2000)..... 20

Figure 2. 1 Flow diagram of methodology followed to create the Mutated sense-arm (Mismatched constructs) and the Gateway (Non-mismatched) RNA silencing constructs..... 43

Figure 2. 2 Schematic representation of head to head ligation of non-mutated strand and mutated strand required for IR formation. 53

Figure 2. 3 A segment of the multiple sequence alignment output screen. Alignment was performed on 8 ACMV isolates to identify a region along the ACMV AC1/4 overlapping region that gives the best sequence alignment. 65

Figure 2. 4 A segment of the multiple sequence alignment output screen. Alignment was performed on 8 A CMV isolates to identify a region along the AC2/3 overlapping region that gives the best sequence alignment. 65

Figure 2. 5 A segment of the multiple sequence alignment performed on 8 EACMV isolates to identify a region along the EACMV AC1/4 overlapping region that gives the best alignment between the isolates. 66

Figure 2. 6 A segment of the multiple sequence alignment performed on 8 EACMV isolates to identify a region along the EACMV AC2/3 that gives the best sequence alignment results. 66

Figure 2. 7 (a) Diagrams of ACMV-[NG:Ogo:90] DNA-A AC1/AC4 (136 nt) and AC2/AC3 (183 nt) and (b) EACMV-[UG2] DNA-A AC1/AC4 (207nt) and AC2/AC3 (174 nt) showing regions that were targeted for efficient siRNA production (targeted areas on the 2 DNA-A molecules shown in green)..... 69

Figure 2. 8 1.2% agaraose gel electrophoresis of PCR amplified targer ORF; 136 bp ACMV AC1/AC4 (lane 2), 183 bp ACMV AC2/AC3 (lane 3), 207 bp EACMV AC1/AC4 and 174 bp EACMV AC2/AC3 (lane 5) and (lane 1) O'GeneRuler 1kb Plus DNA ladder (Fermentas). 70

Figure 2. 9 1.2% agarose gel showing fusion of ORF used to create Hybrid fragments. Fermentas O'GeneRuler 1 kb Plus DNA ladder (lane 1). ACMV AC1/AC4, 136 bp fragment (lane 2), 207 bp EACMV AC1/AC4 fragment (lane 3), fusion of lane 2 and 3 amplicons to yield ~343 bp Hybrid I fragment (lane 4). ACMV AC1/AC4, 136 bp fragment (lane 5), ACMV AC2/AC3, 183 bp fragment (lane 6), fusion of lane 5 and 6 fragment to yield a ~319 bp Hybrid II fragment (lane 7). EACMV AC1/AC4, 207 bp fragment (lane 8), EACMV AC2/AC3, 174 bp fragment (lane 9), fusion of lane 8 and 9 fragments to yield ~381 bp hybrid III fragment (lane 10). 71

Figure 2. 10 1% agarose gel electrophoresis of mutated hybrid fragments amplified from 15min bisulfite treated original hybrid fragments, fragments were clones into pTZR5/T (Fermentas). Fragments were amplified using the mutated modified forward and reverse primers for each Hybrid. M= O'Gene 1kb Plus DNA ladder (Fermentas), mutated 361 bp Hybrid I amplicon (lane 1), mutated 337 bp Hybrid II amplicons (lane 2), mutated 399 bp Hybrid III amplicon (lane 3) and NTC (lane 4). 72

Figure 2.11 (a) A segment of a chromatogram for one of the sequenced clones, with arrows showing points along the Hybrid sequence were C-T mutations were introduced. (b) Original Hybrid sequence prior C-T mutations. Arrows are showing Cs that corresponds with the changed T in fig. 2.11b..... 72

Figure 2. 12 1% agarose gel showing IR clones digested with *Xba*I and *Xho*I to screen clones for successful IR formation following ligation of mutated Hybrid fragment and non-mutated hybrid fragment. Lane 1= O'GeneRuler 1 kb Plus DNA ladder, *Xba*I and *Xho*I restricted empty pTZ57R/T vector (lane 2), 701 bp I-IR released fragment (lane 4), 656 bp II-IR released fragment (lane 3)..... 73

Figure 2. 13 1% agarose gel, screening clones for successful ligation of IR into expression vector pART7, *Not*I digest of IR clones, M= O'GeneRuler 1kb DNA ladder, I-IR cassette (lane 1), II-IR cassette (lane 2), undigested pART7 expression vector (lane 3) and linearised pART7 expression vector (lane 4). 74

Figure 2. 14 0.8% agarose gel electrophoresis. IR expression cassettes PCR amplification using pART7 cassette primers. M= O'GeneRuler 1kb Plus DNA, 2811 bp I-IR cassette amplicon (lane 1), 2766 bp II-IR cassette amplicon (lane 2), 2890 bp III-IR cassette amplicon (lane 3), 2178 bp amplicons amplified from empty pART7 expression vector (lane 4) and NTC (lane 5). 75

Figure 2. 15 1% agarose gel, PCR amplification to screen for successful ligation and presence of IR cassette in plant transformation vector p1305.1. M= O'GeneRuler 1kb Plus DNA ladder (Fermentas), I-IR cassette; 343 bp non-mutated fragment (lane 1), I-IR cassette; 361 bp mutated fragment (lane 7), II-IR cassette 319bp non-mutated fragment (lane 2), II-IR cassette 337 bp mutated fragment (lane 8) and III-IR cassette; 381bp non-mutated fragment (lane 3) and 399 bp mutated fragment (lane 9). Empty p1305.1 vector (lane 10) and NTC (lane 11)..... 75

Figure 2. 16 1.2% agarose gel electrophoresis to confirm presence of SACMV BC1 construct. M= O'GeneRuler 1kb Plus DNA ladder (Fermentas), SACMV BC1 non-mutated 221 bp IR arm amplified from extracted SACMV BC1 construct (lane 4). PCR amplification of mutated 239 bp SACMV BC1 IR arm was unsuccessful (lane 12), NTC (lane 5) and empty p1303 vector (lane 6). 76

Figure 2. 17 PCR amplification of Hyg, GUS and insert genes to screen for construct transformation success in *Agrobacterium* LBA4404. (a) M= 1kb ladder (Fermentas), amplification of 181 bp *GUS* gene in MM1hp, MM2hp, MM3hp, MM4 hp (lane 1-4 resp), positive control (lane 5) and NTC (lane 6). Amplification of 343 bp non-mutated fragment of MM1hp (lane 7), 319 bp non-mutated fragment of MM2hp, 381 bp non-mutated fragment of MM3hp (lane 8), 221 bp non-mutated fragment of MM4hp (lane 10) and NTC (lane 11) (b) M= 1 kb ladder Fermentas), amplification of *Hyg* gene (485bp) 3 in MM1hp, MM2hp, MM3hp and MM4 hp (lane 1-4 resp), positive control (lane 5) and NTC (lane 6), amplification of 361 bp mutated fragment of MM1hp (lane 7), 337 bp mutated fragment of MM2hp (lane 8), 399 bp non-mutated fragment of MM3hp (lane 9), 239 bp mutated fragment of MM4hp (lane 10) and NTC (lane 11). 77

Figure 2. 18 (a) Amplification of 365 bp MM5 *Xba*I fragment (lanes 1-4) and amplification of 365 bp MM5 *Xho*I fragment (lanes 5-8). (b) Amplification of 331 bp MM6 *Xba*I fragment (lanes 1-3) and amplification of 365 bp MM5 *Xho*I fragment (lanes 1-3). (c) Amplification of 393 bp MM7 *Xba*I containing fragment (lanes 1-4) and amplification of 393 bp MM7 *Xho*I containing fragment (lanes 5-8). (d) Amplification of 232 bp MM8 *Xba*I fragment (lanes 1-5) and amplification of 232 bp MM8 *Xho*I containing fragment (lanes 6-10). M= O'GeneRuler 1 kb Plus DNA ladder (Fermentas). 78

Figure 2. 19 Extracted pHellsgate 8 plasmid restricted with *Xba*I (lane 1, 2, 4, 5) and undigested pHellsgate 8 (lane 3). M= O'GeneRuler 1 kb Plus DNA ladder (Fermentas). 79

Figure 2. 20 1% agarose gel electrophoresis, showing MM5XbaI-pH8, MM6XbaI-pH8, MM7XbaI-pH8 and MM8XbaI-pH8 clones containing the correct size construct *Xba*I insert in the desired orientation. Screening of the clones was done using the respective target insert *Xba*I R primer in conjunction with the plasmid P27-3 primer. The P27-3 primer added 103 bp to the expected target insert size. (a) Correct MM5 clone g (lane 7) yielded the expected 468 bp fragment. (b) Lane 1, 3 and 4 with correct 434 bp MM6 fragment. (c) Clones MM7 a, d, e, f and h produced the expected 496 bp amplicon. (d) Clones in lane 1, 4 and 5 are correct, 335 bp amplicon. M= O'GeneRuler 1 kb Plus DNA ladder. 79

Figure 2. 21 1% agarose gel electrophoresis, showing PCR screening of clones for the *Xho*I hairpin arm (a) 474 bp fragment was amplified from MM5*Xba*I: *Xho*I-pH8 clones 1 and 2 (lane 1, 2). (b) MM6*Xba*I: *Xho*I-pH8 screened clones with the expected 412 bp fragment. (c) MM7*Xba*I: *XhoI*-pH8 clones 1-4 with the right size 474 bp insert. (d) MM8*Xba*I: *XhoI*-pH8 clones 1-8, all with the right size 313 bp fragment. M=O'GeneRuler 1 kb Plus DNA ladder 80

Figure 2. 22 1% agarose gel electrophoresis, showing *Not*I digestion of pHellsgate hairpin cassettes. M= O'GeneRuler 1 kb Plus DNA ladder (Fermentas). (a) Undigested original pHellsgate 8 plasmid (lane 1) and *Not*I digestion of pHellsgate 8 (lane 2). Undigested MM7*Xba*I: *XhoI*-pH8 hairpin (lane 3). *Not*I digested MM7*Xba*I: *XhoI*-pH8 releasing a 3745 bp MM7 hairpin cassette (lane 4). (b) *Not*I digested MM5*Xba*I: *XhoI*-pH8 releasing a 3689 bp MM5 hairpin cassette (lane 1). (c) *Not*I digested MM8*Xba*I: *XhoI*-pH8 releasing a 3423 bp MM8 hairpin cassette (lane 1-3) and undigested MM8*Xba*I: *XhoI*-pH8 (lane 4). *Not*I digested MM6*Xba*I: *XhoI*-pH8, releasing a 3621 bp MM8 hairpin cassette (lane 6-8) and undigested MM6*Xba*I: *XhoI*-pH8 (lane 9). *EcoR*I and *Hind*III double digest of plant transformation vector p1305.1 (lane 10 and 11) and undigested pCambia 1305.1 (lane 12)..... 82

Figure 2. 23 Restriction digestion of clones to confirm correct design and construction of the hairpin constructs. M= O'GeneRuler 1kb Plus DNA ladder (Fermentas) (a) MM5 hairpin clone, digested with *Xba*I (lane 1), *Xho*I (lane 2) and *Not*I (lane 3). (b) MM6 hairpin clone, digested with *Xba*I (lane 2), *Xho*I (lane 3) and *Not*I (lane 4). MM7 hairpin clone, digested with *Xba*I (lane 6), *Xho*I (lane 7) and *Not*I (lane 8). MM8 hairpin clone, digested with *Xba*I (lane 10), *Xho*I (lane 11) and *Not*I (lane 12). pHellsgate 8 control *Xba*I, *Xho*I and *Not*I digestion (lane 15-18). Bottom gel is the inverted image to help with visualisation of bands. Undigested MM6hp, MM7hp MM8hp and pHellsgate 8 in lanes 1, 5, 9 and 14, respectively. 84

Figure 2. 24 PCR amplification to screen for presence and orientation of inserts in the completed hairpin constructs. O'GeneRuler 1kb Plus DNA (Fermentas) (a) MM5hp *Xho*I (446 bp) and *Xba*I (468 bp) amplicons. (b) MM6 *Xba*I (434 bp) and *Xho*I (412 bp) amplicons (lanes 1-4). MM7hp *Xba*I (496 bp) and *Xho*I (474 bp) amplicons (lanes 5-8). MM8hp *Xba*I (335 bp) and *Xho*I (313 bp) amplicons (lanes 9-12). (c) Amplification of 465 bp *Hyg*II gene fragment from construct MM5hp, MM6hp, MM7hp and MM8hp and positive 1305.1 control plasmid (lanes 1-5, resp)

and 181 bp *GUS* gene fragment from MM5hp, MM6hp, MM7hp and MM8hp and positive 1305.1 control plasmid (lanes 1-6, resp)..... 86

Figure 3. 1 Flow diagram of work flow to generate transgenic cassava plants. 97

Figure 3. 2 cv.60444 FEC induction (a) Swollen axillary bud after 3 days on CAM. (b) Immature somatic embryos (SE) surrounded by NEFC after 2 weeks on CIM. (c) Maturing SE with a reduction in NEFC after the 2nd transfer to fresh CIM (after 2 weeks); SE then ready for FEC induction on GD. (d) SE maintained on CIM finger-like structures, trumpet shaped and coral-like SE with no NEFC after the 3rd transfer to CIM. (e) Developing FEC with NEFC after the 3rd transfer to GD. (f) Proliferating FEC with no NEFC after the 4th transfer to GD; FEC ready for inoculation with *Agrobacterium* harbouring the constructs. 106

Figure 3. 3 T200 FEC induction (a) Swollen axillary bud, after 3 days on CAM. **(b)** Immature somatic embryos (SE) surrounded by NEFC after 2 weeks on CIM. **(c)** Maturing SE produced after 2nd transfer to fresh CIM (4 weeks later) and ready for FEC induction on GD. **(d)** Mature trumpet shaped and coral-like SE, with choral-like SE being more dominant, and no NEFC after the 4th transfer to CIM (after 2 more weeks). **(e)** Tiny clump of developing FEC with NEFC after the 4th transfer to GD. **(f)** Tiny clump of FEC giving rise to more FEC, proliferating FEC still embedded in NEFC. **(g)** Proliferating FEC after 10 weeks (5th cycle on GD) with hard yellow NEFC structure. **(h)** FEC after 14 weeks (7th cycle on GD); mature and ready to be inoculation with *Agrobacterium* harbouring the constructs..... 107

Figure 3. 4 Regeneration of putatively transformed FEC (a) Blue stained FEC after GUS assay. (b) Developing embryo (on MSN+C250+H15) on a bed of transformed FEC seen as yellow swollen structures. (c) Maturing embryo after 2 weeks on MSN+C250+H15. (d) Yellow green cotyledon after 3 weeks on MSN+C250+H15; cotyledon ready to be moved to CEM+C100. (e) Maturing cotyledon. (f) Appearance of shoot with emerging juvenile leaves after several weeks on CEM+C100. Apical shoot was transferred to rooting media after appearance of mature\true leaves..... 109

Figure 3.5 MM1 transformed cv60444 and T200 FEC. (a) GUS stained FEC. (b) MM1 transformed cv.60444 FEC: FEC not proliferating and not producing embryos after 4 weeks on MSN+C250+H15, turning necrotic. (c) MM1 transformed T200 FEC after 4 weeks on MSN+C250+H15: swollen yellow FEC not forming cotyledons. 110

Figure 3. 6 MM3 transformed cv.60444 FEC (a) GUS stained FEC. (b) cv.60444 FEC producing finger-like structures instead of expected embryo structures. 111

Figure 3.7 Hygromycin rooting test. (a)Transgenic line rooting and growing well on CBM+C50+H10 medium (b) Untransformed cv.60444 not rooting nor growing on CBM+C50+H10 medium. 115

Figure 3. 8 Leaves following O/N incubation at 37 °C in GUS assay solution. (a) Blue stained leaf (positive GUS assay) indicating positive transgene status. (b) Untransformed green wild-type cv.60444 leaf negative for *GUS* 116

Figure 3. 9 1 % agarose gel electrophoresis of *Hyg*, *GUS* and RNAi construct PCR amplicons in 27 A-MM2 putative transgenic lines that were selected for rooting test and GUS assay. Lines were screened for the (a) 181 bp GUS gene fragment, (b) 485 bp *Hyg* gene amplicon, (c) 337 bp mutated sense-arm amplicon and (d) the 319 bp non-mutated antisense-arm amplicon. M= O'GeneRuler 1 kb Plus DNA ladder (Fermentas). 118

Figure 3. 10 PCR confirmation of transgene status of MM4 putative transgenic lines. Lines were screened for the (a) 181 bp *Hyg* fragment, (b) 485 bp *GUS* amplicon, (c) 337 bp mutated sense-arm hairpin amplicon and (d) the 221 bp non-mutated antisense-arm hairpin amplicon. M= O'GeneRuler 1 kb Plus DNA ladder (Fermentas). 119

Figure 3. 11 PCR confirmation of transgene status of putative transgenic B-MM2 lines selected for rooting test and GUS assay. All 50 lines were screened, but gels above only showing results lines B-MM2 16-31. Lines were screening for (a) 181 bp *Hyg* amplicon, (b) 500 bp *GUS* amplicon, (c) 319 bp non-mutated antisense-arm fragment of the hairpin and (d) the 337 bp mutated sense-arm fragment of the hairpin. M= O'GeneRuler 1 kb Plus DNA ladder (Fermentas). 120

Figure 3. 12 PCR screening of putative transgenic B-MM3 lines selected for rooting test and GUS assay. All 42 lines were screened, but gels above show results of B-MM3 31- 42 lines. Lines were screened for (a) 181 bp *GUS* amplicon, (b) 485 bp *Hyg* amplicon, (c) 381 bp non-mutated antisense-arm fragment and (d) 399 bp mutated sense-arm fragment of the construct. M= O'GeneRuler 1 kb Plus DNA ladder (Fermentas). 121

Figure 3. 13 PCR confirmation of transgene status of putative transgenic BMM4 lines that were selected for rooting test and GUS assay. All 50 lines were screened, but gels above only show results for lines BMM4 15-25. Lines were screening for (a) 485 bp Hyg gene amplicon, (b) GUS gene(c) 221 bp non-mutated antisense-arm fragment and (d) the 239 bp mutated sense-arm fragment of the construct. M= O'GeneRuler 1 kb Plus DNA ladder (Fermentas). 122

Figure 3.14 PCR confirmation of putative transgenic C-MM6 lines transgenic status. Lines were screened for (a) 181 bp *GUS* fragment; fragment was successfully amplified in all lines screened. (b) Amplification of the 485 bp hygromycin gene fragment was detected in all lines tested. In both (a) and (b) plasmid amplified positive while no amplicons was seen in both the untransformed cv.60444 and NTC controls. M= O'GeneRuler 1 kb Plus DNA ladder (Fermentas). 123

Figure 3. 15 PCR confirmation of putative transgenic C-MM8 lines transgenic status. Lines were screened for (a) 181bp *GUS* fragment successfully amplified in all lines except line 12 and 23 (b) Amplification of the 485 bp *Hyg* fragment was detected in all lines except line 23. (c) Inverted gel image of 239 bp MM8 *Xba*I amplicons detected in line 2 and 27 and very faintly in lines 1,3,4,5,6,7,8,9,10 and 23 (d) Inverted gel image of 239 bp MM8 *Xho*I-arm detected in line 27 and very faintly in lines 1,2,3,4,5,7,8. M= O'GeneRuler 1 kb Plus DNA ladder (Fermentas). . 124

Figure 3.16 PCR screening of putative D-MM6 transgenic lines for transgene status. (a) Positive amplification of 181 bp *GUS* fragment in all 8 selected lines. (b) Positive amplification of the 485 bp *Hyg* gene fragment in all lines screened. M= O'GeneRuler 1 kb Plus DNA ladder (Fermentas). 125

Figure 3. 17 PCR screening of D-MM8 lines for transgene determination. (a) PCR amplification of the 181 bp *GUS* fragment in 10 lines (lines 1-10) and positive control. (b) Positive amplification of 485 bp gene fragment in all 11 lines and positive control. (c) Amplification of 239 bp MM8 *Xba*I fragment in lines 1, 2, 4, 5, 6, 8, 9 and 10. (d) Amplification of the 239 bp MM8 *Xho*I fragment in lines 1, 3,4,5,9 and 10. M= O'GeneRuler 1 kb Plus DNA ladder (Fermentas). 126

Figure 3. 18 1% agarose gel of PCR DIG labelled *Hyg* and *GUS* fragment probes. M= O'GeneRuler 1 kb Plus DNA ladder (Fermentas). DIG-labelled *Hyg* probe (lane 1) migrating slower than unlabelled 485 bp *Hyg* fragment (lane 2) and DIG-labelled *GUS* probe (lane 3) migrating slower than unlabelled 181 bp *GUS* fragment (lane 4). 127

Figure 3. 19 1% agarose gel of PCR DIG labelled insert probes. M= O'GeneRuler 1 kb Plus DNA ladder (Fermentas), unmodified ACMV AC1/4:AC2/3 (lane 1) migrating slower than unlabelled 319 bp ACMV AC1/4:AC2/3 fragment (lane 3) and DIG-labelled unmodified BC1 unmodified (lane 2) migrating slower than unlabelled 221 bp BC1 (lane 4). 128

Figure 3. 20 Southern blot analysis of A-MM2 transgenic lines for transgene integration using three DIG-labelled probes. M = DIG molecular weight marker (Roche), wt = untransformed cv.60444 and +veC = pC1305.1 (a) *Hind*III-digested genomic DNA, probed with *Hyg* (b) *Hind*III-digested genomic DNA, probed with *GUS* and (c) *Hind*III and *EcoR*I-double digested genomic DNA, probed with ACMV AC1/4:AC2/3 DIG-labelled fragment to detect a 2771 bp MM2hp cassette; +veC = *Hind*III and *EcoR*I-double digested pTZR5/T containing MM2hp cassette. 129

Figure 3. 21 Southern blot analysis of A-MM4 transgenic lines for transgene integration using DIG-labelled probes. M = DIG molecular weight marker (Roche), wt = untransformed cv.60444 and +veC = pC1305.1 (a) *Hind*III-digested genomic DNA, probed with *Hyg*, (b) *Hind*III-digested genomic DNA, probed with *GUS* and (c) *Hind*III and *EcoR*I-double digested genomic DNA, probed with BC1 unmodified DIG-labelled fragment to detect 2575 bp MM4hp cassette; +veC = *Hind*III and *EcoR*I-double digested pTZR5/T containing MM4hp cassette..... 131

Figure 3.22 Southern blot of B-MM2, B-MM3 and B-MM4 *Hind*III-digested genomic DNA probed with DIG-labelled *Hyg* probe for transgene copy number. (a) 13/50 B-MM2 lines (B-MM2 27-39), (b) 13/29 B-MM3 lines (B-MM3 14-26) and (c) 11/50 BMM4 lines (B-MM4 14-24). M = DIG molecular weight marker (Roche), wt = untransformed cv.60444 and +ve = pC1305.1 plasmid control. 133

Figure 3. 23 Southern blot analysis of C-MM6 transgenic lines for transgene integration using DIG-labelled probes. M = DIG molecular weight marker (Roche), wt = untransformed cv.60444 and +veC = pC1305.1 (a) *Hind*III-digested genomic DNA, probed with *Hyg* and (b) *Hind*III-digested genomic DNA, probed with *GUS.* 134

Figure 3. 24 Southern blot analysis of C-MM8 transgenic lines for transgene integration analysis using DIG-labelled probes. M = DIG molecular weight marker (Roche), wt = untransformed cv.60444 and +veC = pC1305.1 plasmid control (a) *Hind*III-digested C-MM8 genomic DNA, probed with *Hyg* and (b) *Hind*III-digested C-MM8 genomic DNA, probed with *GUS.* 136

Figure 3. 25 Southern blot of D-MM6 1-8 lines and D-MM8 1-10 lines, genomic DNA digested with *Hind*III-digested genomic DNA probed with DIG-labelled *Hyg* probe for transgene copy number. M = DIG molecular weight marker, wt = untransformed cv.60444 and +ve = pC1305.1 plasmid control..... 138

Figure 4. 1 Flow diagram of methodology followed to screen transgenic plants for virus resistance. 155

Figure 4. 2 Amplification curves from real-time qPCR of 5 serial (10-fold) dilutions of 10 ng of (a) ACMV-[NG-Ogo] DNA-A in linearised pCambia 1305.1(above). ACMV standard curve was generated from crossing points (read off the exponential phase of the amplification curves) plotted against log ACMV virus concentration (below). (b) Amplification curves from real-time PCR of 5 serial (10-fold) dilutions of 10 ng of SACMV DNA-A in linearised pBS (above). SACMV standard curve generated from crossing points points (read off the exponential phase of the amplification curves) plotted against log SACMV virus concentration (below)..... 163

Figure 4. 3 Images of cassava mosaic disease symptomatic leaves. Leaves scored according to symptom severity scale by Fauquet & Fargette (1990). Two images representing each level of the 0-5 scale (0 being asymptomatic and 5 being fully symptomatic). Images complied from trials performed in this study. 165

Figure 4. 4 A-MM2 transgenic lines and control plants agroinoculated with infectious ACMV-[NG-Ogo] clones. Plants were evaluated at 12dpi (blue), 32dpi (red) and 67dpi (green) for (a) Mean symptom severity scores, (b) Mean plant growth height and (c) Mean absolute viral load quantification (virus molecules/g of TNA). 167

Figure 4. 5 A-MM4 transgenic lines and control plants agroinoculated with infectious SACMV clones. Plants were evaluated at 12dpi (blue), 32dpi (red) and 67dpi (green) for (a) Mean symptom severity scores, (b) Mean plant growth height and (c) Mean absolute viral load quantification (mean viral molecules/g TNA). 169

Figure 4. 6 C-MM6 transgenic lines and control plants infected with infectious ACMV-[NG-Ogo] clones. Plants were evaluated at 12dpi (blue), 32dpi (red) and 67dpi (green) for (a) Mean symptom severity scores, (b) Mean plant growth height and (c) Mean absolute viral load quantification (mean viral molecules/g TNA). 171

Figure 4. 7 C-MM8 transgenic lines and control plants infected with infectious SACMV clones. Plants were evaluated at 12dpi (blue), 32dpi (red) and 67dpi (green) for (a) Mean symptom severity scores, (b) Mean plant growth height and (c) Mean absolute viral load quantification (viral molecules/g TNA). 173

Figure 4. 8 CMD symptoms collected from ACMV and SACMV infected cassava plants at 365 dpi, (a) ACMV infected cv.60444, showing mosaic, leaf curl and size reduction, (b) ACMV infected A-MM2 54 leaf with faint yellow spots on entire leaf surface, (c, d) SACMV infected cv.60444 (WT) with yellow mosaic spotting on entire leaf surface, (e) SACMV infected A-MM4 11 leaf showing slight leaf curl and mosaic on leaf edge and (f) SACMV infected A-MM4 34 showing slight mosaic on the leaf margin and faint yellow spots on leaf surface. 176

Figure 4. 9 Mean viral molecules/g of TNA at 365 dpi, quantified using qPCR, (a) ACMV infected A-MM2 transgenic lines and controls lines and (b) SACMV infected transgenic lines and control plants. 177

Figure 4. 10 1.2% agarose gel electrophoresis (10mg/ml EtBr) of total RNA extracted from (a) A-MM2 transgenic lines 41, 30, 44, 52, 53, 54 and non-transgenic cv.60444 WT, (b) A-MM4 transgenic lines 11, 33, 34, 46, 59, 68 and 79, (c) C-MM6 transgenic lines 2, 1, 8, 10, 11, 19 and non-transgenic cv.60444 and (d) C-MM8 transgenic lines 1, 3, 23, 25, 27 and non-transgenic cv.60444. 178

Figure 4. 11 RT-PCR amplification of transgne cDNA from (a) A-MM2 transgenic lines: 181 bp *GUS* (above) and 485 bp *Hyg* (below). M= O'GeneRuler 1kb Plus DNA ladder (Fermentas), (b) A-MM4 transgenic lines: 181 bp *GUS* (above, left) and 485 bp *Hyg* (below, left), 221 bp non-mutated anti-sense-arm (above, right); GU: 239 bp mutated sense-arm (below, right), (c) C-MM6 transgenic lines: 181 bp *GUS* (above, left) and 485 bp *Hyg* (below, left), 319 bp MM6 *Xba*I-arm (above, right) and 319 bp MM6 *Xho*I-arm (below, right) and (d) C-MM8 transgenic lines: 181 bp *GUS* (above, left) and 485 bp *Hyg* (below, left), 221 bp MM8 *Xba*I-arm and 221 bp MM8 *Xho*I-arm. 180

Figure 4. 12 siRNA detection in healthy transgenic lines and control lines. Probes were radioactively labelled with P^{32}, (a) A-MM2 transgenic lines and controls probes with ACMV AC1/4:AC2/3 generated probe, (b) SACMV BC1-derived probes used to probe A-MM4 transgenic lines, (c) C-MM6 transgenic lines probed with ACMV AC1/4:AC2/3-derived probe, (d) C-MM8 transgenic lines probed with SACMV BC1-derived probe and (e) radioactively labelled 21, 22 and 24 nt oligonucleotides used as markers. 181

Figure 4. 13 Arabidopsis miRNA167 probe used for loading control in siRNA detection experiment to probe healthy control lines and transgenic (a) A-MM2 lines, (b) A-MM4 lines, (c) C-MM6 lines and (d) C-MM8 lines. Left lane is over loaded marker..... 182

List of tables

Table 2. 1 siRNA scan programme computational results predicting regions along the ACMV-[NG:Ogo:90] AC1/AC4 overlapping region were efficient and effective siRNA could be generated. 66

Table 2. 2 siRNA scan programme computational results predicting regions along the ACMV-[NG:Ogo:90] AC2/AC3 overlapping region were efficient and effective siRNA could be generated. 67

Table 2. 3 siRNA scan programme computational results predicting regions along the EACMV-[UG2] AC1/AC4 overlapping region were efficient and effective siRNA could be generated. .. 67

Table 2. 4 siRNA scan programme computational results predicting regions along the EACMV-[UG2] AC2/AC3 overlapping region were efficient and effective siRNA could be generated. .. 68

Table 3. 1 Summary of transformation events including details of RNAi construct used and FEC type transformed. 100

Table 3. 2 Cotyledon and shoot generation efficiency per ~1cm FEC clump for each cultivar/landrace construct transformation event. 113

Table 3.3 Transformation efficiency calculated based on putative transgenic plantlets able to root on hygromycin-containing media and positive blue GUS assay. 116

Table 3.4 Transgene copy numbers of 16 A-MM2 lines detected by DIG-labelled *Hyg*, *GUS* and DIG Hybrid II (ACMV AC1/4:AC2/3) -labelled probes..... 130

Table 3. 5 Transgene copy numbers of 16 A-MM4 lines detected by DIG-labelled *Hyg*, *GUS* and BC1 unmodified fragment probes..... 132

Table 3. 6 Transgene copy numbers of 15 C-MM6 lines detected by DIG-labelled *Hyg* and *GUS* probes. 135

Table 3. 7 Transgene copy numbers of 15 C-MM8 transgenic lines. Lines were probed with DIG-labelled *Hyg* and *GUS* probe. 137

Table 4. 1 Virus challenge trials of transgenic lines. 158

Table 4. 2 Symptom severity scores of A-MM2 transgenic lines at 365 dpi with ACMV 175

Table 4. 3 Symptom severity scores of A-MM4 transgenic lines at 365 dpi with SACMV 175

List of appendices tables

Appendix A Student’s t-test accessing the mean statistical difference between A-MM2transgenic line and cv.60444symptom severity score index, plant height and ACMV viral load, at 12, 32 and 67dpi..... 238

Appendix B Student's t-test accessing the mean statistical difference between A-MM4transgenic line and cv.60444symptom severity score index, plant height and SACMV viral load, at 12, 32 and 67dpi..... 238

Appendix C Student’s t-test accessing the mean statistical difference between C-MM6 transgenic line and cv.60444symptom severity score index, plant height and ACMV viral load, at 12, 32 and 67dpi..... 239

Appendix D Student’s t-test accessing the mean statistical difference between A-MM2transgenic line and cv.60444symptom severity score index, plant height and ACMV viral load, at 12, 32 and 67dpi..... 239

Appendix E Student’s t-test accessing the mean statistical difference between transgenic lines, A-MM2 and AMM4, and cv.60444 viral load at 365 dpi..... 240

Appendix F Pearson’s correlation coefficient measuring the relationship (correlation) between symptom severity score (sss) and plant height, correlation between viral load and symptom severity score and the correlation between viral load and plant height for A-MM2, A-MM4, C-MM6 and C-MM8, at 12, 32 and 67 dpi..... 241

List of abbreviations

ACMV	*African cassava mosaic virus*
AB	axillarybuds
AS	antisense
BAP	6-Benzylaminopurine
bp	base pair
CaMV	*Cauliflower mosaic virus*
CBV	cassava begomovirus
CEM	cassava elongation medium
CIM	callus induction medium
CMD	cassava mosaic disease
CP	coat protein
CTAB	Cetyltrimethylammonium bromide
CMV	*Cucumber mosaic virus*
DNA	deoxyribonucleic acid
dpi	days post inoculation
dsDNA	double-stranded DNA
dsRNA	double-stranded RNA
EACMV	*East African cassava mosaic virus*
EDTA	ethylene diamine tetra-acetate
FEC	friable embryogenic callus
GD	Gresshoff and Doy
GE	genetic engineering
GUS	β-glucuronidase
hp	hairpin
IR	invert repeat
Kb	kilobase
LB	Luria broth
MCS	multiple cloning site
MS	Murashige and Skoog

MP	Movement protein
NAA	α-naphthaleneacetic acid
nt	nucleotide
OD	optical density
O/N	overnight
ORF	open reading frame
pBS	pBluescript
PCR	polymerase chain reaction
PDR	pathogen derived resistance
PTGS	post-transcriptional gene silencing
PVX	potato-virus X
PVY	potato-virus Y
RDR	RNA dependent RNA polymerase
RISC	RNA-induced silencing complex
RNAi	RNA interference
RT-PCR	reverse transcriptase PCR
qPCR	quantitative PCR
S	sense
SACMV	*South African cassava mosaic virus*
SE	somatic embryo
ssDNA	single-stranded deoxyribonucleic acid
siRNA	small interfering RNA
T-DNA	Transfer DNA
TMV	Tomato mosaic virus
TNA	total nucleic acid
ToLCV	*Tomato leaf curl virus*
U	unit
VIGS	virus induced gene silencing
X-gal	5-bromo-4-chloro-3-indolyl-beta-D-galacto-pyranoside
X-gluc	5-bromo-4-chloro-3-indolyl-beta-D-glucuronic acid cyclohexylammonium salt
YEP	yeast extract peptone

CHAPTER: 1 LITERATURE REVIEW

1.1 Cassava crop

Cassava (*Manihot esculenta* Crantz) is a perennial plant grown in tropical and subtropical Africa, Asia and Latin America and 80% of total cassava cultivation occurs in Africa and Asia (Adenle *et al*., 2012). It is mainly cultivated by small resource poor farmers. In low income areas of these countries the crop is a staple food consumed by over 700 million people (Eleazu, *et al.*, 2011). It's recognised as one of 11 crops that contribute to poverty alleviation and food security.

It is thought that cassava was introduced into South Africa from Zimbabwe or Mozambique and Mauritius, and spread across the northern and eastern regions of Natal and Mpumalanga by Tsonga tribesman in the 1830's (Trench *et al.*, 1985). Cassava is mainly cultivated in KwaZulu-Natal (where it is known as *ndumbula*) and Mpumalanga in South Africa (Daphne, 1980). In 1999 a cassava starch processing factory was built in Limpopo and has provided large cash injections for both small and large-scale farmers. This operation has been expanded into Swaziland (Mabasa 2007).

1.2 Cassava mosaic disease (CMD)

CMD contributes to devastating cassava crop losses in Africa and other cassava growing regions of the world (Thresh *et al.*, 1998; Legg & Fauquet, 2004; Legg *et al.*, 2011). Symptoms of CMD were first documented by Warburg in 1894 and only later, in 1906 was it suggested by Zimmerman that the viral pathogen was the causal agent of CMD. CMD results in enormous cassava yield losses annually and is considered one of the most destructive crop disease (Legg *et al*., 2011; Patil & Fauquet, 2009). This crop disease is caused by viruses belonging to the genus *Begomovirus* of the family *Geminiviridae.* These cassava infecting begomoviruses (CBVs) are transmitted by a whitefly vector, *Bemisia tabaci* (Gennadius) (Berry *et al.*, 2004; Bock & Harrison, 1985). CBVs are transmitted by *Bemisia* haplotypes that form a distinct southern African clade (Berry & Rey, 2001; Esterhuizen *et al*., 2013). The virus also spreads through infected cuttings after transmission and produces a range of symptoms that can be observed on plants 3-5 weeks post infection (Varma & Malathi, 2003; von Arnim & Stanley, 1992). Plants

can show mild symptoms such as light-green mosaic patterns or more severe symptoms such as severe leaf shrinkage, curling and chlorotic lesions (**fig.1.1**). Extreme symptoms such as leaf desiccation may result in defoliation and death of young infected plants (Pita *et al.*, 2001). In South Africa CMD was reported as early as 1970 and bulk import of cassava from Mozambique in 1975 caused CMD outbreak (Trench *et al.*, 1985). It was not until the late 1999's and 2000's that two comprehensive studies on the epidemiology and
diversity of cassava begomoviruses were undertaken (Berry & Rey, 2001).



Figure 1. 1 (a) Healthy wildtype cassava plant. **(b)** and **(c)** CBV infected cassava plant showing CMD symptoms.

1.3 Geminiviruses

Geminiviruses have paired icosahedral capsids containing circular single stranded (ss) DNA genomes of 2.5-2.9 kilobases (kb) and are either monopartite or bipartite. The name geminivirus was derived from the Latin word Gemini, meaning twins and was proposed by Harrison *et al.*, 1997). The family *Geminiviridae* has been classified into 7 genera; *Turncurtovirus*, *Eragrovirus*, *Becurtovirus*, *Curtovirus*, *Mastrevirus*, *Topocuvirus* and *Begomovirus* based on virus genome organisation, host range and most importantly the vector transmission (Adams *et al.*, 2013; Fauquet *et al.*, 2008). The genus *Begomovirus* represents 80% of known geminiviruses (Varma & Malathi, 2003). are responsible for several important diseases in southern African crops, including monocots and dicots (Rey *et al*., 2012).

1.3.1 Begomovirus genome organisation

Begomoviruses are whitefly transmitted and most are bipartite, consisting of two DNA components; DNA-A and DNA-B each having a 2.6-2.8 kb genome (**fig. 1.2**). The genomes are bidirectionally transcribed and replicate in the nuclei of infected plant cells (Dry *et al.*, 1993; Gutierrez, 2002). DNA-A encodes 2 genes on its virion-sense strand; *AV1* (coat protein) and *AV2* (responsible for virus accumulation and symptom development and has also been identified as an RNA silencing suppressor) (Wang *et al*., 2014). The complementary-sense strand of DNA A encodes 4 genes; *AC1-AC3* genes encode the replication-protein (Rep), transcriptional activator protein (TrAP) and the replication enhancer protein (REn), respectively and *AC4* gene is involved in virus movement, symptom severity and host range determination (Amin *et al.*, 2011; Settlage *et al*., 2005; Trinks *et al*., 2005). AC2, AC3 and AC4 have all been demonstrated to suppress host gene silencing (Amin *et al.*, 2011; Hanley-Bowdoin *et al.*, 2013). The DNA-B component is required for inter and intra-cellular movement and encodes for 2 genes; *BV1* encodes for a nuclear shuttle protein while *BC1* encodes for proteins required for cell-to-cell movement of the virus (Hehnle *et al.*, 2004; Ward *et al.*, 1997).

DNA-A and DNA-B share a common region (CR) of ~200 base pairs (bp) with a high sequence identity (90-100%) (Harrison & Robinson, 1999). The CR is located within the intergenic region which lies between the virion and the complementary-sense strands of both DNA-A and DNA-B. The intergenic region contains sequence motifs that are necessary for gene replication and

control of gene expression (Eagle *et al*.,1994; Elmer *et al*., 1988; Gutierrez, 2002). Also found in the intergenic region is a nonanucleotide sequence TAATATT↓AC which is conserved across all geminiviruses. Rolling circle replication occurs at this site; ↓ which is known as the initiation site (Stanley, 1995) and initiated and catalyzed by AC1 encoded protein (Settlage *et al.*, 2005).

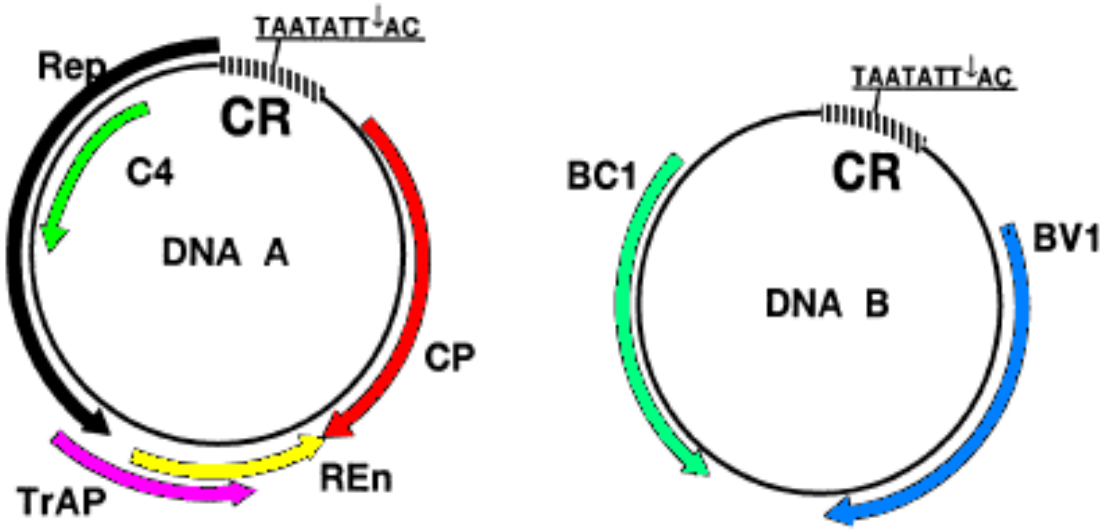


Figure 1. 2 CBV genome organisation, DNA-A and DNA-B (Gutierrez, 2000)

1.3.2 Classification of cassava infecting begomoviruses (CBVs)

Initially 3 distinct groups of whitefly transmitted CBVs were distinguished based on nucleotide sequence by Hong *et al.*, (1993). Berrie *et al.*, 1998; isolated and characterised the 4th distinct group of CBVs from South Africa. This distinct group was named *South African cassava mosaic virus* (SACMV). Making up these 4 groups are 11 distinct species of which 9 infect cassava in Africa: *African cassava mosaic virus* (ACMV), *East African cassava mosaic virus* (EACMV), *East African cassava mosaic Cameroon virus* (EACMCV), *East African cassava mosaic Malawi virus* (EACMMV), *East African cassava mosaic Zanzibar virus* (EACMZV), *East African cassava mosaic Kenya virus* (EACMKV), African cassava mosaic Burkina Faso virus (ACMBFV); Cassava mosaic Madagascar virus (CMMV) and *South African cassava mosaic virus* (SACMV) (Fauquet *et al.*, 2008). Natural recombination has been associated with the occurrence or evolution of new distinct CBV species (Fondong *et al.*, 2000; Pita *et al.*, 2001).

1.3.3 Mixed infections and synergism

Several reports have shown that mixed virus infections in plants occur naturally (Fondong *et al*., 2000). It is during these mixed infections that recombination and pseudo-recombination between the infecting viruses can occur (Pita *et al.*, 2001). Recombination then results in an increase virus molecular diversity (Lima *et al.*, 2013). Recombination between geminiviruses was first reported by Zhou *et al.*, 1997. DNA-A of a novel recombinant isolate Uganda variant (UgV) was found to be extremely similar to Tanzanian isolate of EACMV however the coat protein (CP) was found to be composed of both EACMV and ACMV CP. This novel isolate was found to cause unusually severe CMD symptoms.

During these mixed infections there is an increase in virus titre of both or one of the infecting viruses (Harrison *et al.,* 1997). An increase in virus titre normally results in more severe plant disease symptoms than those observed in single infections, indicating some sort of virus-virus interaction (Rentería-Canett *et al*, 2011; Sanz *et al.*, 2000). Synergistic interaction of viruses was demonstrated between ACMV-[CM] and EACMCV. A seven-fold increase in ACMV-[CM] DNA-A and B was observed in *N. benthamiana* co-infected with EACMCV DNA-A compared with control plants infected with only both components of ACMV-[CM]. Similar results were observed upon co-infection of EACMCV DNA-A and B with ACMV-[CM] DNA-A (Vanitharani *et al.*, 2004). However the same test performed using DNA-B components showed no alteration in viral DNA-A accumulation. Experiments were also performed to identify particular genes involved in the synergistic relationship (discussed later under **Silencing suppressors**).

Designing hybrid RNA silencing constructs targeting several viral regions and several viruses simultaneously ensures greater silencing efficiency and allows successful silencing in the event of mixed infections and in the event that virus recombination or sequence mutations occur.

1.4 RNA silencing

RNA silencing (RNAi) is a conserved innate gene regulatory mechanism that induces sequence-specific mRNA degradation or complete suppression at both transcriptional (TGS) and post-transcriptional gene silencing (PTGS) levels (Agrawal *et al.,* 2003; Wang *et al.,* 2012). In addition, this mechanism has also evolved for protection against virus and transposon invasion (Obbard *et al.,* 2009). This gene regulatory and defense mechanism has been observed in a variety of eukaryotic organisms such as plants, animals, fungi algae, flies, protozoa, nematodes, and many others (Cerutti *et al.,* 2011; Clemens *et al.,* 2000; McRobert and McConkey 2002; Tomoyasu *et al.,* 2008).. An RNAi-like mechanism involving short direct repeat sequences called clustered regularly interspaced short palindromic repeats (CRISPRs) has been reported to also exist in prokaryotes. This RNAi-like mechanism has been termed Prokaryotic silencing (psi) (Barrangou *et al.,* 2007; Brouns *et al.,* 2008). RNA silencing was first documented by Napoli *et al.* (1990) in transgenic petunia flowers. They attempted to up-regulate the key enzyme involved in flavonoid synthesis, chalcone synthase (CHS). Napoli *et al.,* 1990 were expecting to produce transgenic petunia with intensified purple coloured flowers. However contrary to what was expected, 42% of transgenic petunia produced totally white flowers while all the untransformed control produced flowers with normal pigmentation. This phenomenon was termed co-suppression as a result of loss of mRNA of both the endogenous and transgenic *CHS* gene. This was later known as PTGS.

There are three different pathways in gene silencing: the cytoplasmic short-interfering RNA (siRNA) pathway, another pathway that results in the silencing of endogenous mRNAs using microRNAs (miRNAs) and a DNA methylation and transcription suppression pathway (de Felippes *et al.,* 2012; Hamilton, 1999; Ketting *et al.,* 2001; Vaistij *et al.,* 2002). All these different pathways however do share underlying features. In all the various systems, this gene regulatory mechanism occurs in a three step process and the underlying features are similar, (i) formation of double stranded (ds) RNA; (ii) cleavage of dsRNA into siRNA of between 20-27 nt; and (iii) sequence-specific inhibition of complementary cellular or viral mRNA guided by the siRNA (**fig. 1.3**) (Bernstein *et al.,* 2001; Hammond *et al.,* 2000; Parisi *et al.,* 2009; Semizarov *et al.,* 2003).

1.4.1 dsRNA formation and processing into small interfering RNAs

dsRNA was a first identified as a mediator and strong inducer of the silencing process in nematodes *Caenorhabditis elegans* (*C. elegans*) studies (Fire *et al*., 1998). dsRNA was found to be more potent silencing mechanism than either sense or antisense ssRNA. This study also revealed that only a few molecules of dsRNA is required per cell to induce RNAi as silencing of an abundantly expressed *C. elegans* gene was successfully achieved by only a few molecules of dsRNA. This suggested a catalytic or amplification step that resulted in RNAi being very potent, systemic and persistent. Following this discovery, similar supporting reports in plants emerged (Tenllado & Di, 2001). RNA-dependent RNA-polymerase (RDR) was implicated in dsRNA amplification and was found to be critical in the RNA silencing signal potency and systemic spread (Xie *et al.*, 2001). Research by Smardon *et al.* (2000) showed that mutations in an RDR homolog resulted in loss of RNA silencing ability. The presence and amplification of dsRNA also explained dsRNA intermediate synthesis in the RNA silencing of DNA viruses such as geminiviruses (Hanley-Bowdoin *et al.,* 2013; Vanitharani *et al.,* 2005). dsRNA can also result from aberrant RNA, originating from the transcription of foreign virus DNA, this can undergo amplification by RDR (Raja *et al.*, 2010)

1.4.2 Dicer

The unifying feature of all the RNA silencing mechanisms is the cleavage of dsRNA into short RNA fragments of 21-27nt known as siRNA. Reports by Elbashir *et al*. (2001) and Lipardi *et al*. (2001) Lipardi, *et al.* (2001) that the siRNA produced have a 5' phosphate and 3' hydroxyl termini lead to the elucidation that the cleavage of dsRNA into siRNA was by enzymatic activity. The multi-domain ribonuclease called Dicer, belonging to the RNase III protein family, reported as responsible for processing of the initiator dsRNA into the short RNAs (siRNA) of 21, 25 and 27nt (Bernstein *et al*., 2001; Brodersen & Voinnet, 2006; Hammond *et al*., 2000; Weinheimer *et al.*, 2014). This endonucleolytic cleavage activity was reported to start between phosphodiester bonds the lies between the 10^{th} and 11^{th} nucleotide of the dsRNA substrate. Dicer has a 10-residue segment that functions in correctly aligning dsRNA substrates in the enzyme active site. A decrease in catalytic activity and random cleavage of dsRNA is observed when mutations are introduced into the 10-residue Dicer segment (MacRae *et al.*, 2007; Schwab *et al.*, 2006). This work suggested that the structure an d ability of Dicer to align the dsRNA molecule

for into siRNA processing is more dependent on the Dicer enzyme active site rather than the dsRNA sequence. Dicer catalytic activity has also been shown to be unaffected by imperfect U:G wobbles within the dsRNA molecules, both perfect and imperfect dsRNA substrates produce similar cleavage patterns (Soifer *et al.*, 2008). The ability of Dicer to process dsRNA containing wobbles was also demonstrated by Hossbach *et al.,* 2006. Silencing efficiency of both wobble and non-wobble containing hairpins was reported as comparable.

1.4.3 siRNA functional asymmetry

Once the dsRNA has been processed into the siRNA, the siRNA duplexes have to be unwound. Unwinding is as a result of helicase activity (Huang and Liu 2002; Wang *et al.,* 2012). Only a single strand is then incorporated into to the RNA-induced silencing complex (RISC) (Wu-Scharf *et al.,* 2000). Both strands are capable of directing RNA silencing, however it has been shown that Dicer can have a higher affinity for one strand than other and this is known as siRNA functional asymmetry (Schwarz *et al.,* 2003). *In vitro* incubation of luciferase siRNA in an RNAi reaction for 1h in the absence of target mRNA resulted in a 22% accumulation of single stranded (ss) antisense siRNAs while no ss sense siRNAs from the siRNA duplex could be detected. The levels of ss sense siRNAs were however anticipated. This then suggested that the antisense strand is used for directing RNA silencing while the sense stand is degraded. This also proves that there is siRNA asymmetry involved and that the target mRNA is not responsible for any strand bias observed (Schwarz *et al.*, 2003). However, even though a strand bias exists, complete siRNA duplex is required and critical; as single stranded siRNA molecules are approximately 10 fold less effective at directing silencing than siRNA duplexes. This also suggests that this functional asymmetry occurs just before the multicomponent silencing complex termed the RISC is activated (Shao *et al.*, 2007). The RISC complex is comprised of Dicer and the core endonucleolytic cleavage site known as ARGONAUTE (AGO protein) (Meister *et al.,* 2004, 2005; Schuck *et al*., 2013). Studies have proposed that thermodynamics play a role in strand bias; the siRNA strand with the lower thermodynamic stability at the 5' end is incorporated into the RISC complex and used as the guide strand for homologous mRNA degradation (Kini & Walton, 2009; Tomari *et al.*, 2004; Ui-Tei *et al.*, 2012). Introducing a U:G wobble (a less stable base pairing) to the 5' end of the siRNA sense strand and leaving the antisense siRNA strand unchanged resulted in RNA silencing being directed by the sense strand and diminished levels of

the antisense strand was observed and this time round the siRNA functional asymmetry was inverted (Khvorova *et al.*, 2003; Schwarz *et al.*, 2003). Strand asymmetry still remains one of the biggest challenges in siRNA design (Matveeva *et al.*, 2010).

1.4.4 Degradation of mRNA

Once siRNA strand incorporation into the RISC complex has occurred, sequence-specific recognition and degradation of target mRNA follows. The target mRNA is then cleaved into 21-27nt intervals. Target mRNA is only cleaved in regions that are identical to siRNAs produced from the dsRNA (Lu et al., 2004; Pumplin & Voinnet, 2013). Experiments by Hamilton *et al.* (2002) using GFP-expressing *N. benthamiana* also demonstrated two functionally different classes of siRNAs; short and long siRNA, are responsible for sequence-specific degradation of mRNA and systemic spread of the silencing signal. Short siRNAs (21-23nt) were identified to be only involved in mRNA degradation of homologous mRNA and cell-to-cell spread of the signal through the plasmodesmata. Long siRNAs (24-26nt) were implicated in sequence-specific degradation of mRNA as well as systemic RNA silencing through the vascular system (Bai *et al*., 2011; Melnyk *et al.*, 2011). The silencing signal moves from the site of initial mRNA degradation along with or ahead of the virus causing silencing of viral mRNA in newly infected cells (Hamilton *et al.*, 2002). Long siRNAs are also involved in RNA directed methylation of homologous DNA in the cell that the signal has been mobiles to (Bai *et al*., 2011; Hamilton *et al*., 2002).

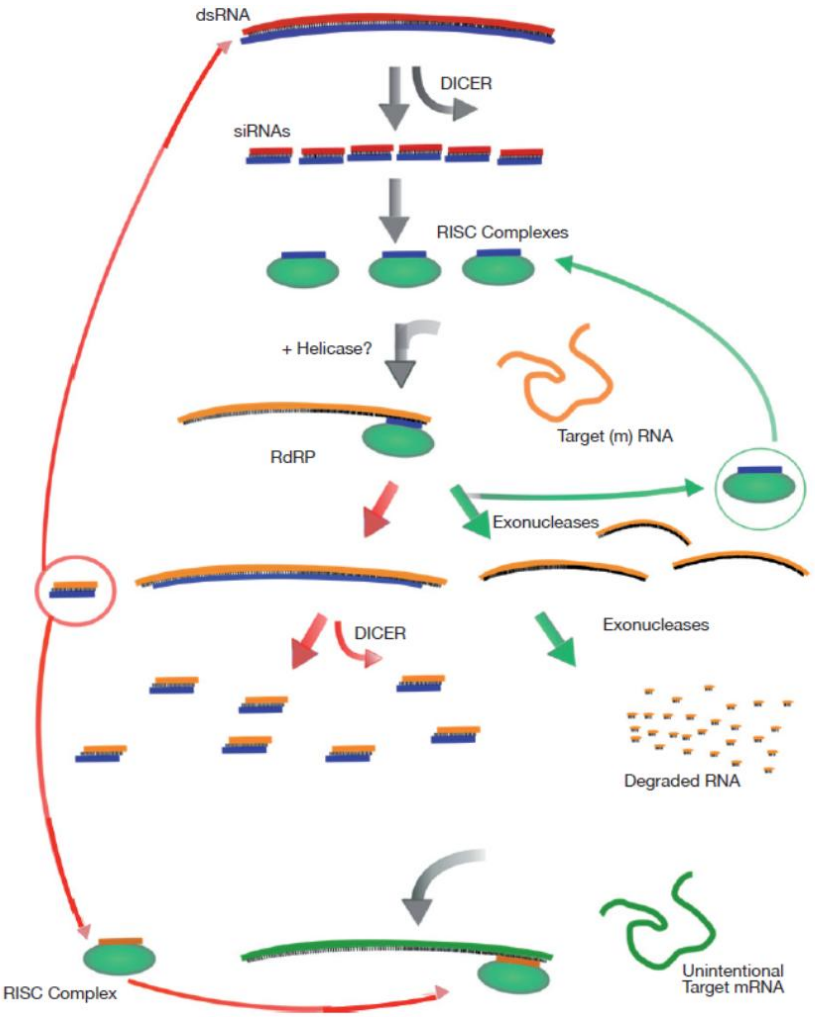


Figure 1. 3 Overview of steps involved in RNA silencing mechanism involving processing of dsRNA intermediates by Dicer into primary siRNA production. Primary siRNA are then used for secondary siRNA production which then enter the RISC complex for sequence-specific degradation of complementary mRNA (Parisi *et al.*, 2009).

1.4.5 DNA methylation

This is a conserved epigenetic mechanism that results in repression of transcription. This silencing mechanism has been reported in both prokaryotes and eukaryotes (Saze *et al.*, 2012). It involves methyltransferase addition of a methyl group to DNA cytosine bases, resulting in a 5-methylcytosine. DNA sequences containing symmetric CG, CHG, and asymmetric CHH (H = A, C, or T) are methylation target sites (Kanno & Habu, 2011). DNA methylation was first reported in potato spindle tuber viroid (PSTVd) transgenic *N. benthamiana* (Wassenegger *et al.*, 1994).

Full PSTVd sequence-specific methylation was reported but no methylation of sequences outside the integration sites was observed. Later experiments reported the existence of two types DNA methylation; a maintenance type that maintains previous methylation patterns present in a particular DNA sequence, and a type that methylates previously unmethylated sequences (Bai *et al.*, 2011; Xie *et al*., 2004; Yu *et al*., 2005). This RNA-directed DNA methylation (RdDM) pathway also involves the biogenesis of siRNA from dsRNA cleavage by a Dicer-like 3 (DLC3) ribonuclease (Xie *et al.*, 2004). Methylation of homologous DNA occurs via another effector complex called the RNA-induced initiation of transcriptional gene silencing (RITS). The long siRNAs incorporate into the RITS and direct chromatin modification/methylation of homologous target DNA sequences (Verdel *et al*., 2004; Wu *et al*., 2010).

1.4.6 Comparison of siRNA and miRNA

MiRNA are endogenously derived regulatory molecules. These were first discovered by Lee *et al.,* (1993) while studying the gene *lin-14* in *C. elegans*. They discovered that the gene does not encode for a particular protein, but instead involved in the control of larval development. The gene was found to produce small RNA molecules of 22nt (Lee *et al.,* 1993) . miRNA, like siRNA have been shown to be involved in DNA methylation (Wu *et al.,* 2010). Like siRNA, miRNA fall under the class of silencing RNA that regulate gene expression (Wilson & Doudna, 2013). Both siRNA and miRNA are involved in post-transcriptional regulation however miRNA are also involved in developmental and cellular processes as well (Khraiwesh *et al.,* 2010). siRNA can be of exogenous and endogenous origin while miRNA are endogenously derived. miRNA differ to siRNA in their biogenesis and can only be differentiated by their precursor transcripts as they are structurally similar to siRNA once processed. miRNA are also 20-24nt long but are mainly processed by Dicer-like 1 ribonuclease (Han *et al.,* 2004; Ketting *et al.,* 2001). siRNA are generated from cleavage of long perfectly complementary dsRNA precursors while miRNA are generated from a longer imperfect pri-miRNA precursor that is processed into a shorter 70nt stemloop pre-miRNA (Bartel, Lee, & Feinbaum, 2004). This is then further processed into a mature miRNA molecule that can then enter the RISC complex. Generally one miRNA is produced from the pri-miRNA, whereas several siRNA can be generated from the dsRNA precursor (Bartel *et al.,* 2004). miRNA have several different mRNA targets and lower off target effects while siRNA generally target one specific complementary mRNA and can have

a higher off target effect as a result of the pool of siRNA fragments generated from the long dsRNA precursor (Bartel *et al.*, 2004). However, plant miRNA tend to have fewer targets of high complementarity than animal miRNA which have been reported to have a broader target of limited complementarity (Schwab *et al.*, 2006).

1.5 Geminiviruses as RNA silencing inducers and targets

In plants, RNA silencing is considered a primary defense mechanism against viral invasion (Zvereva & Pooggin, 2012). It is characterised by formation of primary viral siRNA molecules which are generated from the RISC-mediated cleavage of dsRNA viral transcripts. Primary siRNA molecules are also used for generating secondary siRNA molecules by RDR1 and RDR6 (Blevins *et al.*, 2006). This results in silencing of the viral genome and reduced viral replication. In some cases initiation of this antiviral mechanism correlates with decreased titre of the invading virus, reduction in symptoms, resistance and a recovery phenotype seen in geminivirus-infected plants (Akbergenov *et al*., 2006; Carrillo-Tripp *et al.*, 2007; Ribeiro *et al.*, 2007; Vanderschuren *et al*., 2009; Vu *et al*., 2013) .

Geminiviruses are ssDNA viruses and replicate through a dsDNA intermediate and do not enter a dsRNA phase (Gutierrez 2002; Laufs *et al.*, 1995). But it is believed that dsRNA is generated from Polymerase II (Pol II) directed monodirectional transcription of viral DNA resulting in overlapping regions of viral mRNA (Aregger *et al*., 2012; Hanley-Bowdoin *et al*., 2013; Vanitharani *et al*., 2004). The overlapping regions are used as template by RDR to make dsRNA which is then processed by Dicer producing primary siRNAs as seen in **Fig. 1.4**. Majority of siRNAs generated in ACMV-[CM] plant infections have been found to originate from the AC1 and AC2 ORF overlap region of DNA-A (Chellappan *et al.*, 2004). dsRNA can also be generated from aberrant RNA with regions of homology folding on itself creating the dsRNA required to trigger RNA silencing (fig. 1.4) (Aregger *et al*., 2012; Montgomery & Fire, 1998; Shimura & Pantaleo, 2011; Vanitharani *et al.*, 2005). siRNA molecules derived from aberrant 8S RNA of *Cauliflower mosaic virus* (CaMV) have been identified and its suggested that a Pol II mediated dsRNA intermediate mechanism is involved, however the exact mechanism is still unknown (Blevins *et al*., 2011).

Involvement of siRNA in TGS-directed antiviral defense mechanism against geminiviruses has been extensively shown over the last few years. TGS is associated with promoter inactivation and reduced transcript levels (Vaucheret & Fagard, 2001). DNA methylation does negatively affect geminivirus promoters (Ermak *et al.*, 1993). A recovery phenotype was observed by Vanderschuren *et al*. (2007) in siRNA-directed methylation of ACMV CR and promoter. There were able to detect 24-nt siRNA which are generally associated with DNA methylation which contributes to recovery. In research performed by Akbergenov *et al*. (2006) 21, 22 and 24nt siRNA targeting ACMV and *Cabbage leaf curl virus* (CaLCuV) non coding intergenic region and were associated with and also suggesting involvement of both PTGS and TGS. Involvement of both PTGS and TGS resulting in reduced virus titre and host recovery was observed in pepper plants infected with *Pepper golden mosaic virus* (PepGMV) (Rodríguez-Negrete *et al.*, 2009). Two classes of siRNA molecules were identified; smaller 21-22nt siRNA corresponding mainly to PepGMV coding regions and 24-nt siRNA corresponding to intergenic region. A bisulfite methylation approach was performed to determine methylation levels and patterns focussing on the CP and intergenic regions. Results showed a much higher and constant conserved methylation pattern at all time points for the intergenic region but not for CP. In a more recent geminivirus-plant interaction study the importance of TGS was clearly demonstrated by Hagen *et al*. (2008). *Cucurbit leaf crumple virus* (CuLCrV) infected watermelon and cantaloupe plants had high accumulation of CuLCrV-derived siRNA of 24-27nt and a strong recovery phenotype. Similar results were seen when recovery plants were re-inoculated with CuLCrV. A limited recovery phenotype was observed in CuLCrV-infected zucchini plants as expected methylated CuLCrV DNA was lower CuLCrV infected zucchini plants than CuLCrV-infected watermelon plants. However, CuLCrV infection of zucchini plants inoculated with CuLCrV CR IR construct did result in recovery and reduced virus levels indicating involvement of gene silencing antiviral defense mechanism. Inoculation of CuLCrV recovery leaves with RNA virus, *Cucumber mosaic virus* CMV, resulted in severe disease symptoms and high CuLCrV and CMV titre however surprisingly high siRNA accumulation was observed. This study also emphasised the idea that RNA silencing is more effective on DNA than RNA viruses. The results also suggest that recovery response is virus specific and directed. The increase in CuLCrV also suggests that CMV encodes 2b protein which is a known RNA silencing suppressor (González *et al*., 2010;

Xiuren Zhang *et al.*, 2006). They also implicated virus-virus interaction, similar to that observed by Chellappan *et al*. (2004), as the cause in recovery phenotype loss.

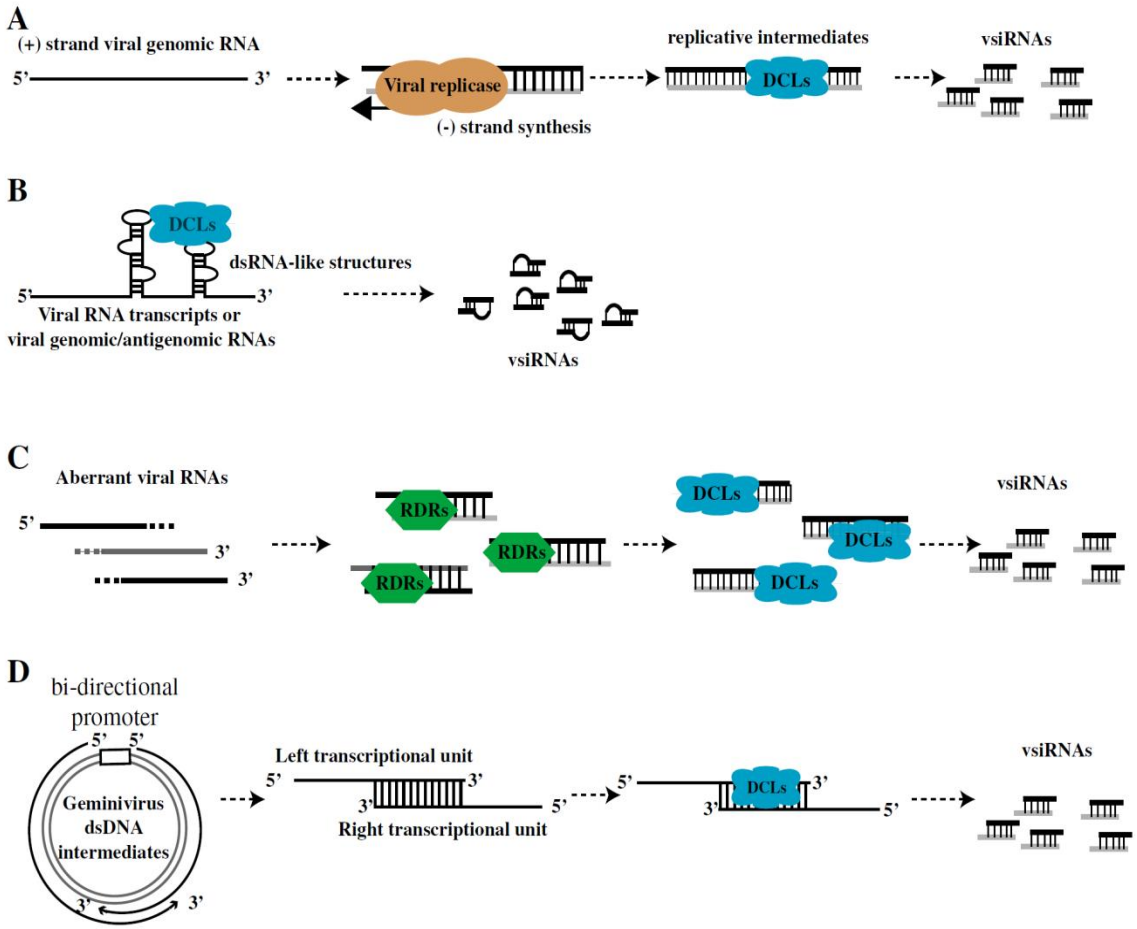


Figure 1. 4 A model depicting formation of dsRNA intermediates for siRNA induced gene silencing of homologous mRNA . **(a)** dsRNA generated from complementary viral RNA strands. **(b)** Imperfect dsRNA-like structures generated from secondary RNA structures. **(c)** dsRNA generated from aberrant RNA with homologous regions folding on itself or those formed by RDR-mediated amplification forming. **(d)** Bidirectional promoter transcribed 3' overlapping RNA transcripts forming perfectly paired dsRNA molecules which can become RDR templates (Shimura & Pantaleo, 2011).

1.6 Viral RNA silencing suppressors

DNA and RNA viruses have evolved suppressor proteins that bind the siRNA duplex or interfere with plant silencing at different stages of the PTGS pathway (initiation, maintenance and systemic signalling). Evasion and silencing of PTGS then enables the virus to replicate and eventually spread systemically resulting in infection (Chapman *et al.*, 2004; Pumplin & Voinnet, 2013). Viral RNA silencing suppressors (VRSS) of different virus families share no similarities suggesting different origins (Senshu *et al.*, 2011). Most VRSS were previously identified as pathogenicity factors and symptom determinants prior to being assigned a secondary function as VRSS (Shimura & Pantaleo, 2011). Some of the earlier work on VRSS identification and confirmation studies were done on potyvirus proteinease HC-Pro (Anandalakshmi *et al.*, 1998; Brigneti *et al.*, 1998; Pruss *et al.*, 1997). This RSS was implicated in interfering with initiation and maintenance of RNA silencing by inhibiting dsRNA processing by DICER and unwinding of the dsRNA duplex (Anandalakshmi *et al.*, 1998). Early studies were also on *Cucumber mosaic virus* (CMV) 2b protein. This VRSS was implicated in prevention of systemic spread of silencing signal (Brigneti *et al.*, 1998). VRSS was also shown to have small dsRNA binding ability (Goto *et al.*, 2007). More recently the mode of silencing suppression has been attributed to interaction and inhibition of the AGO protein (González *et al.*, 2010). Geminiviruses AC2, AC4, V2 and βC1 associated proteins have also been identified as PTGS suppressors. Complexities associated with VSR disruptions in RNA silencing pathways are starting to become more apparent and further investigations are required (Burgyán & Havelda, 2011).

1.6.1 AC2 ORF encoded PTGS suppressor

Voinnet *et al.*, 1999 performed experiments on *N. benthamiana* exhibiting PTGS of the GFP transgene. The plant was infected with a variety of viruses leading to a disruption if GFP PTGS. However the degree of PTGS suppression was found to be virus specific. ACMV infection led to GFP PTGS suppression. Results of previous studies led to the idea of inoculating GFP expressing transgenic *N. benthamiana* exhibiting PTGS with an AC2-PVX expressing vector. More severe necrotic symptoms than those produced by the wild type PVX were observed and this gave an indication that AC2 was a host suppressor. ACMV AC2 was therefore implicated as a PTGS suppressor. To further test that AC2 was indeed a silencing suppressor, PVX vector expressing a single AC2 point mutation (PVX-mAC2) was also used. Unlike the AC2-PVX

vector PVX-mAC2 didn't produce severe symptoms and didn't result in GFP suppression. From the results it was concluded that AC2 was indeed a suppressor of PTGS.

The mechanism of AC2 in PTGS was later suggested to be via transcriptional regulation of host genes involved in negatively regulating the RNA silencing mechanism (Bisaro, 2006). AC2 was shown to have the ability to reverse RNA silencing (Trinks *et al.,* 2005). GFP expressing *N. benthamiana* plants were bombarded with a GFP and AC2 expressing plasmid. Results showed that systemic silencing spread was totally inhibited. This was through AC2-mediated transcriptional activation of host genes that regulate silencing. This was termed transcription-dependent suppression. AC2 seems to also work in a transcription-independent manner by interacting and inactivating adenosine kinase (ADK) which is required in the methylation silencing pathway (Wang *et al*., 2005; Yang *et al*., 2007).

Synergistic relationships occurring in mixed virus infections are known to cause severe disease symptoms (Pruss *et al.*, 1997) but mechanism remained unclear until studies suggested involvement of PTGS suppression (Savenkov & Valkonen, 2001). RNA suppression ability of AC2 was also studied by transient expression leaf assays using *N. benthamiana* agro-infiltrated with a plant transformation vector harbouring EACMV AC2 followed by agro-infection of plant with Cameroon strain ACMV (ACMV-[CM]). An 8 fold accumulation of ACMV-[CM] DNA-A was observed as compared to infections with ACMV-[CM] alone (Vanitharani *et al.,* 2004). Vanitharani *et al*. (2004) also demonstrated a synergistic relationship between ssRNA binding AC4 and AC2 that results in exacerbated disease symptoms.

1.6.2 AC4 ORF encoded PTGS suppressor

The AC4 gene lies entirely within the Rep encoding region and is reported to be a PTGS suppressor and a disease and viral invasiveness enhancer. PTGS suppression by AC4 was also reported to be virus specific (Vanitharani *et al.,* 2004). One of the experiments performed was a transient assay in GFP transgenic *N. benthamiana*. The suppression activity of AC4 from four different CBVs was tested. Two of the tested AC4 proteins were from ACMV-[CM] and *Sri Lankan cassava mosaic virus* and both showed PTGS suppressor activity with increased inhibition of GFP-specific siRNAs. From their extensive studies they were able to categorise

ACMV-[CM] AC4 and EACMCV AC2 as strong PTGS suppressors and ACMV-[CM] AC2 and EACMCV AC4 as week PTGS suppressors. This study provided evidence that similar proteins encoded by different virus species can and do exhibit different silencing suppressor activities.

Chellappan *et al*. (2005) reported that AC4 from ACMV-[CM] but not EACMCV is associated with developmental defects when expressed in *Arabidopsis* though disruption of miRNA pathways. Plants expressing AC4 from ACMV-[CM] appeared stunted and had reduced reproductive tissues. Reduced levels of the most abundant *Arabidposis* leaf miRNA, miR159 were also reported. This suggested that the mature miR159 was inactivated resulting in low miR159 detection levels which therefore caused an over-accumulation of the normal mRNA target producing the developmental defects (Chellappan *et al.,* 2005). It is believed that miRNA pathway suppression is linked to AC4 binding to ss small RNA which then interrupts loading of ss small RNA into the RISC complex or disrupts already existing RISC complexes (Raja *et al.*, 2010).

1.6.3 V2 protein as an RNA silencing suppressor

V2 protein of Israeli isolate TYCLV-Is demonstrated RNA silencing suppressor ability in *N. benthamiana* plants infiltrated with A*grobacterium* containing V2 suppressor gene and A*grobacterium* carrying the RNA silencing initiator *GFP*-reporter gene (Zrachya *et al*., 2007). Elevated GFP expression and GFP protein accumulation in the infiltrated leaves was observed even though accumulation of *GFP*-specific siRNAs was present. Suppression or disruption of the RNA silencing pathway was then speculated to be to subsequent to dsRNA processing into *GFP*-specific siRNA molecules by Dicer unlike AC4 and AC2 which inhibit siRNA accumulation (Vanitharani *et al*., 2004). Co-infiltration with *Agrobacterium* carrying a mutant V2 suppressor gene did not inhibit RNA silencing. According to Glick *et al*. (2008) the suppressor activity of V2 is through inactivation of SGS3, this then disrupts the possible RNA silencing signal transport function of SGS3. SGS3 forms part of the host RNA silencing machine and is involved in RDR6-mediated amplification of the silencing signal (Jauvion *et al*., 2010; Mourrain *et al*., 2000). V2 RNA silencing suppressor activity has also been identified in V2 of *Ageratum yellow vein virus*-Indonesia and *Tomato yellow leaf curl China virus* (Sharma *et al*., 2010; Zhang *et al*., 2012).

1.6.4 Begomovirus associated Betasatellite βC1 encoded PTGS suppressor

Satellites are single stranded sub-viral agents found associated with plant viruses. The first DNA satellite associated with a DNA virus was reported by Dry *et al.* (1997). Satellites depend on co-infection with a helper virus for replication, movement and encapsidation but don't share any sequence similarity to their helper virus (Dry *et al.,* 1997). Satellites can also ameliorate symptoms caused by the helper virus. However, some satellites can also exacerbate helper virus disease symptoms (Roossinck *et al.,* 1992). These sub-viral agents have also been implicated in virus movement as shown by Saeed *et al.* (2007). Co-infection of *Tomato leaf curl New Delhi virus* (ToLCNDV) DNA-A with DNA βC1 associated with cotton leaf curl disease (CLCuD) resulted in systemic infection. However co-infection of DNA-A with a disrupted DNA βC1 did not cause systemic infection. This proved that the movement function of the bipartite begomovirus DNA-B required for systemic infection was replaced by βC1 encoded protein

Betasatellite DNA βC1 encoded protein has been shown to be a VRSS (Amin *et al.,* 2011; Eini *et al.,* 2012; Li *et al.,* 2014). It was suggested that DNA βC1 encoded protein has a strong affinity to dsRNA and therefore interrupts or interferes with dsRNA processing by Dicer (Amin *et al.,* 2011). A decrease in *Tomato leaf curl virus* (ToLCV) siRNA levels and an increase in ToLCV viral load was reported after co-infection of *Cotton leaf curl Multan virus* (CLCuMV) βC1 encoded protein with the helper ToLCV (Eini *et al.,* 2012). However the ability to suppress PTGS has not yet been clearly elucidated.

Mechanism of PTGS suppression by DNA βC1 encoded was suggested to be linked to the interaction of the protein with other plant host effectors that are involved in the RNA silencing pathway. The 1st report of calmodulin-like protein, a cellular component, as an endogenous suppressor of PTGS, was reported by Anandalakshmi, 2000. Developmental abnormalities were observed in calmodulin-like protein (*Nbrgs-CaM*) over-expressing transgenic lines. More recently, Li *et al.,* 2014 showed that *N. benthamiana Nbrgs-CaM* could be unregulated by *Tomato yellow leaf curl China* (TYLCCNV) DNA βC1 encoded protein. GFP expressing *N. benthamiana* were infiltrated with sense and IR-mediated constructs targeting GFP and with calmodulin-like protein (*Nbrgs-CaM*) and βC1. Both *Nbrgs-CaM* and βC1 failed to suppress GFP silencing in IR-mediated PTGS but GFP silencing was observed by both in S-PTGS. These

results that *Nbrgs-CaM* and βC1 disrupts process involved upstream dsRNA generation (Li *et al*., 2014). Li *et al.,* 2014, demonstrated with further experiments using a RDR6-deficient *N. benthamiana* plants that the observed PTGS was through the repression of *N. benthamiana* RDR6 (*NbRDR6*) mRNA levels. RDR6 has been shown to be involved in the biogenesis of secondary siRNA which are required in the PTGS pathway (Cuperus *et al.,* 2011; Rajeswaran and Pooggin 2012).

1.7 Application of RNA silencing to combat plant disease

RNA silencing technology exploiting/improving the innate immune response is currently been used to produce resistant transgenic plants (Duan *et al.,* 2012). This method involves the expression of pathogen-derived genes in transgenic plants. The successful use of pathogen-derived resistance (PDR) technology can be traced as early as 1986. Abel *et al.* (1986) reported a delay in *Tomato mosaic virus* (TMV) induced symptoms in transgenic tobacco expressing TMV coat protein. Over the years PDR technology has evolved from the expression of antisense or sense pathogen-derived RNA transcripts to the currently used technology that involves the simultaneous expression of sense and antisense pathogen-derived RNA transcripts.

1.7.1 Sense and antisense RNA silencing constructs

The first reports of antisense and sense RNA silencing strategies were in bacteria and animal systems and then later in plants (Fire *et al.,* 1991; Takayama 1990). Ecker and Davis (1986) evaluated and compared antisense and sense target gene suppression efficiency in plant protoplasts. Bacterial chloramphenicol acetyltransferase gene was introduced in the sense and antisense orientation. Chloramphenicol acetyltransferase assays showed that antisense strategy to be more effective than sense strategy at blocking target gene expression (Ecker & Davis, 1986). Fire *et al.,* 1991, antisense strategy was reported to be better at inhibiting gene expression than the sense strategy. Similarly, Smith *et al.,* 1990, transformed tomato plants with the polygalacturonase (PG) gene in the antisense orientation and later that year in the sense orientation. However they reported sense technology and antisense technology to be comparable at PG protein reduction and activity (Smith *et al.,* 1990). Findings by Fire *et al.* (1998), that dsRNA itself is a strong inducer of silencing, inspired further later experiments on simultaneous expression of sense and antisense transcripts by Waterhouse *et al.*, 1998.

1.7.2 RNA silencing hairpin constructs

Waterhouse *et al.* (1998) pioneered the simultaneous expression of sense and antisense RNA transcripts in plants. They transformed *N. benthamiana* plants with the NIa-Protease (Pro) gene of potato virus Y (PVY). They reported enhanced and higher resistance to PVY in up to 55% of transgenic *N. benthamiana* simultaneously expressing antisense and sense Pro transcripts than in (less than 15%) transgenic *N. benthamiana* expressing either the sense or the antisense Pro transcripts. Current technology of designing hairpin RNA silencing constructs is derived from findings of Waterhouse *et al.* (1998). These inverted repeat (IR) transgenes form the basis of experimental PTGS in plant systems and has been termed IR-PTGS (Chuang and Meyerowitz 2000; Wesley *et al.,* 2001).

Inverted repeat sequences

Eichman *et al.,* 2000 however showed through crystallization studies that IR sequences can form cruciform structures which are similar in structure to Holliday junctions. These structures were named after Robin Holliday (Holliday *et al.,* 1985). They form as a result of genetic recombination between homologous regions of DNA (Duckett *et al.,* 1988). These four-way junctions can adopt either an open extended-X or more compact stacked X conformation as they are thermodynamically favoured than the linear form (**fig. 1.5**) (Eichman *et al.,* 2000).

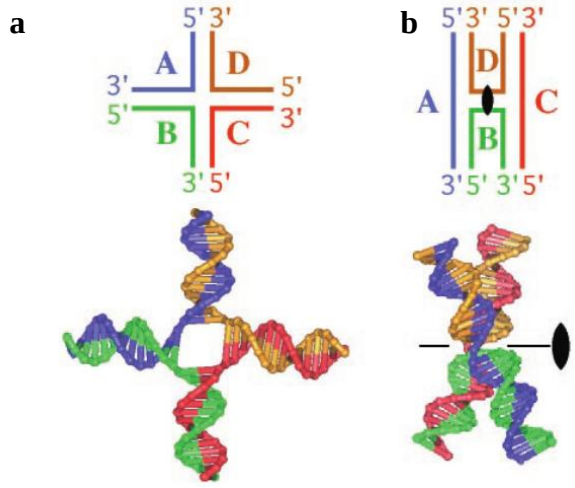


Figure 1. 5 Different 4-way junctions that can be formed by IR sequences; **(a)** Open extended-X conformation and **(b)** compact stacked conformation (Eichman *et al.,* 2000).

These secondary structures associated with palindromes, such as those seen in IR sequences, make cloning, polymerase chain reaction (PCR) amplification and DNA sequencing processes difficult (Bao & Cagan, 2006; Harmse, 2007; Wyman *et al*., 1985). However it was shown that this can be circumvented by designing constructs containing a significantly large spacer sequence between the sense and anti-sense arms of the IR (Smith *et al.,* 2000). Smith *et al.*, (2000) showed that such constructs (intron-spliced RNA hairpin) can induce PTGS with almost 100% efficiency compared to co-suppression and antisense strategy (70% efficiency). The high efficiency has been suggested to be due to the intron aiding alignment of complementary arms of the hairpin, favouring RNA hybridisation, and therefore correct dsRNA formation (Smith *et al.,* 2000; Wesley *et al.,* 2001). Vectors aiding the production of IR constructs with enhanced stability in bacterial and plant cells were designed and introduced by Helliwell and Waterhouse (2003). These vectors; pHANNIBAL, pKANNIBAL and pHELLSGATE, were designed to contain a 700bp *Pdk* intron gene sequence from *Flaveria* between the sense and the anti-sense arm, a *Cauliflower mosaic virus* (CaMV) 35S promoter and an octopine synthase (OCS) terminator based on the pART7 system. However according to Heilersig *et al.,* 2006 an intron whether spliceable or not doesn't seem to enhance PTGS. They reported no noticeable increase in silencing efficiency.

Mutated sense-arm hairpin RNA silencing constructs

Taylor *et al.,* 2012c circumvented the formation of cruciforms by designing hairpin constructs containing several mutations on the sense-arm therefore making the hairpin sense-arm less complementary to the anti-sense arm. This destabilises the DNA secondary structure without destabilising the RNA secondary structure or compromising folding of the RNA hairpin or silencing ability and efficiency of siRNAs generation (Arbuthnot *et al.,* 2010; Taylor *et al.,* 2012c). Cytosine to thymine mutations were introduced using sodium bisulfite (chemical mutagen) which specifically deaminates cytosine without affecting any of the other nitrogenous bases (Arbuthnot *et al.,* 2010; Taylor *et al.,* 2012c). Due to the enhanced stability of mismatched IR constructs observed by Taylor *et al.,* 2012c, mutated sense-arm hairpin RNA silencing constructs were designed and used for cassava cultivar cv.60444 friable embryogenic callus (FEC) transformation (genetic engineering of cassava discussed later). Exactly matched hairpins

using the Gateway-compatible vector such as pHellsgate (Helliwell & Waterhouse, 2003) were also designed.

1.7.3 Artificial miRNA constructs for virus resistance

miRNA were first identified by Lee *et al.,* (1993) and they were described as small non-coding gene regulating RNA molecules that are transcribed from their own genes or from introns. The use of artificial miRNA (amiRNA) constructs has recently become a popular PTGS engineering strategy used to confer virus resistance in plants. Resistance is conferred by targeting viral genes responsible for virus replication, transmission and other important functions in the virus. This technology was first applied in animal cells by Zeng *et al*. (2002) and later by (Parizotto *et al*. (2004) in Arabidopsis (Schwab *et al.,* 2006). More recently this technology has been reported to confer resistance against a bipartite begomovirus. The amiRNA was designed to target the pre-coat and coat protein of *Tomato leaf curl virus* (ToLCV). A 25.3% reduction in ToLCV viral load was observed (Vu *et al.*, 2013).

The mature artificial miRNA consists of a miRNA:miRNA* duplex with a stem-loop. This 21nt duplex is derived from the processing of a naturally occurring 70-80nt precursor miRNA transcript, known as a pre-miRNA (Cuperus *et al.,* 2011; Ketting *et al.,* 2001). The pre-miRNA is processed from a longer transcript known as a primary miRNA (pri-miRNA) (Han *et al.,* 2004). The short 21-25nt sequence length of artificial miRNA is advantageous over the use of siRNA derived from long hairpin sequences, as this reduces the possible chance of recombination between the introduced transgenic sequence and the infecting virus (Ali *et al.,* 2013).

1.8 hpRNA construct design requirements

1.8.1 Sequence length

Several studies have focused on determining the minimum transgene length required for PTGS. This is still however unclear. GFP-transgenic *N. benthamiana* expressing a transgene sequence as short as 23nt were able to provide silencing but efficiency dramatically increased with an increase in transgene length (Thomas *et al.,* 2001). Sequences of less than 16 nt were reported ineffective and showed chimeric silencing in the early stages of infection. Similar studies by

Sijen *et al.* (1996) showed that 60nt was required to promote PTGS. In *N benthamiana* expressing partial nucleocapsid sequence of *Tomato spotted wilt virus Tospovirus*, a minimum transgene length of 236-387 bp was required to induce RNA silencing. However it was found that when the sequence is fused to a non-target gene then a 59-110 bp sequence is still sufficient (Pang *et al.,* 1997). Reasons suggested for the inability of small fragments to promote silencing was inefficient transcription in the nucleus, inefficient processing and less transcript stability in the cytoplasm. These studies showed that length is as important as sequence homology.

Tuschl *et al.,* 1999 performed *in vitro* gene expression studies using *Drosophila* embryo lysates, targeting the luciferase genes and a 75-80% reduction in target mRNA levels with transgene lengths of between 505 – 957 nt was reported. Transgene length of 149 nt was reported to cause a 50% mRNA reduction while 49 nt transgene length was no more effective than buffer controls. However very long transgenes are sometimes not favourable as large siRNAs populations can be produced, and this may seem like an effective strategy but the chance of non-target endogenous plant gene silencing is increased. Therefore it is advisable to produce small populations of highly effective siRNAs to reduce the probability of non-target gene silencing (Galun, 2005).

1.8.2 Sequence complementarity requirements

Length of transgene has been shown to have an effect on RNA silencing efficiency however Mueller *et al.,* 1995 demonstrated the pool of siRNAs derived from the transgene are required to have perfect sequence specificity to target mRNA. PVX expressing *N. benthamiana* was reported to be only effective against PVX and was ineffective against other strains that differed in sequence homology by as little as 22% (Mueller *et al.,* 1995). It is generally believed that in plants, amiRNA and mRNA complementarity is required while in animals, perfect complementarity between the amiRNA and target mRNA is not as essential (Bartel *et al.,* 2004; Montanucci *et al.,* 2008; Rajeswaran and Pooggin 2012). *In planta* experiments by Mallory *et al.* (2004), showed that mismatched within the miR165 complementary site resulted in dramatic *Arabidopsis* leaf developmental effects.

1.8.3 Other important design requirements

There are other set guidelines recommended to helps increase the RNA silencing potency exerted by these short RNA molecules, and siRNA and amiRNA do share common recommended design features. The initial suggestion was that a high GC content was essential; however this was shown to be incorrect. Holen *et al.* (2002) showed there to be no correlation between siRNA potency and high GC content. Instead a low GC content is more favourable (Huesken *et al.*, 2005; Ui-Tei *et al.*, 2004). Other guidelines include: (i) a stretch of adenosine nucleotides at preceding the endonuclease cleavage site at position 10 of the siRNA or amiRNA duplex; (ii) the presence of an AU sequence at the 5' end of the antisense strand of the duplex; and (iii) a GC sequence at the 5' end of the sense strand of the duplex (strand bias discussed above) (Huesken *et al.*, 2005).

1.9 Defective interfering molecule-mediated resistance

Virus resistance can also be mediated by other nucleic acid-based methods other than the expression of virus ORF sequences in either the sense, antisense or sense:antisense (hairpin) orientations. Defective interfering (DI) molecule-mediated resistance is a PDR mechanism that involves the expression of defective viral DNA sequences. These defective sequences are derived from small subgenomic DNA (549-1555 nt) referred to as DI-DNA (Stanley & Townsend, 1985). DI-DNA are found associated with helper full length geminiviruses (Patil *et al.*, 2007; Stanley and Frischmuth 1990). DIs interfere with helper virus replication, production and mobilisation and reduce disease symptoms of infected plants and hence referred to as DI molecules (Stanley & Frischmuth, 1990). DI-DNA lack a complete set of genes required to complete an infectious cycle and therefore require their helper virus to complete replication (Stanley *et al.*, 1997). *N. benthamiana* transformed with a genomic sequence of a DI molecule isolated from an ACMV Kenya isolate, showed symptom amelioration after infection with an ACMV Nigeria isolate and a Kenya isolate. Infection of non-transgenic *N. benthamiana* showed no symptom amelioration (Stanley & Frischmuth, 1990).

1.10 Protein-mediated resistance

This is another form of pathogen-derived resistance (PDR) but unlike nucleic acid-mediated resistance (RNA silencing) this uses protein expression to confer resistance. This method offers resistance to a broader range of viruses however resistance is not as effective as RNA silencing which is highly virus specific and offers high virus resistance (discussed above) (Duan *et al.*, 2012; Nomura *et al.*, 2004). Protein-mediated resistance can be achieved by targeting a number of virus proteins.

1.10.1 Coat protein-mediated resistance

The first report of this was in 1986 in *Tobacco mosaic virus* (TMV) coat protein (CP) expressing *N. benthamiana* plants. Some of the transgenic seedlings inoculated with TMV showed no symptoms while others showed a delay in symptoms. It was proposed that the expressed CP exerted the observed results by interfering with virus disassembly and therefore disabling the virus ability to infect, replicate and systemically spread (Abel *et al.*, 1986). CP-mediated resistance provides broad resistance and resistance against closely related virus species (Beachy *et al.*, 1990; Lomonossoff 1995).

1.10.2 Rep-mediated resistance

This resistance mechanism was first observed in transgenic *Nicotiana tabacum* expressing a 54 kDa component of TMV replicase gene. Upon infection with TMV, plants showed complete virus resistance (Golemboski *et al.*, 1990). However, this resistance mechanism was found to be strain-specific. The exact mode of action was remained unclear as all attempts to extract protein were unsuccessful. Later, Carr *et al.* (1992) suggested that the resistance observed was protein-mediated. They suggested resistance was as a result of 54 kDa protein synthesis and assembly being favoured over synthesis and assembly of the complete 183 kDA replicase of the infecting TMV. Tenllado *et al*. 1995, transformed *N. benthamiana* with a component of *Pepper mild mottle virus* (PMMV) replicase gene. They reported similar results but reported that the observed resistance phenotype was both protein-mediated and transgene RNA-medaited.

Transgenic expression of truncated C1 Rep-associated protein (Rep) of *Tomato yellow leaf curl Sardinia virus* (TYLCSV) resulted in resistance phenotype (Lucioli *et al.*, 2003). Expression of

this protein interfered with challenging (TYLCSV) Rep by inhibiting C1 protein oligomerisation and therefore affecting TYLCSV replication (Lucioli *et al.,* 2003). Oligomersation is required for binding and cleavage of ssDNA at the nanonucleotide sequence found in the common region of both DNA-A and B (Orozco *et al.,* 1997). Once ssDNA has been nicked, then virus replication occurs (Orozco *et al.,* 1997). Once again, resistance was reported to be protein mediated (through oligomerisation inhibition) and nucleic acid-mediated (through PTGS). However, resistance was also reported to be unstable resistance.

1.10.3 Movement protein mediated resistance

The ability of virus to efficiently move locally and systemically plays a role in its pathogenicity and virulence (Ingram *et al.,* 1995; Ward *et al.,* 1997). The movement protein (MP) is responsible for these functions (Ward *et al.,* 1997). A reduction in symptoms and systemic virus levels was seen in transgenic tobacco expressing a gene encoding a defective TMV movement protein (MP) (Cooper *et al.,* 1995). Transgenic tobacco expressing a gene encoding a fully functional TMV MP showed high virus levels and increased symptoms. This showed that the mechanism observed was MP mediated (Cooper *et al.,* 1995).

A reduction or disturbance in virus movement was also observed in tobacco plants expressing a mutated or partially inactive MP sequence (Seppänen *et al.,* 1997). It was suggested that the observed reduction was as a result of non-functional MP competing with infecting virus MP and therefore inhibiting or reducing virus movement in the transgenic plant (Seppänen *et al.,* 1997). This approach offers a broader level of resistance to a number of viruses than PTGS, which is very sequence specific and therefore offers a narrower virus resistance. TMV MP transgenic plants showed tolerance not only to TMV but also to several distantly related and unrelated viruses (Cooper *et al.,* 1995; Seppänen *et al.,* 1997).

1.11 Genetic engineering

Successful production of transgenic plants involves two important processes; development of efficient transformation systems and regeneration procedures (Christou, 1992). Genetic engineering of plants was first reported in *N.tabacum* (Herrera-Estrella *et al.,* 1983). Other earlier reports were in tobacco and tomato (Mccormick *et al.,* 1986; Paszkowski *et al.,* 1984).

Later with the improvement of transformation technology, successes spread to maize, rice, wheat and barley, cassava and other crops (Blechl *et al.*, 1998; Bull *et al.*, 2009; He *et al.*, 2000; Li *et al.*, 1996; Lyznik *et al.*, 1989; Wan and Lemaux 1994). Varying degrees of plant transformation successes have been achieved using transformation systems such as electroporation, particle bombardment and *Agrobacterium tumefaciens* (Christou, 1992). A combination of the correct transformation system, most amenable transformation tissue and reproducible regeneration systems greatly increase transformation efficiencies.

1.11.1 Electroporation

Electroporation of susprension cells involves the use of 2 electrodes passing an electrical current through the suspension and the target DNA (Neumann *et al.,* 1982). Transient pores in the plasma membrane are created allowing the target DNA to enter. The electrodes are then also used to seal the pores, enabling cells to be regenerated (Neumann *et al.*, 1982; Sukharev *et al.*, 1992).

Electroporation of plants usually involves protoplasts; however this has also been successfully achieved in somatic embryo tissue. One of the first successful protoplast electroproration experiments was done in tobacco. Protoplasts were transformed with the aminoglycoside phosphotransferase II gene and successfully regenerated into plantlets (Paszkowski *et al.,* 1984). However the limitations to this method were the low stable transformation efficiencies and difficulty to regenerate plantlets. Prior to 1995, there were only reports of transient gene expression in cassava somatic embryos using electroporation (Luong *et al.*, 1995). Luong and colleagues reported transient expression of β- glucuronidase (GUS) in 75% cassava somatic embryos. Stable transformation of cassava was only later achieved using particle bombardment (Raemakers *et al*., 1997).

1.11.2 Particle bombardment

Particle bombardment also involves the introduction of target DNA into cells, however using metal particles such as gold and tungsten. The DNA coated particles are released at high pressure into plant cells and the target DNA is incorporated into the chromosomal DNA (Christou, 1992).

This transformation approach is considered to be slightly better than electroporation as it allows introduction of target DNA into intact tissue and causes minimal damage to plant tissue and therefore improves the recovery and regeneration of transformed cells (Southgate *et al.,* 1998). Transformation efficiency can be variable depending on species and tissue to be transformed and the efficiency is often lower than that achieved when using *Agrobacterium tumefaciens*-mediated transformation method (Dai *et al.*, 2001). However, unlike *A. tumefaciens*-mediated transformation, bombardment is a universal DNA delivery method and does not depend on crop specificity and host range (Liu *et al.*, 2011; Zheng *et al.*, 1996). Schopke *et al*. (1997) achieved stable *GUS* gene expression in cassava using particle bombardment however only 7 positive transgenic lines were obtained.

Particle bombardment is less host-crop specific than *Agrobacterium*-mediated transformation but does however result in multiple transgene insertions in 90% of reported cases as compared to the lower 50% observed when using *Agrobacterium tumefaciens*-mediated transformation method (Dai *et al.*, 2001). Multiple insertions are undesirable as they can result in transgene silencing and genetic rearrangements (Gelvin 2003a; Tang *et al.*, 1999).

1.11.3 *Agrobacterium tumefaciens*-mediated transformation

Agrobacterium is a gram negative bacterium *A. tumefaciens* (Heberlein *et al.*, 1967). This bacterium contains a tumour inducing (Ti) plasmid (Zaenen *et al.,* 1974). Present are oncogenes which are housed within the transferred (T) DNA (region of the Ti plasmid that integrates into the plant genome) (Chilton *et al.*, 1977). For genetic engineering purposes, these oncogenes are deleted and replaced with foreign genes of interest (Gelvin, 2003a). The T-DNA region is flanked on either side by the left and right borders (25bp imperfect repeat sequences). Any DNA fragment that lies between these borders can be randomly integrated into the plant genome (Gelvin, 2003a). It's this natural ability to transfer genes into plant genomes that has been exploited in the development of transgenic monocotyledonous and dicotyledonous plants (Chen *et al.*, & Yu, 2014; Newell *et al.*, 2010). This method is still considered to be the most favourable transformation method for generating transgenic plants (Gelvin, 2003b). There are numerous reports of successes in cassava genetic engineering of using *A. tumefaciens*-mediated transformation of cassava friable embryogenic callus (FEC). Cassava transformation protocols

have been developed and optimised to make this less time consuming method and a more reliable and reproducible method with high transformation efficiencies (Bull *et al.*, 2009; Chetty *et al.*, 2013; Nyaboga *et al.*, 2013; Zainuddin *et al*., 2012).

1.12 Engineering geminivirus resistance

Great strides in engineering resistance to geminiviruses have been made over the past few decades. Very early attempts included the expression of non-viral protein involved in cell death upon viral infection and transactivation of viral proteins (Hong *et al*., 1997) to coat protein-mediated strategies (discussed above) (Jan *et al*., 2000) and to the more widely and still used RNA silencing-mediated resistance strategy (discussed above) (Ye *et al*., 2014). Previously these strategies were developed and tested in model plants such as *N. benthamiana* but these technologies have since been adopted into other crops and plant systems (Vanderschuren *et al.*, 2007). These strategies have attempted to solve limitations and challenges associated with traditional breeding for resistance. A major limitation to traditional breeding is the availability of naturally occurring geminivirus resistance genes in wildtype cultivars (Vanderschuren *et al*., 2007). Introgression of the available geminivirus resistance genes into farmer preferred cultivars through traditional breeding is also a huge challenge (Lapidot & Friedmann, 2002). Another limitation to traditional breeding for geminivirus resistance was the very variable and limited levels of resistance obtainable (Vanderschuren *et al*., 2007).

Genetic engineering for geminivirus resistance has been demonstrated in other plant systems such in tomato. Resistance to T*omato yellow leaf curl virus* (TYLCV) was reported in tomato plants expressing TYLCV *Rep* gene sequences (Yang *et al*., 2004). Similarly in maize, successful geminivirus resistance was reported in maize streak virus (MSV) resistant maize. This was reported as the first all-African produced MSV resistant maize (Shepherd *et al*., 2007). In gemivirus susceptible *Jatropha curcus*, resistance to Indian cassava mosaic virus (ICMV-Dha) was obtained through expression of hpRNAi constructs targeting ICMV-Dha DNA-A genes (Ye *et al*., 2014). Resistance levels were not only high, but were also reported to be durable and heritable. Resistance to ICMV Singaporean isolate, which shares 94.5% sequence homology to ICMV-Dha, was also reported (Ye *et al*., 2014). Lessons learnt and successful RNAi strategies

developed over the years in other crop systems and the development of efficient tissue culture systems have contributed to geminivirus resistance engineering in cassava.

1.13 Cassava genetic engineering

The major problems in cassava crop cultivation are yield-limiting diseases, such as cassava mosaic disease (CMD), caused by several geminiviruses (Varma & Malathi, 2003) (discussed above, section 1.2). Traditional plant breeding has to date been the only means of selecting for virus tolerant cassava (Lapidot & Friedmann, 2002). However this approach is difficult due to the highly heterozygous nature of this crop and the limited resistance gene available (Solomon-Blackburn & Barker, 2001). Furthermore, cassava's vegetative propagation results in increases of the disease through successive cycles of cultivation (Thresh *et al.*, 1994). Since no chemical control of virus diseases of plants is possible, one approach is via biotechnology, through genetic engineering (GM) of cassava to express virus resistance mechanisms such as RNA silencing (Thresh, 2003).

However lack of reproducible transformation and regeneration systems were previously a major concern in cassava transgenic research and development (Munyikwa *et al.*, 1998). Previously transformation efficiency depending on the transformation method used was very low (3-5%) and intensive and extended tissue culture periods were required (de Vetten *et al.*, 2003). However the technology transfer in cassava FEC induction, transformation and regeneration has made genetic engineering of different cassava cultivars relatively easier and faster with higher transformation efficiencies now achievable (Bull *et al.*, 2009; Chetty *et al.*, 2013; Nyaboga *et al.*, 2013).

The most practical explant for cassava transformation is still FEC and somatic cotyledons (Bull *et al.*, 2009). Insertion of the gene of interest in the explants can be achieved using 3 methods; electroporation particle bombardment and *A. tumefaciens*-mediated transformation (Bull *et al.*, 2009; Fromm *et al.*, 1985; Gonzalez *et al.*, 1998; Schopke *et al.*, 1997). *Agrobacterium tumefaciens*-mediated transformation is still the most efficient and reproducible method (Bull *et al.*, 2009). The method used in this research was *Agrobacterium tumefaciens*-mediated transformation of FECs.

Early RNAi experiments were in model plants such as *N. benthamiana* but efficient transformation and reproducible protocols have allowed RNAi technology transfer to cassava and other crops (Vanderschuren *et al.*, 2007). There have been several reports of successful cassava GE experiments over the years (Taylor *et al*., 2001; Taylor *et al*., 2012b; Vanderschuren *et al.*, 2009; Vanderschuren *et al*., 2007; Zhang *et al.*, 2000; Zhang *et al.*, 2005) and GE successes are even achievable in farmer preferred cultivars (Chetty *et al*., 2013; Nyaboga *et al*., 2013; Zainuddin *et al*., 2012). IR-PTGS derived geminivirus resistance in cassava was first demonstrated by Vanderschuren *et al.* (2009). They produced ACMV AC1 transgenic lines that were resistant and still managed to maintain the resistant phenotype even under high virus pressure and different methods of introducing infectious virus. Prior to this work, Vanderschuren *et al*. (2007) only managed to produce IR-PTGS expressing transgenic cassava lines showing reduced viral load, attenuated symptoms and recovery phenotype. These results were obtained in transgenic lines expressing ACMV CR containing the bidirectional promoter. Currently as it stands successes on cassava geminivirus transgenic research have demonstrated proof in the laboratory and greenhouses. There is no currently available data on geminivirus transgenic cassava confined field trial tests. However, according to Adenle *et al*. (2012), a two year field trial on geminivirus resistant transgenic cassava engineered by the cassava research group from Eidgenössische Technische Hochschule (ETH) Zürich is underway in Puerto Rico. Geminivirus resistant cassava confined field trials involving Danforth Center and ETH Zürich cassava research groups, are underway in Kenya and Uganda (Bailey *et al.*, 2014; Taylor *et al.*, 2012b).

Rationale and Motivation for the study

Cassava (*Manihot esculenta* Crantz) is a staple food and food security crop in sub-Saharan Africa and is cultivated by small resource-poor farmers. Cassava has many uses and application such as animal feeding, ethanol and biofuel production and in the textile and paper industry. Cassava is grown in the Mpumalanga, Limpopo and Kwa-Zulu Natal Provinces in South Africa (SA) by subsistence farmers and commercially in Mozambique and Swaziland for industrial starch. Cassava starch is imported from Thailand for the paper industry in SA, and there has been considerable recognition recently of cassavas' potential contribution to the bioeconomy in terms of agroprocessing, animal feed and bioethanol. Very recently, the Cassava Industry Association of Southern African (CIASA) was registered as an NPO with the Department of Social Welfare. The next step from there will be the registration with the dti (Department of Trade and Industry) SASS Fund and, together with the Agricultural Research Council and Technical Innovation Agency, funds will be committed for cassava germplasm trials for selection of suitable material for large scale commercialized farming development. However cassava mosaic disease (CMD), which is caused by cassava infecting begomoviruses (CBVs), results in devastating cassava crop yield losses in tropical countries where it is cultivated (Elegba *et al.*, 2013). While CMD is endemic to South Africa, no information is available on the actual yield losses. Several approaches have been developed and used to control CMD, including, breeding of natural virus resistant varieties and improved biotechnological strategies to decrease the huge losses experienced annually. Breeding for virus resistant cassava varieties is lengthy, slow and relatively difficult and the use of chemicals to control viruses is not possible. One approach that is effective in combating virus disease is genetic engineering (GE). GE can also be used for developing varieties with increased starch and product yield.

Pathogen-derived resistance (PDR) is a GE strategy that involves the use of virus-derived genes or genome fragments that interfere with a specific step during virus replication or movement. There are several PDR approaches that can be employed for developing transgenic plants; these include nucleic acid-mediated approach (expression of antisense and sense viral sequences and hairpins) and viral protein-mediated resistance mechanism. Cassava is highly recalcitrant to transformation and regeneration, but recently a more reproducible and efficient method of cassava GE, by *Agrobacterium*-mediated transformation of friable embryogenic callus (FEC),

was developed by optimized researchers at Eidgenössische Technische Hochschule (ETH) Zürich. Successful transformation requires efficient FEC induction, gene transfer method, plant regeneration procedures and extensive skills.

According to Bull *et al*. (2011), despite advancements in efficient cassava transformation protocols over the last 15 years by research institutes such as the Danforth Center and ETH Zürich. Technology transfer, development of technical skills and successful implementation on the African continent has been relatively slow. Establishment and implementation of cassava transformation technology on the continent will ensure high quality biotechnology research and training in institutions and universities. This will allow African scientists full control to adapt cassava based on the continent requirements.

RNA silencing could provide a strategy that offers a combination of specificity and the exploitation of a plant cellular pathway that has evolved naturally to combat disease. Combining RNA silencing and cassava transformation protocols available to engineer cassava expressing geminivirus-derived gene sequences provides an effective strategy for combating CMD.

General Objective

Pathogen-derived resistance (PDR) is a GE strategy that involves the use of virus-derived genes to interfere with a specific step during virus replication or movement. With regard to pathogen-derived strategies, several approaches have been taken for CBVs, and these include antisense and sense constructs, construct encoding intron-spliced RNAs and constructs encoding hairpin RNA structures i.e. inverted repeats (IR) which fold to produce dsRNA and hence induce siRNAs. These siRNAs target incoming viral transcripts and reduce infection. This research will test two different RNA hairpin structures for efficient RNA silencing induction, i.e mutated sense-arm hybrid RNA silencing hairpins and Gateway (non-mutated) RNA silencing hairpins. Mismatched haripins were designed in order to overcome the problem of cruciform structures or holliday junctions (Eichman *et al.*, 2000) and to stabilize the long IRs during cloning.

Studies in South Africa have shown that ACMV, SACMV and EACMV isolates exist (Berry and Rey 2001; Rey *et al*., 2012). Additionally, infections normally occur as single and also as mixed

infections therefore the aim of the study was to design mismatched and non-mismatched hairpin RNA silencing constructs that provide the most efficient siRNA production and virus knockdown against ACMV-[NG-Ogo], EACMV-UG2, SACMV and other cassava infecting geminivirus isolates. Furthermore, comparisons of RNA silencing efficiency between the mismatched and non-mismatched IR were undertaken.

General Aims

1. Design virus-derived hairpin RNA silencing constructs targeting ACMV, EACMV and SACMV. Constructs were designed using two different methods; using the mutated sense-arm method and the Gateway technology method.

2. Cultivar 60444 and landraceT200 FEC induction. *Agrobacterium*–mediated transformation of cv.60444 and T200 FEC with hpRNA constructs and regeneration of transgenic plantlets.

3. Evaluation of transgenic lines for ACMV and SACMV resistance

CHAPTER 2

CONSTRUCTION OF THE MUTATED SENSE-ARM HAIRPIN RNA SILENCING CONSTRUCTS AND GATEWAY RNA SILENCING CONSTRUCTS AGAINST AFRICAN CASSAVA MOSAIC VIRUS, EAST AFRICAN CASSAVA MOSAIC VIRUS AND SOUTH AFRICAN CASSAVA MOSAIC VIRUS

\

2.1 Introduction

RNAi strategy was first observed in petunia plants unexpectedly by Napoli *et al.* (1990) and over the years it has become a widely used method in PTGS for developing virus resistant transgenic crops and also for plant gene function studies. Self-complementary (IR or hairpin) constructs are considered to be more effective for RNAi strategy against viral pathogens than sense or antisense strategies as dsRNA is the actual (Wang *et al.*, 2008; Waterhouse *et al.*, 1998) RNAi trigger.

A spacer region is required between the IR for stability of the IR DNA in the bacteria and host plant. However in 2000, Smith *et al.*, observed that only 60% of plants transformed with spacer region containing constructs had a single transgene copy number and were virus resistant. When the spacer sequence was replaced with a functional intron that is spliced out during pre-mRNA processing and 100% of plants transformed with the spliceable intron showed increased silencing efficiency. Based on the findings by Smith *et al.,* (2000) Helliwell and Waterhouse *et al.,* 2003 then developed high throughput silencing vectors such as the pHannibal and pHellsgate. These vectors are designed with a functional PDK intron instead of the spacer sequence and facilitate rapid and simple construction of silencing construct. An increase in RNA silencing efficiency was observed in 100% plants transformed using these vectors. Helliwell and Waterhouse *et al.,* 2003 have developed a technology called the Gateway system that has reduced the number of cloning steps. They have designed vectors that allow PCR products containing specific primer sites on either end to recombine with pHellsgate vectors. Recombination occurs at appropriate vector sites allowing formation of the two arms of the hairpin in a single recombination reaction (Helliwell & Waterhouse, 2003).

Gateway technology is rapid, however a more desirable and improved method of construct design that eliminates the use of a very large intron and therefore the transfer of a very large T-DNA region during plant transformation has been adopted in our lab. This method is based on the knowledge that repeat sequences of DNA are prone to Holliday junction formation and hence the need for a spacer/intron to stabilize the DNA (Eichman *et al.,* 2000). DNA containing extensive regions of very close homology, such as IR DNA sequences has been known to form junctions known as helical junctions or Holliday intermediates (Duckett *et al.*, 1988). These structures are important in biological cells during genetic recombination events, rearrangements

and repair of double strand breaks in DNA. In naturally occurring biological systems these structures are resolved by enzymes. The IR form stable cruciform structures. Junctions then form in the arms of the cruciform (Lilley & Norman, 1999).

Therefore in designing IR DNA with a few mismatches we believe that the tendency of IR forming these stable cruciform structures will be circumvented. Mismatches reduce the long stretch of homologous sequence and therefore circumvent the formation of stable cruciform structures. Mismatches were introduced in the DNA sequence by exposing DNA to sodium bisulfite treatment. Sodium bisulfite treatment deaminates unmethylated cytosines to uracil (Shapiro *et al.*, 1970). The mutated strand is used in an amplification reaction resulting in the incorporation of a thyamine in the newly synthesised stand, hence C-T conversion.

In this study mutated sense-arm hairpin RNA silencing constructs **(section 2.2)** and Gateway silencing constructs **(section 2.3)** were designed to against ACMV and SACMV and the silencing efficiency compared between the two approaches. Additionally, mixed infections are a common occurrence in nature and hence stacked (chimeric/hybrid) constructs with the ability to target a variety of CBVs were designed. Stacked constructs were also designed to target two CBV ORF simultaneously. All constructs were transformed into cassava FEC T200 landrace and cv.60444 FEC (Chapter 3).

2.2 Specific Aims

The aim of this chapter was to design virus-derived hairpin RNA silencing constructs (MM1; MM2 and MM3) targeting ACMV, EACMV and SACMV. Constructs were designed using two different methods; using the mutated sense-arm method and the Gateway technology method. A mutated SACMV BC1 hpRNA construct previously tested in *N. benthamiana* (Taylor *et al*., 2012c; Rey *et al*., 2012) was included in the transformation and virus-challenge trials of cassava (chapters 3 and 4).

2.2.1 Construct mutated sense-arm hairpin RNA silencing constructs

MM1hp: Construct I (ACMV AC1/AC4 + EACMV AC1/AC4)

MM2hp: Construct II (ACMV AC1/AC4 + ACMV AC2/AC3)

MM3hp: Construct III (EACMV AC1/AC4 + EACMV AC2/AC3)

Steps for construction of mutated sense-arm hybrid RNA silencing hairpins

i. Target sequence amplification of selected regions.
ii. Fuse selected amplicon fragments to make the required hybrid combinations
iii. Sodium bisulfite treat the hybrid fragments required for the sense-arm of the IR construct
iv. Assemble the different IR constructs consisting of a mutated sense and unmodified antisense-arm.
v. Clone the mismatched IR constructs into pART7 expression vector.
vi. Clone the hairpin cassette constructs into plant transformation vector pCAMBIA 1305.1.
vii. Transform *Agrobacterium* LBA 4404 with the 4 mutated sense-arm hybrid RNA silencing hairpins.

2.2.2 Construct non-mismatched (Gateway) RNA silencing hairpin constructs

MM5hp: Construct V (ACMV AC1/AC4 + EACMV AC1/AC4)

MM6hp: Construct VI (ACMV AC1/AC4 + ACMV AC2/AC3)

MM7hp: Construct VII (EACMV AC1/AC4 + EACMV AC2/AC3)

MM8hp: Construct VIII (SACMV BC1)

Steps for Gateway RNA silencing hairpins

i. Target sequence amplification from hybrid sequences generated in **2.4.1.6**. Hybrid sequence PCR modification to incorporate *Xba*I and *Xho*I restricted sites

ii. Cloning of *Xba*I and *Xho*I containing amplicons into *Xba*I and *Xho*I restricted sites of pHellsgate 8

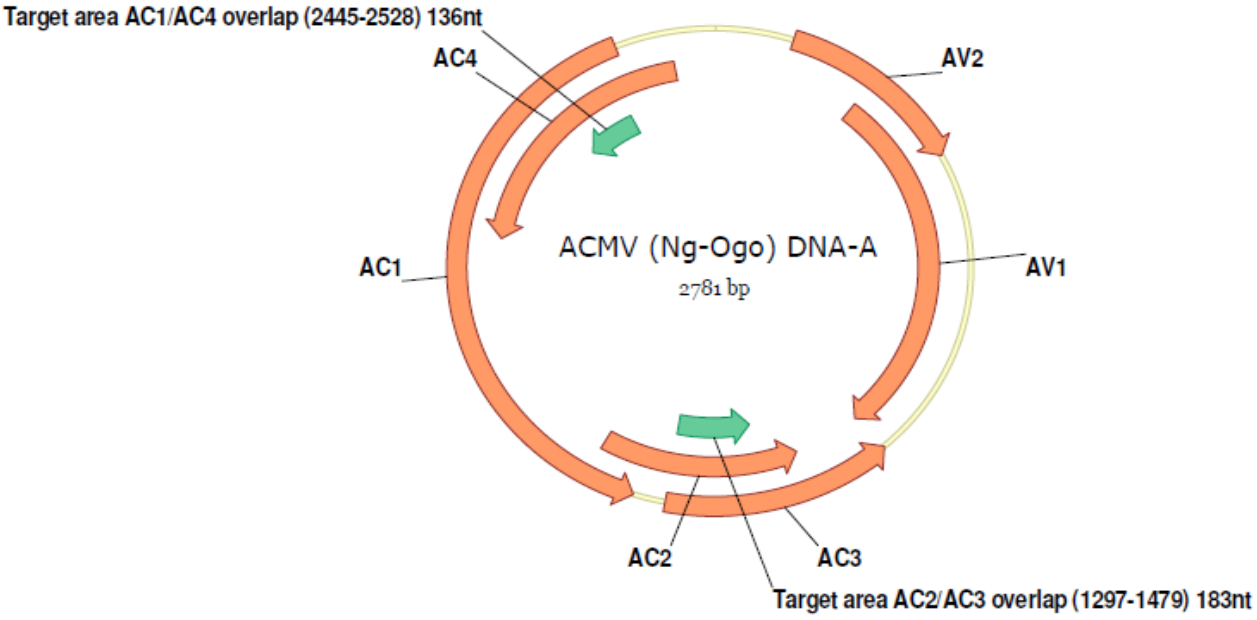
iii. *Not*I digest of pHellsgate 8 hairpin cassette (promoter, IR sequences separated by intron and terminator) and ligation into pCAMBIA1305.1

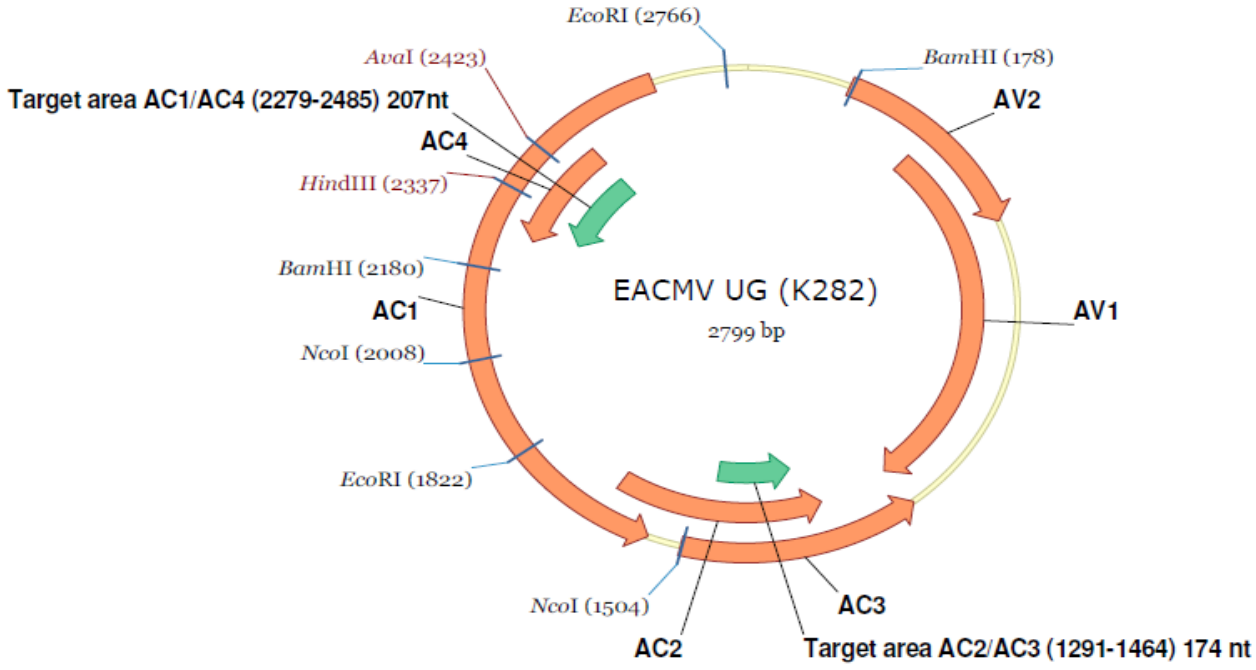
iv. Transformation of *Agrobacterium* LBA 4404 with the 4 different Gateway RNA silencing hairpin constructs

2.3 Methodology flow chart

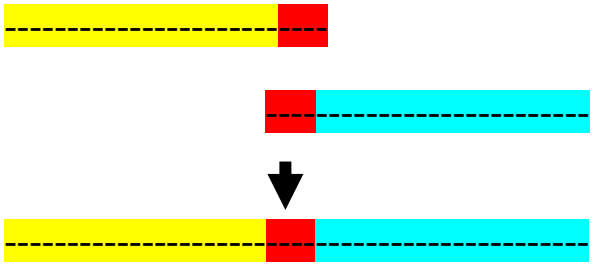
2.3.1 Target region selection and amplification

1) PCR amplification of target regions





2) PCR-mediated fusion of target regions to make hybrid



2.3.2 Mutated sense-arm hairpin RNA silencing constructs

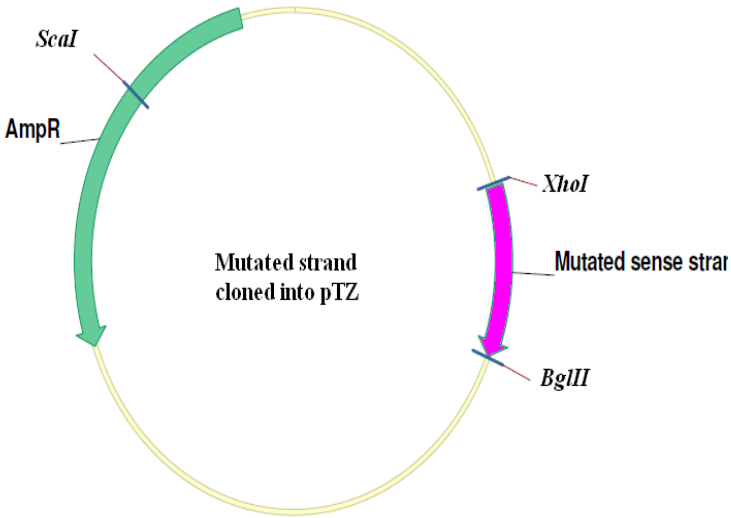
1) Mutation of hybrid strand using sodium bisulfite

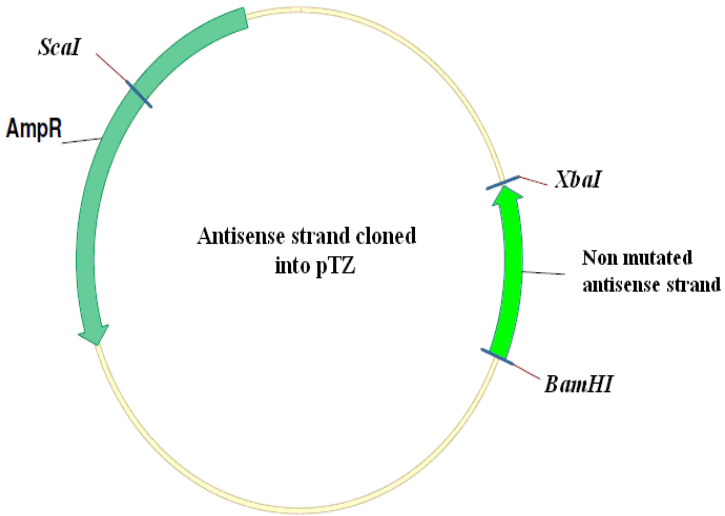
2) PCR amplification of mutated hybrid strand using modified primers that contain restriction enzymes to facilitate downstream cloning

2) PCR amplification of original (nonmutated) hybrid strand using original target region primers

***Xho*I** ---------- ***Bgl*II**

3) T/A cloning of fragments into pTZ57R/T and screening for orientation

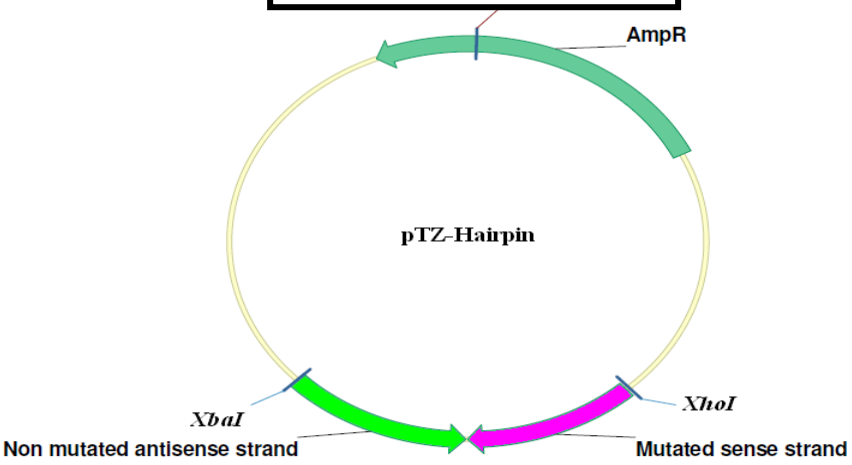




3) Digestion with *Sca*I and *Bgl*II

3) Digestion with *ScaI* and *BamHI*

4) Ligation of fragments



5) Sub-cloning into pART7 expression cassette and 9) Sub-cloning into pCambia 1305.1

2.3.3 Non-mismatched (Gateway) RNA silencing hairpin constructs

----

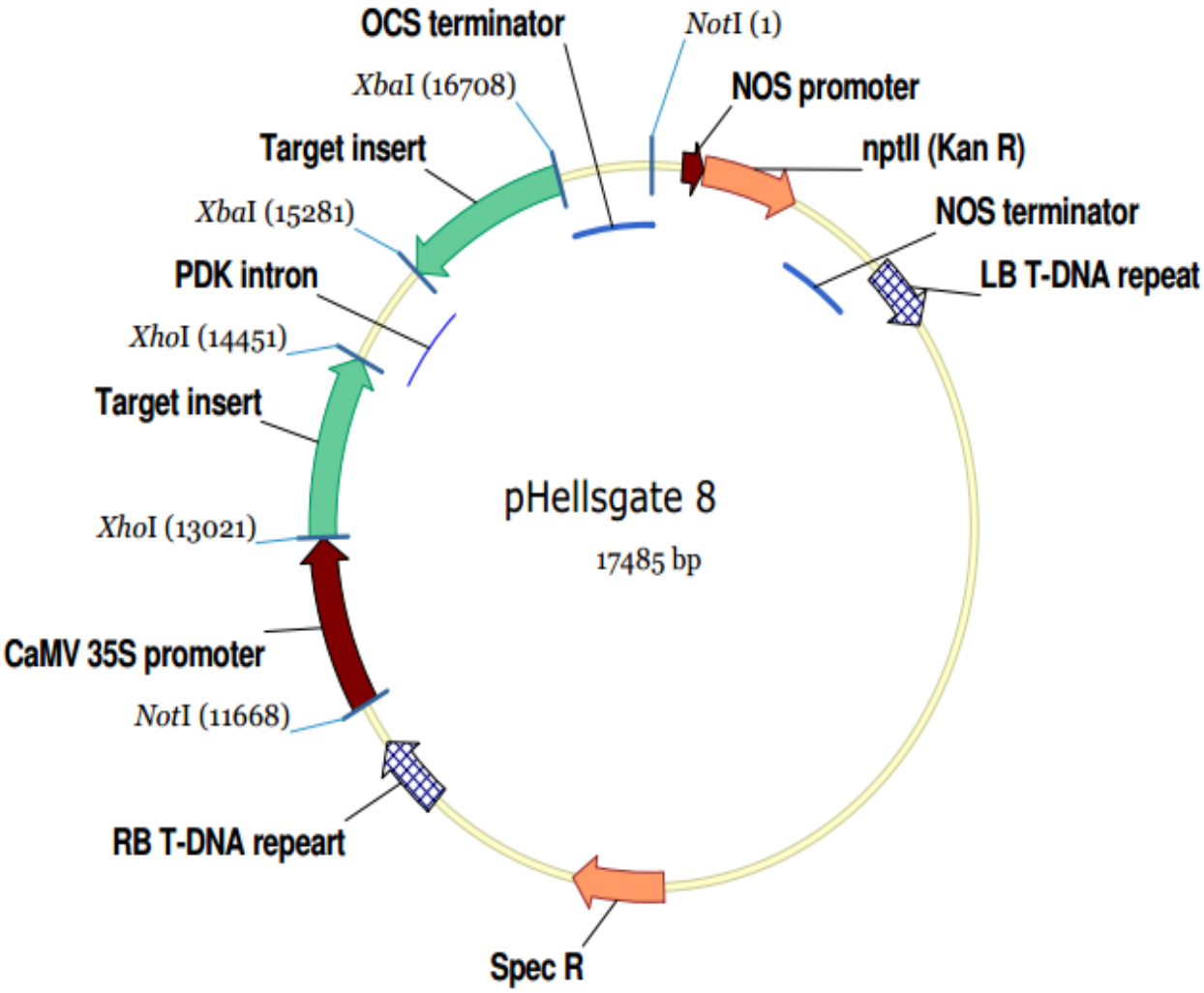
(hybrid fragment generated in section 2.3.1)

1) PCR incorporation of *Xho*I and *Xba*I restriction sites on either side of the target hybrid fragments

Xho*I**----------Xho*I**

Xba*I**----------Xba*I**

2) Ligation of *Xho*I and *Xba*I containing target amplicons into pHellsgate 8



3) Sub-cloning of pHellsgate 8 hairpin cassette into pCambia 1305.1

4) *A. tumerfaciens* LBA4404 transformation with pCambia 1305.1-pHellsgate hairpin constructs (nonmutated RNA silencing hairpin/Gateway constructs)

Figure 2. 1 Flow diagram of methodology followed to create the Mutated sense-arm (Mismatched constructs) and the Gateway (Non-mismatched) RNA silencing constructs.

2.4 Materials and Methods

2.4.1 Target selection, alignment and amplification

2.4.1.1 Sequence alignment and selection of CBV ORF targets for RNAi constructs

The paper by Fauquet *et al.* (2008) was used to obtain the accessions numbers of DNA-A of 8 ACMV isolates; ACMV-[Nigeria: Ogoroco: 1990] ([NG:Ogo:90]), ACMV-Cameroon: 1998 ([CM: 98), ACMV– [Nigeria] (NG), ACMV– [Cameroon-DO2:1998] (DO2:98), ACMV–[Cote d'Ivoire:1999] ([CI:99]), ACMV–[Kenya:844:1982] ([KE:844:82]), ACMV–[Uganda] (ACMV-[UG]), ACMV-Uganda: Mild: 1997) ([UGMld]:97) and ACMV–Uganda:Severe:1997 [UG:Svr:97]) and DNA-A of 6 EACMV isolates; EACMV–Uganda2 ([UG2]), EACMV–[Uganda:Mild2:1997] ([UG:Mld2:97]), EACMV–[Uganda:Severe2:1997] ([UG:Svr2:97]), EACMV– [Kenya:K2B:1996] ([[KE:K2B:96]), EACMV-Tanzania [Tanzania:YV] ([TZ:TV]) and East African mosaic Zanzibar virus ([EACMZV]).

The accession numbers of all the 14 CBV isolates were entered into the National Center for Biotechnological Information site (NCBI) to obtain the sequences. The selected CBV isolates are representatives of EACMV and ACMV diversity in Africa. Multiple sequence alignment was performed using Clustal X Multiple Sequence Alignment Program (version 1.8, 1999). ACMV ([NG:Ogo:90]), DNA-A and EACMV–[UG2] DNA-A were chosen as reference sequences (these are isolates that are available in the lab and therefore available for PCR amplification of desired target regions). The reference sequences were aligned with the DNA-A sequences of the other 7 ACMV and 5 of the EACMV to find regions with sequence similarity within the overlapping gene regions of AC1/AC4, AC2/AC3 for both ACMV and EACMV. Well conserved regions amongst ACMV and EACMV isolates were identified as potential targets against sites. Sequences of regions selected were entered into a program called siRNA Scan (Xu *et al*., 2006) to identify potential RNA silencing off-targets and to also identifying regions along the potential target sequence were efficient siRNAs will be produced.

Overlapping ORF fragments were computationally identified

- ACMV AC1/AC4 =136 bp
- ACMV AC2/AC3 =183 bp
- EACMV AC1/AC4 =207 bp
- EACMV AC2/AC3 =174 bp

2.4.1.2 Polymerase chain reaction amplification of identified overlapping ORF regions

Integrated DNA Technologies (IDT) programme was used to design primers to amplify the target overlapping ORF regions. Each of the 4 preliminary fragments were amplifies using High fidelity enzyme mix (Fermentas) using the following 4 sets of primers. For amplification of ACMV AC1/4, primer ACMV AC1/AC4F (forward) (5'-AAGTGAGGTTCCCCATTCTG-3') and ACMV AC1/AC4R (reverse) (5'-ATGTCTTTCTCACATACCCAAAGTG-3') combination was used. Primer set had an annealing temperature (Ta) of 60°C. For ACMV AC2/3, primer ACMV AC2/3F (5'-CTCCTTCCTCAGGTTGTGATTG-3') and ACMV AC2/3R (5'-CCAATCATGGATTTACGCACA-3') were used, Ta was 60°C. For EACMV AC1/4 the primers EACMV AC1/4R (5'-TTCTGGCATCGACTTGGAA-3') and EACMV AC1/4R (5'-ATGGGGTGCCTCATCTCC-3') were used, Ta was 56°C. For EACMV AC2/3, primers EACMV AC2/3F (5'- CCAGACCTTGAAGTTCAGAAAA-3') and EACMV AC2/3R (5'-AGGAATGGCGTTTTTACCTG-3') were used, Ta was 58°C. The reaction mixture contained 0.2µM of each primer, 5X High fidelity buffer, 2mM dNTPs, 1U High fidelity enzyme mix (creates both blunt ends and 3'-dA overhangs), 20ng of template DNA and nuclease free water to a final volume of 50µl. The polymerase chain reactions (PCR) were cycled in a thermal cycler (Bio-Rad) set at 94 °C for 2min and 35 cycles 94°C for 30s, appropriate Ta for 30s, primer extension at 72°C for 30s and final extension step of 72°C for 10min the appropriate cycling conditions. Amplification products were run in 1.2% agarose gel containing 10µg/ml ethidium bromide run in 1X TAE.

2.4.1.3 Cloning of PCR products

PCR amplicons were T/A cloned into pTZ57R/T vector (Fermentas). The ligation mixture contained 1X ligation buffer, 1U T4 DNA ligase (Fermentas), 4µl of PCR amplified fragment, 3µl pTZ57R/T vector and nuclease free water to a final volume of 30µl. Ligation control was also performed using the kit provided control PCR fragment. The ligation mixtures were incubated at 22°C for a minimum of 1 hour (h). Chemically treated competent *E.coli* DH5α cells stored at -70°C were thawed on ice. To this 15 µl of ligation mix was added to 100µl competent cells and incubated on ice for 15min. Cells were heat shocked at 42°C for 90s and then placed on ice for 3-5min. Transformation control was also performed using control vector with insert (Fermentas). Cells were spread onto LB agar plates containing 100µg/ml ampicillin (to select for transformants), 20mg/ml X-Gal and 0.1M IPTG, for blue/white colony screening. Plates were incubated at 37°C overnight. White colonies were selected and inoculated into 5ml LB broth containing 100µg/ml ampicillin and incubated at 37°C overnight shaking at 200 revolutions per minute (rpm).

2.4.1.4 Screening of clones

Plasmid DNA was extracted from the presumptive clones using the High pure plasmid miniprep kit (Roche) and quantified on the Nanodrop 1000 spectrophotometer (Nanodrop).Clones were screened for presence of insert using the M13pUC F (5'-GTAAAACGACGGCCAG-3') and M13pUC R (5'-CAGGAAACAGCTATGAC-3') primers, corresponding to the N-terminus of galactosidase. Insert primers used to amplify the regions in **2.4.1.2** were also used to confirm the presence of target insert. The reaction mixture contained 1X Taq buffer, 2mM $MgCl_2$, 0.2mM dNTPs, 0.2µM of each primer, 1U Taq recombinant enzyme (Fermentas), 20ng of template DNA and nuclease free water to a final volume of 50µl. Reactions were cycled in a thermal cycler (Bio-Rad) set at 94 °C for 2min and 35 cycles 94°C for 30s, 55°C for 30s, primer extension at 72°C for 30s and final extension step of 72°C for 10min the appropriate cycling conditions. Amplification products were run in 1.2% agarose gel containing 10µg/ml ethidium bromide run in 1XTAE.

Once the overlapping ORF fragments had been identified, amplified and cloned we explored different fragment fusion combinations that could be used to generate hybrid fusion fragments

required to produce 3 different mutated sense-arm RNA silencing hairpin constructs. The following combinations were selected:

- I-ACMV AC1/AC4 + EACMV AC1/AC4 =343 bp
- II-ACMV AC1/AC4 + ACMV AC2/AC3 =319 bp
- III-EACMV AC1/AC4 + EACMV AC2/AC3 =381 bp

2.4.1.5 Designing bridge primers and producing PCR fragments with complementary overlapping ends

In order to fuse 2 fragments required to make the 3 hybrid constructs, chimeric bridge primers were designed. Bridge primers introduced complementary overlapping ends between 2 fragments and therefore facilitated the fusion of the fragments forming the hybrid virus target sequence. For each of the 3 constructs a bridge primer was designed. Bridge primers were designed by adding the F primer sequence of the 2nd fragment to the R primer sequence of the 1st fragment creating a 40-47nt bridge primer.

Bridge primer for **Hybrid I** was made by adding the EACMV AC1/4F primer sequence to the 5' end of ACMV AC1/4 R primer sequence creating a 44nt ACMV1/4 + EACMV1/4 HYBRID R primer (5'-TTCCAAGTCGATGCCAGAAATGTCTTTCTCACATACCCAAAGTG-3'). The ACMV AC1/4 fragment required for **Hybrid I** was re-amplified from extracted plasmid **(2.4.1.4)** using ACMV AC1/4F and ACMV AC1/4 + EACMV AC1/4 Hybrid R producing an ACMV AC1/4 amplicon with EACMV AC1/4 overlap (Product A).

Bridge primer for **Hybrid II** was made by adding the ACMV AC2/3 F primer sequence to the 5' end of ACMV AC1/4 R primer sequence creating a 47nt ACMV1/4+ ACMV2/3 HYBRID R primer (5'-CAATCACAACCTGAGGAAGGAGATGTCTTTCTCACATACCCAAAGTG-3'). The ACMV AC1/4 fragment was also required for **Hybrid II**, the fragment was once again re-amplified from extracted plasmid **(2.4.1.4)** however this time round using ACMV AC1/4F and

the ACMV AC1/4 + ACMV AC2/3 Hybrid R primers producing ACMV AC1/4 amplicons with ACMV AC2/3 overlap (Product B).

Bridge primer for **Hybrid III** was made by adding the EACMV AC2/3 F primer sequence to the 5'end EACMV AC1/4 R primer sequence creating a 40nt EACMV 1/4 + EACMV 2/3 HYBRID R (5'-TTTTCTGAACTTCAAGGTCTGGATGGGGTGCCTCATCTCC-3'). To amplify the EACMV AC1/4 fragment required to generate the **Hybrid III**, EACMV AC1/4F primer and EACMV AC1/4+EACMV AC2/3 Hybrid R primer were used. The fragment was amplified from plasmid extracted in **2.4.1.4** creating an EACMV AC1/4 amplicon with EACMV AC2/3 overlap (Product C).

The PCR reaction mixture to amplify all the 3 hybrid fragments consisted of 0.2µM of each appropriate primer, 1X High fidelity buffer, 0,2mM dNTPs, 1U High fidelity enzyme mix (Fermentas), 20ng of appropriate plasmid and nuclease free water to a final volume of 50µl. PCR Reactions were cycled in a Thermal cycler (Bio-Rad) set at 94 °C for 2min and 35 cycles 94°C for 30s, appropriate Ta for 30s, primer extension at 72°C for 30s and final extension step of 72°C for 10min. Ta used to create ACMV AC1/4 with EACMV AC1/4 overlap (Product A) was 58°C. Ta to create ACMV AC1/4 with ACMV AC2/3 overlap (Product B) was 60°C. Ta to create EACMV AC1/4 with EACMV AC2/3 overlap (Product C) was 58°C. Fragments were run in 1.2% agarose gel containing 10µg/ml ethidium bromide run in 1XTAE. The remaining PCR products were PCR purified using the High pure PCR purification kit (Roche) and also cloned into pTZ5R/T following the same method as **2.4.1.3** Method used to screen clones was the same as **2.4.1.4**.

2.4.1.6 Fusion PCR for creating hybrid fragments I, II,

Target overlapping regions (EACMV AC1/4, ACMV AC2/3 and EACMV AC2/3) were again amplified from extracted plasmid from **2.4.1.4**, regions were amplified following the same conditions used in **2.4.1.5**. Products A, B and C were also re-amplified from the plasmid clones generated above.

PCR was used to fuse fragments required to make each hybrid fragment. PCR Product A (1µg) was mixed with EACMV AC1/4 overlap fragment (1µg). PCR product B (1µg) was mixed with ACMV AC2/3 (1µg) and PCR product C was mixed with EACMV AC2/3 (1µg). Mixed products were placed in a thermal cycler (Bio-Rad) for 3min at 95°C to denature the strands then cooled down to 50°C for 5min to allow the overlapping in each reaction to align (ref to methodology flow diagram 2.1, point 2). PCR reaction tubes were set up with 1X High fidelity buffer, 0,4mM dNTPs, 5U High fidelity enzyme mix (Fermentas) and nuclease free water to a final volume of 50µl. No primers were included in this reaction as this reaction was only performed to elongate the overlapping regions generated after the 50°C for 5min cooling step. The reaction tubes were 1st heated to 95°C for 30sec and machine paused and to this 10µl of the mixed DNA was added. The reaction tubes were then placed back into the Thermal cycler (Bio-Rad) for 30sec at 55°C followed by 30min at 72°C to allow for overlapping ends to be extended creating the dsDNA.

2.4.1.7 Amplification of the hybrid fragments

PCR reactions were set up for each of the 3 hybrid fragments. Primer combinations specific for amplifying each of the above products were used. To amplify **Hybrid I**, ACMV AC1/4F and EACMV AC1/4R primers were used. To amplify **Hybrid II**, ACMV AC1/4F and ACMV AC2/3R primers were used. To amplify **Hybrid III**, EACMV AC1/4F and EACMV AC2/3R primers were used. dsDNA molecules generated above were used as template, 1µl was placed in a PCR tube containing 1X High fidelity buffer, 0,2mM dNTPs, 0.2µM of each primer, 1U High fidelity enzyme mix (Fermentas) and nuclease free water to a final volume of 50µl. PCR cycling conditions were as follows, 94 °C for 2min and 35 cycles 94°C for 30s, Ta of 58°C for 30s was used for all primer sets, primer extension at 72°C for 30s and final extension step of 72°C for 10min. Hybrid PCR products were run in 1% agarose gel containing 10µg/ml ethidium bromide run in 1X TAE.

2.4.1.8 Cloning and screening of hybrid fragments

Hybrid fragments I, II and III were PCR purified using pure PCR purification kit (Roche) and cloned following the same method as **2.4.1.3**. Plasmid DNA was extracted from the presumptive clones using the High pure plasmid miniprep kit (Roche) and plasmid quantified on the

Nanodrop 1000 spectrophotometer (Nanodrop). Clones were screened using the same method as **2.4.1.4**. Clones were further screened for orientation using the M13pUC F primer, the EACMV AC1/4R primer for Hybrid I, M13pUC F primer and ACMV AC2/3 R primer for Hybrid II and M13pUC F primer and EACMV AC1/4 R primer for Hybrid III. PCR reaction mixture used and cycling conditions used were same as **2.4.1.4.** Amplification products were run in 1% agarose gel containing 10µg/ml ethidium bromide run in 1X TAE. Clones containing the hybrid fragments in the antisense orientation were kept for later use and those containing sense fragments were used for sodium bisulfite treatment reaction.

2.4.2 Construction of mutated sense-arm hairpin RNA silencing constructs

2.4.2.1 C-T mutation of PCR products

Hybrid I, II and III were amplified from extracted plasmid DNA using High fidelity enzyme mix (Fermentas). Primers used were the same as the ones used in **2.4.1.7** and the thermal cycling conditions were also the same. The reaction mixture contained 0.2µM of each primer, 1X High fidelity buffer, 2mM dNTPs, 1U High fidelity enzyme mix (Fermentas). PCR amplicons were PCR purified (Roche) and quantified on the Nanodrop 1000 spectrophotometer (Nanodrop). The EZ DNA Methylation-Gold kit (Zymo Research) was used to catalyze the deamination of Cytosine residues to Thymine residues. Following manufactures instructions 130µl CT reagent (containing sodium bisulfite) was added to 20µl (200ng-500ng) of respective purified PCR products I, II and III. Tubes were then placed in a Thermal cycler (Biorad). DNA was denatured at 98°C for 10min, then deaminated at 64°C for various time periods (5, 10, 15, and 30min), followed by cooling at 4°C for 10min. Deaminated DNA was then used immediately and not stored for longer than 24hrs. Deaminated DNA products were then purified with desulphonation buffer and an ethanol-containing wash buffer. The recovered purified deaminated DNA was then eluted from a silica-based spin-column and used for downstream PCR.

2.4.2.2 Strand specific amplification of the deaminated PCR products

To preferentially amplify the sodium bisulfite treated PCR products, modified primers designed. These primers were designed to incorporate appropriate restriction endonuclease (RE) sites to the 5’ and 3’ ends of the PCR products, this was essential for downstream processing restriction and

ligations. To the F primer *XhoI* and *SpelI* sites were added and a *BglII* recognition site was added to the R primer.

To preferentially amplify mutated Hybrid I fragment, primer set ACMV AC1/4F (mod-*XhoI*+*SpeI*) (5'-GATCCTCGAGACTAGTAAGTGAGGTTTCCCATTTTG-3') and EACMV AC1/4R (mod-*BglI*) (5'-GATCAGATCTATAGGATGCCTCATCTCC-3') was used. To preferentially amplify mutated Hybrid II fragment, primer set ACMV AC1/4 F (mod-*XhoI*+ *SpeI*) (5'-GATCCTCGAGACTAGTAAGTGAGGTTTCCCATTTTG'-3) and ACMV AC2/3R (mod-*BglII*) (5-'GATCAGATCTCCAATCATAGATTTACACACAGG-3**'**) was used. To preferentially amplify mutated Hybrid III, primer set EACMV AC1/4F (mod-*XhoI*+ *SpeI*) (5-GATCCTCGAGACTAGTTTTTGGCATCGATTTGGAA-3') and EACMV AC2/3 R (mod-*BglII*) (5-'GATCAGATCTAAGAATAGCGTTTTTACCTGG-3') was used. The PCR reaction mixture consisted of 0.2µM of each primer, 1X High fidelity buffer, 0,2mM dNTPs, 1U High fidelity enzyme mix (Fermentas), 1µl of the recovered mutated DNA was added and nuclease free water added to a final volume 50µl. The mutated hybrid PCR products were then run in a 1 % agarose gel containing 10µg/ml ethidium bromide in 1XTAE.

Mutated hybrid fragments were expected to be 18 bp longer than the nonmutated hybrid fragments. The 18 bp extra nucleotides were from RE sites that were introduced to the 5' end of the F and R primers used to amplify the mutated hybrid fragments.

- **Expected mutated hybrid fragment sizes**
- I mutated hybrid =361 bp
- II mutated hybrid =337 bp
- III mutated hybrid =399 bp

2.4.2.3 Cloning of mutated hybrid fragments

Mutated hybrid PCR products were purified using the High Pure PCR product purification Kit (Roche) and quantified using the Nanodrop. Fragments were then T/A cloned into pTZ57R/T vector (Fermentas) following method described in **2.4.1.3**. Plates were incubated at 37°C O/N.

White colonies were randomly selected and inoculated in LB broth containing 100µg/ml amplicillin.

2.4.2.4 Screening of clones for insert and orientation

Plasmid DNA was extracted from presumptive clones using High Pure Plasmid Miniprep kit (Roche) and quantified using the Nanodrop. Clones were first screened for correct size using the M13 primer set following same method described in **2.4.1.4**. Positive clones containing the right size insert were then further screened for correct orientation using the M13F pUC primer and the mutated hybrid insert reverse primer. PCR amplicons were examined by electrophoresis on a 1% agarose gel, containing 10µg/ml ethidium bromide run in 1X TAE.

2.4.2.5 Sequencing and sequence analysis of clones

Following screening, clones presumed to contain the mutated and original unmodified strands were sent for automated sequencing by Inqaba Biotechnical Industries (Pretoria, South Africa). The universal M13/pUC F primer and the M13/pUC R primer were used to sequence the multiple cloning site (MCS) of pTZ57R and any insert contained within. Raw sequencing data was edited using the Chromas software (version 1.45) (Griffith University, Australia). Subsequent sequence analysis was performed using Vector NTI Advance suite of software (version 10.3) (Invitrogen, 2006). A multiple sequence alignment was done to compare the sequences of mutated overlapping clones to the full length sequence to determine the number of cytosine to thymine mutations. Sequencing data was also used to confirm the orientation of inserts.

2.4.2.6 Construction and cloning of the inverted (IR) repeat

Plasmid DNA was extracted from the desired mutated hybrid and nonmutated hybrid clones. Plasmid containing the mutated hybrid fragment was restricted with *Sca*I and *Bgl*II (Fermentas) while plasmid containing the nonmutated hybrid fragment was restricted with *Sca*I and *Bam*HI (Fermentas). The restriction fragments were then analysed on a 1% agarose gel. Bands corresponding to approximately 1.5kb (nonmutated hybrid) and 2.2kb (mutated hybrid) were excised and gel extracted using the QiAquick gel extraction kit (Qiagen) followed by

quantification using a nanodrop. Restriction digest with *Bgl*II and *Bam*HI produced compatible cohesive ends therefore enabling mutated hybrid and nonmutated hybrid fragments to be ligated forming an IR. A 1:1 ligation ratio between the 2 fragments was performed. Ligation mixture contained 1X ligation buffer, 1U T4 DNA ligase (Fermentas) and 1:1 ratio purified fragments. This was incubated for a minimum of 1hr at 22°C. Chemically competent DH5α cells (100µl) were transformed with 15µl of the ligation mixture and spread on 100 µg/ml ampicillin containing LB agar plate and incubated O/N at 37°C. Colonies were randomly selected and inoculated in LB containing 100 µg/ml ampicillin and incubated O/N at 37°C. Plasmid DNA from the presumptive clones was then extracted. Clones were successfully screened using *Xba*I and *Xho*I (Fermentas) as it was to PCR to amplify through the IR sequence. Restriction fragments were examined by electrophoresis on a 0.8% agarose gel containing 10 µg/µl ethidium bromide run in 1X TAE.

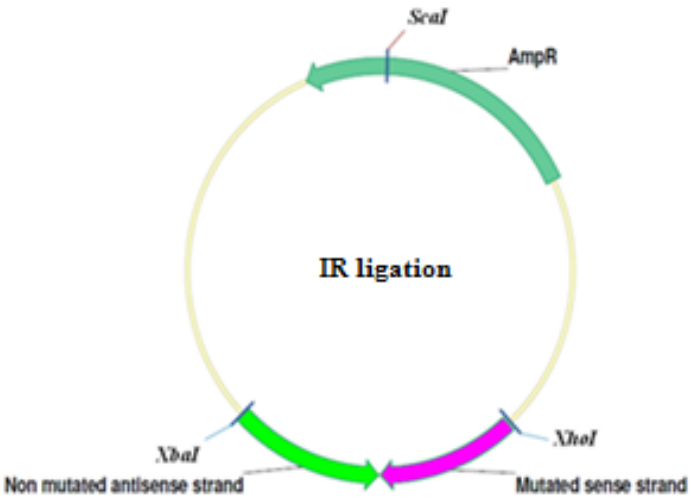


Figure 2. 2 Schematic representation of head to head ligation of non-mutated strand and mutated strand required for IR formation.

- **Expected IR hairpin fragment sizes**

- I-IR: non-mutated hybrid I + mutated hybrid I = 698 bp
- II-IR: non-mutated hybrid II + mutated hybrid II = 650 bp
- III- IR: non-mutated hybrid III + mutated hybrid III = 774 bp

2.4.2.7 Sub-cloning of IR into expression cassette

A double digest using *Xba*I and *Xho*I (Fermentas) was performed to restrict the IRs to restrict out of pTZR5/T. Following restriction, the vector and fragments of interest were separated by electrophoresis run in 1X TAE. The IR fragements was excised from a 1% agarose gel containing10ug/µl ethidium bromide. IR fragments were gel purified using a QiAquick gel Extraction Kit (Qiagen), and quantified on a Nanodrop. Expression pART7 vector was linearized using *XbaI* and *XhoI* (Fermentas) and also dephosphorylated using FastAP (Fermentas). Vector was then purified using the High Pure PCR product purification Kit (Roche). The gel purified fragments were then ligated in the pART7 multiple cloning site (MCS), between CaMV35S promoter and octopine synthase transcriptional terminator sites. A 1:1 insert (100ng) vector (100ng) ligation reaction was performed and incubated at 22°C for a minimum of 1hour. This transformed into DH5α following the same method as **2.4.1.3**. Transformed cells were plated on LB agar plate containing 100µg/ml amplicillin and incubated O/N at 37°C. Colonies were randomly picked and plasmid DNA extracted using the High Pure plasmid extraction kit (Roche) followed by screened using *Xho*I and *Xba*I (Fermentas). Correct clones were assigned the following ID/codes MM1-IR cassette, MM2-IR cassette and MM3-IR cassette.

2.4.2.8 PCR amplification of IR expression cassette

Due to the lack of available REs required to restrict the IR expression cassette out of pART7 and ligate into pCAMBIA 1305.1, it was necessary to amplify out the whole IR expression cassette (promoter, IR insert and terminator). The IR expression cassette was amplified using the following primer set; Cassette 7 F (5'-TTAACGTTTACAATTTCCCATTCGC-3') and Cassette 7 R (5'-GTTATCCGCTCACAATTCC-3') primers. The PCR reaction mixture consisted of 0.2µM of each primer, 1X High fidelity buffer, 0,2mM dNTPs, 1U High fidelity enzyme mix (Fermentas), 20ng of template DNA and nuclease free water to a final volume of 50µl. PCR cycling conditions were as follows, 94 °C for 2min and 35 cycles 94°C for 30s, 55°C for 30s, primer extension at 72°C for 3min and final extension step of 72°C for 10min. PCR products were run in a 1 % agarose gel containing 10µg/ml ethidium bromide in 1X TAE. Amplicons produced of ~3000 bp were T/A cloned into pTZ57R/T as described in **2.4.1.3**. Ligation mixture was transformed into *E.coli* DH5α using following method described in **24.1.3**. Transformed cells were plated on LB agar plate containing 100µg/ml ampicillin and incubated O/N at 37°C.

Colonies were randomly selected and plasmid DNA extracted using the High Pure plasmid extraction kit (Roche).

2.4.2.9 Screening of clones for presence and orientation of IR expression cassette

Colonies were screened using M13 primers for presence of IR expression cassette following method described in **2.4.1.4**. The PCR reaction mixture contained 1X Taq buffer, 2mM $MgCl_2$, 0.2mM dNTPs, 0.2µM of each primer, 1U Taq recombinant enzyme (Fermentas), 20ng of template DNA and nuclease free water to a final volume of 50µl. Reactions were cycled in a thermal cycler (Bio-Rad) set at 94 °C for 2min and 35 cycles 94°C for 30s, 55°C for 30s, primer extension at 72°C for 3min 30secs and final extension step of 72°C for 10min th. Amplification products were run in 0.8% agarose gel containing 10µg/ml ethidium bromide run in 1X TAE.

Colonies containing IR expression cassettes were further screened for orientation. PCR was used to screen. Different primer combinations were used. M13pUCF primer was used along with cassette 7 R primer. M13pUCR was used with cassette 7 F primer. Reaction mixture and cycling conditions were the same as above. Amplification products were then run in 0.8% agarose gel containing 10µg/ml ethidium bromide run in 1XTAE.

2.4.2.10 Sub-cloning of IR hairpin cassette into pCambia 1305.1

Double digest was performed using *EcoR*I and *Hind*III (Fermentas) to restrict the IR hairpin cassette out of pTZ57R/T. Expected restricted fragments (~3-3.3kb) were gel extracted and purified from a 0.8% agarose gel containing 10µg/ml ethidium bromide run in 1XTAE. Plant transformation vector pCAMBIA 1305.1 was linearized with *EcoR*I and *Hind*III (Fermentas) and blunt end polished using T4 DNA polymerase (Fermentas). Blunt polished ends were then dephosphorylated using FastAP (Fermentas). The vector was then PCR purified using the High Pure PCR product purification Kit (Roche). Quality and quantity of fragments was determined using a Nanodrop. A ligation reaction of the IR cassette and the vector 1305.1 was set up. Ligation reaction was set up following method described in **2.4.1.3**. Concentration of IR cassettes DNA (insert) was 81.81ng and 100ng vector 1305.1 was used for a 3:1 insert to vector ratio creating MM1-IR/1305.1, MM2-IR:1305.1 and MM2-IR:1305.1. Competent *E.coli* DH5α cells were transformed with 15µl of the ligation reaction mixture following method described in

2.4.1.3. Transformed cells were plated on LB plates containing 50µg/ml kanamycin and incubated O/N at 37°C. Clones were randomly selected and inoculated into 5ml LB containing 50µg/ml kanamycin broth, and incubated at 37°C overnight.

2.4.2.11 Screening of plant transformation vector for presence of IR cassette.

Plasmid DNA was extracted from the presumptive clones using the High Pure plasmid extraction kit (Roche). Restriction digest was performed on the clones using *Xho*I and *Xba*I (Fermentas) to screen putative recombinant plasmids for the presence of IR cassette. Screening was also performed by PCR using Hybrid primers, annealing temperatures and procedure described in **2.4.1.7** and Mutated hybrid primers, annealing temperatures and procedure described in **2.4.2.2**. The reaction mixture contained 1X Taq buffer, 2mM $MgCl_2$, 0.2mM dNTPs, 0.2µM of each primer, 1U Taq recombinant enzyme, 20ng of template DNA and nuclease free water to a final volume of 50µl. Reactions were cycled in a thermal cycler (Bio-Rad) set at 94 °C for 2min and 35 cycles 94°C for 30s, appropriate Ta for 30s, primer extension at 72°C for 30s and final extension step of 72°C for 10min. Fragments were analysed by electrophoresis on a 1% agarose gel containing 10µg/ml ethidium bromide in a 1X TAE buffer. One screening was completed and correct RNA silencing hairpin constructs identified the following ID/codes were aligned to each of the 3 constructs; MM1hp construct, MM2hp construct and MM3hp construct.

2.4.2.12 Transformation of *A. tumefaciens* LBA 4404 with IR hairpin cassettes

Plasmid DNA extracted from clones containing the correct RNA silencing hairpin constructs was then used to transform *A. tumefaciens* LBA 4404 using the freeze thaw method (Holsters *et al*., 1978). Chemically competent *A. tumefaciens* LBA 4404 cells stored at -70°C were placed on ice to thaw. Once thawed, 100ng of RNA silencing hairpin (MM1hp construct, MM2hp construct and MM3hp) construct was added to 100µl of the competent cells. This was then snap frozen in liquid nitrogen for 5min followed by heat shock on a heating block at 37°C for 5min, 1ml Yeast extract-phosphate (YEP) broth was then added. This was incubated at 28 °C for 2-4 hrs with gentle shaking (50rpm). After the incubation period, transformed cells were centrifuged for 30secs at maximum speed and the supernatant discarded. The pellet was resuspended in 100µl YEP. Transformed cells were then spread on YEP plate containing 50µg/ml rifampicin, 50µg/ml

kanamycin and 100µg/ml streptomycin and incubated at 28 °C for 1-2 days until colonies appeared.

2.4.2.13 Transformation of BC1 hairpin cassette into *A. tumefaciens* LBA 4404

The SACMV BC1 mutated hybrid RNA silencing construct used to transform *N. benthamiana* (Taylor *et al*., 2012c) was included in this study as transformation of cassava had not been attempted. This construct was engineered in exactly the same way as the 3 above (MM1hp, MM2hp and MM3hp) constructs. The only differences being, this SACMV BC1 construct was derived from a single ORF (not hybrid ORF), the target ORF was DNA-B derived and not DNA-A derived, the construct was in plant transformation pCAMBIA 1303 and not pCAMBA 1305.1. pCAMBIA 1303 is very similar to pCAMBIA 1305.1, the only difference is the presence of both GFP and GUS gene in pCAMBIA 1303 while pCAMBIA only has the GUS reporter gene. Lastly, this construct was in a different *A. tumefaciens* strain. Construct was in *A. tumefaciens* Agl and not LBA4044 like the other 3 constructs. *A. tumefaciens* Agl is more virulent than LBA4044 and was therefore not suitable *Agrobacterium*-mediated transformation of FEC. Agl is more suitable for virus infectivity studies. This construct was extracted from Agl and mobilised into LBA4044.

SACMV BC1 containing Agl was cultured in YEP containing 50µg/ml kanamycin and 100µg carbenicillin O/N at 28°C and shaking at 180rpm. Plasmid DNA was isolated using the High Pure plasmid extraction kit (Roche). Plasmid was used to transform chemically competent *E.coli* DH5α cells following method described in **2.4.1.3**. Colonies were cultured in LB containing 50µg/ml kanamycin, O/N at 37°C shaking at 200rpm. Plasmid DNA was again isolated using the High Pure plasmid extraction kit (Roche). Presence of the SACMV-[ZA] BC1hp was screened using BC1 non-mutated fragment primer set, BC1F (5'-AAACATTCCACGGACATACG-3') and BC1R (5'TGGTAGCCCAATCTGAGACCTT-3'). Plasmid was also screened for the presence of the BC1 mutated fragment using the primer set, BC1F (mod–*Xho*I+*Spe*I) (5-'GATCCTCGAGACTAGTAAATATTCTACGGACATACG-3') and BC1R (mod-*BglII*) (5'-GATCAGATCTTAGTAGCCCAATCTAAGACCTTGT-3'). The reaction mixture for each contained 1X Taq buffer, 2mM $MgCl_2$, 0.2mM dNTPs, 0.2µM of each primer, 1U Taq recombinant enzyme (Fermentas), 20ng of template DNA and nuclease free water to a final

volume of 50µl. Reactions were cycled in a thermal cycler (Bio-Rad) set at 94 °C for 2min and 35 cycles 94°C for 30s, 54°C for 30s, primer extension at 72°C for 30s and final extension step of 72°C for 10min. Fragments were analysed by electrophoresis on a 1% agarose gel containing 10µg/ml ethidium bromide in a 1X TAE buffer.

Once BC1hp construct had been identified and verified to be correct we renamed this RNA silencing hairpin construct MM4hp. Construct MM4hp was then used to transform *A. tumefaciens* LBA4404 following the method described in **2.4.2.12**

2.4.2.14 Screening of *A. tumefaciens* LBA4404 for the presence RNA silencing hairpin constructs.

Colonies from each of the four *A. tumefaciens* LBA4404 transformation plates were selected and inoculated into YEP broth containing 50µg/ml rifampicin, 50µg/ml kanamycin and 100µg/ml strepotomycin. Broths were incubated at O/N at 28°C and 200rpm. Plasmid DNA was then extracted from presumptive clones and screened for the presence of the hairpin constructs; MM1hp, MM2hp, MM3hp and MM4hp. Clones were screened by restriction digest using *Xho*I and *Xba*I (Fermentas). An empty pCAMBIA1305.1 (p1305.1) was also digested accordingly and used as a negative control.

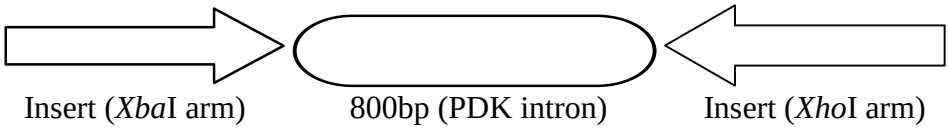
Clones were also screened by PCR amplification of beta-glucuronidase (GUS) gene. GUS gene is found on the p1305.1 vector. To amplify the gene, the following primer set was used; GUSPlus F (5'-CAACATCCTCGACGACGATAGCA-3') and GUSPlus R (5'-GGTCACAACCGAGATCTCCT-3') were used. These amplify a 181 bp fragment. Clones were also screened the following primer set; Hyg F (5'-TCTCGATGAGCTCATGCTTTGG-3') and Hyg R (5'-AGTACTTCTACACAGCCATGGG-3'). These primers amplify a 444 bp amplicons; a portion of the Hygromycin resistance gene found on the p1305.1 vector. The reaction mixture for amplification of each of the reporter genes contained 1X Taq buffer, 2mM $MgCl_2$, 0.2mM dNTPs, 0.2µM of each primer, 1U Taq recombinant enzyme (Fermentas), 20ng of template DNA and nuclease free water to a final volume of 50µl. Reactions were cycled in a thermal cycler (Bio-Rad) set at 94 °C for 2min and 35 cycles 94°C for 30s, 58°C for 30s, primer extension at 72°C for 30s and final extension step of 72°C for 10min. Clones were also screened using target

insert primers following method described in **2.4.1.7** and **2.4.2.2**. Fragments were analysed by electrophoresis on a 1% agarose gel containing 10µg/ml ethidium bromide in a 1X TAE buffer. *A. tumefaciens* LBA 4404 successfully transformed with the pCAMBIA 1305.1.

2.4.3 Construction of non-mismatched (Gateway) RNA silencing hairpin constructs

Method used to make the Gateway (pHellsgate) constructs was slightly different to the method described by the Invitrogen protocol. The BP recombinase method of going through the pDon entry clone was omitted and instead target fragments were cloned into the *Xho*I and *Xba*I sites of pHellsgate 8 using restriction enzyme digestion and ligation.

Gateway RNA silencing hairpin constructs to be designed



- MM5hp: ACMV AC1/AC4 + EACMV AC1/AC4 =343 bp
- MM6hp: II-ACMV AC1/AC4 + ACMV AC2/AC3 =319 bp
- MM7hp: IV-EACMV AC1/AC4 + EACMV AC2/AC3 =381 bp
- MM8hp: SACMV BC1=221 bp

2.4.3.1 Addition of *Xba*I and *Xho*I restriction sites to hairpin fragments

To facilitate ligation of Hybrid I, II and III and BC1 fragments into pHellsgate 8, *Xba*I and *Xho*I restriction enzyme sites were added to the 5'end of each of the forward and reverse primers.

***Xho*I and *Xba*I restriction site was added to the following primers**

Hybrid I: ACMV AC1/4F and EACMV AC1/4R

Hybrid II: ACMV AC1/4F and ACMV AC2/3R

Hybrid IV: EACMV AC1/4F and EACMV AC2/3R

SACMV BC1: BC1F and BC1R

Hybrid fragments used were created above in steps **2.4.1.1-2.4.1.8, BC1 fragment** was obtained from previous student (Harmse, 2009). The restriction sites were added to each of the 4 fragments in a PCR reaction.

To amplify Hybrid I fragment with *Xba*I restriction sites on either ends, primer set; ACMV AC1/4 *Xba*I F (5'-GATCTCTAGAAAGTGAGGTTCCCCATTCTG-3') and EACMV AC2/3 *Xba*I R (5'-GATCTCTAGAAGGAATGGCGTTTTTACCTG-3') was used. Another Hybrid I fragment was amplified and modified to contain *Xho*I restriction sites to either ends of the fragment. This was achieved by designing primers that were the same as the *Xba*I primers however the underlined section of the primer was replaced with CTCGAG.

To amplify Hybrid II fragment with *Xba*I restriction sites on either ends, primer set; ACMV AC1/4 *Xba*I F (5'-GATCTCTAGAAAGTGAGGTTCCCCATTCTG-3') and ACMV AC2/3 *Xba*I F (5'- GATCTCTAGACCAATCATGGATTTACGCACA-3') was used. Another Hybrid II fragment was amplified and modified to contain *Xho*I restriction sites to either ends of the fragment. This was achieved by designing primers that were the same as the *Xba*I primers however the underlined section of the primer was replaced with CTCGAG.

To amplify Hybrid III fragment with *Xba*I restriction sites on either ends, primer set; EACMV AC1/4 *Xba*I F (5'-GATCTCTAGATTCTGGCATCGACTTGGAA-3') and EACMV AC2/3 *Xba*I R (5'-GATCTCTAGAAGGAATGGCGTTTTTACCTG-3') was used. Another Hybrid fragment was amplified and modified to contain *Xho*I restriction sites to either ends of the fragment. This was achieved by designing primers that were the same as the *Xba*I primers however the underlined section of the primer was replaced with CTCGAG.

To amplify SACMV BC1 fragment with *Xba*I restriction sites on either ends, primer set; BC1 *Xba*I F (5'- GATCTCTAGAAAATATTCTACGGACATACG-3') and BC1 *Xba*I R (5'-GATCTCTAGATGGTAGCCCAATCTGAGACCTT-3') was used. Another SACMV BC1 fragment was amplified and modified to contain *Xho*I restriction sites to either ends of the fragment. This was achieved by designing primers that were the same as the *Xba*I primers however the underlined section of the primer was replaced with CTCGAG.

The PCR reaction mixture contained 1 X High fidelity buffer, 2mM dNTPs, 1U High fidelity enzyme mix (Fermentas), 0.2µM of each primer, 20ng of template DNA and nuclease free water to a final volume of 50µl. Reactions were cycled in a thermal cycler (Bio-Rad) set at 94 °C for 2min and 35 cycles of 94°C for 30s, 58°C 30s, primer extension at 72°C for 30s and final extension step of 72°C for 10min. Amplicons were run in 1.2% agarose gel containing 10µg/ml ethidium bromide run in 1X TAE.

2.4.3.2 Ligation of fragments (hairpin arms) into pHellsgate 8

PCR fragments generated were digested with either *Xba*I or *Xho*I (Fermentas). Digested fragments were PCR purified using the High pure PCR purification kit (Roche). pHellsgate 8 was first digested with *Xba*I (Fermentas) to digest out the 1.5kb ccdB gene and simultaneously dephoshorylated using FastAP (Fermentas). The digestion reaction was analysed on a 1% agarose gel. Bands corresponding to 16 485bp (vector backbone) was excised and gel extracted using the QiAquick gel extraction kit (Qiagen), followed by quantification using a nanodrop. The *Xba*I digested PCR fragments required for each hairpin construct were ligated into the *Xba*I digested pHellsgate 8 backbone. A 3:1 insert to vector ligation ratio was performed. Ligation mixture contained 1X Rapid ligation buffer, 1U T4 DNA ligase (Fermentas) and 3:1 ratio purified fragments. This was incubated for 10min at 22°C. Chemically competent DB3.1 cells were then transformed following method used in **2.4.1.3**. Transformed cells were plated onto LB agar plates containing 100µg/ml spectinomycin. Plates were incubated at 37°C O/N. Colonies were cultured in LB broth with 100µg/ml spectinomycin.

2.4.3.3 Screening of clones for presence and orientation of *Xba*I hairpin arm

Plasmid DNA from the O/N cultures was extracted using plasmid isolation kit (Fermentas). Presence of insert was confirmed by PCR using the *Xba*I modified primers from **2.4.3.1**. The reaction mixture contained 1X Taq buffer, 2mM $MgCl_2$, 0.2mM dNTPs, 0.2µM of each primer, 1U Taq recombinant enzyme (Fermentas), 20ng of plasmid DNA and nuclease free water to a final volume of 50µl. Reactions were cycled following same cycling conditions used for **2.4.3.1**. Amplification products were run in 1.2% agarose gel containing 10µg/ml ethidium bromide run in 1X TAE.

Clones containing insert were also screened for presence and orientation of insert using a combination of the *Xba*I F insert primer and the pHellsgate 8 P27-5 sequencing primer and also the combination of *Xba*I R and pHellsgate 8 P27-5. Clones containing *Xba*I hairpin arm in the correct orientation were expected to yield an amplicon for the *Xba*I F primer and P27-5 primer combination and no amplicon for the *XbaI*R and P27-5 combination.

2.4.3.4 Ligation of the 2nd arm (*Xho*I fragment) required to complete the hairpin

Clones containing the correct orientation *Xba*I fragments were digested with *Xho*I (Fermentas) to digest out the other 1.5kb ccdB gene house in the pHellsgate 8 vector. Digestion and dephosphorylation (Fermentas FastAP) was performed simultaneously. The digestion reaction was analysed on a 1% agarose gel. Bands corresponding to vector backbone were excised and gel extracted using the QiAquick gel extraction kit (Qiagen) followed by quantification using a nanodrop. *Xho*I fragments (hairpin arm) from **2.4.3.1** were also digested with *Xho*I and PCR purified using PCR purification kit (Roche). Ligation of the vector backbone and the *Xho*I digested hairpin arm was performed following method described in **2.4.3.2**. Following ligation transformation of competent DB3.1 cells was performed following method used in **2.4.3.2**.

2.4.3.5 Screening of clones for presence and orientation of *Xho*I hairpin arm

Plasmid DNA from the O/N cultures was extracted using plasmid isolation kit (Fermentas). Presence of insert was screening by PCR using the *Xho*I modified primers from **2.4.3.1**. Screening was performed following method used in **2.3.3.3** however the *Xho*I insert primers were used and clones containing insert were screened for insert orientation using primer hybrid *XhoI* F and P27-3 combination and *Xho*I R and P27-3 combination. Clones containing *Xho*I hairpin arm in the correct orientation were expected to yield an amplicon for the *Xho*I F primer and P27-5 primer combination and no amplicon for the *XhoI*R and P27-3 combination.

2.4.3.6 Sub-cloning of pHellsgate IR into pCambia 1305.1

Digestion of IR cassette out of plant transformation vector pHellsgate 8 into plant transformation vector pCAMBIA 1305.1 was necessary so that silencing efficiency comparison between the mutated-sense arm hairpin constructs and the Gateway hairpin constructs can be made.

Once both IR ams (*Xba*I and *Xho*I hairpin arms) were confirmed to be present and in the correct orientation, the IR cassette (35S promoter, IR arms and the octopine synthase terminator) were digested with *Not*I (Fermentas). The digestion reaction was analysed on a 1% agarose gel. Bands corresponding to right size for each IR cassette were excised and gel extracted using the QiAquick gel extraction kit (Qiagen) followed by quantification using a nanodrop. Purified excised fragments were blunt end polished using T4 DNA polymerase (Fermentas) to facilitate blunt end ligation with blunt-end polished dephosphorylated pCambia 1305.1 vector generated from **2.4.2.10**. For the ligation reaction, a 3:1 IR cassette to pCambia 1305.1 ratio was used, other reaction components included 1X Rapid ligase buffer, 10X PEG 4000 (V/V), 5U T4 DNA ligase (Fermentas) and nuclease water to a final volume of 30µl. The ligation reaction was incubated for 10min at 22°C. Chemically competent *E.coli* DH5α cells were then transformed following method used in **2.4.5.3**. Transformed cells were plated onto LB agar plates containing 50µg/ml kanamycin. Plates were incubated at 37°C O/N. Colonies were cultured in 5ml of LB broth with 100µg/ml kanamycin.

2.4.3.7 Screening of plant transformation vector for presence IR hairpin cassette.

Plasmid extraction from O/N liquid cultures was performed using the Plasmid extraction kit (Fermentas). Screening of clones was performed following **2.4.3.3** (screening of *Xba*I arm) and **2.4.3.5** (screening of the *Xho*I arm).

Following screening, 1 clone presumed to be correct for each of the 4 constructs (MM5hp, MM6hp, MM7hp and MM8hp) were sent off for automated sequencing by Inqaba Biotechnical Industries (Pretoria, South Africa). Each clone was sequenced using 4 different primers (P27-3, P27-5, *Xho*I F and *Xba*IF). Raw sequencing data was edited using the Chromas software (version 1.45) (Griffith University, Australia). Multiple sequence alignment to confirm correct orientation of the *Xba*I and *Xho*I arms if the IR cassette was performed using Clustal X Multiple Sequence Alignment Program (version 1.8, 1999).

2.4.3.8 Transformation of *A. tumefaciens* LBA 4404 with IR hairpin cassettes

Transformation was performed as described in **2.4.2.12**. Plasmid was extracted from randomly selected colony for each construct; plasmid was extracted using the Plasmid extraction kit (Fermentas). Colonies were also screened as described **2.4.3.3** and **2.4.3.5**. Clones were also screened using the GUS and Hyg gene primers following method described in **2.4.2.14**.

2.5 Results

2.5.1 Sequence alignment and target region identification

Regions in ACMV AC1/4 overlapping ORF and ACMV AC2/3 overlapping ORF that had high sequence identity were selected for potential targeting (fig 2.3 and 2.4). Less perfect alignment sequence similarity between the EACMV AC1/4 and EACMV AC2/3 overlapping reading frames of the 8 EACMV isolates was observed (fig 2.5 and 2.6). The selected EACMV isolates showed only 83% and 75% sequence similarity within the EACMV AC1/4 and EACMV AC2/3 overlapping regions, respectively. This was expected as it is known that there is more variation in EACMV isolates than ACMV.

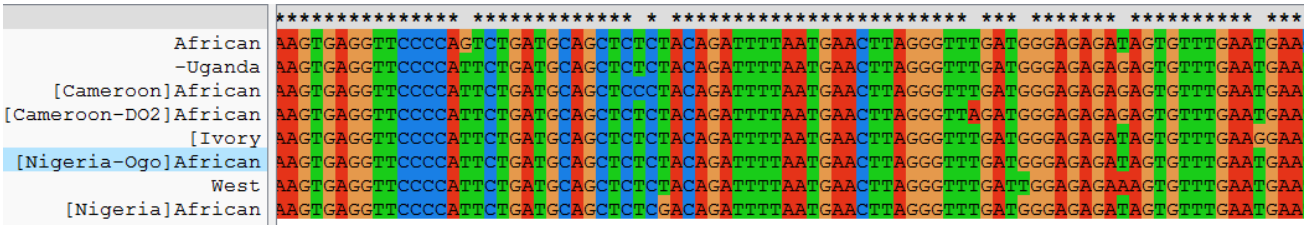


Figure 2. 3 A segment of the multiple sequence alignment output screen. Alignment was performed on 8 ACMV isolates to identify a region along the ACMV AC1/4 overlapping region that gives the best sequence alignment.

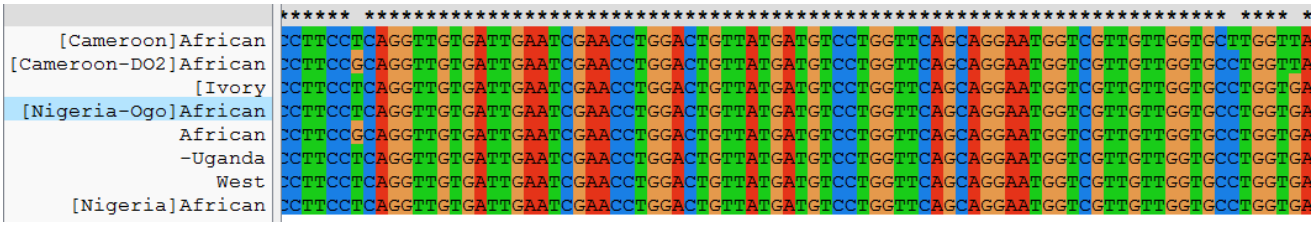


Figure 2. 4 A segment of the multiple sequence alignment output screen. Alignment was performed on 8 A CMV isolates to identify a region along the AC2/3 overlapping region that gives the best sequence alignment.

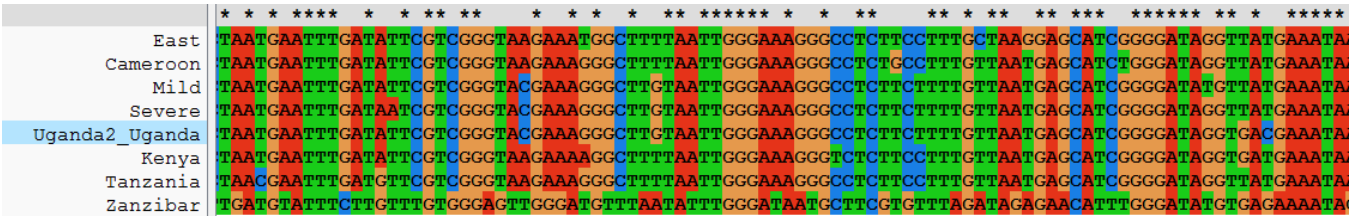


Figure 2. 5 A segment of the multiple sequence alignment performed on 8 EACMV isolates to identify a region along the EACMV AC1/4 overlapping region that gives the best alignment between the isolates.

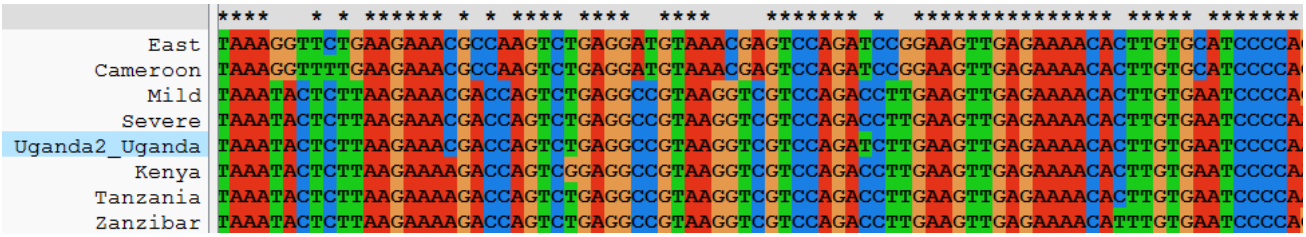


Figure 2. 6 A segment of the multiple sequence alignment performed on 8 EACMV isolates to identify a region along the EACMV AC2/3 that gives the best sequence alignment results.

siRNA hotspots from the conserved ACMV AC1/4, ACMV AC2/3. EACMV AC1/4 and EACMV AC2/3 overlapping regions were identified using siRNA Scan programme. Regions generating possible efficient siRNA hit/hotspots are shown in red and regions considered non-hits shown in black in tables 2.1-2.4.

Table 2. 1 siRNA scan programme computational results predicting regions along the ACMV-[NG:Ogo:90] AC1/AC4 overlapping region were efficient and effective siRNA could be generated.

Number	Fragment	siRNA AS (3' - 5')	Hits
12	query_seq (289 - 309)	UUCACUCCAAGGGGUAAGACU	1
13	query_seq (306 - 326)	GACUACGUCGAGAGAUGUCUA	1
14	query_seq (309 - 329)	UACGUCGAGAGAUGUCUAAAA	1
15	query_seq (310 - 330)	ACGUCGAGAGAUGUCUAAAAU	1
27	query_seq (395 - 415)	AUCUUGUGAAACCCAUACACU	1
28	query_seq (404 - 424)	AACCCAUACACUCUUUCUGUA	1

Table 2. 2 siRNA scan programme computational results predicting regions along the ACMV-[NG:Ogo:90] AC2/AC3 overlapping region were efficient and effective siRNA could be generated.

Number	Fragment	siRNA AS (3' - 5')	Hits
1	query_seq (38 - 58)	UCCAGCAGGUCUGGAACUUCA	1
4	query_seq (46 - 66)	GUCUGGAACUUCAAGUCUUUU	0
7	query_seq (156 - 176)	CAGCACCAGCCACUAAAGCUU	1
8	query_seq (157 - 177)	AGCACCAGCCACUAAAGCUUU	1
9	query_seq (159 - 179)	CACCAGCCACUAAAGCUUUAU	1
10	query_seq (160 - 180)	ACCAGCCACUAAAGCUUUAUA	0
11	query_seq (171 - 191)	AAGCUUUAUAUCCCCUAAACA	0
12	query_seq (172 - 192)	AGCUUUAUAUCCCCUAAACAA	1
13	query_seq (188 - 208)	AACAAUACAGGGUCCAUUUUU	1
14	query_seq (199 - 219)	GUCCAUUUUUGCGGUAAGGAA	1

\

Table 2. 3 siRNA scan programme computational results predicting regions along the EACMV-[UG2] AC1/AC4 overlapping region were efficient and effective siRNA could be generated.

Number	Fragment	siRNA AS (3' - 5')	Hits
1	query_seq (28 - 48)	AAGACCGUAGCUGAACCUUUU	1
2	query_seq (30 - 50)	GACCGUAGCUGAACCUUUUCA	1
3	query_seq (59 - 79)	UUCUUUAAGGGGAGGGAAAAA	0
4	query_seq (65 - 85)	AAGGGGAGGGAAAAAUUACAU	0
5	query_seq (66 - 86)	AGGGGAGGGAAAAAUUACAUU	0
6	query_seq (70 - 90)	GAGGGAAAAAUUACAUUCGAA	0
7	query_seq (90 - 110)	AACUGUAGCCUGCUACUAAAU	1
8	query_seq (103 - 123)	UACUAAAUCGAGGGACUUACA	1
9	query_seq (114 - 134)	GGGACUUACAAGCCUACCUUU	1
10	query_seq (120 - 140)	UACAAGCCUACCUUUACACAA	1
11	query_seq (123 - 143)	AAGCCUACCUUUACACAACUA	1
12	query_seq (139 - 159)	AACUAGCCCUACCCCUUUACU	1
13	query_seq (142 - 162)	UAGCCCUACCCCUUUACUCUA	1

Table 2. 4 siRNA scan programme computational results predicting regions along the EACMV-[UG2] AC2/AC3 overlapping region were efficient and effective siRNA could be generated.

Number	Fragment	siRNA AS (3' - 5')	Hits
1	query_seq (1 - 21)	UCCAGCAGGUCUGGAACUUCA	1
2	query_seq (4 - 24)	AGCAGGUCUGGAACUUCAAGU	0
6	query_seq (71 - 91)	GGCAUAGACCUCUCACUACUA	0
7	query_seq (119 - 139)	CAGCACCAGCCACUAAAGCUU	1
8	query_seq (120 - 140)	AGCACCAGCCACUAAAGCUUU	1
9	query_seq (122 - 142)	CACCAGCCACUAAAGCUUUAU	1
10	query_seq (123 - 143)	ACCAGCCACUAAAGCUUUAUA	0
11	query_seq (134 - 154)	AAGCUUUAUAUCCCCUAAACA	0
12	query_seq (135 - 155)	AGCUUUAUAUCCCCUAAACAA	0
13	query_seq (151 - 171)	AACAAUACAGGGUCCAUUUUU	1
14	query_seq (162 - 182)	GUCCAUUUUUGCGGUAAGGAA	1

Based on the computational results, two final specific target regions were selected on the ACMV ([NG:Ogo:90]) reference target begomovirus (**fig. 2.6a**).

a) ACMV-[NG:Ogo:90] AC1/AC4 overlapping region (2445-2528) 136 nt

b) ACMV-[NG:Ogo:90] AC2/AC3 overlapping region (1297-1479) 183 nt

Using EACMV–Uganda2 ([UG2]) as the reference virus, the following 2 overlapping target regions were chosen (**fig. 2.6b**).

c) EACMV-[UG2] AC1/AC4 overlapping region (2279-2485) 207 nt

d) EACMV-[UG2] AC2/AC3 overlapping region (1291-1464) 174 nt

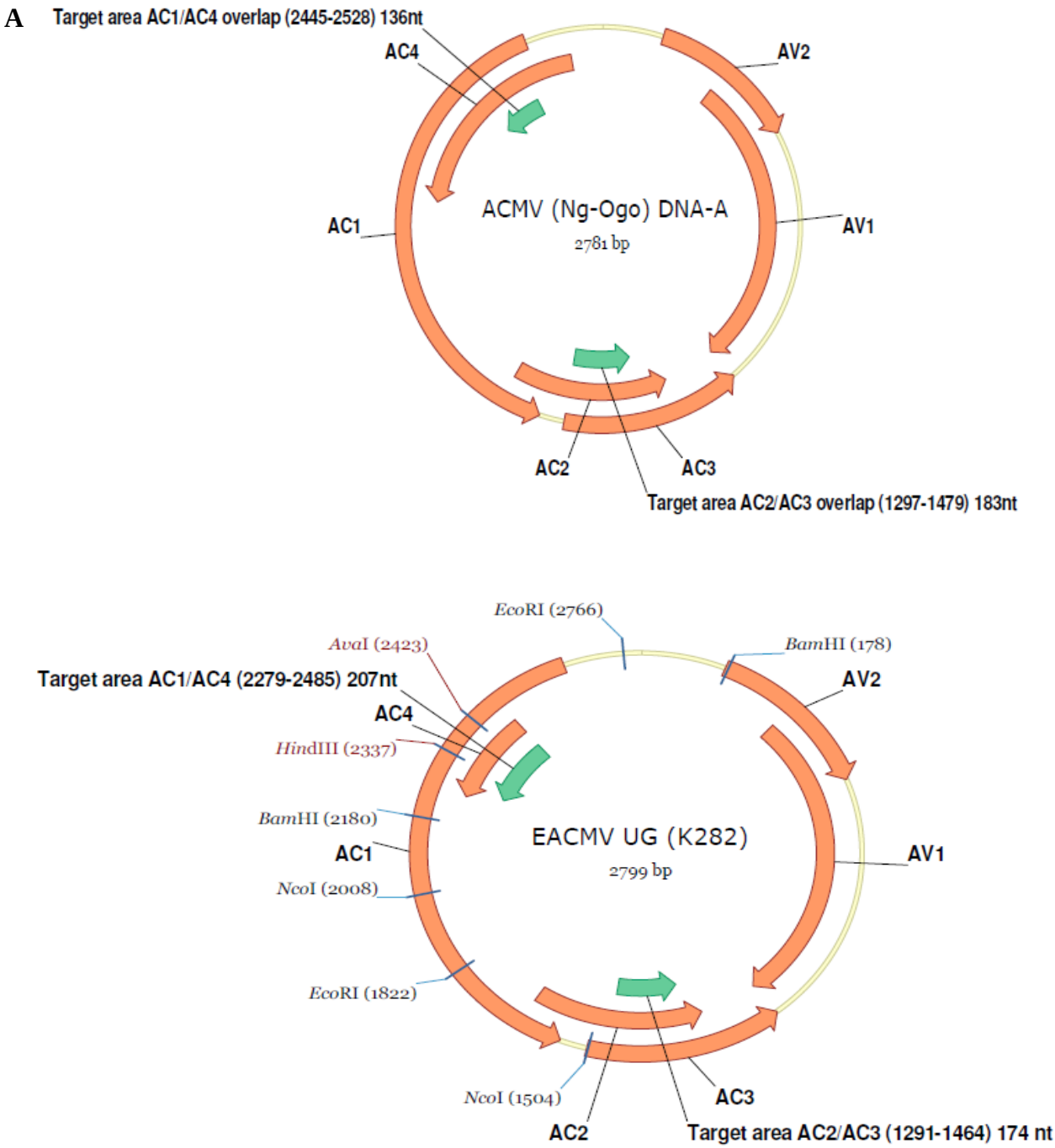


Figure 2. 7 (a) Diagrams of ACMV-[NG:Ogo:90] DNA-A AC1/AC4 (136 nt) and AC2/AC3 (183 nt) and **(b)** EACMV-[UG2] DNA-A AC1/AC4 (207nt) and AC2/AC3 (174 nt) showing regions that were targeted for efficient siRNA production (targeted areas on the 2 DNA-A molecules shown in green).

2.5.2 Mutated sense-arm hairpin RNA silencing constructs

2.5.2.1 Amplification of the target ORF and fusion of fragments to make the hybrids

All four regions were successfully amplified from the full length reference clones ACMV ([NG:Ogo:90]) and EACMV-[UG2]. Fragment size of 136 nt was amplified for ACMV AC1/4, 183 nt for ACMV AC2/3, 207 nt for EACMV AC1/4 and 174 nt for EACMV AC2/4 (fig 2.8). Fragments were successfully cloned into pTZR5/T (Fermentas).

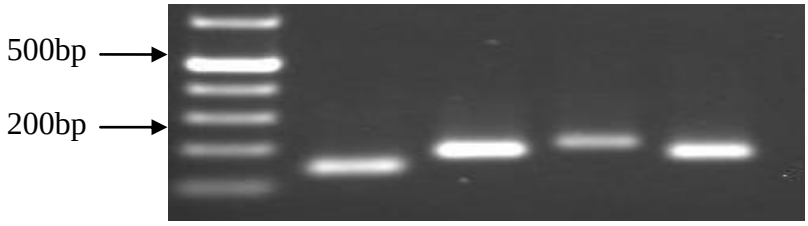


Figure 2. 8 1.2% agaraose gel electrophoresis of PCR amplified targer ORF; 136 bp ACMV AC1/AC4 (lane 2), 183 bp ACMV AC2/AC3 (lane 3), 207 bp EACMV AC1/AC4 and 174 bp EACMV AC2/AC3 (lane 5) and (lane 1) O'GeneRuler 1kb Plus DNA ladder (Fermentas).

2.5.2.2 Fusion of fragments to create hybrids

Following cloning, target ORF fragments were re-amplified from the clones. However primer-introduced modifications were included to facilitate fusion of the target ORF. Fusion/hybrid fragments, 343 bp Hybrid I fragment (fig 2.9 lane 4), 319 bp Hybrid II (fig 2.9 lane 7) and 381 bp hybrid III fragment (fig 2.9 lane 10), were generated. Fragments were also successfully cloned into pTZR5/T (Fermentas).

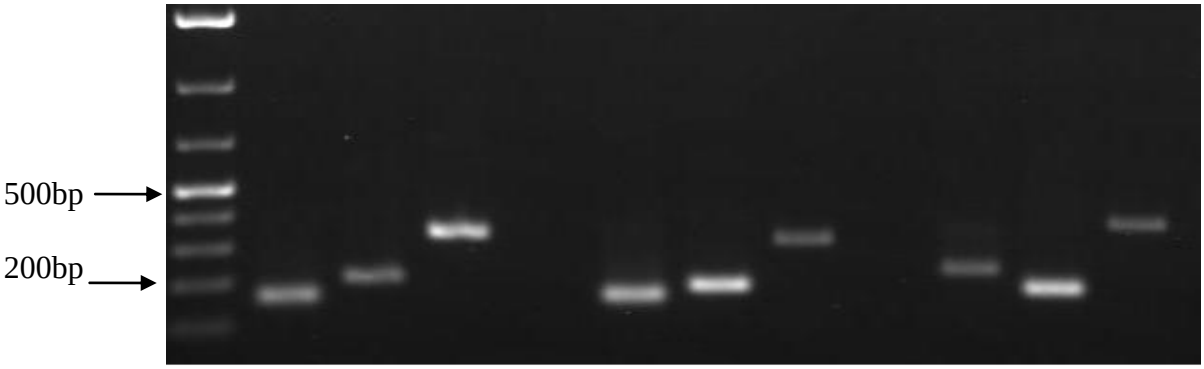


Figure 2. 9 1.2% agarose gel showing fusion of ORF used to create Hybrid fragments. Fermentas O'GeneRuler 1 kb Plus DNA ladder (lane 1). ACMV AC1/AC4, 136 bp fragment (lane 2), 207 bp EACMV AC1/AC4 fragment (lane 3), fusion of lane 2 and 3 amplicons to yield ~343 bp Hybrid I fragment (lane 4). ACMV AC1/AC4, 136 bp fragment (lane 5), ACMV AC2/AC3, 183 bp fragment (lane 6), fusion of lane 5 and 6 fragment to yield a ~319 bp Hybrid II fragment (lane 7). EACMV AC1/AC4, 207 bp fragment (lane 8), EACMV AC2/AC3, 174 bp fragment (lane 9), fusion of lane 8 and 9 fragments to yield ~381 bp hybrid III fragment (lane 10).

2.5.2.3 Sodium bisulfite treatment of hybrid fragments and sequence analysis for C-T mutations in the sequence

Preferential amplification of mutated hybrid fragments was successful using the modified primers containing few C-T base changes in the F primer and G-A base changes in the R primer. PCR amplification could only be achieved from fusion products sodium bisulfite treated for 15min. Therefore in our study 15min bisulfite treatment of products was the optimal time. Preferentially amplified mutated fragments were cloned into pTZR5/T (Fermentas) and sequenced. Mutated hybrid I mutagenesis showed 81 % C-T (38/47 C-T mutations). There was an overall 11% change in the 343 bp Hybrid I fragment, however the cloned and sequenced mutated Hybrid I fragment also contained 1 undesirable G-A mutation. Mutated Hybrid II had 56% C-T mutation (29 out of 52 C's were converted to T's). There was an overall 9% change in the 319 bp Hybrid II sequence. Mutated hybrid III mutagenesis showed 78% C-T (59/76 C mutation to T's), representing an overall 16% change 381 bp Hybrid III sequence.

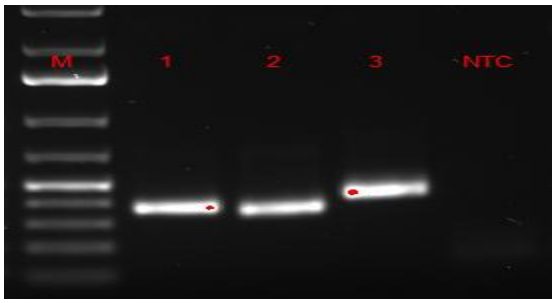


Figure 2. 10 1% agarose gel electrophoresis of mutated hybrid fragments amplified from 15min bisulfite treated original hybrid fragments, fragments were clones into pTZR5/T (Fermentas). Fragments were amplified using the mutated modified forward and reverse primers for each Hybrid. M= O'Gene 1kb Plus DNA ladder (Fermentas), mutated 361 bp Hybrid I amplicon (lane 1), mutated 337 bp Hybrid II amplicons (lane 2), mutated 399 bp Hybrid III amplicon (lane 3) and NTC (lane 4).

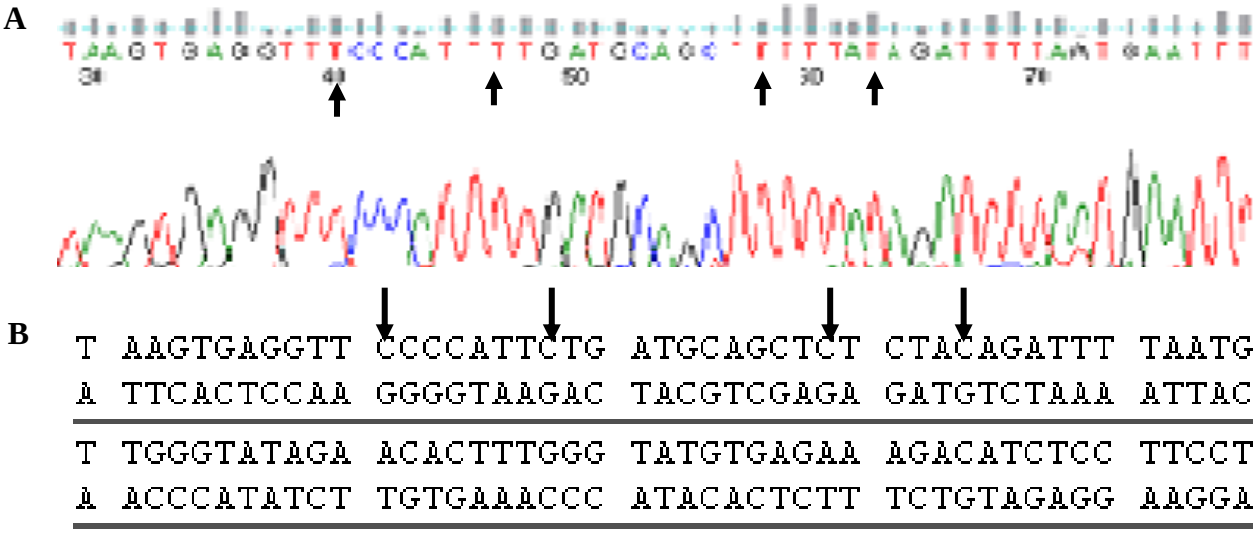


Figure 2.11 (a) A segment of a chromatogram for one of the sequenced clones, with arrows showing points along the Hybrid sequence were C-T mutations were introduced. **(b)** Original Hybrid sequence prior C-T mutations. Arrows are showing Cs that corresponds with the changed T in fig. 2.11b.

2.5.2.4 Ligation of nonmutated original hybrid fragment and the mutated hybrid fragment required to make the IR.

Ligation of the mutated and non-mutated hybrid fragments generated. I-IR, II-IR and III-IR and these were cloned into pTZ57R/T. Putative IR clones were screened with enzymes *Xho*I and *Xba*Iand expected fragment size of 704 bp for I-IR, 656 bp fragment for II-IR and 780 bp for III-IR were obtained **(fig. 2.12,** III-IR digest not shown on gel**)**.

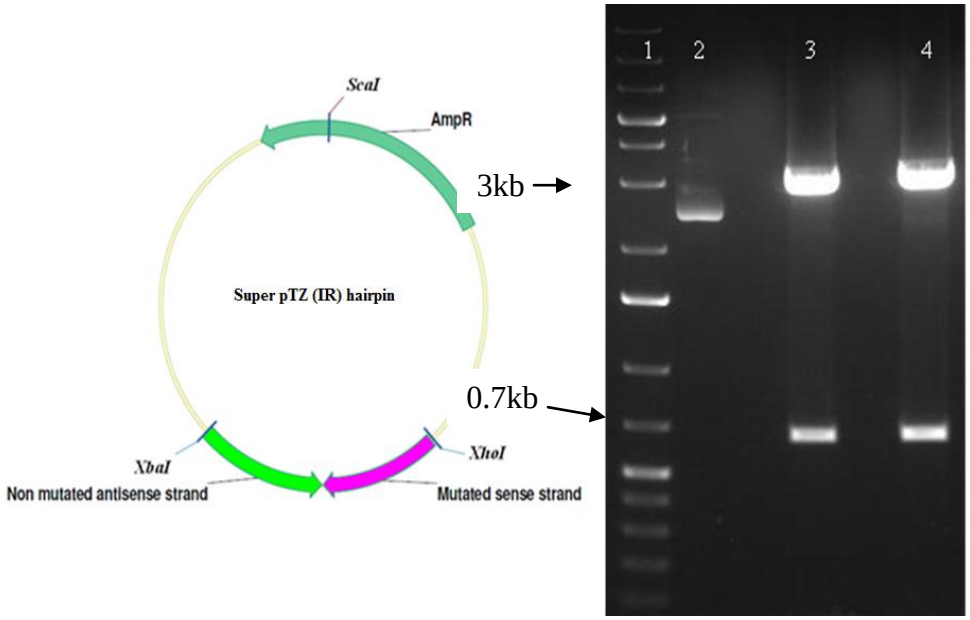


Figure 2. 12 1% agarose gel showing IR clones digested with *Xba*I and *Xho*I to screen clones for successful IR formation following ligation of mutated Hybrid fragment and non-mutated hybrid fragment. Lane 1= O'GeneRuler 1 kb Plus DNA ladder, *Xba*I and *Xho*I restricted empty pTZ57R/T vector (lane 2), 701 bp I-IR released fragment (lane 4), 656 bp II-IR released fragment (lane 3).

2.5.2.5 Ligation of IR into pART7

*Xba*I and *Xho*I digested IR clones were sub-cloned and ligated into expression vector pART7. Clones containing the expected IR fragment sizes of 701 bp for I-IR and 656 bp for II-IR and 780 bp for III-IR selected (gel not shown). Selected clones were also screened using *Not*I. *Not*I releases the entire expression cassette (CaMV35S promoter, target IR and the 765 bp terminator)

Expected size for *Not*I digested I-IR clone was 2811 bp, *Not*I digested II-IR clone released a 2766 bp and 2890 bp fragment was released following *Not*I digest of III-IR clone **(fig. 2.13).**

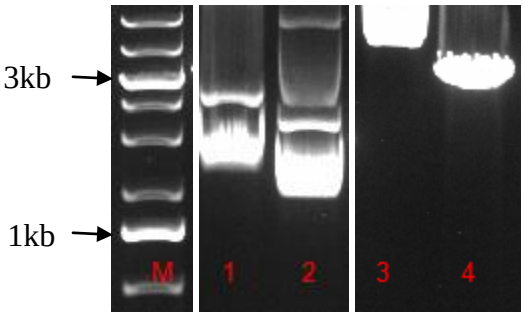


Figure 2. 13 1% agarose gel, screening clones for successful ligation of IR into expression vector pART7, *Not*I digest of IR clones, M= O'GeneRuler 1kb DNA ladder, I-IR cassette (lane 1), II-IR cassette (lane 2), undigested pART7 expression vector (lane 3) and linearised pART7 expression vector (lane 4).

2.5.2.6 Sub-cloning of IR into plant transformation vector pCAMBIA 1305.1

Final destination vector for IR expression cassettes was plant transformation vector pCAMBIA 1305.1. To facilitate sub-cloning of the expression cassette into p1305.1, entire 2811 bp amplicon for I-IR, 2766 bp for II-IR and 2890 bp for III-IR were amplified and **(fig. 2.14)** and products T/A cloned into pTZR5/T. Successful ligation into p1305.1 was confirmed by PCR amplification of the mutated and non-mutated hybrid fragments. Plasmid of clones containing the entire completed RNA silencing hairpin construct (MM1hp, MM2hp and MM3hp) was then ready to be used for transformation *Agrobacterium* LBA4404 **(fig 2.15)**.

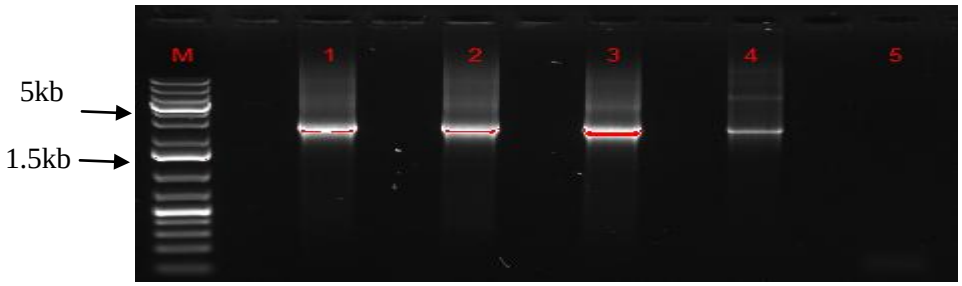


Figure 2. 14 0.8% agarose gel electrophoresis. IR expression cassettes PCR amplification using pART7 cassette primers. M= O'GeneRuler 1kb Plus DNA, 2811 bp I-IR cassette amplicon (lane 1), 2766 bp II-IR cassette amplicon (lane 2), 2890 bp III-IR cassette amplicon (lane 3), 2178 bp amplicons amplified from empty pART7 expression vector (lane 4) and NTC (lane 5).

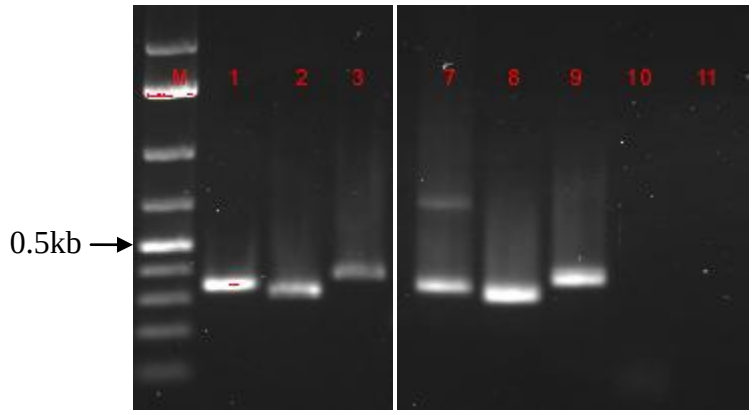


Figure 2. 15 1% agarose gel, PCR amplification to screen for successful ligation and presence of IR cassette in plant transformation vector p1305.1. M= O'GeneRuler 1kb Plus DNA ladder (Fermentas), I-IR cassette; 343 bp non-mutated fragment (lane 1), I-IR cassette; 361 bp mutated fragment (lane 7), II-IR cassette 319bp non-mutated fragment (lane 2), II-IR cassette 337 bp mutated fragment (lane 8) and III-IR cassette; 381bp non-mutated fragment (lane 3) and 399 bp mutated fragment (lane 9). Empty p1305.1 vector (lane 10) and NTC (lane 11).

2.5.2.7 SACMV BC1 (MM4hp) construct

The SACMV BC1 mutated sense-arm hairpin construct was mobilised from the more virulent *Agrobacterium Agl*1 strain (Taylor *et al*., 2012c) to *Agrobacterium* LBA4404 for cassava transformation purposes. Successful plasmid mobilisation was confirmed by amplification of a 221 bp non-mutated fragment however amplification of the 239 bp mutated fragment was unsuccessful. Amplification of IR fragments is often problematic due to tight secondary

structures and therefore we proceeded with *Agrobacterium* LBA4404 transformation of cassava FEC.

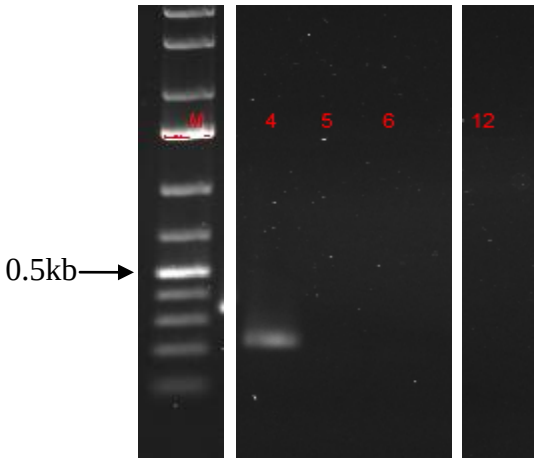


Figure 2. 16 1.2% agarose gel electrophoresis to confirm presence of SACMV BC1 construct. M= O'GeneRuler 1kb Plus DNA ladder (Fermentas), SACMV BC1 non-mutated 221 bp IR arm amplified from extracted SACMV BC1 construct (lane 4). PCR amplification of mutated 239 bp SACMV BC1 IR arm was unsuccessful (lane 12), NTC (lane 5) and empty p1303 vector (lane 6).

2.5.2.8 Transformation of constructs into *Agrobacterium* LBA4404

All four (MM1hp, MM2hp, MM3hp and MM4hp) constructs were successfully mobilised into LBA4404. Transformation success was confirmed by PCR amplification of the Hyg, GUS and insert gene (fig 2.17).

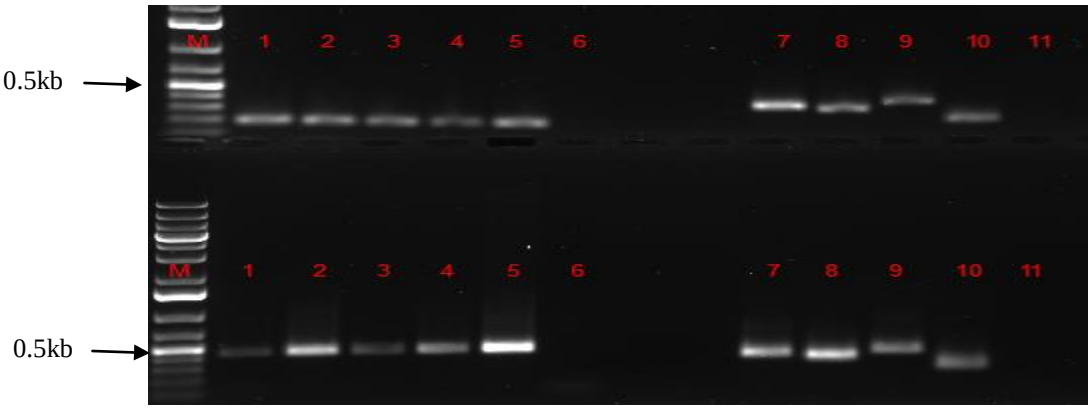


Figure 2. 17 PCR amplification of Hyg, GUS and insert genes to screen for construct transformation success in *Agrobacterium* LBA4404. **(a)** M= 1kb ladder (Fermentas), amplification of 181 bp *GUS* gene in MM1hp, MM2hp, MM3hp, MM4 hp (lane 1-4 resp), positive control (lane 5) and NTC (lane 6). Amplification of 343 bp non-mutated fragment of MM1hp (lane 7), 319 bp non-mutated fragment of MM2hp, 381 bp non-mutated fragment of MM3hp (lane 8), 221 bp non-mutated fragment of MM4hp (lane 10) and NTC (lane 11) **(b)** M= 1 kb ladder Fermentas), amplification of *Hyg* gene (485bp) 3 in MM1hp, MM2hp, MM3hp and MM4 hp (lane 1-4 resp), positive control (lane 5) and NTC (lane 6), amplification of 361 bp mutated fragment of MM1hp (lane 7), 337 bp mutated fragment of MM2hp (lane 8), 399 bp non-mutated fragment of MM3hp (lane 9), 239 bp mutated fragment of MM4hp (lane 10) and NTC (lane 11).

2.5.3 Non-mismatched (Gateway) RNA silencing hairpin constructs

2.5.3.1 PCR incorporation of *Xho*I and *Xba*I restriction sites and fragment ligation into pHellgate 8

*Xba*I and *Xho*I-containing amplicons for MM5hp, MM6hp, MM7hp and MM8hp were successfully amplified . A 365 bp MM5*Xba*I and 365 bp MM5*Xho*I fragment were amplified for MM5hp construct **(fig. 2. 19a)**. A 331 bp MM6*Xba*I and 331 bp MM6*Xho*I fragment were amplified for MM6hp construct **(fig. 2. 19b)**. A 393bp MM7*Xba*I and 393 bp MM7*Xho*I fragment were amplified for MM7hp construct **(fig. 2. 19c).** A 232 bp MM8*Xba*I and 232 bp MM8*Xho*I fragment were amplified for the MM8hp construct **(fig. 2. 19d)**.

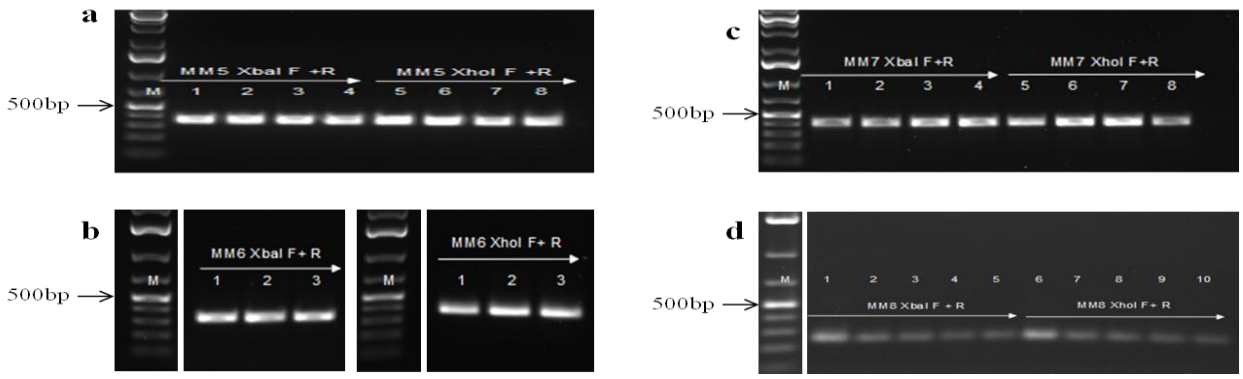


Figure 2. 18 **(a**) Amplification of 365 bp MM5 *Xba*I fragment (lanes 1-4) and amplification of 365 bp MM5 *Xho*I fragment (lanes 5-8). **(b)** Amplification of 331 bp MM6 *Xba*I fragment (lanes 1-3) and amplification of 365 bp MM5 *Xho*I fragment (lanes 1-3). **(c)** Amplification of 393 bp MM7 *Xba*I containing fragment (lanes 1-4) and amplification of 393 bp MM7 *Xho*I containing fragment (lanes 5-8). **(d)** Amplification of 232 bp MM8 *Xba*I fragment (lanes 1-5) and amplification of 232 bp MM8 *Xho*I containing fragment (lanes 6-10). M= O'GeneRuler 1 kb Plus DNA ladder (Fermentas).

2.5.3.2 *Xba*I ligation into pHellsgate 8 vector

The site-specific recombinase method was not utilised to replace the *ccdB* gene sites with the target genes. Instead conventional restriction and ligation was used. The *ccdB* gene fragment flanked by *Xba*I sites was digested out, releasing a 1428 bp fragment **(fig. 2. 20)**. The resulting linear dephoshorylated plasmid (~16kb) from each digestion reaction was gel extracted and gel purified and *Xba*I containing fragment for each construct ligated into the linear vector. Amplicons generated from plasmid P27-3 primer and *Xba*I reverese primer combination suggested correct ligation orientation. For MM5, only one clone was obtained, clone g (lane 7), a 468 bp amplicon was produced, the other clones were empty (fig. 2. 21 a). For MM6, 3 clones producing a 434 bp amplicon were selected (lanes 1,2 and 4) (fig. 2. 21 b). A 496 bp amplicon could be amplified in 5 MM7 clones (lanes 1, 4, 5, 6, 8) (fig. 2. 21 c). A 335 bp fragment was correctly amplified in 3 of the MM8 clones (fig. 2.21 d). One clone for each construct was selected for downstream *Xho*I restriction digest and ligation of the *Xho*I arm required to complete the hairpins. Selected clones were labelled as MM5*Xba*I-pH8, MM6*Xba*I-pH8, MM7*Xba*I-pH8 and MM8*Xba*I-pH8.

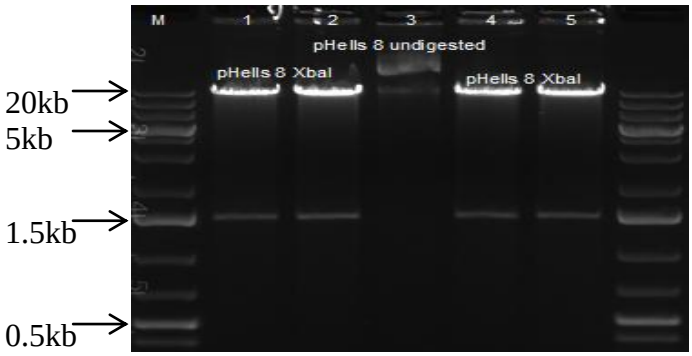


Figure 2. 19 Extracted pHellsgate 8 plasmid restricted with *Xba*I (lane 1, 2, 4, 5) and undigested pHellsgate 8 (lane 3). M= O'GeneRuler 1 kb Plus DNA ladder (Fermentas).

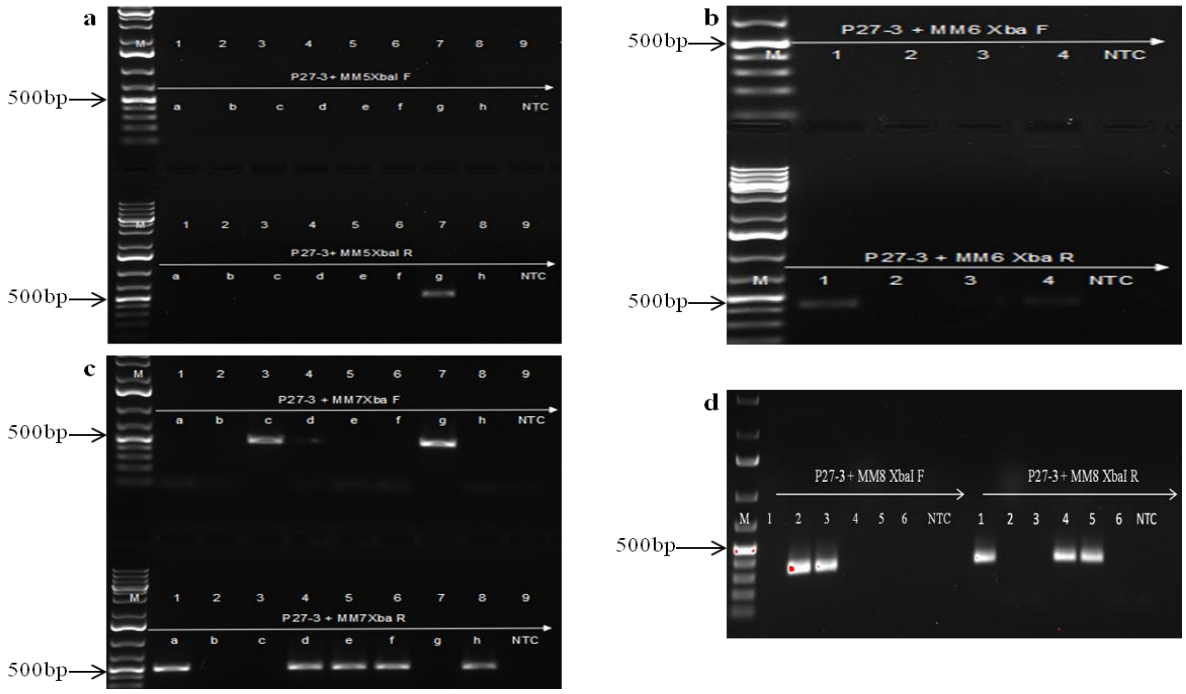


Figure 2. 20 1% agarose gel electrophoresis, showing MM5XbaI-pH8, MM6XbaI-pH8, MM7XbaI-pH8 and MM8XbaI-pH8 clones containing the correct size construct *Xba*I insert in the desired orientation. Screening of the clones was done using the respective target insert *Xba*I R primer in conjunction with the plasmid P27-3 primer. The P27-3 primer added 103 bp to the expected target insert size. **(a)** Correct MM5 clone g (lane 7) yielded the expected 468 bp fragment. **(b)** Lane 1, 3 and 4 with correct 434 bp MM6 fragment. **(c)** Clones MM7 a, d, e, f and h produced the expected 496 bp amplicon. **(d)** Clones in lane 1, 4 and 5 are correct, 335 bp amplicon. M= O'GeneRuler 1 kb Plus DNA ladder.

2.5.3.3 Ligation of the *Xho*I arm of the hairpin replacing the 2nd *ccdB* gene

Clones MM5*Xba*I-pH8, MM6*Xba*I-pH8, MM7*Xba*I-pH8 and MM8*Xba*I-pH8 were restricted with *Xho*I to remove the other *ccdB* gene to allow for insertion of the *Xho*I arm of the hairpin. Clones were screened using the respective insert *Xho*I R primer and the plasmid P23-5 primer combination. Two positive clones containing the MM5*Xba*I: *XhoI*-pH8 hairpin for the MM5hp construct, these 2 clones produced the expected 446 bp amplicon **(fig. 2. 22a)**. All 8 clones screened for MM6 *Xho*I were positive for the 412 bp amplicon **(fig. 2. 22b)**. Four positive were obtained for MM7*Xho*I, expected 474 bp amplicon, and 1 of the 5 clones had no insert **(fig. 2. 22c)**. For MM8*Xho*I, all 8 clones screened were positive for the 313 bp **(fig. 2. 22d)**. One from each was selected for further downstream processing and these clones were labelled MM5*Xba*I: *XhoI*-pH8, MM6*Xba*I: *XhoI*-pH8, MM7*Xba*I: *XhoI*-pH8 and MM8*Xba*I: *XhoI*-pH8.

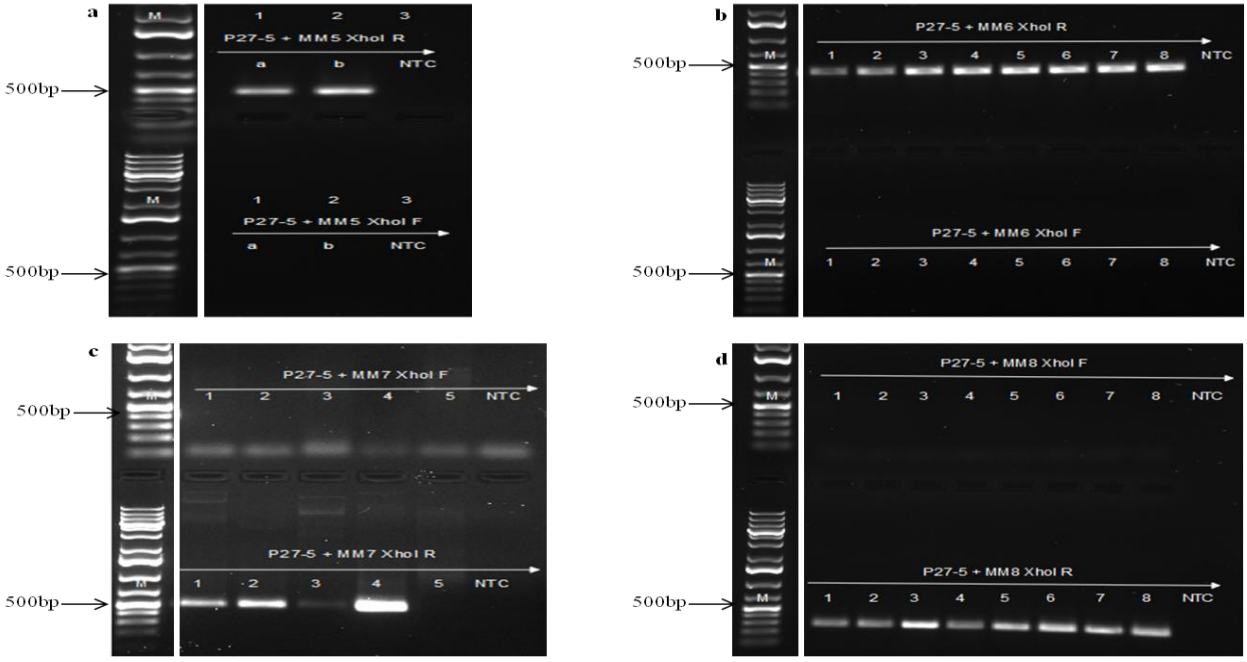


Figure 2. 21 1% agarose gel electrophoresis, showing PCR screening of clones for the *Xho*I hairpin arm **(a)** 474 bp fragment was amplified from MM5*Xba*I: *Xho*I-pH8 clones 1 and 2 (lane 1, 2). **(b)** MM6*Xba*I: *Xho*I-pH8 screened clones with the expected 412 bp fragment. **(c)** MM7*Xba*I: *XhoI*-pH8 clones 1-4 with the right size 474 bp insert. **(d)** MM8*Xba*I: *XhoI*-pH8 clones 1-8, all with the right size 313 bp fragment. M=O'GeneRuler 1 kb Plus DNA ladder

2.5.3.4 *Not*I digestion of pHellgate 8 hairpins and ligation into pCambia 1305.1

pHellsgate 8 hairpins; MM5*Xba*I: *XhoI*-pH8, MM6*Xba*I: *XhoI*-pH8, MM7*Xba*I: *XhoI*-pH8 and MM8*Xba*I: *XhoI*-pH8 were sub-cloned into plant transformation vector pCAMBIA 1305.1, as the other 4 mutated sense-arm hairpin silencing constructs (designed in **2.4.2**) were cloned into this plant transformation vector.

*Not*I digestion of control original 17485 bp pHellsgate 8 produced 2 fragments; 11667 bp vector backbone fragment and a 5818 bp fragment that lies with the 2 *Not*I restriction sites (**fig. 2. 23a**, lane 2). *Not*I digest of MM5*Xba*I: *XhoI*-pH8 produced the 11667 bp vector backbone fragment as well as a 3689 bp hairpin cassette (CaMV35S promoter, the two 365 bp sense and antisense hairpin arms and the OCS terminator) (**fig. 2. 23b**, lane 1). *Not*I digest of MM6*Xba*I: *XhoI*-pH8 produced the vector backbone fragment and a 3621bp hairpin cassette (CaMV35S promoter, the two 331 bp sense and antisense hairpin arms and the OCS terminator) (**fig. 2. 23c**, lane 6-8). MM7*Xba*I: *XhoI*-pH8 *Not*I digest produced the vector backbone fragment and the 3745bp hairpin cassette (CaMV35S promoter, the two 393 bp sense and antisense hairpin arms and the OCS terminator) (**fig. 2. 23a**, lane 4). *Not*I digest of MM8*Xba*I: *XhoI*-pH8 released the 3423 bp hairpin cassette (CaMV35S promoter, the two 232 bp sense and antisense hairpin arms and the OCS terminator and the 14626 bp vector backbone (**fig. 2. 23c**, lane 1-3). Plant transformation vector pCambia 1305.1 was simultaneously double digested using *Hind*III and *EcoR*I and dephosphorylated (**fig. 2. 23c**, lane 10-11). Linear dephosphorylated p1305.1 was gel extracted and purified and made ready for ligation of the hairpin cassettes into the MCS of the vector.

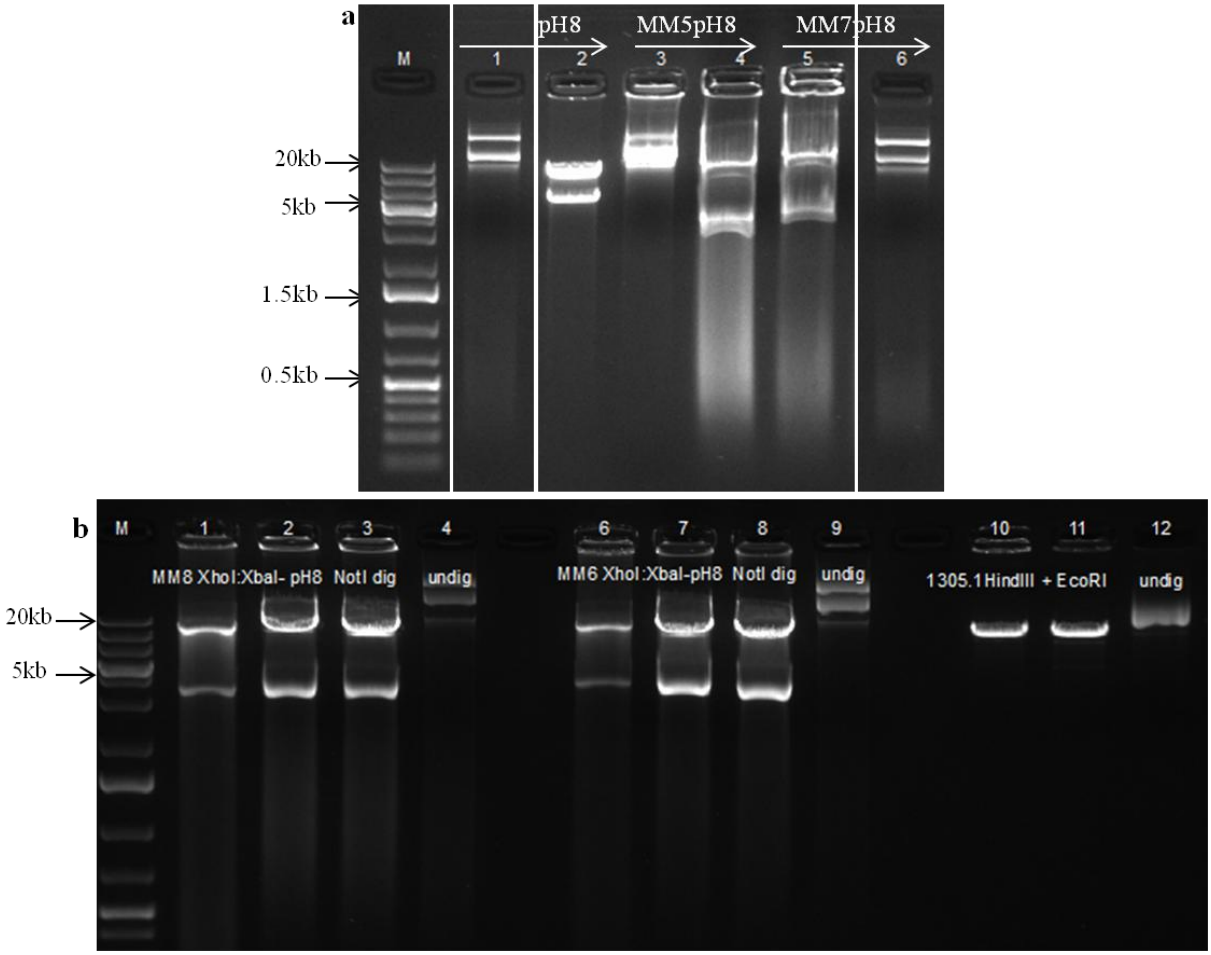


Figure 2. 22 1% agarose gel electrophoresis, showing *Not*I digestion of pHellsgate hairpin cassettes. M= O'GeneRuler 1 kb Plus DNA ladder (Fermentas). **(a)** Undigested original pHellsgate 8 plasmid (lane 1) and *Not*I digestion of pHellsgate 8 (lane 2). Undigested MM7*Xba*I: *XhoI*-pH8 hairpin (lane 3). *Not*I digested MM7*Xba*I: *XhoI*-pH8 releasing a 3745 bp MM7 hairpin cassette (lane 4). **(b)** *Not*I digested MM5*Xba*I: *XhoI*-pH8 releasing a 3689 bp MM5 hairpin cassette (lane 1). **(c)** *Not*I digested MM8*Xba*I: *XhoI*-pH8 releasing a 3423 bp MM8 hairpin cassette (lane 1-3) and undigested MM8*Xba*I: *XhoI*-pH8 (lane 4). *Not*I digested MM6*Xba*I: *XhoI*-pH8, releasing a 3621 bp MM8 hairpin cassette (lane 6-8) and undigested MM6*Xba*I: *XhoI*-pH8 (lane 9). *Eco*RI and *Hind*III double digest of plant transformation vector p1305.1 (lane 10 and 11) and undigested pCambia 1305.1 (lane 12).

2.5.3.5 Screening of completed hairpin constructs prior to DNA sequencing

Prior to sending hairpin construct clones off for sequencing, PCR verification and restriction enzyme digestion was performed on the clones once more to confirm presence and orientation of the hairpin arms and the entire hairpin cassette. This was also done to confirm that the hairpin cassettes had been successfully ligated into plant transformation vector pCambia 1305.1.

Restriction digest screening

Restriction digestion of the MM5hp construct clone with *Xba*I and *Xho*I confirmed that the target inserts were present. The two 365 bp fragments corresponding to the sense and anti-sense arms of the MM5hp construct were released by digestion with *Xba*I and *Xho*I **(fig. 2. 24a, lane 1 and 2)**. The entire 3689 bp hairpin cassette was also released after *Not*I digestion of the hairpin clone **(fig. 2. 24a, lane 3)**.

Both *Xba*I and *Xho*I restriction digestion of MM6hp construct clone released the two 331 bp insert fragments corresponding to the sense and anti-sense arms of MM6hp construct **(fig. 2. 24b lane 2 and 3)**. Digestion of the clone with *Not*I released the expected 3621 bp hairpin cassette **(fig. 2. 24b, lane 4)**.

Restriction digestion of MM7hp construct clone with *Xba*I and *Xho*I released the expected two 393 bp fragments corresponding to the sense and antisense arms of the hairpin construct **(fig. 2. 24b, lane 6 and 7)**. *Not*I restriction digestion of the clone released the 3745 bp hairpin cassette **(fig. 2. 24b, lane 8)**.

*Xba*I and *Xho*I restriction digestion of the MM8hp construct clone released the two 232 bp fragments corresponding to the sense and anti-sense arm of the hairpin construct **(fig. 2. 24b, lane 10 and 11)**. *Not*I restriction digestion of the hairpin construct clone released the expected 3423 bp hairpin cassette **(fig. 2. 24, lane 12)**.

Control pHellsgate 8 restriction digestions with *Xba*I and *Xho*I was also performed and fragments corresponding to the 1428 bp of the sense *ccdB* gene was observed and the 1431bp fragment corresponding to the anti-sense ccdB gene fragment was seen (**fig. 2. 24b, lane 15 and**

16). *Not*I restriction digestion released the 5818 bp fragment consisting of the CaMV35S promoter, the two *ccdB* genes and the OCS terminator **(fig. 2. 24b, lane 16)**.

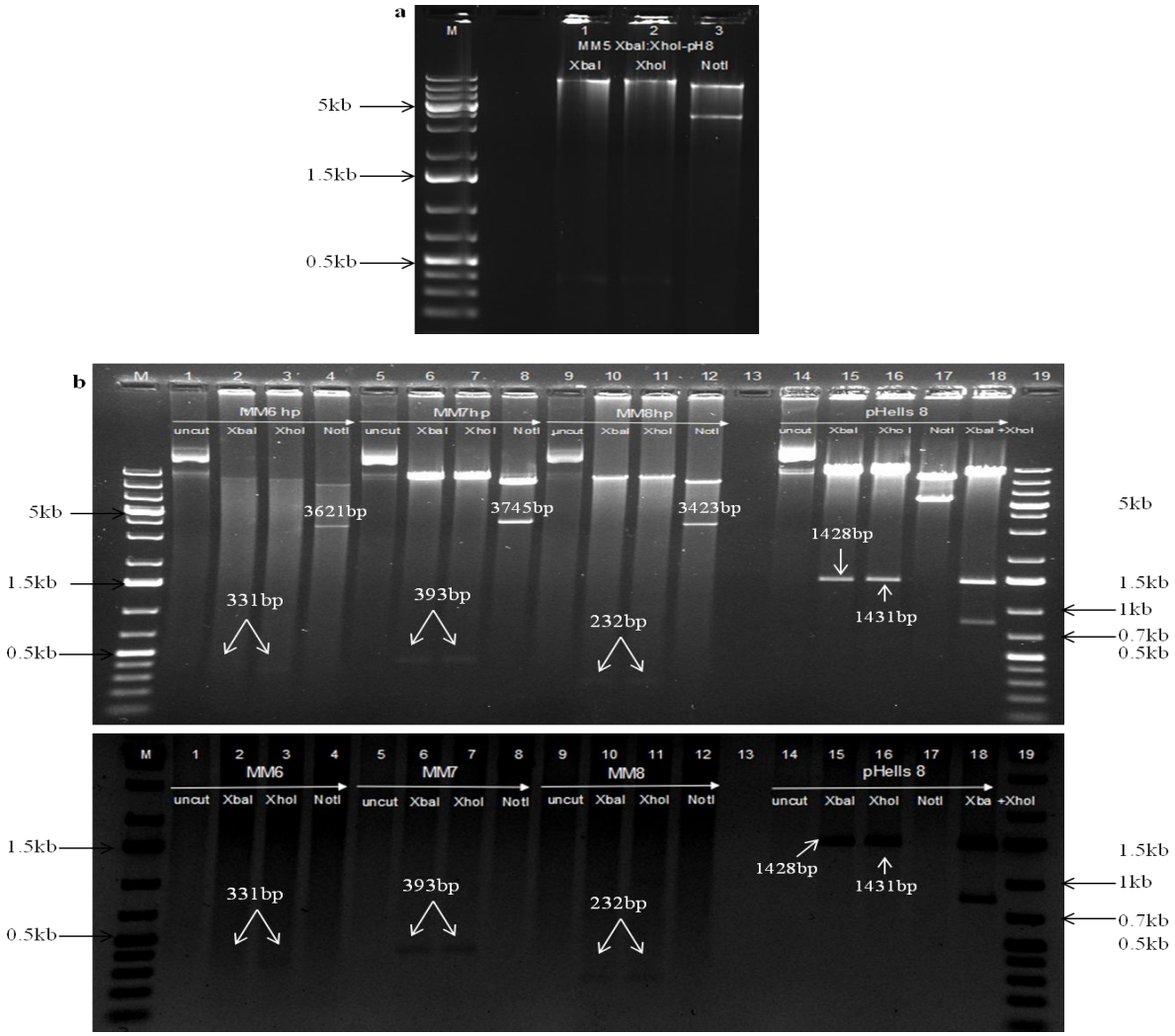


Figure 2. 23 Restriction digestion of clones to confirm correct design and construction of the hairpin constructs. M= O'GeneRuler 1kb Plus DNA ladder (Fermentas) **(a)** MM5 hairpin clone, digested with *Xba*I (lane 1), *Xho*I (lane 2) and *Not*I (lane 3). **(b)** MM6 hairpin clone, digested with *Xba*I (lane 2), *Xho*I (lane 3) and *Not*I (lane 4). MM7 hairpin clone, digested with *Xba*I (lane 6), *Xho*I (lane 7) and *Not*I (lane 8). MM8 hairpin clone, digested with *Xba*I (lane 10), *Xho*I (lane 11) and *Not*I (lane 12). pHellsgate 8 control *Xba*I, *Xho*I and *Not*I digestion (lane 15-18). Bottom gel is the inverted image to help with visualisation of bands. Undigested MM6hp, MM7hp MM8hp and pHellsgate 8 in lanes 1, 5, 9 and 14, respectively.

PCR screening

Following restriction enzyme screening, hairpin construct clones were PCR screened once again before sequencing. PCR screening was used to validate correct insert orientation and to once again confirm that hairpin cassettes had been successfully ligated into p1305.1 before immobilising hairpin constructs into *Agrobacterium* LBA4404. To verify correct orientation, clones were screened once again with the plasmid primer and the insert reverse primer for both the *Xba*I and *Xho*I inserts. MM5hp construct screening with the primers amplified the expected 446 bp and 468 bp fragments **(fig. 2. 24a, lanes 1-3 and 4-6)**. MM6hp construct screening amplified a 412 bp and 434 bp fragment **(fig. 2. 24b, lanes 1-4)**. MM7hp construct screening amplified a 474 bp and 496 bp fragment **(fig. 2. 24b, lanes 5-8)**. Amplification from MM8hp construct amplified a 313 bp and 335 bp fragment **(fig. 2. 24b, lanes 9-12)**.

Plant transformation vector p1305.1 primers amplifying the 465 bp HygII gene fragment and 181 bp GUS gene fragment were used to complete the screening process of the MM5hp, MM6hp, MM7hp and MM8hp constructs. Both fragments were successfully amplified in all construct clones and the positive controls **(fig. 2. 24 c)**.

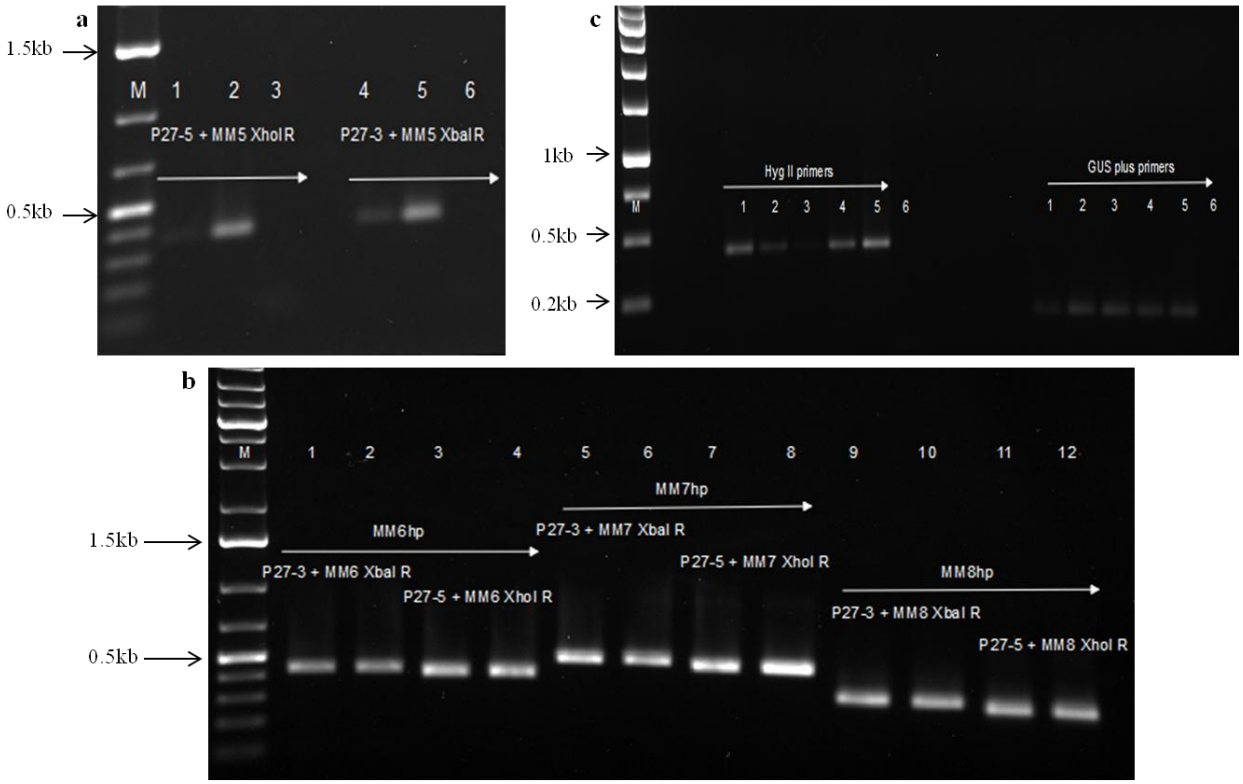


Figure 2. 24 PCR amplification to screen for presence and orientation of inserts in the completed hairpin constructs. O'GeneRuler 1kb Plus DNA (Fermentas) **(a)** MM5hp *Xho*I (446 bp) and *Xba*I (468 bp) amplicons. **(b)** MM6 *Xba*I (434 bp) and *Xho*I (412 bp) amplicons (lanes 1-4). MM7hp *Xba*I (496 bp) and *Xho*I (474 bp) amplicons (lanes 5-8). MM8hp *Xba*I (335 bp) and *Xho*I (313 bp) amplicons (lanes 9-12). **(c)** Amplification of 465 bp *Hyg*II gene fragment from construct MM5hp, MM6hp, MM7hp and MM8hp and positive 1305.1 control plasmid (lanes 1-5, resp) and 181 bp *GUS* gene fragment from MM5hp, MM6hp, MM7hp and MM8hp and positive 1305.1 control plasmid (lanes 1-6, resp).

2.6 Discussion

The overall objective of this study was to engineer geminivirus resistance cassava using RNA silencing hairpin constructs derived from SACMV or ACMV open reading frames. We employed two different design methods; mutated sense-arm RNA silencing hairpin and the more conventional intron-containing RNA silencing hairpin technology. Four sense strand-mutated transgene constructs (MM1hp-MM4hp) and four Gateway-based (pHellsgate8) hairpin were successfully constructed (MM5hp-MM8hp). Constructs were designed to target multiple ORFs from the same species as this method has been showed to be more efficient than single ORF targeting constructs. Hybrid constructs targeting ORF of different species were designed to try and address the severity of losses experienced from mixed infections as to offer multiple species resistance. Regions were also targeted because begomovirus AC2 and AC4 have been identified as PTGS suppressors.

Variation in DNA-A of ACMV and EACMV isolates

Due to CBV sequence conservation, the nature and spread of cassava infecting geminivirus and the severe losses reported from mixed virus infections, constructs were designed to target multiple species and strains (Harrison *et al.*,1997; Pita, Fondong, Sangar, *et al.*, 2001). Sequence variation in the DNA-A of ACMV isolates was found to be lower irrespective of the geographical location. However the same was not observed when sequences of DNA-A of EACMV isolates were aligned. High variation in DNA-A of EACMV isolates was also observed by Zhou *et al*. (1997). Pita *et al.* (2001) attributed the high variation seen in EACMV DNA-A to the high recombination frequency. Alignment of the AC1/4 of the 6 EACMV isolates was found to have less variation than the AC2/3 region. Our results are similar to those observed by Fondong *et al.*, 2000 from the alignment of EACMV Tanzania. Recombination maps of EACMV DNA-A showed AC2/3 to be a recombination hotspot and hence the reason for the high variation observed. Regions of ACMV and EACMV showing higher sequence conservation were targeted.

Target sequence selection for efficient siRNA production

A programme called siRNA Scan programme was used. The aim of the programme is to predict regions within the identified conserved sequence where efficient siRNA are generated (Xu *et al.*, 2006b, http://bioinfo2.noble.org/RNAiScan.htm). This was done to ensure that only regions

offering maximum silencing efficiency were selected. This ensured that the final dsRNA hairpin length was as short as possible. Short hairpins were preferred even though the successful use of long dsRNA in plant systems has been reported (Lu *et al*., 2004; Tenllado *et al.*, 2001; Vanitharani *et al*., 2003). Expression of long dsRNA is more unfavourable in animal systems. Another more crucial reason for using shorter target sequences as possible was to reduce possible off-target silencing effects (Pang *et al.*, 1997).

Sodium bisulfite treatment for deamination of cytosine to thymine (C-T)

Sodium bisulfite treatment is commonly used in applications for studying DNA methylation patterns; however in this study sodium bisulfite was used for introducing C to T (C-T) mutations in the sense-arm of hairpin RNA silencing constructs. This is the second report of bisulfite treatment application for use in hairpin RNA silencing technology. Designing intron containing RNA silencing hairpin constructs is the most commonly used technology for producing hairpin constructs. An intron positioned within the sense and antisense arms has been reported to be important in allowing correct hairpin folding (Smith *et al.*, 2000). It is also believed that the intron helps in stopping the formation of cruciform structures known to occur in IR sequences (Eichman *et al.*, 2000).

In this research, introns-containing hairpins as well as non-intron (mutated sense-arm) hairpins were explored. It was shown by Taylor *et al.*, 2012c that introduction of C-T mutations in the sense-arm of the hairpin disrupts the perfect complementarity of the IR sequences and therefore stops the formation of cruciform structures. C-T mutations were achieved by exposing the target sequence to sodium bisulfite. Exposure of sequence to sodium bisulfite for a specific period of time results in deamination of cytosine residues to thymine (Shapiro and Weisgras 1970). In our study the optimum exposure time was 10 min. We observed that exposure periods of more than 10 min resulted in the inability to PCR amplify the specific sequence post treatment. This could have been as a result of undesired bases changes other than the anticipated C-T conversion or due to DNA degradation. Ehrich *et al.*, 2007 and Raizis *et al.*, 1995 showed that C-T conversion time requires optimisation to achieve optimum C-T conversion with minimal DNA degradation. They showed that treatment exposures of 30 min and longer results in fragmented ssDNA caused DNA depurination. However previously in our lab, Harmse, 2009 (MSc thesis) reported no

difference in PCR amplification efficiency after prolonged bisulfite treatment exposure. Tusnády *et al.*, 2005 implicated primer design as the main contributor of low bisulfite PCR efficiency due to high T and A presence in the sense and antisense primers, respectively. They developed a primer search design tool with an algorithm aimed at circumventing this problem.

Sequence specific amplification of the correctly mutated strand

It was expected that post treatment, C-T mutations would be introduced in the positive strand of the sequence when read in the 5' to 3' direction and conversely producing G-A base changes in the negative strand. With this is mind, primers were designed to specifically amplify only the mutated template strands as it was possible that a population of mutated and non-mutated template was present. The forward primers were designed to contain C-T changes along the length of the primer, while the reverse primers were designed to contain several G-A base changes along the length of the primer. As little as 2 base changes in the forward and reverse primers were enough to ensure strand specific amplification.

Successfully amplified strands were sent off for sequencing and successful strand specific selection was confirmed by the sequence analysis results. From the sequencing results we observed that after 10 min treatment periods that the sense arm of MM1hp had a 81 % C-T conversion rate, MM2hp sense arm; a 56 % conversion rate and MM3hp sense arm; a 78 % conversion rate. A lower conversion rate was seen in MM2hp than in MM1hp and MM3hp, indicating that MM2hp sequence contained more methylated Cs as sodium bisulfite treatment targets non-methylated C and deaminates the Cs to Ts. Harmse, 2009 reported a 56 % deamination of C-T in the sense arm of the SACMV BC1 (MM4hp) construct after a 10 min treatment.

A**dvantages of using mutated sense arm hairpin construct technology**

Mutated sense-arm hairpin construct technology was relatively cheaper than the Gateway construct system but did however involve more restriction enzyme digests, ligations and cloning steps and therefore was more time consuming. Using this method of engineering imperfect IR sequences reduces the formation of cruciform and any unwanted tertiary structures associated with IR sequences. This is important as cloning of IR sequences is known to be difficult (Bao &

Cagan, 2006; Rattray, 2004). Cloning difficulties arise from IR sequence re-arrangement and deletion ability possessed by certain conventional *E.coli* strains, such as *E.coli* DH5α (Bao & Cagan, 2006). Unlike the Gateway IR system, this imperfect IR technology does not required specialised IR tolerant cells, such as SURE *E.coli* cells, are required. These cells are IR endonuclease and recombinase deficient (Casali, 2003). Other specialised *E.coli* DB3.1 cells are also required for the Gateway system, *E.coli* DB3.1 cells these cells are resistant to the toxic effects of the *ccd*B gene carried by plasmids such as pHellsgate 8 and pHellsgate 10. Piccin *et al.*, 2001 circumvented these IR-induced cruciform structures by including a GFP intron/spacer between the target hairpin arms. Gateway pHellsgate vectors are based on a similar approach with approximately a 800 bp PDK intron positioned between both arms of the hairpin (Wesley *et al.*, 2001). This PDK intron is relatively large in relation to the shorter 300-500bp target sequences required for the hairpin arms and this increases the hairpin cassette which can make ligation and cloning even more difficult. However with this said, cloning of large fragments has improved since the early years of Burke and colleagues in 1987 (Tao & Zhang, 1998).

Imperfect IR technology is relatively cheaper than the Gateway recombinase kits as conventional restriction enzymes, standard TA cloning vectors, expression vectors and standard *E.coli* strains that are routinely found in the lab were used and therefore costs were significantly reduced. However we employed a slightly different method to produce the desired non-mismatched constructs. This approach was cheaper than the manual-prescribed Gateway recombinase kit. This method used conventional restriction and ligation methods in molecular cloning however did require slightly more ligation, assembly and cloning steps than the kit described Gateway recombinase method.

CHAPTER 3

AGROBACTERIUM-MEDIATED TRANSFORMATION OF CV.60444 AND T200 FEC WITH MUTATED AND NON-MUTATED RNA SILENCING HAIRPIN CONSTRUCTS AND REGENERATION OF TRANSFORMED FRIABLE EMBRYOGENIC CALLUS

3.1 Introduction

Cassava transformation

Cassava production is sub-Saharan Africa is faced with a number of biotic constraints. Cassava mosaic disease (CMD) is the major biotic constraint in cassava cultivation and causes severe cassava yield losses annually (Hong *et al.,* 1993; Patil and Fauquet, 2009). Disease control relies on development of virus resistant plants. Virus resistant transgenic cassava varieties have been developed by different approaches, and by introducing different virus-derived transgenes (Vanderschuren *et al*., 2009; Vanderschuren *et al.*, 2012; Vanderschuren *et al.*, 2007; Zhang *et al.*, 2005). However the key element in successful cassava genetic engineering is reliable and efficient transformation and regeneration methods. The most efficient and reliable method is the use of *Agrobacterium tumefaciens* (*A. tumefaciens*) to introduce the DNA of interest (Bull *et al*., 2009).

Agrobacterium-mediated transformation

A. tumefaciens is a soil plant pathogenic gram-negative bacterium. This bacterium naturally infects dicotyledonous plants causing the formation of crown gall tumours (Cleene & Ley, 1976; Newell *et al*., 2010; Smith & Townsend, 1907). Proliferation of the induced tumour in the plant cells doesn't require the continuous presence of the bacterium, indicating that cells become genetically transformed upon infection. This is the only organism that is capable of inter-kingdom gene transfer (Pitzschke & Hirt, 2010; White & Braun, 1942). It is believed that this inter-kingdom gene transfer ability might be evolutionary related to bacterial conjugation (Lessl & Lanka, 1994). It is this natural ability to insert foreign genes into plant genomes that has been exploited to produce transgenic plants (Gelvin, 2003b).

The *A. tumefaciens* harbours a Ti plasmid, and located on this plasmid is a segment of DNA called the T-DNA and the *vir* genes which are required for both virulence and tumor formation (Gelvin, 2003a; Zaenen *et al.*, 1974). This T-DNA is flanked by 25 bp direct repeat sequences called the right border (RB) and left border (LB) based on the polarity and genes involved in the T-DNA transfer. Chilton *et al.*, 1977 demonstrated that the T-DNA segment is transferred and integrated into the plant genome. Reports later revealed that the RB is very important as it determines the direction of T-DNA transfer from the *Agrobacterium* to the plant genome

(Kononov *et al.*, 1997; Wang *et al.*, 1984). Once the segment has been transferred and transcribed reprogramming of plant cells occurs and tumour formation occurs.

There are several steps and processes involved in infection. Plant phenolic compounds that are produced during wounding first autophosphorylates the VirA protein. This then activates the VirG protein which then binds to the *vir* gene promoter thereby activating *vir* gene transcription (Brencic & Winans, 2005). The *Agrobacterium* then attaches to the plant cell using chromosomally encoded bacterial genes (Douglas *et al*., 1982; Newell *et al*., 2010). Following this, a transporter complex is formed by the VirB and VirD4 protein to allow the Vir proteins and T-DNA to be transported. VirD2 then nicks and binds to the 5'end of the T-DNA and guides it through the transporter complex into the plant cell (De Vos & Zambryski, 1989). Located on the C terminus of the VirD2 is a nuclear localisation signal which then helps direct and attach the T-DNA to the plant nucleus. The VirD2 has been implicated in of the host genome and ligation of T-DNA into the plant genome is mediated by host proteins. Integration of the T-DNA occurs in a non-homologous end-joining mechanism (Koukolíková-Nicola *et al*., 1993). Upon infection the plant also attempts to mount a defence response using the plant innate immunity however the T-DNA and the Vir protein act as defence response suppressors (Ditt *et al.*, 2001).

Integration of the T-DNA in the host genome results in the expression of the T-DNA encoded bacterial genes (oncogenes). These oncogenes encode enzymes responsible in the synthesis of plant growth hormones, auxins and cytokinins. This then results in reprogramming of plant cells for tumour formation and the activation of genes involved in opine synthesis (Binns & Thomashaw, 1988). These opines are in the form of nopaline or octopine which the bacteria then uses as growth substances once the T-DNA has been integrated (Dessaux *et al*., 1988; Pitzschke & Hirt, 2010).

Manipulation of *Agrobacterium* for plant genetic engineering

Implication of the Ti plasmids in tumorgenesis, and the scientific evidence that demonstrated that only a segment (T-DNA) of the Ti plasmid is transferred and integrated into the plant genome, and that gene transfer ability of the bacterium was across plant kingdoms, lead to the proposal that the Ti plasmid could be used for foreign DNA transfer into plant genomes. Following this

proposal, T-DNA binary vectors were developed. The reasons for not using the Ti plasmid and developing the T-DNA binary vectors were : 1) The Ti plasmid lacked appropriate restriction sites for cloning of the gene of interest, 2) the Ti plasmid had a large size and 3) the discovery that the ability to transfer DNA required only the LB and RB (Gelvin, 2003a).

The binary vector system is based on the use of two plasmids simultaneously; the binary vector carrying the T-DNA segment and the Ti (*vir*) plasmid disarmed of the oncogenic genes with only the origin of replication present (Hoekema *et al* in 1983). The presence of both plasmids in a desired *Agrobacterium* strain ensures that the T-DNA is transferred into the plant genome. pCambia are a group of plant transformation binary vectors that are derived from the pPZP vectors and were constructed by Hajdukiewicz *et al.* in 1994. These vectors contain RB and LB flanking the region to be transferred. Within this region flanked by the RB and LB is a multiple cloning site (MCS) and this follows after the RB following the MCS is the gene encoding for herbicide or antibiotic resistance and selectable marker gene. This arrangement ensures that the gene of interest is closest to the RB as transfer is initiated at the RB followed by the plant markers then to the LB. Once the foreign gene of interest is cloned into the MCS the plasmid is then used to transform a disarmed strain of *A. tumefaciens* with only the *vir* genes and the origin of replication present (Hajdukiewicz *et al*., 1994). LBA4404 is one of the *A. tumefaciens* stains developed to contain a non-oncogenic *vir* helper plasmid. The earliest reports of gene transfer into plant cells was in *N. benthamiana* and this technology has since been exploited in a variety of other plants (Eamens *et al*., 2008).

Cassava transformation

Cassava genetic engineering technology has matured and developed significantly since the first reports of successful cassava genetic engineering in the 1990s. Some of the first cassava genetic transformation experiments involved the expression of selectable markers such as the phosphinotricin resistance (*bar*) gene and the β-glucuronidase (*uid*A) genes. Transformation is mainly based on the production of friable embryogenic callus (FEC) through somatic embryogenesis which is considered be the most promising target tissue (Bull *et al.*, 2009; Chetty *et al.*, 2013; Hankoua *et al*., 2006; Li *et al*., 1998; Nyaboga *et al*., 2013; Schopke *et al*., 1997; Taylor *et al*., 2001; Zainuddin *et al*., 2012).

In 1996, cassava expressing a luciferase gene was engineered by Raemakers *et al.,* 1996. This luciferase reporter gene was introduced into cassava somatic embryos using particle bombardment. This was the first report of successful bombardment of cassava embryos. Later Schopke *et al.,* 1997 also reported successful cassava transformation using embryogenic suspension cultures as target tissue, however, particle bombardment was used to introduce the DNA. Gonzalez *et al.,* 1998 also used embryogenic suspension cultures as target tissue for the introduction of the *uid*A gene into the cassava genome however this foreign DNA was introduced using *Agrobacterium*-mediated transformation. In other experiments, somatic embryo derived-cotyledons were selected as target tissue for transformation using *Agrobacterium* (Li *et al.,* 1996 and Sarria *et al.,* 2000). Zhang *et al.,* 2000 also reported stable and successful transformation of cotyledons however using particle bombardment. The use of embryogenic suspension cultures as target tissue was initially considered to be more favourable and efficient than using cotyledons as it offered better transgene selection because of constant contact with the selection medium. Another reason was that the chance of obtaining chimeric plants was considered to be lower than when using organised tissue such as cotyledons (Gonzalez *et al*., 1998). Technology has shifted to the use of FEC as the target tissue, first described by Taylor *et al*. in 1996.

The chance of obtaining chimeric transgene expression is greatly reduced when FEC is used as the target tissue unlike when somatic embryos and organised tissue like cotyledons are used. This reduction can be seen when either *Agrobacterium* or particle bombardment are used (Raemakers *et al.,* 1997). This therefore makes FEC the most practical target tissue for particle bombardment and *Agrobacterium*-mediated transformation. Using FEC also decreases the level of escapes (untransformed plantlets) unlike when cotyledons are used. The high susceptibility of the FEC to *Agrobacterium* makes *Agrobacterium*-mediated transformation of FEC the most efficient, reproducible and favoured method for DNA introduction than particle bombardment. *Agrobacterium*-mediated FEC transformation experiments by Schreuder *et al.* (2001) showed that up to 100 transgenic lines per 100 mg FEC starting material. Their results also revealed that transformation success was *Agrobacterium* strain dependent. Munyikwa *et al.* (1998) reported an extremely low transformation efficiency using particle bombardment. Their results showed

that about 1 transgenic line was produced per 100 mg FEC starting material. The comparatively high *Agrobacterium*-mediated transformation efficiency of FEC compared to other starting material, and lack of very high technology equipment required, makes this the transformation method of choice. FEC induction does however still require lengthy and fastidious tissue culture procedures and is genotype dependent (Chetty *et al.*, 2013; Nyaboga *et al*., 2013; Zainuddin *et al.*, 2012), and requires also a certain level of training and skills. More recently, Bull *et al.* (2009) adapted some of the earlier protocols, leading to a more robust and streamlined procedure, which was used to establish vector transformation of cassava in our laboratory (Chetty *et al*., 2013). However, this has not been achieved, to date, for transformation for SACMV and ACMV resistance until this study. This was also the first undertaking to transform the cassava landrace/genotype T200 with anti-viral hpRNA constructs.

3.2 Specific Aims

i. Cassava cv.60444 and T200 FEC induction
ii. *Agrobacterium*-mediated transformation of FEC with mutated and non-mutated constructs (described in chapter 2)
iii. Regeneration of transformed FEC
iv. Selection of plants for transgene integration using visual and molecular screening
v. Selection of transgenic plants for virus infection to screen for resistance

3.3 Methodology flow chart

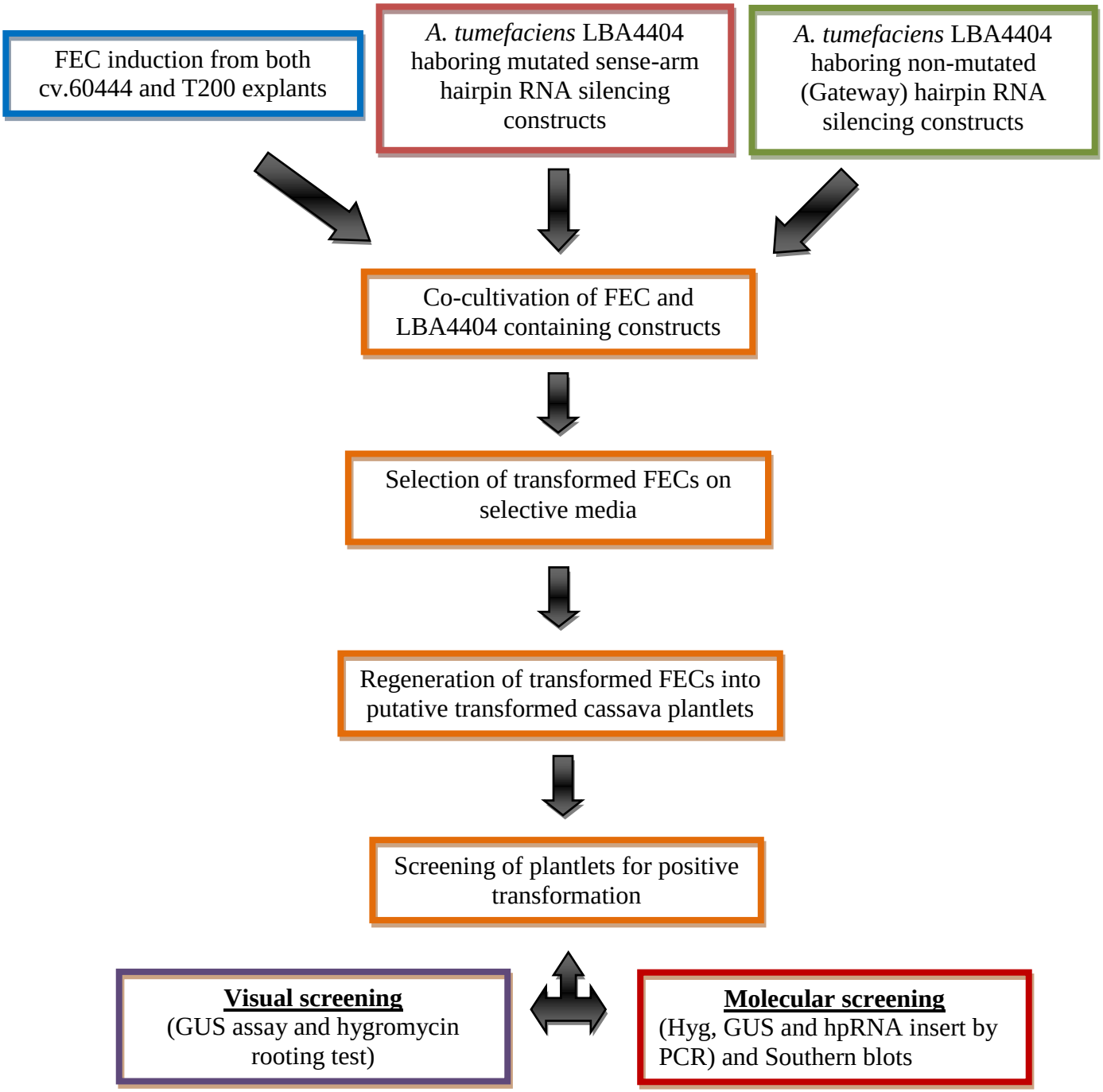


Figure 3. 1 Flow diagram of work flow to generate transgenic cassava plants.

3.4 Materials and Methods

3.4.1 Friable embrogenic callus (FEC) induction

cv.6044 FEC induction from cassava explants material was performed following (Bull *et a*l., 2009). Induction of T200 FEC followed (Chetty *et al*., 2013). On each GD plate, 10 FEC clusters were placed. All non-embryogenic friable callus (NEFC) was removed with each sub-culturing.

3.4.2 Preparation of *Agrobacterium* inoculum

Mismatched and non-mismatched RNA silencing hairpin constructs (chapter 2; MM1hp, MM2hp, MM3hp, MM4hp, MM5hp, MM6hp, MM7hp and MM8hp) transformed into *Agrobacterium* LBA4044, and *Agrobacterium* harbouring empty pCambia 1305.1 plant transformation vector, were streaked each on Yeast extract peptone (YEP) medium (5 g/L Yeast extract, 5g Bacto-peptone and 10 g/L Sodium chloride, solidified with 15 g/L bacterial agar and pH was adjusted to 7.2). YEP medium was supplemented with antibiotics (50 µg/ml kanamycin, 50 µg/ml rifampicin and 100 µg/ml streptomycin). Streaked plates were inverted and incubated at 28°C in the dark for 2 days. A single colony for each construct was removed using a sterile inoculating loop and inoculated in YEP + 50 µg/ml kanamycin, 50 µg/ml rifampicin, 100 µg/ml streptomycin and 2 mM $MgSO_4$. This was cultured O/N in the dark at 28 °C with shaking at 200 rpm.

Cultures were allowed to grow until they reached an optical denstity (OD) of 0.7-1.0, at λ=600nm. From this culture 0.5 ml was removed and inoculated in 25 ml of YEP containing 50 µg /ml kanamycin, 50 µg/ml rifampicin, 100 µg/ml streptomycin and 2 mM $MgSO_4$. This was grown O/N in the dark at 28 °C with shaking at 200 rpm. The OD was measured and when an OD of 0.7-1.0 at λ=600nm was obtained, the bacterial suspension was placed in a sterile 50 ml centrifuge tube and centrifuged at 4000 g for 10 min at room temperature. The supernatant was removed and the pellet resuspended in 25 ml of liquid GD medium. Suspension was again centrifuged at 4000g for 10 min at room temperature. Following this, the supernatant was removed and excess liquid removed. The pellet was resuspended in GD liquid and diluted to an OD_{600} of 0.5. Once the correct OD had been reached, acetosyringone to a final concentration of

200 µM was added. The cultures were placed on a horizontal shaker (50 rpm) at room temperature for 45 min.

3.4.3 *Agrobacterium*-mediated transformation of FEC

Seven FEC plates, consisting of 10 FEC clumps of approximately 0.8 - 1 cm diameter were used for each transformation experiment. Each FEC clump was co-cultivated with 100 µl of prepared *Agrobacterium*: construct inoculums (prepared in section **3.4.4)**. The same was also performed for the 2 plates using the *Agrobacterium* with the control pCAMBIA vector. One plate was not transformed and was monitored for regeneration. Pipetting of the bacterial suspension was done in a manner as not to flood the plate but rather just soak the FEC clusters. Plates were then left in the laminar flow uncovered for ~5 min and then sealed with parafilm. FEC with the bacterial suspensions were co-cultivated at 24 °C for 4 days in 16 h light/8h dark photoperiod.

Table 3. 1 Summary of transformation events including details of RNAi construct used and FEC type transformed.

Constructs	cv.60444 FEC	T200 FEC
MM1hp Mismatch (ACMV AC1/AC4 + EACMV AC1/AC4)	**Group A transformation**	**Group B transformation**
MM2hp Mismatch (ACMV AC1/AC4 + ACMV AC2/AC3)		
MM3hp Mismatch (EACMV AC1/AC4 + EACMV AC2/AC3)		
MM4hp Mismatch (SACMV BC1)		
MM5hp Non-Mismatch/Gateway (ACMV AC1/AC4 + EACMV AC1/AC4)	**Group C transformation**	**Group D Transformation**
MM6hp Non-Mismatch/Gateway (ACMV AC1/AC4 + ACMV AC2/AC3)		
MM7hp Non-Mismatch/Gateway (EACMV AC1/AC4 + EACMV AC2/AC3)		
MM8hp Non-Mismatch/Gateway (SACMV BC1)		

3.4.4 Removal of excess *Agrobacterium*

Following the co-cultivation period, FEC were gently scraped off the plates using sterile forceps and placed in 50 ml tubes containing 25 ml of GD liquid plus 500 µg/ml carbenicillin. The suspension was vortexed briefly for 5-10 sec and the FEC were then allowed to settle. Using a 10 ml pipette the supernatant was aspirated, leave the FECs as dry as possible. Washing of FEC in

the GD liquid containing 500µg/ml carbenicillin was repeated ~5 times or until the supernatant became clear. Once clear, the supernatant was discarded and the FEC resuspended in ~10 ml of GD liquid containing 500 µg/ml carbenicillin. The FEC suspensions were pipetted and spread thinly and evenly onto ~10 sterile plastic meshes (pour size of 100 µm). Meshes were then each placed on top of 3 layers of sterile filter paper to allow for absorption of excess liquid off the FEC.

3.4.5 Recovery and maturation of transformed FEC

Mesh:FEC were then transferred to GD plates with 250 µg/ml carbenicillin to help with FEC recovery. Plates were sealed with parafilm and incubated at 28 °C for 4 days at 16 h light/8 h dark photoperiod. For the selection of transformed FEC and to improve the regeneration efficiency mesh/FEC were placed on a stepwise increase of hygromycin. After 4 days, mesh:FEC were placed for a week on to GD containing 250 µg/ml carbenicillin and 5 µg/ml hygromycin followed by one week on GD containing 250 µg/ml carbenicillin and 8 µg/ml hygromycin and one further week on GD with 250 µg/ml carbenicillin and 15 µg/ml hygromycin. All plates were sealed with parafilm and placed at 28 °C with 16 h light/8 h dark photoperiod.

3.4.6 GUS assay to determine transformation success

To visually detect transformation success a small section of the putatively transformed material on the mesh/FEC was removed using sterile forceps and placed in GUS assay solution (100 mM Tris/NaCl buffer, 1 mg/ml 5-bromo-4-chloro-3-indolyl-β-D-glucuronic acid (X-Gluc) and 1 % Triton X-100). Untransformed cv.60444 FEC were also included as a negative control. These were incubated at 37 °C O/N. GUS solution was removed and material destained in 70% ethanol, and leaves viewed.

3.4.7 Regeneration of transgenic plants

For the regeneration of transformed FEC, MSN medium was used. MSN consists of MS2 medium containing 250 µg/ml carbenicillin, 1 µg/ml 1-Naphthaleneacetic acid (NAA) and 15 µg/ml hygromycin and solidified with 8 g/L Noble agar. Mesh: FECs were transferred to MSN and maintained on MSN for 10 days at 28 °C with 16 h light/8 h dark photoperiod. After 10

days, this was transferred to fresh MSN for a further 10 days using the same incubation conditions. This cyclic MSN transfer process was performed not more than 8 times. This was to decrease the possibility of regenerating escapee non-transformed FEC. During these MSN 10 days transfers, any green or white emerging cotyledons were moved to cassava elongation medium (CEM). CEM was composed of MS2 supplemented with 0.4 µg/ml BAP and 2 µM $CuSO_4$ and 100 µg/ml carbenicillin and solidified with 8 mg/ml Nobel agar. Cotyledons were moved to fresh CEM every 14 days, and this was repeated until juvenile leaves and shoots appeared. Shoots were removed and placed in sterile small bottles on solid cassava basic medium (CBM) [MS2 with 2 µM $CuSO_4$; 50 µg/ml carbenicillin and solidified 3 mg/ml phytagel]. Plates were incubated for 28 °C with 16 h light/8hrs dark photoperiod, and approximately 2 weeks later, roots developed forming small plantlets.

3.4.8 GUS assay on plantlets

Developing shoots were selected and GUS assays were performed following the procedure used in section **3.4.8**.

3.4.9 Preliminary screening using a rooting experiment

A rooting test on hygromycin-containing media to screen for successful hygromycin-resistant transformants was performed. The apical shoots from the plantlets generated in section **3.4.9** were isolated and placed in sterile tissue culture bottles on CBM containing 50 µg/ml carbenicillin and 10 µg/ml hygromycin. Two holes were punctured in the top of the tissue culture bottle lids and puncture wholes were then covered with sterile micropore tape. Regenerated wild-type untransformed cv.60444 plantlets were also included as a negative control.

3.4.10 Propagation of transgenic plant lines

Plants showing positive GUS and positive rooting in the hygromycin were selected and propagated on MS2 medium following method described in section **3.4.1**.

3.4.11 Regeneration test of untransformed wild-type cv.60444 FEC

As mentioned in **3.4.5**, a plate of untransformed cv.60444 was included with every transformation experiment. This was done to determine the regeneration efficiency of the FEC selected for the transformation experiment. Untransformed FEC clusters were removed off the GD plates where they were maintained and propagated and placed on sterile mesh. The mesh with the FEC was then placed onto MSN medium without the hygromycin and 250 µg/ml carbenicillin (to test that the carbenicillin had no effect on FEC maturation and regeneration into plantlets). Upon placing on hygromycin-free MSN, the FEC clusters were gently pressed down to ensure FEC contact with the medium. FEC were maintained hygromycin-free MSN and transferred to fresh medium every 10 days following method described in **3.4.9.** Developing cotyledons were also treated following the same method as described in **3.4.9.** Plantlets produced on the CBM medium were propagated following the same method described in **3.4.1**.

3.4.12 Total nucleic acid extraction from plantlets

Approximately 50 mg of leaf tissue was collected from the plantlets, and snap- frozen in liquid nitrogen, and crushed into a fine powder. Total nucleic acid (TNA) was isolated from the harvested samples using the CTAB based method (Doyle and Doyle 1987). To each eppendorf of crushed sample, 500 µl of preheated CTAB extraction buffer (2 % hexadecyltrimethylammonium bromide, 1.4 M NaCl, 0.2 % 2-mercaptoethanol, 20 mM EDTA, 100 mM Tris-HCl, pH 8.0) was added and thoroughly vortexed and incubated in a water-bath at 65 °C for 60 min and the tube occasionally inverted. After incubation, 500 µl of chloroform-isoamyl alcohol (24:1) was added followed by mixing and centrifugation at 13 400 rpm for 10 min at 4 °C. The aqueous layer containing the DNA was placed into a clean tube and the above chloroform-isoamyl alcohol extraction step repeated. Purified TNA in the upper aqueous layer was precipitated using 500 µl isopropanol and centrifugation for 10 min at 13 400 rpm at 4 °C. TNA pellet was washing with 1 ml of ice-cold 70 % ethanol followed by centrifugation for 10 min at 13 400 rpm at 4 °C, this pellet washing step was repeated. The pellet was air dried and resuspended in 50 µl TE (10 mM Tris pH 8.0 and 1 mM EDTA) containing 20 µg/ml RNase A (Fermentas). The extracted DNA was quantified on the Nanodrop 1000 spectrophotometer (Nanodrop).

3.4.13 PCR-based screening for further confirmation of transformation success

Plants were screened for transgene using insert primers following method described in sections **2.4.1.7** and **2.4.2.2** for screening of mutated sense-arm hairpin RNA transgenic plantlets and the method described in sections **2.4.3.4** and **2.4.3.5** for non-mutated (Gateway) hairpin RNA transgenic plants. Both sets of transgenic plants were also screened with both GUS and Hyg primers following the method described in section **2.4.2.14**.

3.4.14 Southern blot screening of transgenic plants

Some of the extracted DNA from **3.4.14** was used for transgene copy number analysis following DIG-High Prime DNA Labelling and Detection Starter Kit II (Roche) protocol. A total of 20 µg of extracted DNA was digested with enzyme and incubated O/N at 37 °C. Digestion reaction was deactivated and run O/N in a 1 % agarose gel in 1X TAE. Capillary transfer of DNA from agarose gel to positively charged nylon Hybond-N+ membrane (Amersham) was performed for 6-8 h. Membranes were hybridised O/N at 42 °C with DIG-labelled Hyg gene probe. Probe was labelled following the DIG-High Prime DNA Labelling and Detection Starter Kit II (Roche) protocol. Washing off of all unbound probe membrane and antibody detection was performed following DIG-High Prime DNA Labelling, and the Detection Starter Kit II (Roche) protocol. Membranes were developed on Lumi-film chemiluminescent detection film (Roche).

Samples were digested with Hind*III* and then probed separately with *Hyg* DIG-labelled probe and the *GUS* DIG-labelled probe. Samples were also digested with both Hind*III* and EcoR*I* simultaneously and then probed with target gene labelled probe.

3.5 Results

3.5.1 FEC induction from cv.60444

SE developed 2 weeks after being placed on CIM, however these were still immature, and at this stage there was more non-desirable soft tissue than SE **(fig. 3.2 b)**. The immature SE were then placed on fresh CIM for 2 more weeks, and after this the appearance of finger-like structures, coral-shaped and torpedo-like structures, resembling mature SE, became visible **(fig. 3.2 c)**. At this stage some of the mature SE were divided and split and some placed on GD media for FEC induction and some were used for further SE production on fresh CIM (this was the 3rd transfer) **(fig 3.2. d)**. Biweekly maintenance and cycling of SE on fresh CIM ensured that a constant SE supply was available for FEC induction at any one time. However, SE could only be transferred to fresh CIM for 10 more weeks (at 2 week intervals, therefore 5 CIM transfers) as the ability to produce finger-like structures diminished with every successive transfer to CIM. Towards the 8th transfer to CIM, a green colour around the SE edges was observed. SE also appeared more coral shaped and lost the finger-like structure and torpedo appearance. SE induction had to therefore be initiated every 16 weeks to maintain stocks and for production of high quality FEC induction.

High quality cv.60444 FEC **(fig. 3.2 f)** was obtained after approximately 11 weeks (from the start of explant axillary bud swelling to the development of FEC on the 4th transfer on GD media).

3.5.2 T200 FEC induction

T200 FEC induction followed a similar process to cv.60444 induction; however T200 FEC induction was a lengthier process as it required additional cycling steps compared with cv.60444 FEC induction. Mature SE only appeared after the 3rd SE transfer to fresh CIM **(fig. 3.3 c).** As with cv.60444, the SEs were split for SE maintenance **(fig. 3.3 d)** or FEC induction **(fig. 3.3 e)**. FEC suitable for transformation were obtained after a total of 14 weeks from the 1st GD transfer to the 7th GD transfer. Therefore it took a total of 18 weeks from the start of explant swelling to mature FEC formation **(fig. 3.3 h)**. T200 FEC was a slightly light yellow-pale colour unlike cv.60444 FEC which were a more yellow colour.

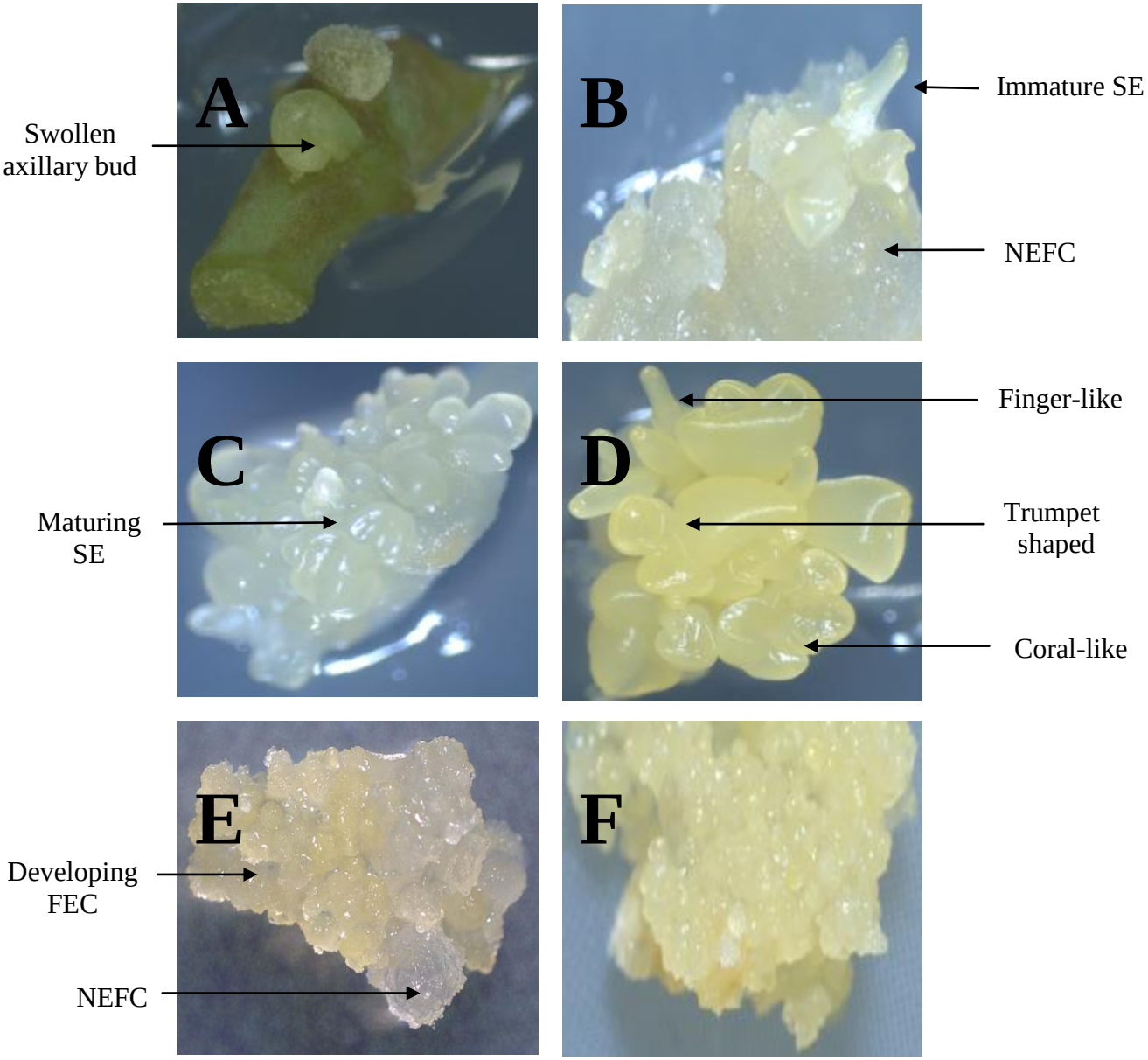


Figure 3. 2 cv.60444 FEC induction (a) Swollen axillary bud after 3 days on CAM. **(b)** Immature somatic embryos (SE) surrounded by NEFC after 2 weeks on CIM. **(c)** Maturing SE with a reduction in NEFC after the 2nd transfer to fresh CIM (after 2 weeks); SE then ready for FEC induction on GD. **(d)** SE maintained on CIM finger-like structures, trumpet shaped and coral-like SE with no NEFC after the 3rd transfer to CIM. **(e)** Developing FEC with NEFC after the 3rd transfer to GD. **(f)** Proliferating FEC with no NEFC after the 4th transfer to GD; FEC ready for inoculation with *Agrobacterium* harbouring the constructs.

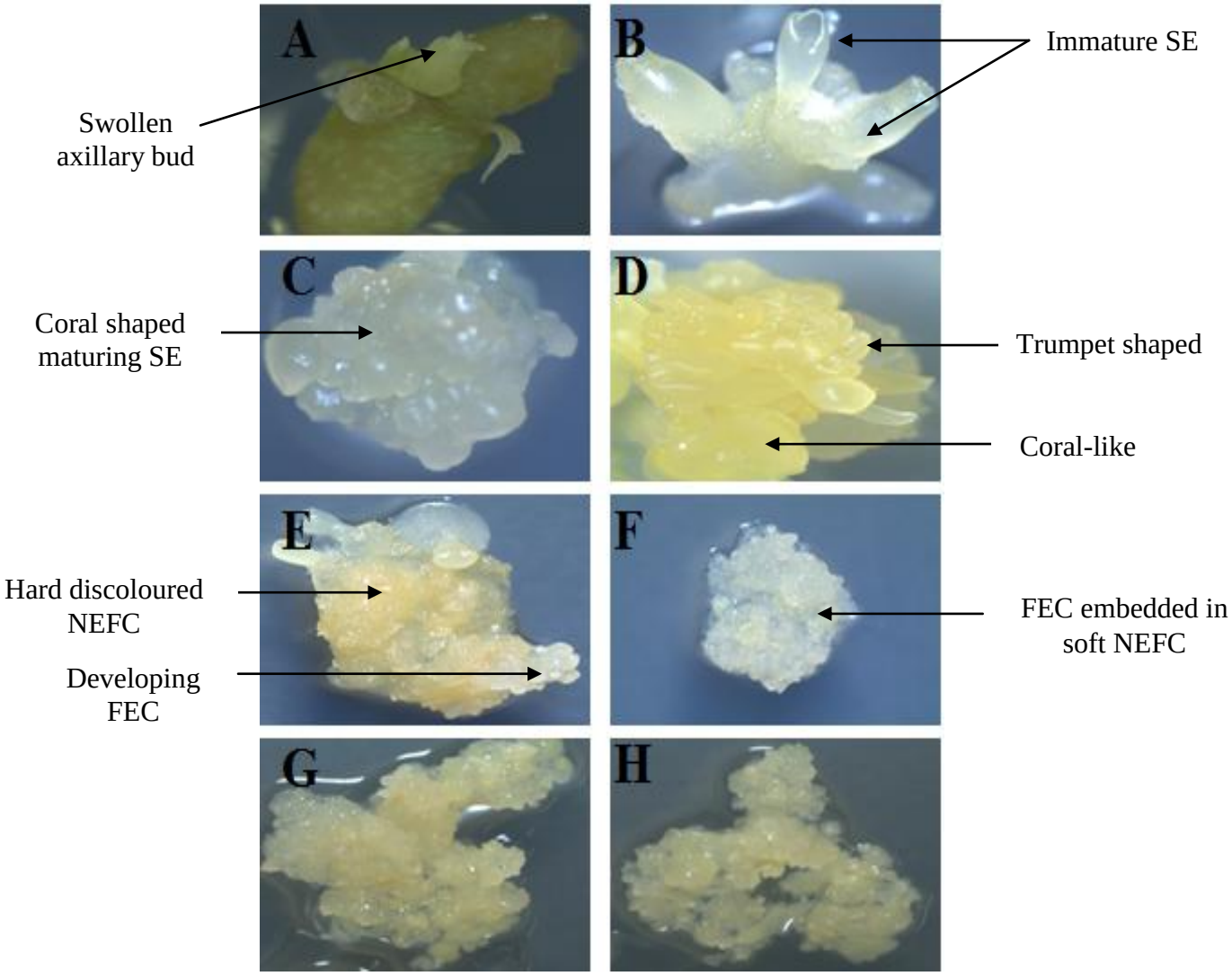


Figure 3. 3 T200 FEC induction (a) Swollen axillary bud, after 3 days on CAM. **(b)** Immature somatic embryos (SE) surrounded by NEFC after 2 weeks on CIM. **(c)** Maturing SE produced after 2nd transfer to fresh CIM (4 weeks later) and ready for FEC induction on GD. **(d)** Mature trumpet shaped and coral-like SE, with choral-like SE being more dominant, and no NEFC after the 4th transfer to CIM (after 2 more weeks). **(e)** Tiny clump of developing FEC with NEFC after the 4th transfer to GD. **(f)** Tiny clump of FEC giving rise to more FEC, proliferating FEC still embedded in NEFC. **(g)** Proliferating FEC after 10 weeks (5th cycle on GD) with hard yellow NEFC structure. **(h)** FEC after 14 weeks (7th cycle on GD); mature and ready to be inoculation with *Agrobacterium* harbouring the constructs.

3.5.3 Mismatched (mutated sense arm) RNA silencing hairpin construct transformation of cv.60444 and T200 FEC and regeneration of transformed FEC

3.5.3.1 FEC transformation and cotyledons

To distinguish between cv.60444 and T200 transformation with mismatched constructs, transformation events were labelled as group A and group B, respectively.

For group A and group B transformation experiments, 7 plates with 10 FEC clumps of approximately 1cm diameter were used as starting material. After the co-cultivation step, FEC were moved weekly onto GD media containing increments of hygromycin (5 mg/ml-15 mg/ml). This step was necessary to promote selection and later regeneration of transformed FEC. A GUS assay was performed and positive transformation was confirmed by the blue stained FEC **(fig. 3.4 a).** FEC that failed to be transformed turned a dull creamy colour, while transformed FEC turned a more intense yellow colour and appeared to double in size.

The next step following selection was regeneration of transformed FEC on media containing increments of hygromycin minimise regeneration of untransformed FEC (escapees). Transformed cv.60444 FEC produced embryos as early as 10 days after being placed on MSN+H15 media **(fig. 3.4 b)**. On the 2nd transfer to MSN+H15 tiny green cotyledons were already forming and the production of more embryos and cotyledons increased with every transfer to fresh MSN+H15 **(fig. 3.4 d)**. FEC were transferred to fresh MSN+H15 6 times (after every 10 days). The same process was followed for T200 transformed FEC, however for T200 transformed FEC, formation of embryos and cotyledons only occurred on the 3rd MSN+H15 transfer.

Cotyledons only developed from MM2 and MM4 transformed cv.60444 FEC (A-group) and from T200 FEC transformed with MM2, MM3 and MM4 constructs (B group) **(Table 3.2)**. Cotyledons failed to regenerate from MM1, MM5 and MM7 transformed FEC. Up to a 50% reduction in cotyledon number was seen for T200 transformed FEC compared with cv.60444 FEC transformed with the same constructs.

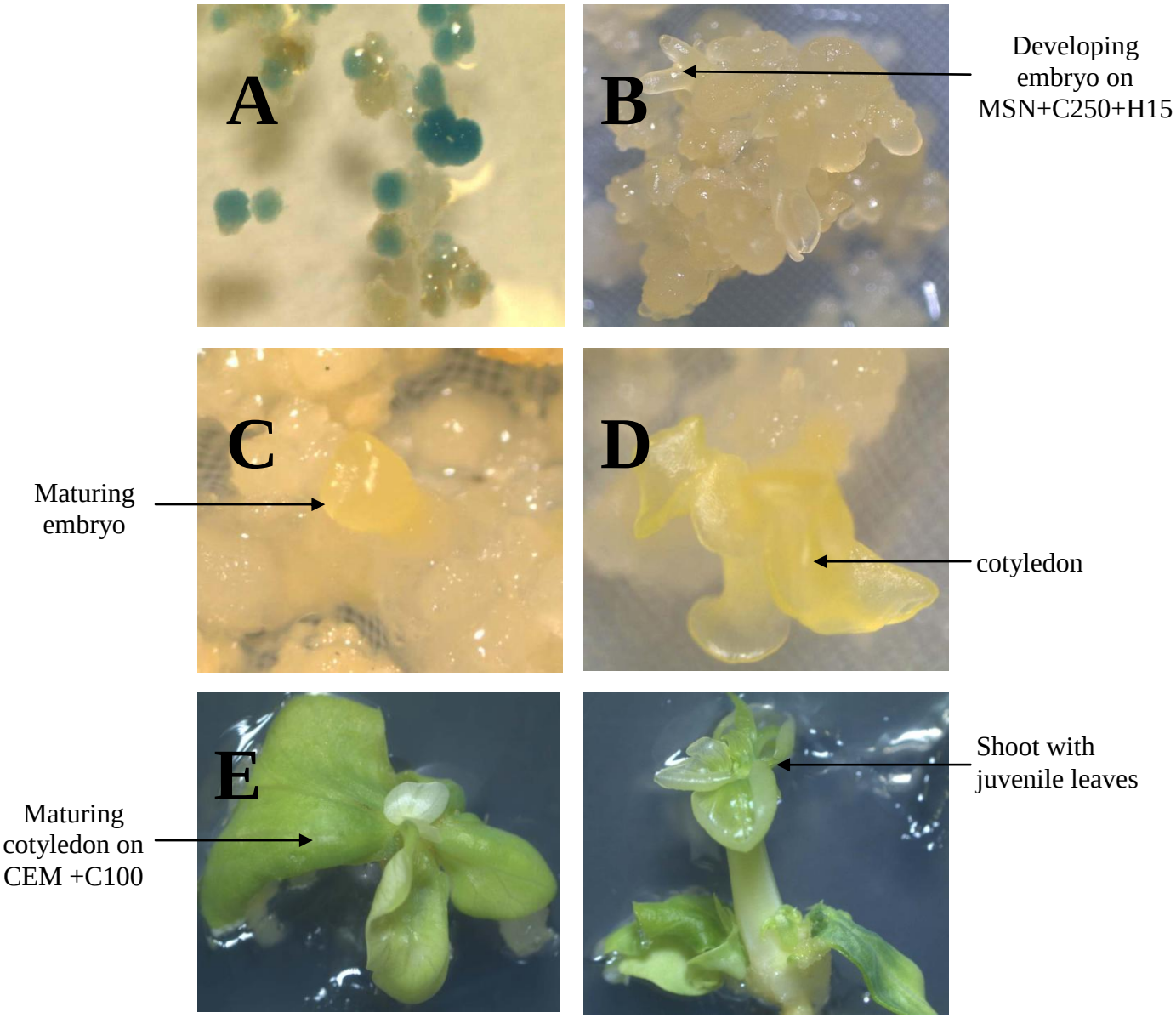


Figure 3. 4 Regeneration of putatively transformed FEC (a) Blue stained FEC after GUS assay. **(b)** Developing embryo (on MSN+C250+H15) on a bed of transformed FEC seen as yellow swollen structures. **(c)** Maturing embryo after 2 weeks on MSN+C250+H15. **(d)** Yellow green cotyledon after 3 weeks on MSN+C250+H15; cotyledon ready to be moved to CEM+C100. **(e)** Maturing cotyledon. **(f)** Appearance of shoot with emerging juvenile leaves after several weeks on CEM+C100. Apical shoot was transferred to rooting media after appearance of mature\true leaves.

3.5.3.2 Undesirable FEC developmental retardation and defects

MM1 transformed cv.60444 FEC turned a cream and brown colour and failed to proliferate even 4 weeks after the co-cultivation step, and no cotyledons were formed **(fig. 3.5 b)**. FEC did however stain blue, indicative of successful transformation **(fig. 3.5 a)**. Similar results were observed for T200 FEC transformed with MM1; however amongst the brown FEC were clumps with an intense yellow colour that is associated with transformed FEC **(fig. 3.5 c)**. These also failed to produce cotyledons.

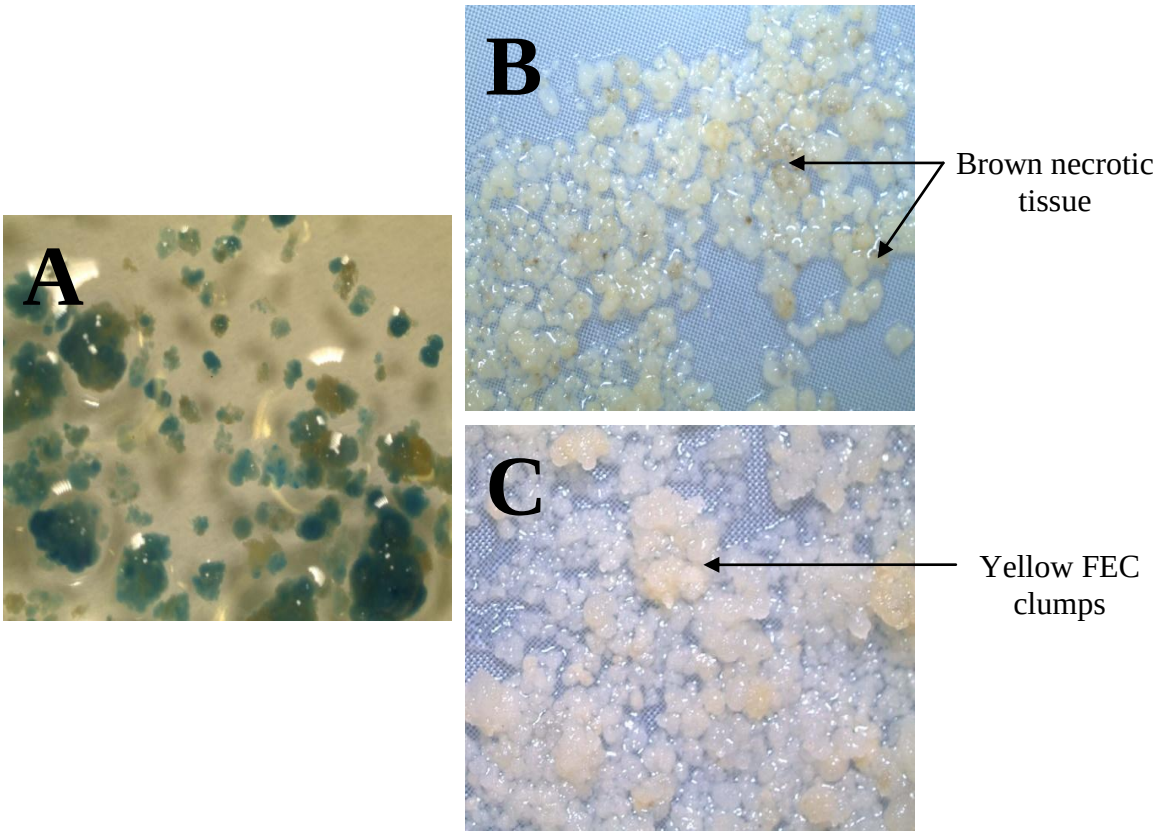


Figure 3.5 MM1 transformed cv60444 and T200 FEC. **(a)** GUS stained FEC. **(b)** MM1 transformed cv.60444 FEC: FEC not proliferating and not producing embryos after 4 weeks on MSN+C250+H15, turning necrotic. **(c)** MM1 transformed T200 FEC after 4 weeks on MSN+C250+H15: swollen yellow FEC not forming cotyledons.

Interesting and unusual finger-like structures, instead of the expected embryo structures, were observed from cv.60444 FECs transformed with MM3 constructs **(fig. 3.6 b)** despite positive transformation, indicated by blue-stained FEC (GUS assay) **(fig. 3.6 a)**.

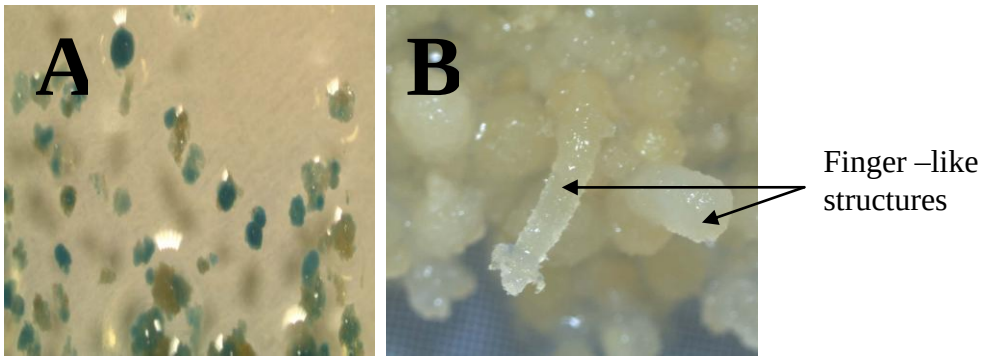


Figure 3. 6 MM3 transformed cv.60444 FEC **(a)** GUS stained FEC. **(b)** cv.60444 FEC producing finger-like structures instead of expected embryo structures.

3.5.3.3 Shoot development and rooting of putative transgenic lines

Group A and B cotyledons emerging from FEC transformation and regeneration events were transferred to shoot-promoting media containing 100 mg/ml carbenicillin (CEM+C100). After placing the cotyledons on CEM+C100 for 2 weeks, shoots with juvenile leaves emerged from the middle of the cotyledons **(fig. 3.4 f)**. Approximately 65% of the cotyledons produced shoots.

Group A and group B shoots were excised and placed on rooting media with 50 mg/ml carbenicillin (CBM+C50). Overall a high percentage of shoots placed on CBM+C50 produced roots efficiently. Each shoot that rooted was treated as an independent putative transgenic line. Less than 5 % of shoots failed to root. Over 100 putative transgenic A-group lines were generated on CBM+C50, however for handling purposes only 100 A-MM2 lines and 100 A-MM4 lines **(table 3.2)** were selected and maintained for transgene status characterisation.

B-group shoots were able to develop roots at a high efficiency with the exception of B-MM3 transgenic lines. Only 50 putative transgenic lines were selected for maintained and transgene status determination, and again this was done to help keep the number of lines analysed at a

manageable size. As a result of the lower rooting efficiency observed for B-MM3 lines, only 43 putative transgenic lines were generated **(Table 3.2)**.

3.5.4 Non-mismatched RNA silencing hairpin constructs transformation of cv.60444 and T200 FEC and regeneration of transformed FEC

3.5.4.1 FEC transformation and cotyledons

Cultivar 60444 and T200 FEC transformation events with non-mismatched constructs were given the codes Group C and Group D, respectively. Selection of cv.60444 and T200 FEC transformed with non-mismatched constructs followed the same sequence of events as observed for cv.60444 and T200 FEC transformed with mismatched constructs (**3.5.3)**. Transformed FEC were selected for on GD media containing increasing concentrations of hygromycin. Embryos were formed after moving FEC to MSN+H15 media. Results were similar to those observed in **3.5.3.** Once again a delay in embryo production was observed in T200 transformed FEC compared with cv.60444 transformed FEC.

Embryos matured and gave rise to cotyledons. Approximately a 10-fold decrease in cotyledon numbers was observed in both cv.60444 and T200 FEC transformed with non-mismatched constructs compared to cotyledons generated from mismatched transformed cv.60444 and T200 FEC (reported in **3.5.3)**.

3.5.4.2 Shoot development of cotyledons

Cotyledons were placed on CEM+C100 media and green shoots with immature leaves emerged. C-MM6 generated cotyledons had a shooting efficiency of 66% and 60% for C-MM8 generated cotyledons. D-MM6 and D-MM8 generated cotyledons had a 71% and 54% shooting efficiency, respectively **(table3.2)**.

Table 3. 2 Cotyledon and shoot generation efficiency per ~1cm FEC clump for each cultivar/landrace construct transformation event.

Cultivar/landrace transformed,construct and experiment group	**RNAi construct**	**Number of ~1 cm FEC clumps**	**Number of cotyledons generated**	**Number of cotyledons/ ~1 cm FEC clump**	**Number of emerging shoot**	**Number of shoots/ ~1 cm FEC clump**
cv.60444 transformation with Mutated sense-RNAi constructs (A-group)	MM2hp	70	850	12	535	8
	MM4hp	70	640	9	408	6
cv.60444 transformation with Non-mutated-RNA constructs (C-group)	MM6hp	40	107	3	71	2
	MM8hp	40	117	3	67	2
T200 transformation with Mutated sense-RNAi constructs (B-group)	MM2hp	50	317	6	197	4
	MM3hp	50	108	2	65	1
	MM4hp	50	343	7	230	5
T200 transformation with Non-mutated-RNAi constructs (D-group)	MM6hp	30	40	1	28	1
	MM8hp	30	70	2	38	1

3.5.4.3 Shoot rooting to generate putative transgenic lines

As a result of low cotyledon numbers, fewer shoots were available for transfer to rooting media CBM+C50. Roots started appearing as early as 2 weeks after placing excised shoots in rooting media. Shoot and roots matured over 6-8 weeks giving rise to putative transgenic lines. Up to 95% of shoots placed on rooting media managed to produce roots however as s a result of the low starting shooting number, fewer putative transgenic lines were available for further transgene status characterisation **(table 3.2).**

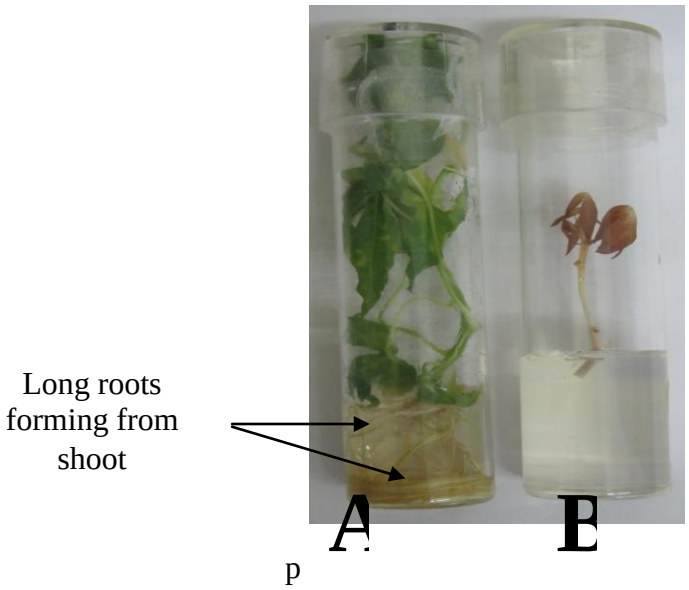
3.5.5 Visual screening of Group A, Group B, Group C and Group D generated lines for transgene status

A total of 98 A-MM2 lines, 99 A-MM4 lines, 50 B-MM2, 42 B-MM3 and 50 B-MM4 putative transgenic lines were screened The number of putative transgenic lines from group C and D that were screened was reduced to 30 lines for C-MM6, 40 lines for CMM-8, 20 lines for D-MM6 and 30 lines for D-MM8.

All the selected putative transgenic lines (generated and selected in **3.5.3** and **3.5.4)** were tested for transformation success using visual tests: (i) hygromycin rooting test and GUS assay and (ii) molecular methods: PCR of the *Hyg*, *GUS* and transgene, southern blots and northern blots.

3.5.5.1 Hygromycin rooting test

Apical shoots of putative transgenic lines were placed on CBM media containing 10 µg/ml hygromycin (CBM+C50+H10), this was to test the rooting ability in media containing hygromycin selection. Successfully transformed lines were able to produce roots and grow in media containing hygromycin, while untransformed cv.60444 and T200 failed to produce roots, and the apical shoot failed to grow, turned brown and died **(fig. 3.7)**. A-MM2 and A-MM4 putative transgenic lines had 86% and 88% rooting success, respectively. B-MM2, B-MM3 and BMM4 had 95%, 98% and 98% respectively. C-MM6 and C-MM8 putative transformed lines showed a 66% and 75% rooting success, respectively. C-MM5 and C-MM7 putative transgenic lines all failed to root. D-MM6 and D-MM8 had 66% and 83% rooting success, respectively **(table 3.2)**.

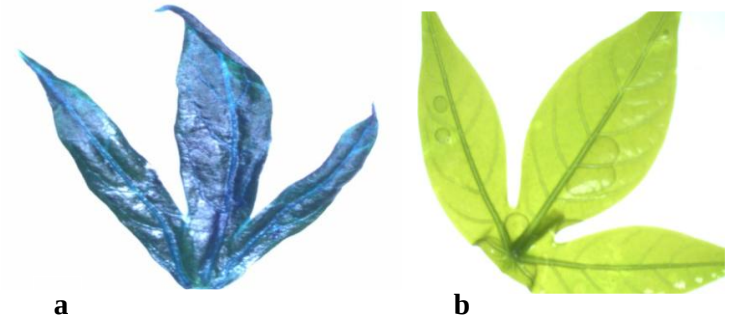


p

Figure 3.7 Hygromycin rooting test. **(a)**Transgenic line rooting and growing well on CBM+C50+H10 medium **(b)** Untransformed cv.60444 not rooting nor growing on CBM+C50+H10 medium.

3.5.5.2 GUS assay

Along with the rooting test, putative transgenic lines were also screened for transformation success using a GUS assay. Lines that had been successfully transformed turned blue following O/N incubation in GUS assay solution (**fig. 3.8a**). Leaves that remained green following staining suggested that plant was not transgenic (**fig. 3.8b**). GUS assay results demonstratedthat 74 % of A-MM2 and 80 % of A-MM4 lines were transgenic. Seventy four percent, 76 % and 64 % of B-MM2, B-MM3 and B-MM4 lines assayed were positive for GUS, respectively. A low 37 % of C-MM6 lines assayed tested positive for GUS and 63 % of C-MM8 lines tested positive. All C-MM5 and C-MM7 lines tested negative for GUS. GUS assay results of D group putative transgenic lines suggested that 43 % of D-MM6 and 60 % of D-MM8 selected lines had been successfully transformed **(table 3.2)**. As expected, untransformed cv.604444 and untransformed T200 control plants were negative for GUS, with the leaves not staining blue **(fig. 3.8 b)**.



a **b**

Figure 3. 8 Leaves following O/N incubation at 37 °C in GUS assay solution. **(a)** Blue stained leaf (positive GUS assay) indicating positive transgene status. **(b)** Untransformed green wild-type cv.60444 leaf negative for *GUS*

Table 3.3 Transformation efficiency calculated based on putative transgenic plantlets able to root on hygromycin-containing media and positive blue GUS assay.

Transformation group ID	**Number of Lines screened**	**Transformation efficiency**	
		Hygromycin Rooting test (%)	**GUS assay (%)**
A-MM2	98	86	74
A-MM4	99	88	80
B-MM2	50	98	74
B-MM3	42	95	64
B-MM4	50	98	76
C-MM6	68	66	37
C-MM8	65	75	62
D-MM6	21	67	62
D-MM8	36	83	50

3.5.6 PCR-based validation of group A, group B, group C and group D transgene status

For validation of visual screening results, PCR amplification of *Hyg*, *GUS* and insert were performed.

3.5.6.1 Mismatched cv.60444 lines (group A) and mismatched T200 lines (group B) - Transgene status screening using PCR amplification of *GUS*, *Hyg* and transgene

- **Group A lines:**

A-MM2 lines

PCR amplification of a 181 bp *GUS* fragmentwas successful in 85 % of the 98 A-MM2 lines, however only 83 % of the same lines were positive for the 485 bp *Hyg* amplicon. Positive and negative controls gave the expected results **(fig 3.9a and b)**. The **337 bp** mutated sense-arm (of the construct) was detected in 80 % of the lines **(fig. 3.9c)**. However the **319 bp** non-mutated antisense-arm of the hairpin could not be amplified in all 98 lines, but the positive control amplified from plasmid gave the expected fragment size **(fig. 3.9d)**. *GUS*, *Hyg* and RNAi construct PCR amplification results suggested that some lines had only certain regions of the T-DNA integrated. An example of this was line, A-MM2-3, where only the *Hyg* and the hpRNA mutated sense-arm could be amplified **(fig. 3.9)**. A total of 98 lines were screened, but the agarose electrophoresis gels below show results for only 27 lines.

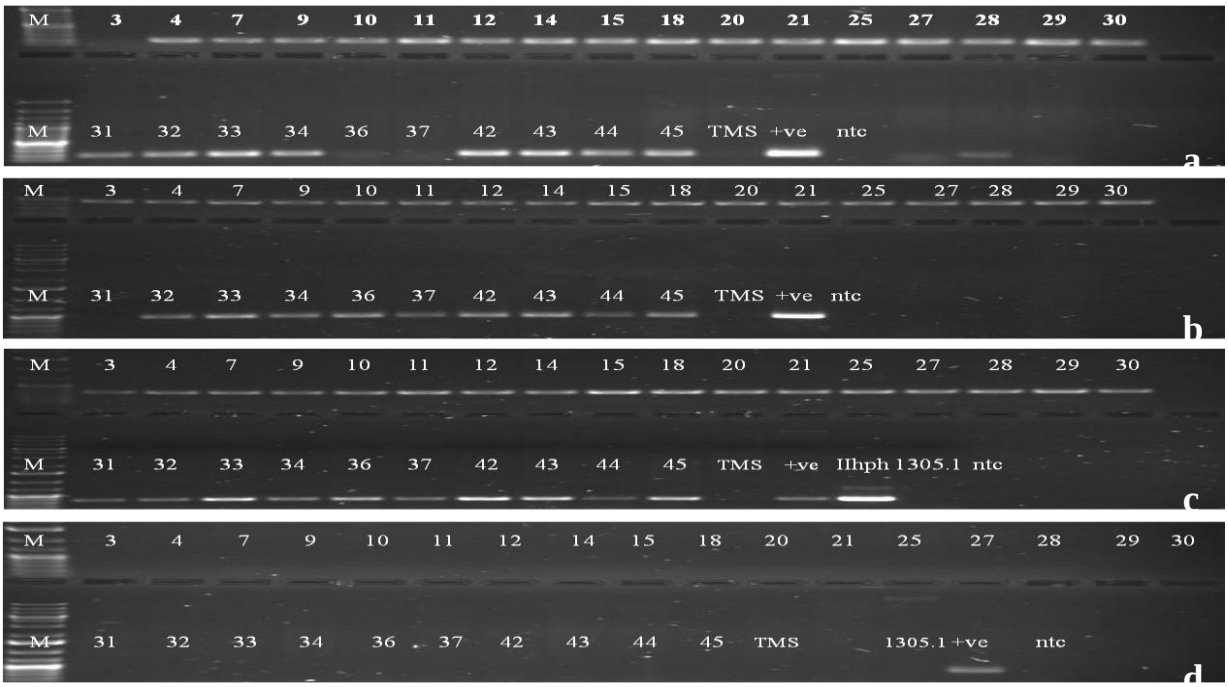


Figure 3. 9 1 % agarose gel electrophoresis of *Hyg*, *GUS* and RNAi construct PCR amplicons in 27 A-MM2 putative transgenic lines that were selected for rooting test and GUS assay. Lines were screened for the **(a)** 181 bp GUS gene fragment, **(b)** 485 bp *Hyg* gene amplicon, **(c)** 337 bp mutated sense-arm amplicon and **(d)** the 319 bp non-mutated antisense-arm amplicon. M= O'GeneRuler 1 kb Plus DNA ladder (Fermentas).

A-MM4 lines

A *GUS* amplicon was detected in 93 % of the 99 MM4 lines tested **(fig. 3.10a)**. The *Hyg* amplicon was amplified in 99 % of the lines **(fig. 3.10b)**. Lines were also tested for the mutated sense-arm of the hairpin, and the 239 bp fragment was amplified in 89 % of the lines **(fig. 3.10c)**, however, the non-mutated antisense-arm of the hairpin could not be detected in any of the 99 lines. Positive control reactions yielded the expected results **(fig. 3.10d).** In certain lines, for example A-MM4 90, the Hyg rooting test was positive, however PCR amplification of the *Hyg*, *GUS*, mutated sense-arm and non-mutated antisense-arm were all negative.

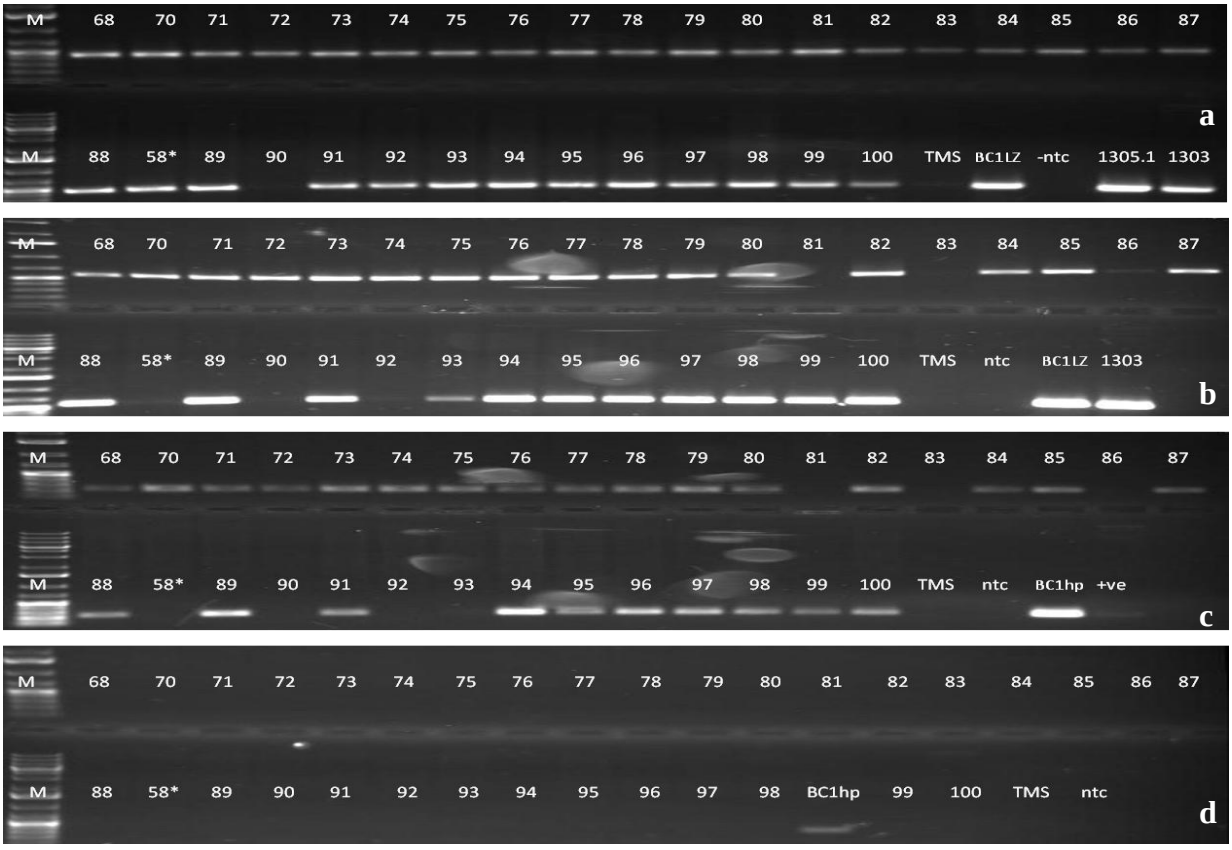


Figure 3. 10 PCR confirmation of transgene status of MM4 putative transgenic lines. Lines were screened for the **(a)** 181 bp *Hyg* fragment, **(b)** 485 bp *GUS* amplicon, **(c)** 337 bp mutated sense-arm hairpin amplicon and **(d)** the 221 bp non-mutated antisense-arm hairpin amplicon. M= O'GeneRuler 1 kb Plus DNA ladder (Fermentas).

- **Group B lines:**

<u>B-MM2 lines</u>

PCR amplification of the 181 bp *GUS* fragmentwas successful in 96 % of the 50 B-MM2 lines and the 485 bp *Hyg* fragment was detected in 98 % of the 50 BMM2 lines **(fig. 3.11a and b)**. Transgene screening using the non-mutated sense-arm primers was positive in only 40 % of the lines **(fig. 3.11c)**. Screening of the same lines using the mutated-sense arm primers amplified positive in 96 % of the lines **(fig. 3.11d)**. Agarose gels below show results for only 15/50 lines that were screened.

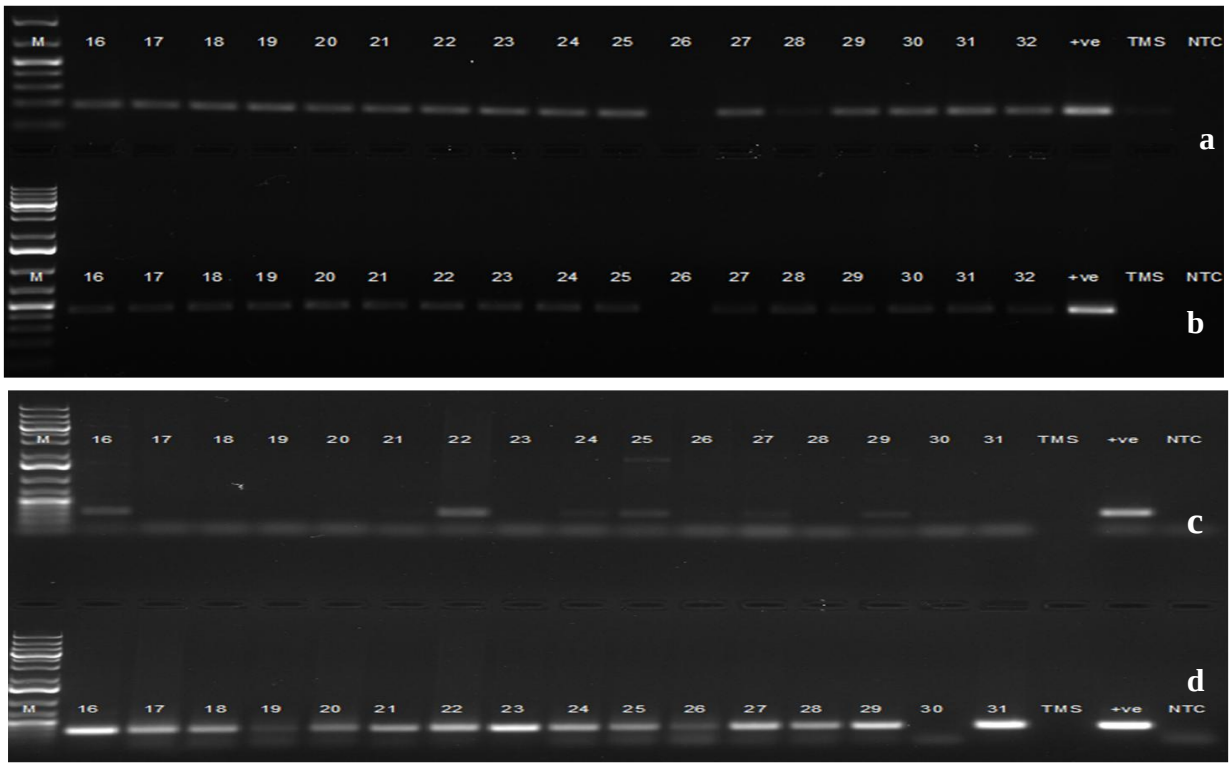


Figure 3. 11 PCR confirmation of transgene status of putative transgenic B-MM2 lines selected for rooting test and GUS assay. All 50 lines were screened, but gels above only showing results lines B-MM2 16-31. Lines were screened for **(a)** 181 bp *Hyg* amplicon, **(b)** 500 bp *GUS* amplicon, **(c)** 319 bp non-mutated antisense-arm fragment of the hairpin and **(d)** the 337 bp mutated sense-arm fragment of the hairpin. M= O'GeneRuler 1 kb Plus DNA ladder (Fermentas).

B-MM3 lines

The 181 bp *GUS* amplicon was detected in all of the 42 lines screened **(fig. 3.12a)**. The same lines were screened for the *Hyg* region of the transgene, and this was only detected in 95 % of the lines **(fig. 3.12b)**. The lines were further screened for the non-mutated antisense-arm of the transgene, and this was only detected in 31 % of the lines **(fig. 3.12c)**. Screening of the mutated sense-arm fragment of the hairpin was only detected in an even lower 21 % of the lines **(fig. 3.12d)**. Mutated sense-arm and antisense-arm amplicons were very faint **(fig. 3.12c and d)**. Gels below show results of only 12/50 of the lines screened.

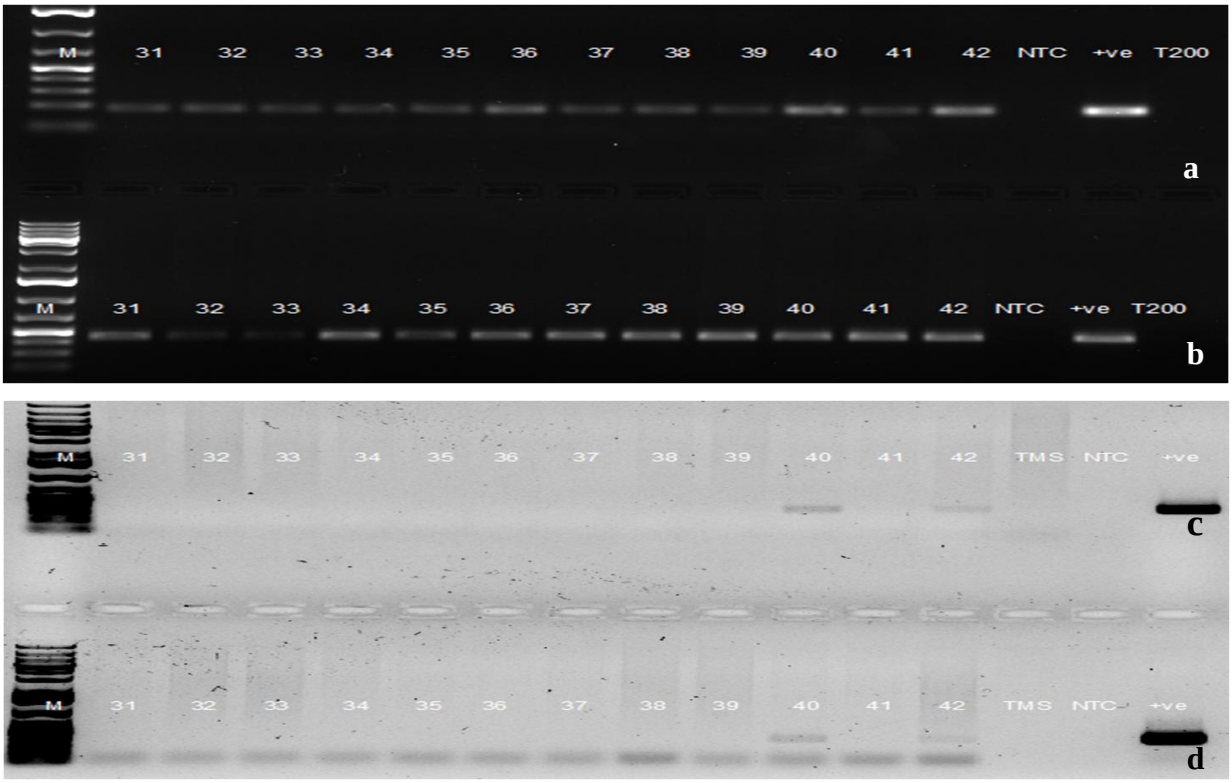


Figure 3. 12 PCR screening of putative transgenic B-MM3 lines selected for rooting test and GUS assay. All 42 lines were screened, but gels above show results of B-MM3 31- 42 lines. Lines were screened for **(a)** 181 bp *GUS* amplicon, **(b)** 485 bp *Hyg* amplicon, **(c)** 381 bp non-mutated antisense-arm fragment and **(d)** 399 bp mutated sense-arm fragment of the construct. M= O'GeneRuler 1 kb Plus DNA ladder (Fermentas).

B-MM4 lines

The *Hyg* fragment was detected in 92 % of the 50 lines screened **(fig. 3.13a)**. The *GUS* amplicon was detected in 96 % of the 50 lines screened (**fig. 3.13b)**. The non-mutated antisense-arm of the construct was amplified in 96% of the lines **(fig. 3.13c)**. The mutated sense-arm was amplified in only 88 % of the lines **(fig. 3.13d)**. The negative and positive control PCR reactions yielded the expected results. Gels below are showing results for only 11 lines.

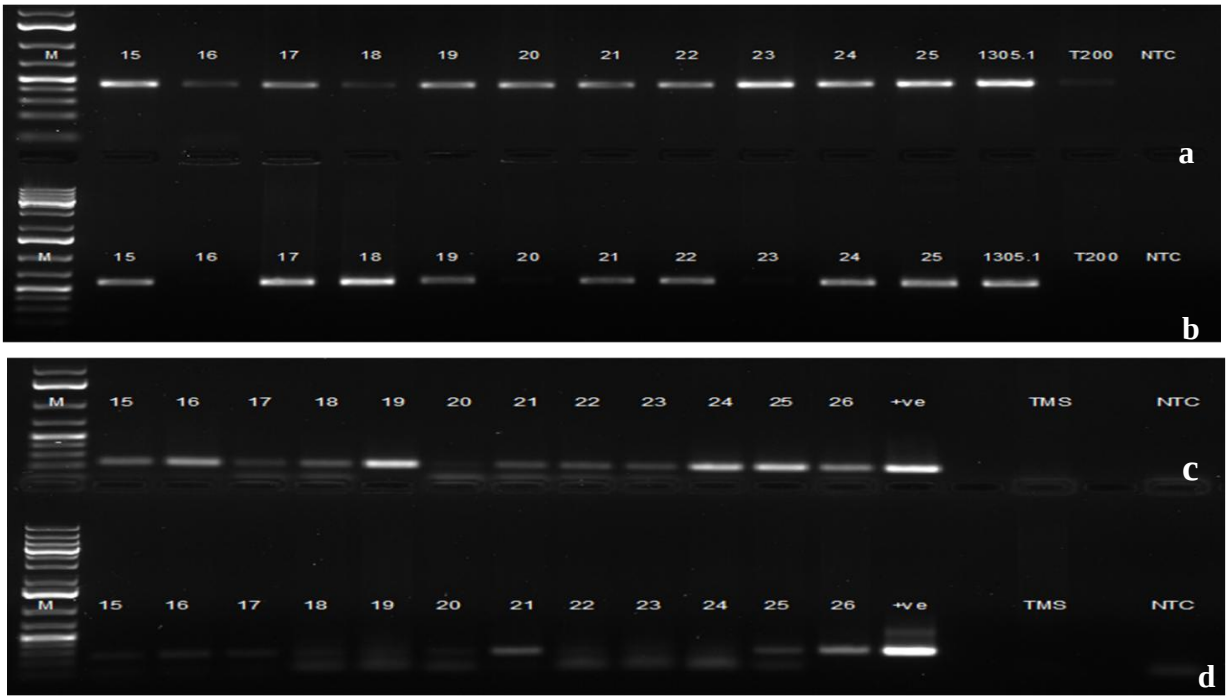


Figure 3. 13 PCR confirmation of transgene status of putative transgenic BMM4 lines that were selected for rooting test and GUS assay. All 50 lines were screened, but gels above only show results for lines BMM4 15-25. Lines were screened for **(a)** 485 bp Hyg gene amplicon, **(b)** GUS gene**(c)** 221 bp non-mutated antisense-arm fragment and **(d)** the 239 bp mutated sense-arm fragment of the construct. M= O'GeneRuler 1 kb Plus DNA ladder (Fermentas).

3.5.6.2 Non-mismatched cv.60444 lines (group C) and non-mismatched T200 lines (group D) - Transgene status screening using PCR amplification *GUS*, *Hyg* and RNAi construct

C-MM6 lines

Molecular screening of C-MM6 lines was performed on 17 lines. All the 17 lines were positive for both the 181 bp *GUS* amplicons **(fig. 3.14 a)** and the 485 bp *Hyg* fragment **(fig. 3.14 b)**. Positive amplification was achieved for both plasmid controls while no amplicons were obtained for the negative control untransformed cv.60444 and the NTC. None of the samples tested positive for PCR amplification of both the 331 bp MM6 *Xba*I-arm and the 339 bp MM6 *Xho*I-arm of the construct (gel not shown).

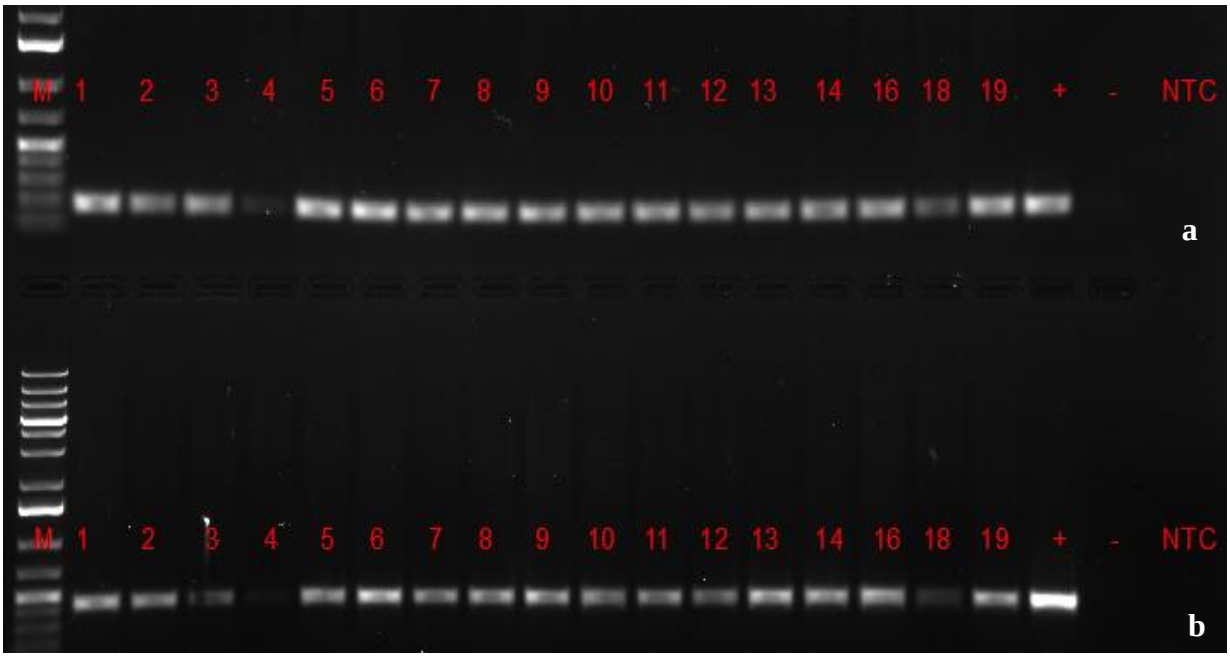


Figure 3.14 PCR confirmation of putative transgenic C-MM6 lines transgenic status. Lines were screened for **(a)** 181 bp *GUS* fragment; fragment was successfully amplified in all lines screened. **(b)** Amplification of the 485 bp hygromycin gene fragment was detected in all lines tested. In both **(a)** and **(b)** plasmid amplified positive while no amplicons was seen in both the untransformed cv.60444 and NTC controls. M= O'GeneRuler 1 kb Plus DNA ladder (Fermentas).

C-MM8 lines

Amplification of the 181 bp *GUS* was positive in 15/17 lines screened while 16/17 were positive for the 485 bp *Hyg* gene fragment. Positive controls amplified positive for both the *GUS* and *Hyg*. The negative control, untransformed cv.60444, and NTC were negative for the both GUS and *Hyg* gene fragments. Amplification of the 239 bp MM8 *Xba*I-arm was strongly amplified in only 2 of the 17 samples tested. Faint amplification of this 239 bp fragment was observed in the 10 remaining lines. The 236 bp MM8 *Xho*I-arm was amplified at high intensity in only 1 of the 17 lines tested while very faint amplicons were seen in 7 lines and no amplicons was seeing in 9/17 lines. Positive and negative controls gave expected results.

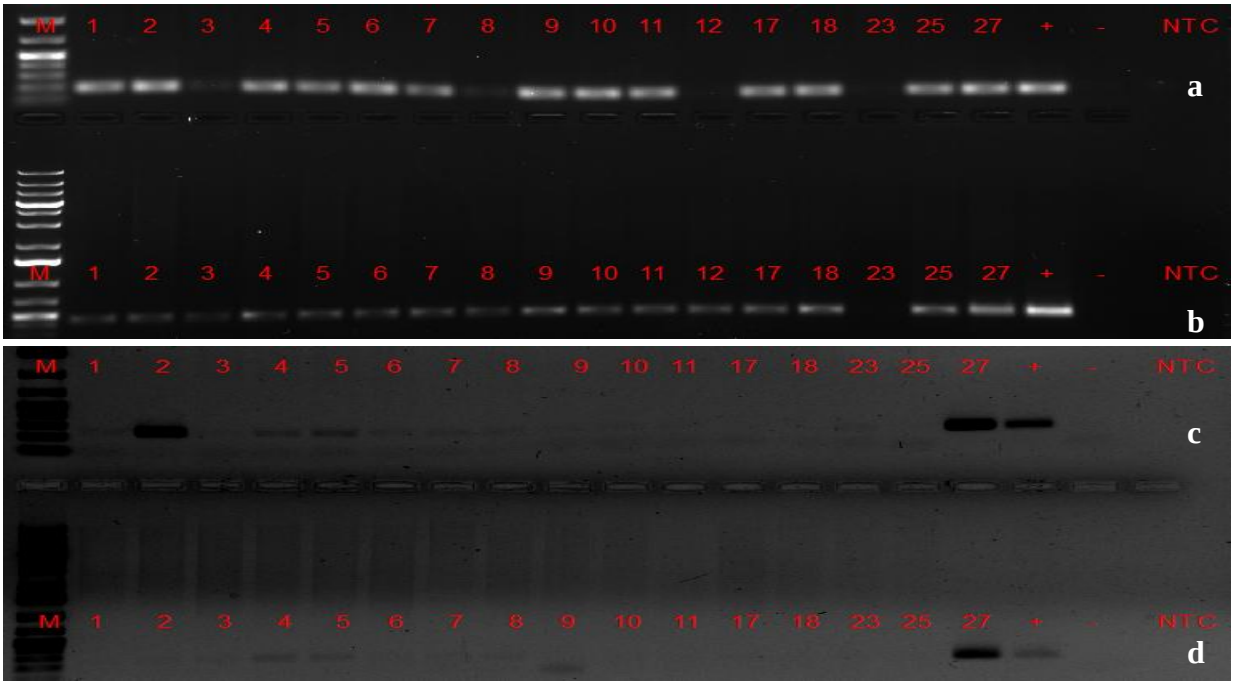


Figure 3. 15 PCR confirmation of putative transgenic C-MM8 lines transgenic status. Lines were screened for **(a)** 181bp *GUS* fragment successfully amplified in all lines except line 12 and 23 **(b)** Amplification of the 485 bp *Hyg* fragment was detected in all lines except line 23. **(c)** Inverted gel image of 239 bp MM8 *Xba*I amplicons detected in line 2 and 27 and very faintly in lines 1,3,4,5,6,7,8,9,10 and 23 **(d)** Inverted gel image of 239 bp MM8 *Xho*I-arm detected in line 27 and very faintly in lines 1,2,3,4,5,7,8. M= O'GeneRuler 1 kb Plus DNA ladder (Fermentas).

D-MM6 transgenic lines

All 8 D-MM6 lines screened were positive for presence of the 181bp *GUS* fragment **(fig. 3.16 a)** and positive for the 485 bp *Hyg* fragment **(fig. 3.16 b)**. Lines were also screened for the 331 bp MM6 *Xba*I-arm of the hairpin and the 331 bp MM6 *Xho*I-arm however both these fragments could not be amplified in all the 8 lines screened (gels not shown).

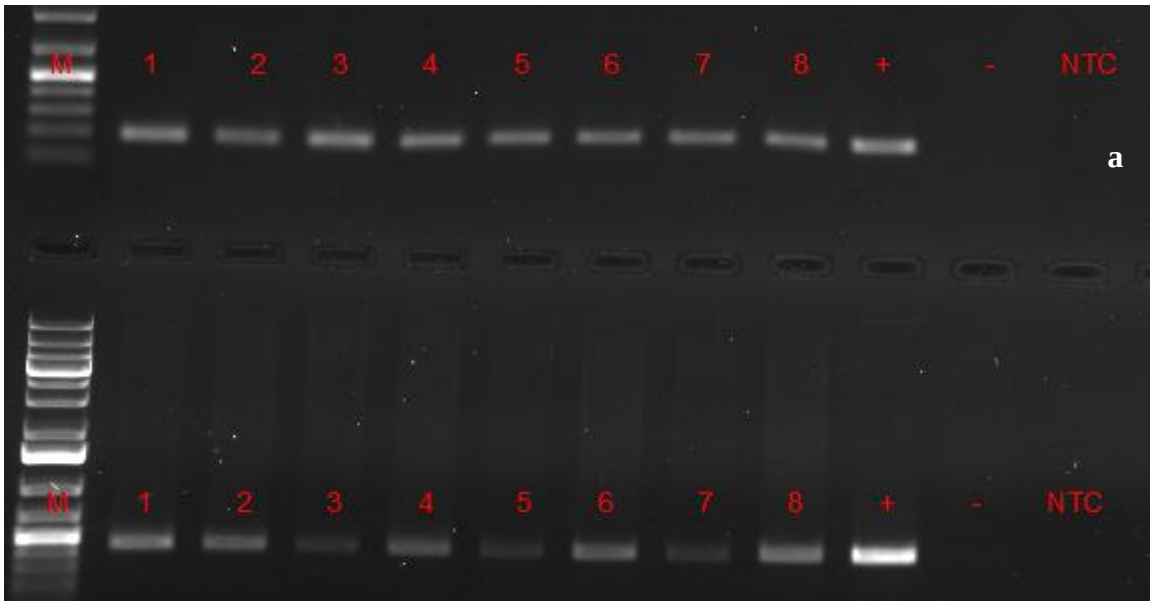


Figure 3.16 PCR screening of putative D-MM6 transgenic lines for transgene status. **(a)** Positive amplification of 181 bp *GUS* fragment in all 8 selected lines. **(b)** Positive amplification of the 485 bp *Hyg* gene fragment in all lines screened. M= O'GeneRuler 1 kb Plus DNA ladder (Fermentas).

D-MM8 lines

The 181 bp *GUS* fragment was positively amplified in all 10 out of 11 D-MM8 lines screened. **(fig. 3.17 a)**. These 11 lines were also screened for the presence of the 485 bp *Hyg* gene fragment, all 11 lines amplified positive **(fig. 13.7 b)**. Both *GUS* and *Hyg* positive controls amplified successfully while as expected the negative control, untransformed cv.60444 and the NTC produced no amplicons. Lines were also screened for the presence of the hairpin arm of the construct. The 239 bp MM8 *Xba*I-arm was amplified in 8 of the 11 lines screened; however the amplicons were very faint. The 239 bp MM8 *Xho*I-arm was amplified in 6 out of the 11 lines screened; the amplicons were also faintly amplified.

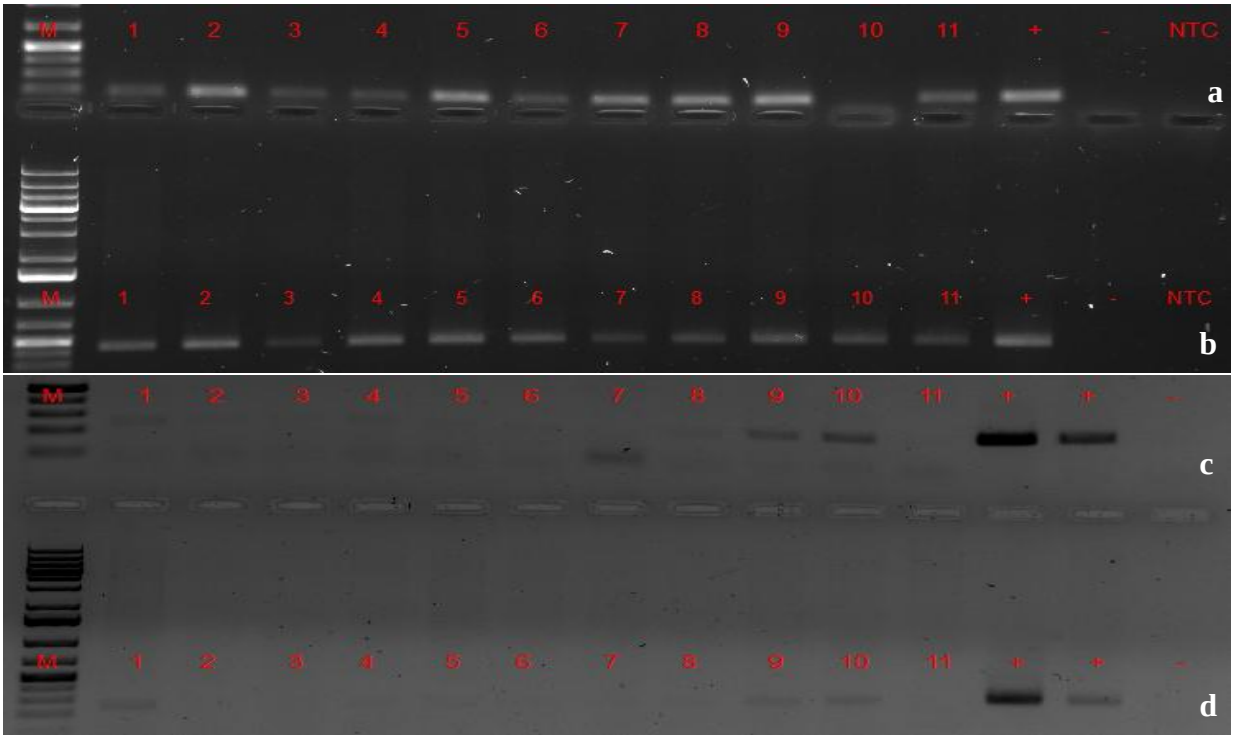


Figure 3. 17 PCR screening of D-MM8 lines for transgene determination. **(a)** PCR amplification of the 181 bp *GUS* fragment in 10 lines (lines 1-10) and positive control. **(b)** Positive amplification of 485 bp gene fragment in all 11 lines and positive control. **(c)** Amplification of 239 bp MM8 *Xba*I fragment in lines 1, 2, 4, 5, 6, 8, 9 and 10. **(d)** Amplification of the 239 bp MM8 *Xho*I fragment in lines 1, 3,4,5,9 and 10. M= O'GeneRuler 1 kb Plus DNA ladder (Fermentas).

3.5.7 Transgene integration analysis using Southern blot

Selected lines from the screening tests above were maintained in tissue culture for further processing and analysis.

Group A (mismatched cv.60444) and group C (non-mismatched cv.60444) transgenic lines were probed with 3 probes (*Hyg*, *GUS* and RNAi construct DIG-labelled probes). Group B (mismatched T200) and group D (non-mismatched T200) transgenic lines were probed with *Hyg* DIG labelled probe.

3.5.7.1 DIG Probe labelling and synthesis

Probes were successfully synthesised following the Roche DIG PCR labeled kit. Synthesis and labeling was confirmed by agarose gel electrophoresis. Successfully labelled gene fragments migrated slower than the respective unlabelled control gene fragment. Slower migration was as a result of the incorporation of the heavier DIG-11-dUTP deoxyribonucleotide contained in the mixture of deoxyribonucleotides. The DIG-labelled *Hyg* and *GUS* probes appeared higher than the 485 bp **(fig. 3.18 lane 1 and 2)**, and 181 bp *GUS* **(fig. 3.18 lane 3 and 4)** unlabelled counterparts. The unmodified ACMV AC1/4:AC2/3 DIG-probes appeared higher than unlabelled 319 bp ACMV AC1/4:AC2/3amplicon **(fig. 3.19 lane 1 and 3)** while unmodified BC1 labelled probe also appeared higher than 221 bp BC1 unlabelled amplicons. **(fig. 3.19 (lane 2 and 4)**. Probes were then used in Southern blot hybridisation experiments.

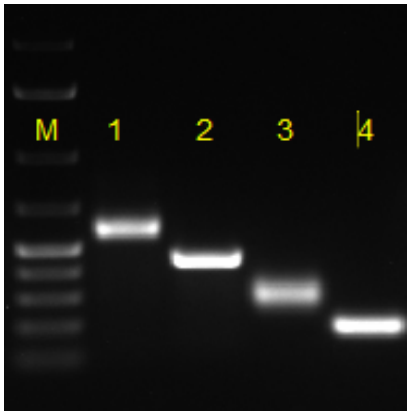


Figure 3. 18 1% agarose gel of PCR DIG labelled *Hyg* and *GUS* fragment probes. M= O'GeneRuler 1 kb Plus DNA ladder (Fermentas). DIG-labelled *Hyg* probe (lane 1) migrating slower than unlabelled 485 bp *Hyg* fragment (lane 2) and DIG-labelled *GUS* probe (lane 3) migrating slower than unlabelled 181 bp *GUS* fragment (lane 4).

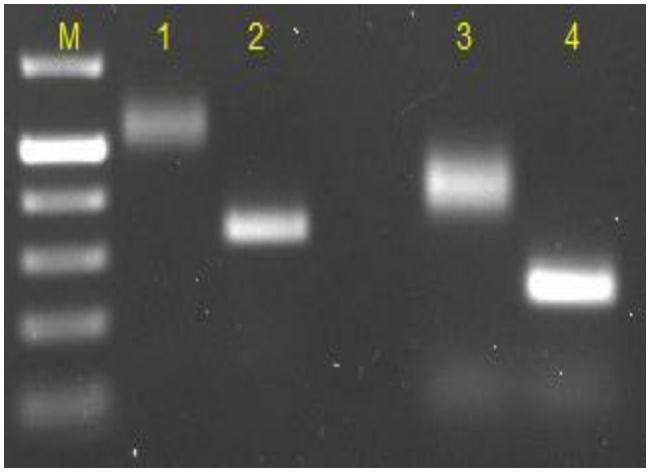


Figure 3. 19 1% agarose gel of PCR DIG labelled insert probes. M= O'GeneRuler 1 kb Plus DNA ladder (Fermentas), unmodified ACMV AC1/4:AC2/3 (lane 1) migrating slower than unlabelled 319 bp ACMV AC1/4:AC2/3 fragment (lane 3) and DIG-labelled unmodified BC1 unmodified (lane 2) migrating slower than unlabelled 221 bp BC1 (lane 4).

3.5.7.2 Group A transgenics

A-MM2 lines

Transgene integration study was performed on 16 of the 98 A-MM2 lines. Probing with DIG labelled-*Hyg* indicated that 12/16 lines had a single transgene copy integrated, 3/16 lines had 2 transgene copies integrated, while no transgene could be detected in one of the lines **(fig. 3.20a)**. Probing of the same 16 lines with DIG labelled-*GUS* 8/16 lines had a single transgene copy integrated, 2/16 had 2 transgene integrations, 3/16 lines had 3 transgenes integrated, 1/16 had 4 transgenes integrated, while in 1 line there was no transgene detection **(fig. 3.20b)**. The 16 lines were also screened for transgene copy number using the DIG labelled-ACMV AC1/4:AC2/3. Analysis showed that 11/16 of the lines had 1 copy of an intact MM2hp cassette (CaMV35S-ACMV AC1/4:AC2/3 IR- terminator), 2/16 lines had 1 copy of the intact cassette as well as a truncated MM2hp cassette and in 3/16 of the lines, no MM2hp cassette could be detected suggesting a deletion of the ACMV AC1/4:AC2/3 fragment of the MM2hp cassette **(fig. 3.20c)**.

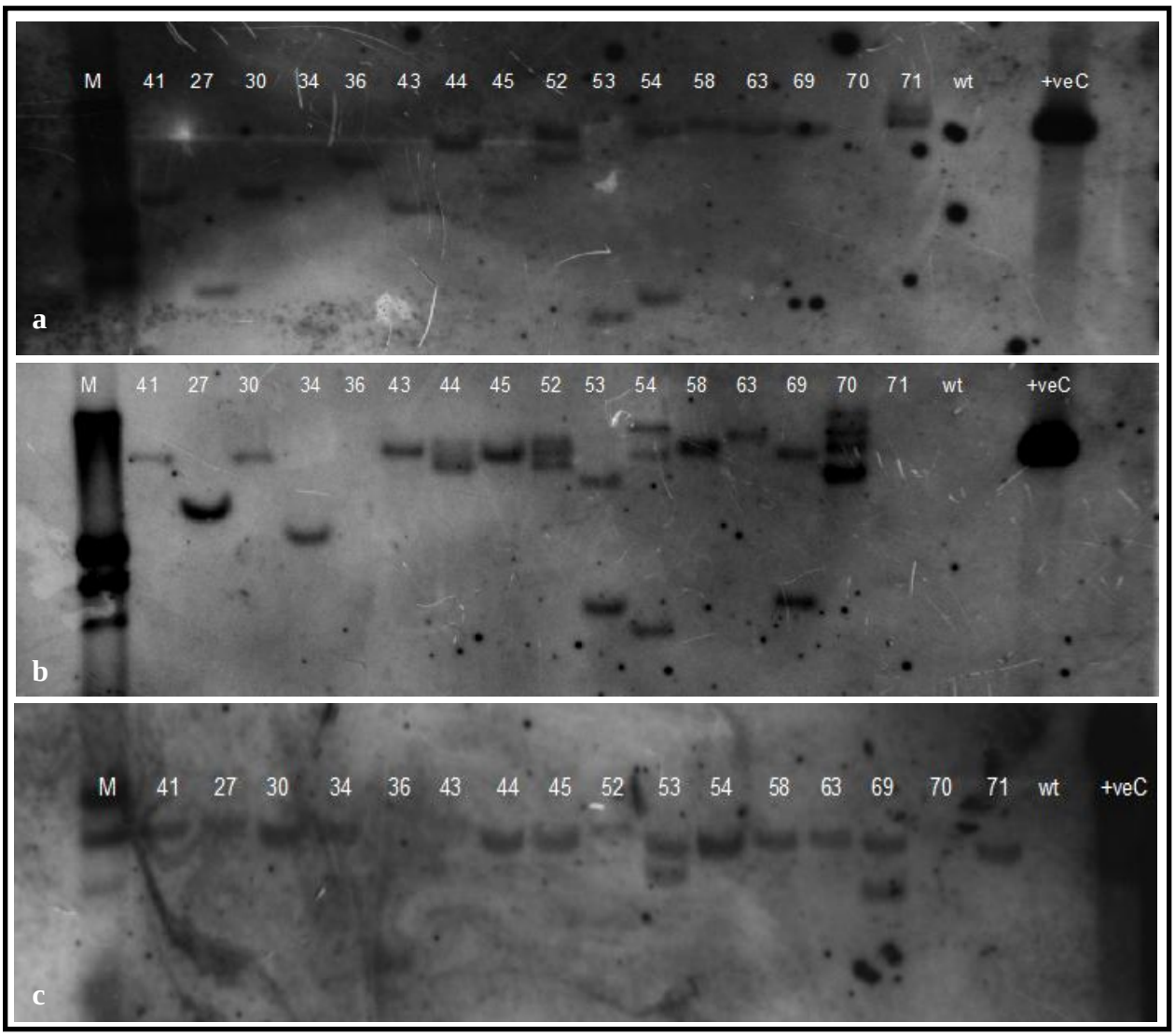


Figure 3. 20 Southern blot analysis of A-MM2 transgenic lines for transgene integration using three DIG-labelled probes. M = DIG molecular weight marker (Roche), wt = untransformed cv.60444 and +veC = pC1305.1 **(a)** *Hind*III-digested genomic DNA, probed with *Hyg* **(b)** *Hind*III-digested genomic DNA, probed with *GUS* and **(c)** *Hind*III and *Eco*RI-double digested genomic DNA, probed with ACMV AC1/4:AC2/3 DIG-labelled fragment to detect a 2771 bp MM2hp cassette; +veC = *Hind*III and *Eco*RI-double digested pTZR5/T containing MM2hp cassette.

Table 3.4 Transgene copy numbers of 16 A-MM2 lines detected by DIG-labelled *Hyg*, *GUS* and DIG Hybrid II (ACMV AC1/4:AC2/3) -labelled probes

Line ID	*Hyg*	*GUS*	MM2hp cassette
21	1	1	1
27	1	1	1
30	1	1	1
34	1	1	1
36	1	0	0
43	1	1	0
44	1	3	1
45	1	1	1
52	2	3	1
53	1	2	1 and a truncated copy
54	2	3	1
58	1	1	1
63	1	1	1
69	1	2	1 and a truncated copy
70	0	4	0
71	2	0	1

A-MM4 lines

Out of 98 A-MM4 transgenic lines, 17 lines were selected to analyse transgene integration patterns. Transgene copy results, when probed using the DIG-labelled *Hyg* indicated that 14/17 lines had single transgene copy, 1/17 lines had 2 copies, and there was no detection in 2/17 A-MM4 lines **(fig.3.21a)**. When probing the same 17 lines with DIG-labelled *GUS* probes, 10/17 lines had a single transgene copy and 7/17 lines had 2 transgene copies **(fig. 3.21b)**. Lines were also probed with DIG-labelled BC1 unmodified fragment. Probing showed that 13/17 lines had an intact MM4hp cassette (CaMV35S-SACMV BC1 IR-terminator), 1 line had an intact MM4hp cassette as well as 4 other copies containing insertions within the cassette, 1/17 had an intact cassette and an insertion containing copy, and in 2/17 lines no MM4hp cassette could be detected suggesting a possible deletion of the unmodified arm of the MM4hp **(fig. 3.21c)**.

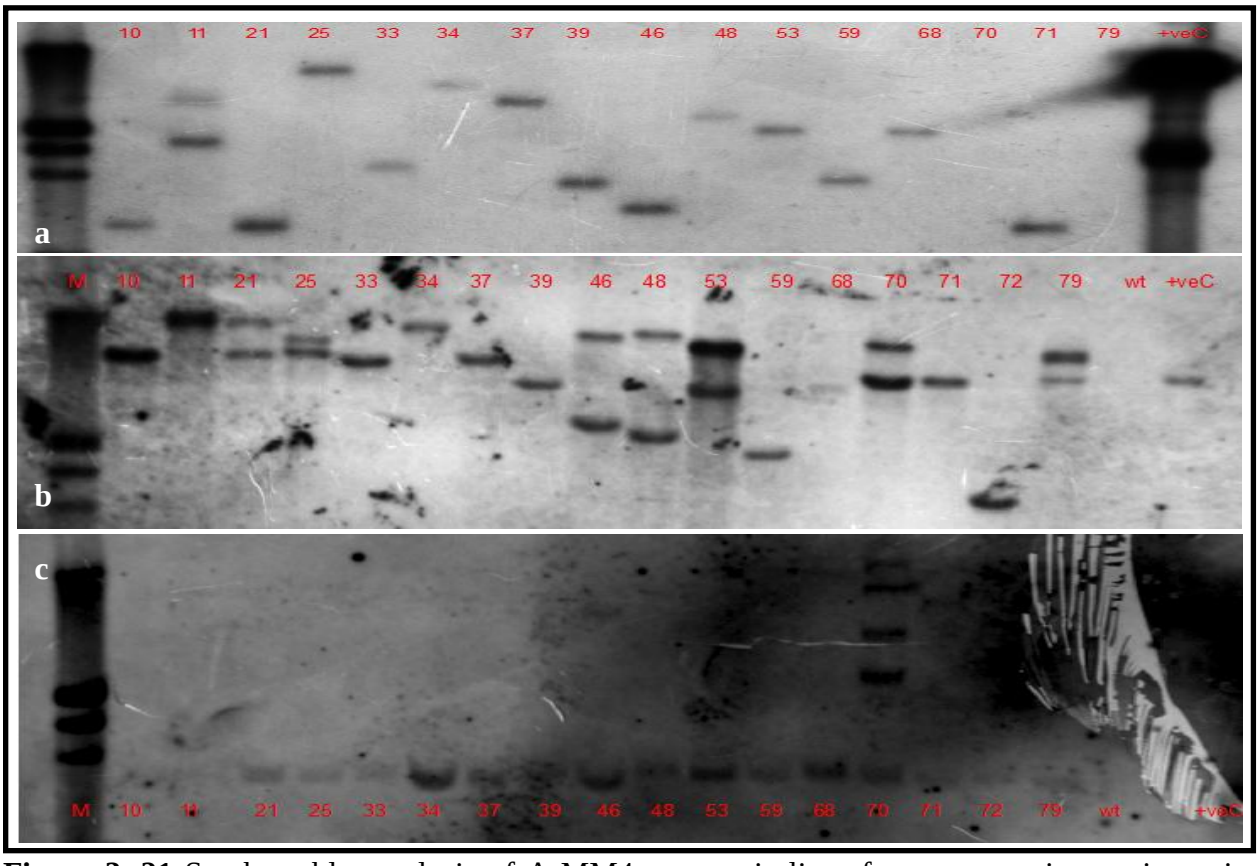


Figure 3. 21 Southern blot analysis of A-MM4 transgenic lines for transgene integration using DIG-labelled probes. M = DIG molecular weight marker (Roche), wt = untransformed cv.60444 and +veC = pC1305.1 **(a)** *Hind*III-digested genomic DNA, probed with *Hyg*, **(b)** *Hind*III-digested genomic DNA, probed with *GUS* and **(c)** *Hind*III and *Eco*RI-double digested genomic DNA, probed with BC1 unmodified DIG-labelled fragment to detect 2575 bp MM4hp cassette; +veC = *Hind*III and *Eco*RI-double digested pTZR5/T containing MM4hp cassette.

Table 3. 5 Transgene copy numbers of 16 A-MM4 lines detected by DIG-labelled *Hyg*, *GUS* and BC1 unmodified fragment probes

Line ID	*Hyg*	*GUS*	MM4hp cassette
10	1	1	0
11	2	1	0
21	1	2	1
25	1	2	1
33	1	1	1
34	1	1	1
37	1	1	1
39	1	1	1
46	1	2	1 + an insertion containing copy
48	1	2	1
52	1	2	1
59	1	1	1
68	1	1	1
70	0	2	1 +4 insertion containing copies
71	1	1	1
79	0	2	1

3.5.7.3 Group B transgenics

B-MM2, B-MM3 and B-MM4 transgenic lines (T200 transformed with mismatched RNAi constructs) were screened for transgene copy number using DIG labelled-*Hyg* probe. A total of 50 B-MM2 lines, 29 B-MM3 and 50 B-MM4 lines were screened. Screening results of B-MM2 lines indicated that 44/50 had a single transgene copy, 2/50 lines had 2 transgene copies while no transgene could be detected in 4/50 of the lines **(fig. 3.22a)**. Screening of 29 B-MM3 transgenic lines with *Hyg* probe indicated that 25/29 had a single transgene copy, 3/29 lines had 2 transgene copies and 1 line was negative **(fig 3.22b)**. A total of 50 B-MM4 lines were screened; 43/50 had a single transgene copy number, 4/50 lines had 2 transgene copies and no transgene could be detected in 3/50 lines **(fig 3.22c)**. Not all B-MM2, B-MM3 and B-MM4 Southern blot pictures have been included; only one Southern blot figure for each is shown.

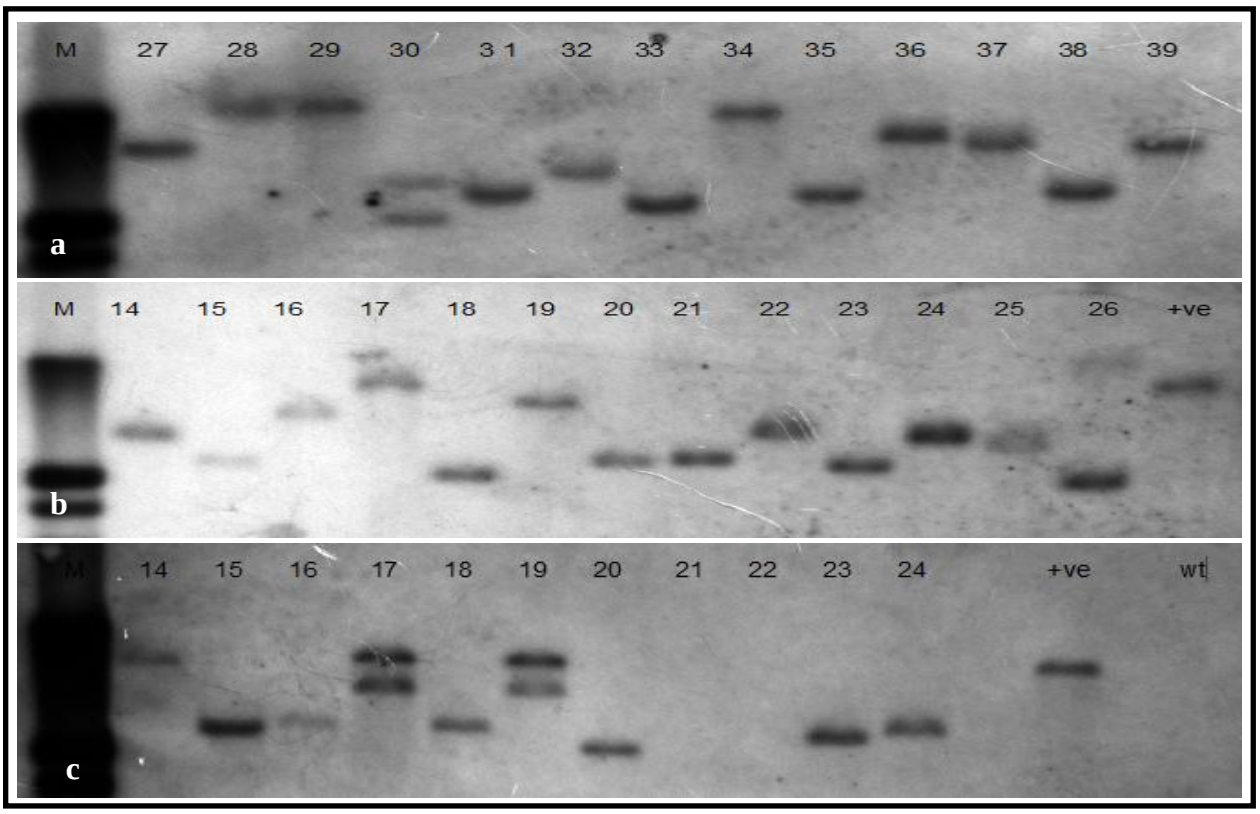


Figure 3.22 Southern blot of B-MM2, B-MM3 and B-MM4 *Hind*III-digested genomic DNA probed with DIG-labelled *Hyg* probe for transgene copy number. **(a)** 13/50 B-MM2 lines (B-MM2 27-39), **(b)** 13/29 B-MM3 lines (B-MM3 14-26) and **(c)** 11/50 BMM4 lines (B-MM4 14-24). M = DIG molecular weight marker (Roche), wt = untransformed cv.60444 and +ve = pC1305.1 plasmid control.

3.5.7.4 Group C transgenic lines

C-MM6 transgenic lines

Transgene integration analysis was performed on 15 C-MM6 lines using DIG-labelled *Hyg*, *GUS* and MM6 *XbaI* fragment probes. Probing with DIG labelled-*Hyg*, 6/15 lines had a single transgene copy, 4/15 had 2 transgene copies, 2/15 had 4 transgene copies while no transgene could be detected in 3/15 lines **(fig. 3.23a)**. When probing the same 15 lines with DIG-labelled *GUS* probe, 9/15 lines had a single transgene copy, 2/15 had 2 copies and while no transgene could be detected in 4/15 lines **(fig. 3.23b)**.

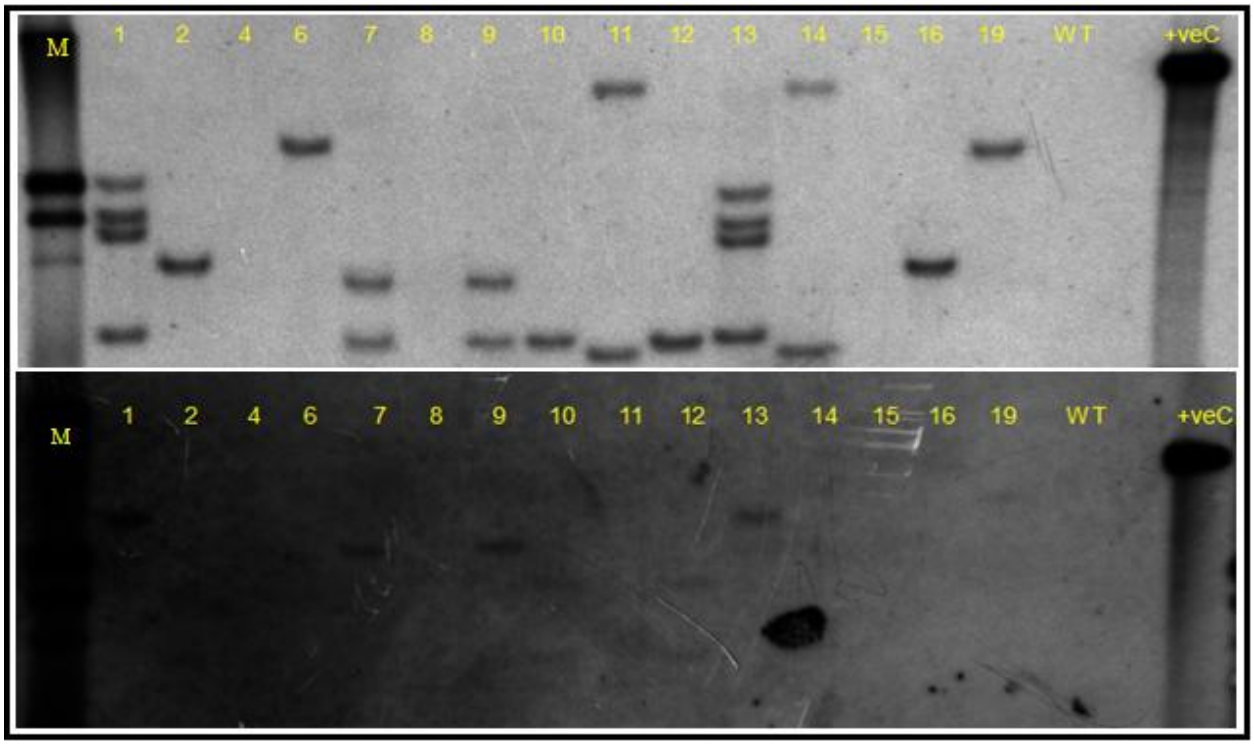


Figure 3. 23 Southern blot analysis of C-MM6 transgenic lines for transgene integration using DIG-labelled probes. M = DIG molecular weight marker (Roche), wt = untransformed cv.60444 and +veC = pC1305.1 **(a)** *Hind*III-digested genomic DNA, probed with *Hyg* and **(b)** *Hind*III-digested genomic DNA, probed with *GUS.*

Table 3. 6 Transgene copy numbers of 15 C-MM6 lines detected by DIG-labelled *Hyg* and *GUS* probes.

Line ID	*Hyg*	*GUS*
1	4	1
2	1	1
4	0	1
6	1	1
7	2	1
8	0	0
9	2	1
10	1	2
11	2	0
12	1	2
13	4	1
14	2	0
15	0	0
16	1	1
19	1	1

C-MM8 lines

Fifteen of 30 lines were selected for transgene integration pattern analysis. When screening with DIG-labelled *Hyg* gene probe 1 line had a single transgene copy, 12/15 lines had 2 transgene copies and no transgene was detected in 2/15 lines **(fig. 3.24a)**. DIG-labelled *GUS* probe results showed that, 12/15 lines had a single transgene copy and no transgene was detected 3/15 lines **(fig. 3.24b)**.

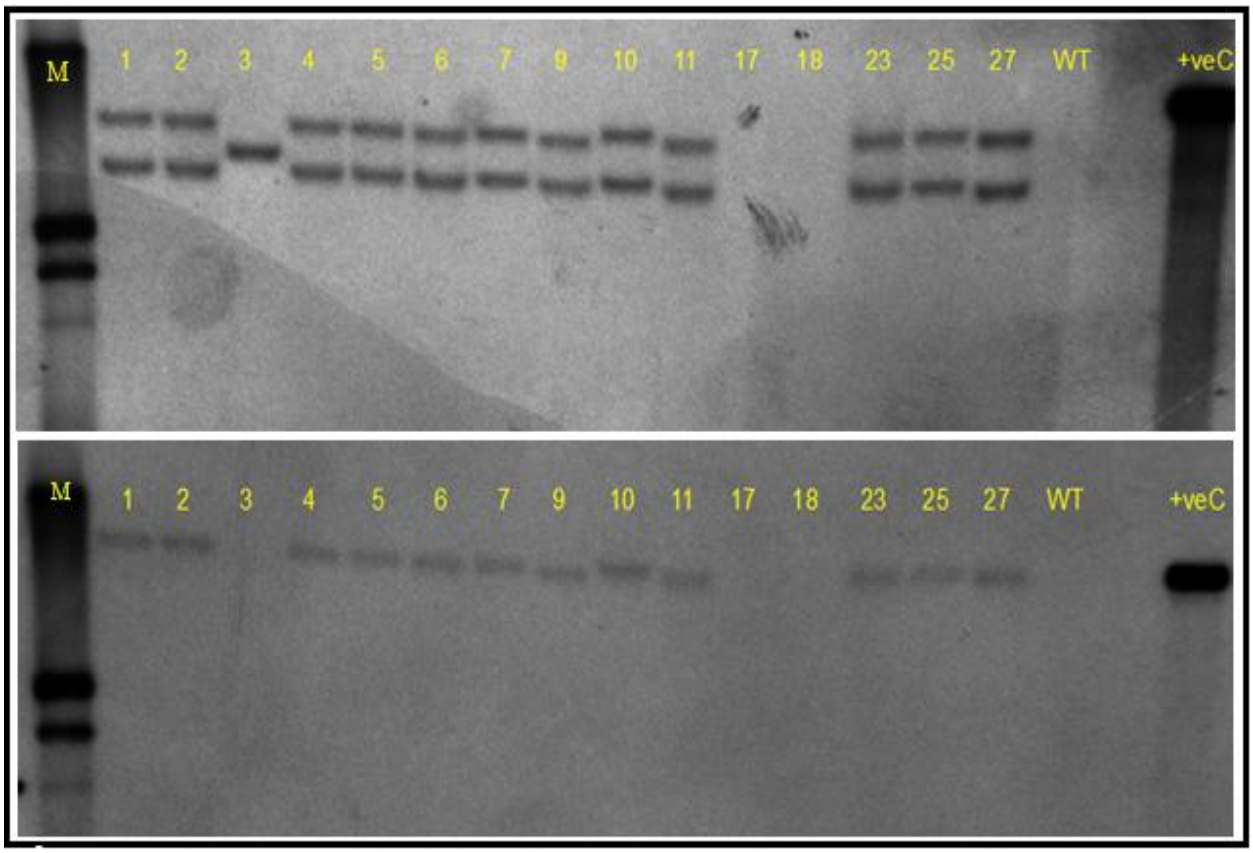


Figure 3. 24 Southern blot analysis of C-MM8 transgenic lines for transgene integration analysis using DIG-labelled probes. M = DIG molecular weight marker (Roche), wt = untransformed cv.60444 and +veC = pC1305.1 plasmid control **(a)** *Hind*III-digested C-MM8 genomic DNA, probed with *Hyg* and **(b)** *Hind*III-digested C-MM8 genomic DNA, probed with *GUS*.

Table 3. 7 Transgene copy numbers of 15 C-MM8 transgenic lines. Lines were probed with DIG-labelled *Hyg* and *GUS* probe.

Line ID	Hyg	GUS
1	2	1
2	2	1
3	1	0
4	2	1
5	2	1
6	2	1
7	2	1
9	2	1
10	2	1
11	2	1
17	0	0
18	0	0
23	2	1
25	2	1
27	2	1

3.5.7.5 Group D transgenic lines

D-MM6 and D-MM8 lines were screened for transgene copy number using DIG-labelled *Hyg* probe. Southern blot results of D-MM6 lines showed that 6/8 had a single transgene copy and 2/8 D-MM6 lines had 2 transgene copies. D-MM8 results showed that 7/10 lines had a single transgene copy, 2/10 lines had 2 transgene copies and 1 line had 3 transgene copies.

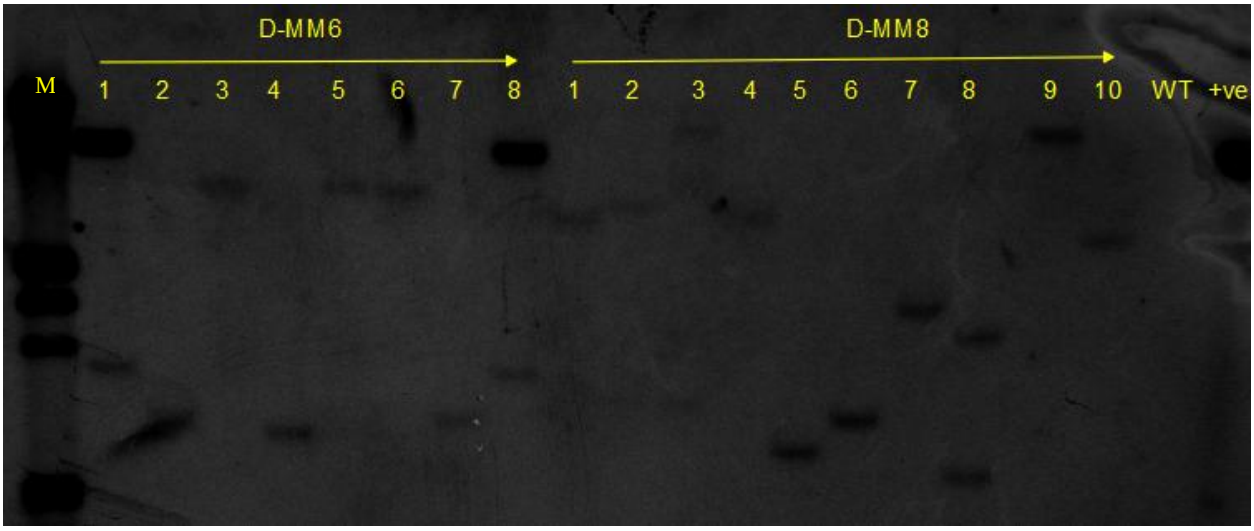


Figure 3. 25 Southern blot of D-MM6 1-8 lines and D-MM8 1-10 lines, genomic DNA digested with *Hind*III-digested genomic DNA probed with DIG-labelled *Hyg* probe for transgene copy number. M = DIG molecular weight marker, wt = untransformed cv.60444 and +ve = pC1305.1 plasmid control.

Selected single-copy group A and C transgenic lines with positive transgene inserts were used for virus challenge trials (chapter 4) to determine level of virus resistance. Group B and D transgenic lines were maintained in tissue culture for screening at a later stage.

3.6 Discussion

Cassava SE and FEC induction

High quality somatic embryos (SE) from both cv.60444 and T200 axillary buds were successfully generated. Similar to Nyaboga *et al*. (2013), initiation of primary (immature) SE was achieved within 2 weeks. Mature cv.60444 SE were obtained after 4 weeks of SE induction while T200 required an additional 2 weeks. Cultivar 60444 SE were more finger-like and trumpet shaped in morphology compared with the flat and coral shaped T200 SE. However after 8 weeks, cv.60444 started proliferating into predominantly flat coral shaped SE. At 10 weeks of culture and maintenance, choral- shaped SE started changing from the characteristic pale yellow colour and developed a green tinge around the edges. At this stage the SE were discarded and a new SE induction was initiated.

Using the SE as starting material, high quality mature cv.60444 FEC, suitable for transformation experiments, was induced after the 4th transfer (8 weeks). This was similar to the results obtained by Bull *et al*. (2009), but different to the study by Hankoua *et al*. (2006), who reported a 12 week FEC induction period for cv.60444 using a slightly different FEC induction protocol compared to Bull *et.al*. In contrast, high quality T200 FEC was only obtained after the 7th GD media transfer and therefore required a total of 14 weeks. Hankoua *et al*. (2006) also reported longer FEC induction periods for other cassava genotypes other than cv.60444. Similar to Chetty *et al*. (2013), in this study T200 FEC proliferated better in constant darkness unlike cv.60444 FEC which were maintained in 16 h light and 8 h dark. Chetty *et al*. (2013), Nyaboga *et al*. (2013) and Zainuddin *et al*. (2012) reported that FEC induction conditions and ease of induction is cultivar or landrace dependent. The length of time to generate FEC was also found to vary in the East African cultivars tested by Nyaboga *et al*. (2013), ranging from 9 to 22 weeks. Obtaining high quality FEC is critical for successful cassava genetic transformation. High transformation efficiencies also depend on efficient FEC regeneration protocols.

Agrobacterium-mediated transformation of FEC

Using the Bull *et al*. (2009) protocol, we were able to successfully transform cassava cv.60444 and T200 FEC. Embryo formation from hpRNA construct-transformed T200 FEC was slower

than cv.60444 FEC. Embryo initiation from transformed cv.60444 FEC occurred a few days after the 1st transfer to MSN+H15 while T200 FEC embryo initiation only occurred on the 2nd MSN+H15 transfer. This was seen for all mismatch and non-mismatch hpRNA construct-transformed FEC. Green cotyledons emerged for transformed cv.60444 and T200 FEC on the 2nd and 3rd MSN+H15 transfer, respectively. On average, 57% more cotyledons were produced per cv.60444 FEC clump than per T200 FEC clump. Results suggest that cotyledon regeneration efficiency is genotype-dependent and further shows that cv.60444 is more amenable to transformation than most cassava cultivars or landraces. It was also observed that mismatched hpRNA construct transformation experiments generated 4 fold more cotyledons per FEC clump than non-mismatched transformation experiments. This could be linked to T-DNA transfer efficiency. Reports have shown that the efficiency and stability of T-DNA integration into plant genomes decreases with T-DNA size (Hamilton *et al.*, 1996). Non-mismatched constructs in this study have a 800 bp larger T-DNA region as a result of the 800 bp PDK intron associated with pHellsgate vectors.

Regeneration problems from FEC and off-target effects on host plants

MM1hpRNA-transformed cv.60444 FEC become necrotic 4 weeks after co-cultivation with *Agrobacterium*. T200 FEC transformation with MM1hp produced a mixture of necrotic and yellow swollen FEC-like tissue. Both cv.60444 and T200 MM1hp transformed FEC did not regenerate however both showed distinct phenotypic differences on MSN media. Since transformation with the vector only did not demonstrate this necrotic phenotype, this suggests possible negative transgene effect in the two different cassava genotypes, which may have led to suppression or misregulation of gene expression pathways involved in FEC development and regeneration. This detrimental effect on development of transformed FEC may be due to insertion locations, and also variable preferences between T200 and cv.60444, dictating resultant phenotypes. Even though transgene integration cannot be controlled and is not well understood it is suggested that insertion-site integration is non-random (as previously thought) and may be host genome sequence-dependent (Bartlett *et al.*, 2014; Li *et al.*, 2006; Salvo-Garrido *et al.*, 2004). Siddiqui *et al.* (2008) researched the phenotypic effects caused by the expression of transformed virus RNA silencing suppressors in *N. benthamiana* and *N. tabacum*. They reported that expressing RNA silencing suppressor, P1, of *Rice yellow mottle virus* (RYMV) *N.*

benthamiana and *N. tabacum* resulted in distinctly different symptoms. Expression of this silencing suppressor in *N. benthamiana* resulted in severe stunting and leaf malformation. These results were seen even at very low expression levels. Expression of the same suppressor in *N. tabacum* produced no adverse effects. Based on these findings we postulate that the developmental defects in FEC development seen in MM1 transformed cv.60444 and T200 FEC could partially be transgene-cultivar/landrace induced phenotypic changes due location insertion.

Interestingly, however, transformation success and undesirable FEC phenotypic differences were also observed in transformation experiments of cv.60444 and T200 FEC with the MM3 hpRNAi construct. In cv.60444, FEC produced finger-like protrusions could not be regenerated into plantlets, however transgenic plantlets were regenerated from MM3-transformed T200 FEC. Notwithstanding possible effects of transgene insertion-cassava germplasm genetic differences contributing to FEC or cotyledon regeneration, it seems more likely that off-target effects occurred, caused by the transcribed transgene hpRNA derived siRNAs. Both MM1 transformed T200 and cv. 60444 did not regenerate, and additionally neither did MM3 and MM7 (mismatched and non-mismatched hybrid EACMV AC1/4: EACMV AC2/3, respectively) transformed cv.60444 and T200 FEC, respectively, regenerate lines. Co-cultivation of both cv.60444 and T200 FEC with the MM5construct also did not generate any transformed lines, and FEC failed to develop and regenerate cotyledons. MM1and MM5 hybrid hp RNA constructs both target ACMV-NG:Ogo:90 and EACMV-UG2 AC1/4 ORFs, but the difference is that MM1 is a mismatched hybrid while MM5 is a non-mismatched hybrid construct. However, what these four constructs have in common is an AC1/AC4 overlap fragment of EACMV-UG2 in the transgene. AC4 is a potent virus suppressor of host RNA silencing and is also known to induce developmental effects in plants (Incarbone & Dunoyer, 2013; Vanitharani *et al*., 2004; Zvereva & Pooggin, 2012). Developmental abnormalities were reported in cassava expressing AC4 of ACMV-[CM] (Chellappan *et al*., 2005). They suggested that these abnormalities were caused as a result of ACMV-[CM] AC4-derived siRNA that were negatively inactivating miRNA regulating plant development. ACMV-[CM] AC4 was reported to cause developmental abnormalities in ACMV-[CM] AC4 expressing *Arabidopsis thaliana* plants (Chellappan *et al*., 2005). We therefore postulate that the off-target inducing siRNAs are more likely to be generated from the EACMV AC1/4 targeted region and not the ACMV-NOg:90 AC1/4 gene

sequence, also based on the observation that the same ACMV-NOg:90 AC1/4 gene sequence is present in two other hpRNA constructs, MM2 and MM6, and yet no undesired off-target developmental effects were observed from FEC transformed with these constructs. Additionally, MM3 transgene has an EACMV-UG2 AC2/3 fragment, and AC2 is also a known virus suppressor of RNA silencing, and modulator of symptom severity in plants (Pumplin & Voinnet, 2013; Trinks *et al*., 2005; Vanitharani *et al.*, 2004).

EACMV-UG induced more severe symptoms in cassava compared to ACMV in *N. benthamiana* (Sserubombwe *et al*., 2008), and this may in part also be due to the RNA silencing suppressor proteins encoded by AC1/4 and AC2/3 ORFs, as discussed above. Vanitharani *et al*. (2004) provided evidence that similar proteins encoded by different virus species can and do exhibit different silencing suppressor activities (discussed in chapter 1). Njock (2014) reported more severe symptoms in ACMV-CM infected *N. benthamiana* than in EACMV-CM infected *N. benthamiana*. Arabidopsis-expressing suppressors from different plant viruses resulted in developmental abnormalities and disease-like symptoms (Chapman *et al*., 2004). Observed effects were reported to be a result of a disruption in the miRNA pathway involved in plant development. Collectively, this would support the hypothesis that in cv.60444, specific siRNAs generated from the MM1 (stacked ACMV AC1/4 and EACMV or MM3 (stacked EACMV AC1/4: EACMV AC2/3) constructs are causing toxicity, either each overlapping ORF, or synergistically. Transgene-derived siRNAs could have negatively affected miRNA regulatory pathway(s) involved in FEC or cotyledon development. We were able to generate putative transgenic MM3hp plantlets from T200 FEC but not from cv.60444 FEC. This suggests that T200 FEC were not negatively affected by the MM3 transgene with regard to cotyledon initiation or development. Again, as suggested previously, this may have been due to the genetic differences between these two germplasm, in the miRNA-responsive pathways. Despite strong evidence from this study for a role of geminivirus genotype and transgene ORF-derived RNA in off-target detrimental effects on FEC and cotyledon development, we do not rule out a role for cultivar background genetics in these interactions.

However not all morphological off-types can be attributed to the constructs and gene-derived sequences. Taylor *et al*. (2012a) reported 5% off-types from regenerated transgenic plantlets,

and these lines were usually discarded. The authors suggest that FEC (cv. 60444) should not be cycled more than three cycles at the time of *Agrobacterium* co-culture. In our first FEC transformation experiment, using 15-24 months old FEC, we did encounter mismatched hpRNA construct-transgenic plants showing abnormal phenotypes. Many transgenic lines generated from this transformation event were stunted, had emerging leaves that appeared lancolate as opposed to trifoliate, some plants had thin contorted stems and very short internodes (data and figure not shown). However, in a repeat transformation experiment, using younger than 20 months old FEC, we obtained transgenic cassava displaying morphology similar to the untransformed control. We attributed the undesirable phenotypic differences to prolonged FEC cycling prior to *Agrobacterium* co-cultivation and not to the mismatched constructs. Taylor *et al*. (2001) reported leaf morphological aberrations when using older embryonic tissue. The authors suggested a disturbance in endogenous auxin metabolism due to prolonged picloram exposure in the cycling medium. Raemakers *et al*. (2001) also reported morphological aberrations, reduced transformation efficiencies and longer plantlet regeneration periods when using 24 months old FEC compared with 6 months old FEC. However in contrast, the cassava research group at ETH Zurich (Bull *et al*., 2009) cycle the FEC for up to 20 rounds (10-12 months) with comparable low off-type percentages.

Early cassava transformation experiments reported low transformation efficiencies (Raemakers *et al*., 2001; Taylor *et al*., 2004; Zainuddin *et al*., 2012). During the earlier experiments, cassava transformation involved co-cultivation of explants, such as cotyledons generated from somatic embryo, with the *Agrobacterium*-construct inoculum. These methods produced low (1-30 %) putative transgenic shoots and therefore results in low transformation efficiencies (Raemakers *et al*., 1997; Sarria *et al*., 2000). According to Raemakers *et al.* (2001) construct-transformed FEC have a greater chance of regenerating into embryos than untransformed FEC. They state that a 'strict correlation' exists between the percentage transgenic FEC and percentage transgenic embryos generated. They go further and say that there is a positive correlation between the number of putative transgenic lines and final number of actual transgenic lines generated. In this study we observed a similar trend in group A transformation event, where 12 cotyledons per FEC clump were generated, and this in turn resulted in 8 putative transgenic shoots per FEC clump, resulting in high (over 100) putative transgenic lines being generated and this then has a direct

effect on high (94-98 %) transgenic transformation efficiencies (**table 3.3**). And as suggested by Raemakers *et al*. 2000 low cotyledon regeneration efficiency per FEC clump, resulted in low shoot production efficiency per FEC clump. Low shooting efficiency negatively affected the number of putative transgenic lines produced, and resulted in lower transformation efficiencies (67-83 %) observed in group C and D transformation event.

Transformation efficiencies and transgenic plant production

With the advent of more robust, improved protocols, much higher transformation efficiencies are now attainable. Recovery of independent putative transgenic lines is assured using methods by Bull *et al*. (2009) and Taylor *et al*. (2012). However as reported by Nyaboga *et al*. (2013) comparing transformation efficiencies is relatively complicated because of different transformation protocols, different cultivars and FEC quality and age. In this study we regenerated 1639 putative transgenic cv.60444 lines per 430 FEC clumps with a ~1 cm diameter (average of 4 putative transgenic lines per FEC clump). Bull *et al*. (2009) anticipated in excess of 50 putative transgenic lines per 100 FEC clumps (average of 0.5 putative transgenic lines per FEC lump). Chetty *et al*. (2013) regenerated 154 putative transgenic lines per 140 FEC clumps (average of 1.1 putative transgenic lines per FEC clump). Zainuddin *et al*. (2012) regenerated 59 putative transgenic lines from 72 FEC clumps (average of 0.8 putative transgenic lines per FEC clump). All these studies used FEC clusters on solid media, and the range of transformation efficiencies from these collective studies, including this study, was 0.1 – 4.0 transgenic lines per ~1cm FEC clump. Taylor *et al*. (2012a) on the other hand transform FEC in liquid culture, and reported an average of 22 putative transgenic lines per 1 cm^3 of FEC settling volume.

Transformation and regeneration of cassava is also genotype dependent and few cultivars or landraces have been successfully transformed in Asian cultivars (Raemakers *et al*., 2001) and African cultivars (Hankoua *et al*., 2006; Nyaboga *et al*., 2013; Zainuddin *et al*., 2012), suggesting an underlying genetic control in the capability of a given genotype. In the study by Nyaboga *et al*. (2013) three local farmer-preferred cultivars were successfully transformed and regenerated, although not all somatic embryos produced plantlets, and L-tyrosine was required to improve regeneration of FEC (Zainuddin *et al*., 2012). Nyaboga *et al*. (2013) did however report lower efficiencies for three East African farmer-preferred cultivars (Serere, Kibandameno and

Ebwanateraka) compared with cv.60444. In the study by Zainuddin *et al*. (2012), on cassava landraces provided by IITA-Ibadan, an increase in the number of maturing embryos was achieved by doubling FEC time on recovery and proliferation medium, this was done prior to placing construct-transformed FEC on MSN medium. Lower transformation efficiencies are usually obtained for cultivars and landraces other than the model cv.60444 cultivar. In the first cassava transformation report in our lab, using the Bull *et al.* (2009) method, we reported transformation efficiencies of 45 % and 33% for cv.60444 and T200, respectively (Chetty *et al*., 2013). These transformation efficiencies were based on putative transgenic cv.60444 and T200 shoots that rooted successfully on hygromycin-containing rooting media. Here we demonstrate a great improvement in transformation efficiencies for both cv.60444 and T200. We obtained an average transformation efficiency of 79 % and 76 % for cv.60444 and T200, respectively. According to Bull *et al*. (2009), transformation efficiency is directly proportional to FEC quality and regeneration capacity, and therefore the establishment of efficient and reproducible transformation platform in our lab could have had resulted in the higher efficiencies observed in this study.

Molecular-based techniques proved to be reliable transformation screening methods. PCR screening and Southern blot were more reliable than histochemical GUS assays. Using PCR amplification of *Hyg* and *GUS* to screen putative transgenic plantlets we were able to report average transformation efficiency of 92 %. PCR screening using hpRNA primers were not as efficient in amplification of the hairpins (inverted repeats) and demonstrate an average transformation efficiency of 44 %. Difficulties associated with amplifying through IR sequences, especially those longer than 200 bp, could cause the discrepancies in transformation efficiencies (Hauge *et al.*, 2009; Hommelsheim *et al*., 2014; Rattray, 2004; Yang *et al*., 2014). Hommelsheim *et al.* (2014) proposed several models to explain difficulties in IR amplification, and they suggested disturbances in polymerase activity due to complex structures that form during PCR re-annealing and denaturation cycles and polymerase dissociation as IR sequences are approached. They suggested using polymerases with better strand displacement activity, using polymerase cocktails and even including thermostable polymerase-associated proteins in IR-PCR amplification.

Overall, lower transformation efficiency results were obtained in this study from GUS assay-based screening, when transformation efficiency was calculated on the number of putative transgenic shoots showing positive blue GUS assay. The GUS assay results provided high under-representation of the true transformation efficiency results. The observed under-representation was suggested to be a result of assaying the uppermost leaves of tissue culture plantlets. Jefferson *et al*. (1987) reported decreased GUS activity in young leaves of transgenic *N*. *tabacum* var. Samsun expressing *GUS*. They also reported tissue dependent *GUS* expression levels with differential *GUS* transcription and translation being observed in leaves and stems. They reported that maximal *GUS* transcription requires mature chloroplasts. GUS assays are widely used but from our results and other transformation groups, and according to Halder & Kombrink (2015), it is subjective and 'biased hit selection' prone. Halder & Kombrink (2015) developed a more robust and reliable GUS assay-based method in *Arabidopsis thaliana* that is both qualitative and quantitative. This fluorimetric assay quantifies the fluorescence released from 4-methylumbelliferyl-β-D-glucuronide (4-MUG) cleavage by β-*galactosidase*. Similar less reliable results were reported in transformation experiment of farmer-preferred cultivars, Ebwanatereka, Kibandameno and Serere, by Nyaboga *et al*. (2013). In cassava landraces, Oko-iyawo and Abbey-ife, GUS assay transformation efficiency results were also lower than rooting test results (Zainuddin *et al*., 2012). From our data we also observed that the rooting test is more accurate than the GUS assay. Rooting test results closely correlated with molecular screening results, and provided a good starting point for screening for selected transgenics, particularly when a large number of putative transgenic lines needed to be screened. We then consolidated and verified visual screening and PCR based screening tests by performing Southern blot analysis, which not only confirms integration, but provides transgene copy number.

T-DNA integration analysis

In addition to performing Southern blot analysis for copy number using the routine *Hyg* probe (Bull *et al*., 2009; Hiei *et al*., 1994) or *npt*II probe (Honda *et al*., 2002; Schreuder *et al*., 2001; Taylor *et al*., 2012) we probed with *GUS* , and in the A group of transformations, with hpRNA construct probes. These regions lie within the vector T-DNA borders. Most cassava transformation studies have used plant transformation binary vector reporter genes, such as *Hyg* (Bull *et al*., 2009; Vanderschuren *et al*., 2009; Zainuddin *et al*., 2012) or *nptII* (Taylor *et al*.,

2012) to determine transgene copy number only. This method however is slightly limited in providing crucial information regarding transgene organisation post integration in the plant genome. Detailed analysis of T-DNA integrations, re-arrangements, deletions, insertions and inversions have been a focus only in a few transformation studies, in context of transgene detection, organization and expression. Several studies (Bartlett *et al*., 2014; Latham *et al*., 2006; Liu *et al*., 2014; Zeng *et al*., 2009) have shown that integration does not always follow the expected and predicted insertion of all genes lying within the right and left borders of the transformation vector. Transgene truncations, deletions, insertions, inversions, re-arrangements and segregation into different loci have been reported (Liu *et al*., 2014; Müller *et al*., 1999). T-DNA integration of several transgenic lines was analysed in this study (data not shown) using Southern blot, we discovered that using just one gene probe did not give a true reflection of T-DNA integration integrity. In A-MM4 line 70, failure to probe with *Hyg* suggested that the line had no transgene integrated, while probing with *GUS* we were able to identify two transgene copies, and surprisingly, when probing with a hpRNA probe, one intact T-DNA and four additional copies which appeared to have insertions were identified. The majority of C-MM8 lines appeared to be single copy transgenics when probed with *Hyg*, however probing with *GUS*, lines appeared to have two transgene copies. Our observed results also suggest possible additional truncated transgene and gene insertions and deletions. T-DNA usually integrates from right to left border (Gelvin, 2003a; Pitzschke & Hirt, 2010; Riva *et al*., 1998; Wang *et al*., 1984). On plant transformation vector, pCAMBIA 1305.1, *Hyg* is located closer to the left border while *GUS* is located closer to the right border and in addition the right border is associated with 'overdrive' sequences which are known to enhance right border transmission and insertion (Gelvin, 2003a). This could explain the suggestion that integration of an intact T-DNA does not always occur.

In a study by Müller *et al.* (1999) transgene re-arrangements and illegitimate recombination was seen in twelve tobacco transgenic lines. They discovered that all sites of recombination contained palindromic sequences. Kohli *et al*. (1999) implicated the CaMV35S promoter in the re-arrangements events observed in the 12 transgenic tobacco lines. They demonstrated that imperfect palindromic sequences and AT rich DNA sequences present in CaMV35S promoted illegitimate recombination events. These sequences form secondary structures, such as hairpins

which are amenable to re-combination and rearrangements. A combination of Southern blot analysis, PCR-based methods and sequencing would give a more detailed picture of transgene integrity. Identification of integration site/location by amplifying junction sequences as described by Bartlett *et al*. (2014) would also prove valuable information.

In conclusion, comparable high efficiencies of FEC transformation and transgenic plant regeneration, was achieved with both the model cultivar cv. 60444 and the SA high-starch landrace T200. However despite this success, cassava transformation remains laborious and fastidious, requiring a large amount of technical resources and screening of a large number of lines for selection of single copy insertions of non-truncated transgenes. T-DNA integration detection using the current methods also remains somewhat unreliable. Two of the most successful cassava transformation platforms (Taylor *et al*.2012a and Vanderschuren *et al*.2009 at the Donald Danforth Plant Science Center and ETH Zurich, respectively) have both similarities and differences, one notable one being the use of *hpt*II hygromycin resistance gene (Bull *et al*., 2009) and *npt*II kanamycin resistance gene (Taylor *et al*., 2012). In our hands, we find *hpt*II gives better results (compared to experiments using kanamycin in our laboratory in the early 2000's; data not reported), while Taylor *et al.* 2012a found that kanamycin worked better in their hands. Again, this points out that cassava transformation is not entirely reproducible in different conditions, and certainly we know it is genotype dependent. Furthermore, if more traits are to be engineered in cassava in future, the scale and reproducibility of cassava transformation needs further investigation.

CHAPTER 4

SCREENING OF TRANSGENIC PLANTS FOR SACMV AND ACMV RESISTANCE

4.1 Introduction

4.1 Development of virus resistant transgenic cassava

On the African subcontinent food insecurity is a major problem with small and large scale farmers as well as subsistence farmers relying on cassava cultivation (Kolawole *et al.*, 2010). However, cassava infecting begomoviruses cause a huge threat to cassava cultivation. Methods used to try and limit these losses include traditional breeding for resistance, which is time consuming, and introgression of resistance genes into preferred cultivars is challenging (Fargette *et al.*, 1996; Rudi *et al.*, 2010). Various transgenic strategies to engineer virus resistant or tolerant lines have been explored (Shepherd *et al.*, 2009). Over the last two decades different research groups working toward engineering begomovirus resistance in cassava have reported varying levels of susceptibility, tolerance and resistance.

However within the plant virology community there are disparities associated with the terms susceptibility, tolerance and resistance. The terms have no standard definitions (Lapidot & Friedmann, 2002). For purposes of this research we have adopted a similar definition as that described by Lapidot and Friedmann. We define resistance as *showing no symptoms and supporting very low to no virus replication*, tolerance as *supporting normal to lower virus replication however with reduced/mild symptoms* and susceptible as *supporting normal or even higher virus replication and high to severe symptoms*. Recovery *is defined as no to mild symptoms and low viral load*. It would also seem that plant breeders and farmers have a different view or concerns to virologists with regards to plant - virus interactions and disease. Farmers and plant breeders are more concerned about the visual and crop yield effects of the virus on the plant (Lapidot & Friedmann, 2002). Plants showing normal to high viral load but with low virus symptoms are still considered comparatively more favourable, as this has a lesser impact on yield. Plant pathologists and virologists on the other hand are more interested in the behavior of the virus in the plant and virus replication (Lapidot & Friedmann, 2002), as plants with high virus levels may exacerbate vector transmission in the field..

4.2 Challenges associated with engineering resistance

Several factors can contribute to reduced levels of resistance; these factors can be virus, plant and environmentally derived. Geminiviruses are able to overcome RNA silencing mechanism by

encoding silencing suppressors (Bisaro, 2006). The multigenic nature of resistance is also a potential problem in breeding and engineering for virus resistance (Rabbi *et al.*, 2014). In certain reports the resistance phenotype has been broken by slight changes in temperature, light and virus inoculum dosage (Chellappan *et al.*, 2005; Kotakis *et al.*, 2010; Vanderschuren *et al*., 2009). Chellappan *et al.* (2005) reported temperature-induced changes in PGTS-based silencing levels in cassava and *N. benthamiana.* An overall attenuation in symptoms was observed at higher temperatures (30 °C) than at 25 °C in cassava and *N. benthamiana* infected with ACMV-[CM], EACMCV and EACMV-[UG]. Decrease in symptoms was linked to a 6-fold increase in virus-derived siRNA accumulation at higher temperatures. The study by Kotakis *et al.* (2010) in GFP transgenic *N. benthamiana* showed that an increase in light intensity resulted in increased mRNA levels of enzymes involved in the RNA silencing pathway and in siRNA accumulation. More recently, it has also been shown that light intensity and temperature affects systemic spread of the silencing signal (Patil & Fauquet, 2014). In transient *Nicotiana benthamiana* agroinfiltrated with seven species on cassava mosaic geminiviruses, at higher light intensities and higher temperatures (>30 ^{o}C), gene silencing was localized to infiltrated leaves only, and the plants recovered from viral symptoms due to reduced systemic spread of the silencing signal (Patil & Fauquet, 2014). Additionally, in a study by Vanderschuren *et al*. (2009), an increase in infection rate from 22 % to 90 % was observed when transgenic cassava expressing ACMV AC1 was infected with higher a ACMV-NOg virus inoculum dosage. They concluded that an increase in virus titre can break resistance.

Once proof of concept has been shown in greenhouse trials, the next step is confined field trials (CFT). However environmental factors can contribute to the different results observed between repeat greenhouse trials and between greenhouse trials and CFT (Anand *et al.*, 2003; Viswanath et *al.*, 2011). Data from cassava CFT for virus resistance transgenic cassava (Taylor *et al*., 2012b) and β-carotene bio-fortification (Sayre *et al*., 2011) is not fully available as CFT are still underway. CMD-resistant transgenic cassava has been confirmed in CFT at the National Research Institute, UK, however CFT using natural virus pressure still need to be performed (Taylor, *et al.*, 2012b). Virus Resistant Cassava for Africa (VIRCA) was established in Uganda in October 2009. Since its establishment three CFT on CMD-resistant cassava and one on cassava brown streak disease (CBSD)-resistant cassava have been performed. Two CMD CFT in

Kenya are also currently underway (Taylor et *al*., 2012b). The VICRA report by Taylor *et al*. (2012b) on CFT has confirmed greenhouse trial data of transgenic cv.60444 targeting EACMV. CFT of CMD-resistant cv.60444 developed by ETH are still ongoing in Puerto Rico (Adenle *et al*., 2012; Vanderschuren *et al*., 2009; Zhang *et al*., 2005). At the time of print, CFT in Africa, on ETH-developed CMD-resistant cassava were still yet to occur (Adenle *et al*., 2012).

4.3 Methods used to infect plants

Begomovirus transmission in nature is whitefly-mediated (Bock *et al.*, 1978), however in the laboratory, agro-inoculation or biolistics with infectious clones and grafting are performed especially for DNA viruses (Ariyo *et al*., 2006; Kheyr-Pour *et al*., 1994; Vanderschuren *et al*., 2012). Mechanical transmission, such as rubbing leaves with virus infected sap, is effective for a large number of RNA viruses and plant species, such as tobacco plants, but is not suitable for cassava (Berrie *et al.*, 1997). Grafting can be time consuming, and requires a large starting number of virus-infected scions but can result in 75-85% infection success (Wagaba *et al.*, 2013). In CBSD, grafting has been found to be more reliable in virus transmission for transgenic evaluation of cassava plants, but again this takes a longer time period before evaluations can be performed (Mohammed *et al*., 2012; Wagaba *et al*., 2013). Virus transmission using biolistics is faster, however requires optimisation, has low infectivity rate and it is relatively more expensive (Ariyo *et al.*, 2006; Lapidot *et al.*, 2007). Agro-inoculation of plants is time consuming, however it is low cost with high infectivity success (Kheyr-Pour *et al.*, 1994). Agro-inoculation of virus clones can be used for a wide range of plant hosts and is the choice for geminivirus infection (Biswas & Varma, 2001; Saeed, 2008), as in many cases these ssDNA viruses are not mechanically transmitted (Lal *et al*., 2015; Rigden *et al*.,1996).

Parameters and scales for monitoring and scoring of CMD is variable. At present no procedures and protocols defining plant inoculation age, sample size, amount of virus inoculum, symptom evaluation (whole plant or leaf scoring), sampling procedure, time and frequency of sampling, have been standardised. Symptom severity scoring indices vary slightly between different plant transformation and screening scientific groups with the scoring scale ranging from 0-5 (0= no symptoms and 5= most severe symptoms) (Fauquet & Fargette, 1990) or 1-5 (1= no symptoms and 5= most severe symptoms) (Hahn *et al*., 1980) or 0-4 (0= no symptoms and 4= most serve

symptoms) (Calvert & Thresh, 2002). Some scoring systems even include intermediate scores such as 0.5 and 1.5. More recently Ntui *et al*. (2015) adopted a 0-3 scale in evaluating *Sri Lankan cassava mosaic virus* (SLCMV) in genetically engineered cassava cv.KU50. Another factor that should be considered is that symptom severity can be both cultivar and virus dependent (Fauquet & Fargette, 1990). There also are two approaches to calculating the mean severity score, namely collecting symptom scores for all plants, including asymptomatic, or only considering diseased plants, and to an extent, both approaches can be misleading and confusing (Sseruwagi *et al*., 2004).

Along with visual symptom analysis, viral load quantification is also essential when evaluating plant resistance levels. The most reliable and sensitive technique is real-time PCR (qPCR). A positive correlation between observed symptoms and viral load is often reported and it is suggested that correlation is also cultivar specific (Chellappan *et al*., 2004; Kaweesi *et al*., 2014; Medina-Hernández *et al*., 2013; Moreno *et al*., 2011). However this is not always the case, and a lack of correlation was reported in tomato infected with single or mixed *Pepino mosaic virus* (PepMV) strains (Gómez *et al*., 2009). A correlation was also not established in pepper plants infected with the begomovirus *Pepper golden mosaic virus* (PepGMV) (Carrillo-Tripp *et al*., 2007). Surprisingly, a positive correlation between PepGMV siRNA accumulation and symptom severity was observed; siRNA accumulation was associated with severe symptoms. High virus-derived siRNA accumulation was also reported in severely infected transgenic *N. benthamiana* expressing the *Rep* gene of *Tomato yellow leaf curl Sardinia virus* **(**TYLCV) (Lucioli *et al*., 2003). Nonetheless, there are several reports relating to the inverse correlation between siRNA accumulation levels and viral load as well as symptoms. Such observations were seen in *N. benthamiana* and cassava infected with ACMV-[CM], and symptom recovery was also observed (Chellappan *et al*., 2004). Plant recovery was reported in transgenic cassava expressing bidirectional promoter of ACMV, where recovery correlated with high accumulation of virus-derived siRNA (Vanderschuren, Akbergenov, et al., 2007). In transgenic cassava expressing ACMV AC1-derived hairpin construct, total immunity against ACMV was also associated with high accumulation of virus derived siRNA accumulation (Vanderschuren *et al*., 2009), and more recently resistance positively correlating to PTGS and transgene-derived siRNAs was reported in SLCMV-transgenic cassava (Ntui *et al*., 2015).

In our study, transgenic cassava lines expressing virus-derived RNAi constructs were screened for resistance by agro-inoculation with infectious ACMV and SACMV clones for the DNA A and B components, respectively. Transgenic lines were then monitored for symptom development and resistance/tolerance levels. Virus load and siRNA production was also monitored.

4.2 Specific Aims

i. Micro-propagation of cv.60444 transgenic lines (MM2 MM4 MM6 and MM8) and acclimatization for (6 weeks)
ii. Agro-infection of cv.60444 transgenic lines with infectious virus clones
iii. Plant evaluations for virus infection severity, plant height, and leaf harvesting at 12, 32 and 67 days post inoculation (dpi)
iv. Viral load quantification using absolute real time qPCR
v. siRNA screening for final selection trials

4.3 Methodology flow chart

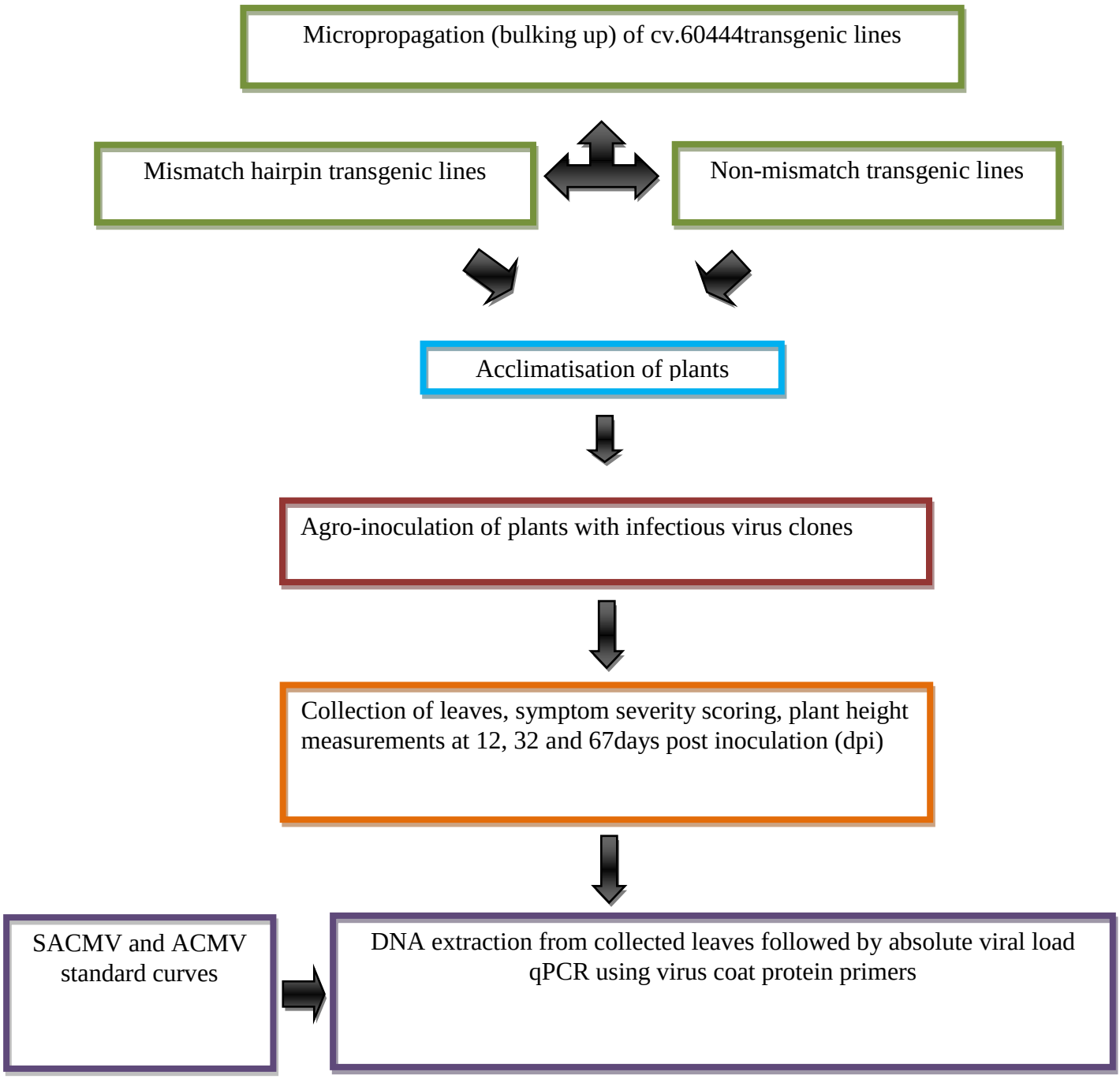


Figure 4. 1 Flow diagram of methodology followed to screen transgenic plants for virus resistance.

4.4 Materials and Methods

4.4.1 Bulking up and acclimatisation of selected transgenic plants

Mismatch (MM2 and MM4) and non-mismatch (MM6 and MM8) cv.60444 transgenic lines (generated in Chapter 3) were micro-propagated for virus-challenge experimental trials. Following bulking up, transgenic and non-transgenic control plants were acclimatised using the procedure described below. The acclimatisation protocol was initiated with propagation of transgenic cassava plantlets in tissue culture on MS2 media. After roots developed (10-14days) plantlets were removed from tissue culture and transferred to peat jiffies (Jiffies International), placed in plastic trays and covered with plastic wrap. Trays were placed in a phytotron facility at 28 °C, with 16 h light (8000-10000 lux) and 8 h dark cycles and 60 % humidity. Over a period of 3-4 weeks, slits were cut through the plastic wrap to gradually help acclimatise the plants. A total of 20-30 plants were acclimatised for each transgenic line and additional plants for controls.

4.4.2 Agro-inoculation of plants

Following successful acclimatisation, 15-20 transgenic lines were agro-inoculated with infectious virus clones. ACMV (MM2) transgenic plants were agroinoculated with *A. tumefaciens* C58C1 ACMV-[NG-Ogo:90] DNA-A and DNA-B infectious dimers and SACMV (MM4) transgenic plants were infected with *A. tumefaciens* AGL1 SACMV DNA-A and DNA-B infectious dimers. DNA-A and DNA-B components for each pair were grown overnight to an OD_{600} of 2. Cultures were centrifuged and pellets resuspended in Yeast extract peptone (YEP) broth to obtain an OD_{600} of between 1.8 and 2.0. Equal amounts of the appropriate components were mixed. To each plant, 100µl of the culture was inoculated in the stems and petioles just below the apical leaves. Plants were then covered with plastic wrap and slits introduced over 3 days until all the plastic had been removed. Non-transgenic cassava plants (tolerant TME3 and susceptible cv.60444) were agro-inoculated, as virus infection controls, in the same manner. Uninfected transgenic lines and wild-type uninfected plants were also included in the trial. The infected plants kept in the phytotron chamber for the duration of the experiment. The growth conditions mentioned above in **4.4.1** were maintained.

4.4.3 Sampling and symptom monitoring

At 3 time points post infection (12, 32 and 67dpi) plant height was measured, and the upper-most fully grown leaves were scored for symptom development using a symptom severity score index by Fauquet and Fargette (1990) (0= no symptoms, 1= faint mosaic, 2= yellow mosaic with slight leaf deformation and 5% size reduction, 3=severe mosaic, leaf distortion and reduced size, 4= severe mosaic, severe distortion and up to 5 0% size reduction and 5= leaf reduced to veins and 50-80 % size reduction). These upper-most fully grown leaves were harvested and frozen in liquid nitrogen and stored at -70 °C until further processing. For each transgenic line and control plant, 6 plants showing symptoms were selected, scored and monitored.

A total of 12 A-MM2 and 16 A-MM4 transgenic lines were randomly selected and challenged over 4 separate trials following methods **4.4.1-4.4.3**. However from the screening results (symptom severity scores and viral load quantified) 7 A-MM2 and 7 A-MM4 transgenic lines showing promising virus resistance/tolerance were identified and selected for a large scale virus challenge trial (**table 4.1**). Six C-MM6 and 5 C-MM8 transgenic lines were also selected for trials (**table 4.1**). Virus-free tissue culture stocks of these lines were used and micro-propagated, acclimatised, challenged and re-evaluated for resistance levels following methods described in 4.4.1-4.4.3. Agro-inoculated plants were evaluated at 12, 32, 67 dpi, and transferred to larger pots and monitored for a further 10 months (300 days) in the greenhouse at a temperature between 25-30 °C day temperature and 15-22°C night temperature, and a mid-day light intensity ranging between 8000-10,000 lux in summer (September- April). Winter light intensity was not measured.

Student's t-test was performed on values obtained for symptom severity scores, plant height and viral load. This was performed to determine if the observed values between the transgenic lines and cv.60444 and TME3 were significantly different. Pearson's correlation test was performed to determine if a correlation between viral load and symptom existed. Tests were performed using Microsoft Excel.

Table 4. 1 Virus challenge trials of transgenic lines.

Trial number	Infectious virus clone	Transgenic lines screened	dpi monitoring
Trial 1 (A-MM2)	ACMV-[NG-Ogo:90]	A-MM2 45, 41, 54, 52, 53, 44, 30	12, 32, 67, 365
Trial 2 (A-MM4)	SACMV	A-MM4 11, 33, 34, 46, 59, 68, 79	12, 32, 67, 365
Trial 3 (C-MM6)	ACMV-[NG-Ogo:90]	C-MM6 2, 1, 8, 10, 11, 19	12, 32, 67
Trial 4 (C-MM8)	SACMV	C-MM8 1, 3, 23, 25, 27	12, 32, 67

4.4.4 TNA extraction and absolute viral load quantification

TNA was isolated from the harvested samples using CTAB based method described by Doyle and Doyle (1987). For each harvested plant sample, approximately 50 mg of leaf tissue was snap frozen in liquid nitrogen and crushed into a fine power. To each eppendorf of crushed leaf tissue, 500 µl of preheated CTAB extraction buffer (2% hexadecyltrimethylammonium bromide, 1.4 M NaCl, 0.2 % 2-mercaptoethanol, 20 mM EDTA, 100 mM Tris-HCl, pH 8.0) was added and thoroughly vortexed, and incubated in a water-bath at 65 °C for 60 min and the tube occasionally inverted. After incubation, 500 µl of chloroform-isoamyl alcohol (24:1) was added followed by mixing and centrifugation at 13400 rpm for 10 min at 4 °C. The aqueous layer containing the DNA was placed into a clean tube and the above chloroform-isoamyl alcohol extraction step repeated. Purified TNA in the upper aqueous layer was precipitated using 500 µl isopropanol and centrifugation for 10 min at 13400 rpm at 4 °C. TNA pellet was washing with 1ml of ice-cold 70 % ethanol followed by centrifugation for 10 min at 13400 rpm at 4 °C, this ethanol pellet washing step was repeated. The pellet was air dried and resuspended in 50 µl TE (10 mM Tris pH 8.0 and 1 mM EDTA) containing 20 µg/ml RNase A (Fermentas) and incubated at 37 °C for at least an hour. The extracted DNA was quantified on the Nanodrop 1000 spectrophotometer (Nanodrop).

4.4.5 Generation of ACMV and SACMV standard curves

To quantify SACMV and ACMV viral load, standard curves for both SACMV and ACMV were generated by real-time PCR using the Maxima SYBERGreen (Fermentas) in the LightCycler 480 instrument (Roche Applied Science). Standard curves were generated using tenfold dilutions (ranging from 1 ng/ul to 0.1 pg/ul) of pBS SACMV DNA-A and pBS ACMV DNA-A clones. To generate a standard curve for each virus, qPCR reaction mixture was set up according to manufactures instructions, 1X master mix, 0.3 mM of appropriate reverse and forward primers, 1 µl of appropriate standards (1 ng/µl -0.1 pg/µl) and nuclease free water to a final volume of 10µl. To generate the ACMV standard curve, forward primer APA9 FP2 5'CAATTTCCACCCCAACATTCA3' and reverse primer APA9 RP2 5'GCGTAAGCATCATTCGCTGAT3' were used. The SACMV standard curve was generated using forward primer CCPF 5' GCACAAACAAGCGTCGA3' and reverse primer CCPR 5'CTGCCAGTATGCTTAACGTCA3' The cycling conditions consisted of initial denaturation at 95 °C for 10 min and 40 cycles of denaturation at 95 °C for 15 s, annealing at 60 °C for 30 s and extension at 72 °C for 30 s.

4.4.6 ACMV and SACMV viral load quantification

The amount of virus DNA A present in the harvested leaf samples was quantified using qPCR in the LightCycler 480 instrument (Roche Applied Science). Extracted TNA of infected transgenic lines, infected untransformed control plants and healthy negative control plants were diluted to 50 ng/µl. For each transgenic line and control plants, extracted TNA from 6 plants were randomly pulled into 3 groups of two to reduce leaf-to-leaf variation. Viral load quantification of each pooled sample was performed in triplicate and non-template control was also included. The qPCR reaction was performed as described in **4.4.5**. The viral load in ACMV (A-MM2 and C-MM6) and SACMV (A-MM4 and C-MM8) infected transgenic lines, and infected control plants, was calculated from the ACMV and SACMV standard curves, respectively. The viral load was expressed as the mean viral molecules per g of extracted TNA, and graphs plotted using Microsoft Excel.

4.4.7 Trangene expression and Northern blots for siRNA detection

Total RNA was isolated from *in vitro* plant stocks of transgenic lines (table 4.1) selected for virus challenge experiments. Total RNA was isolated using the QIAzol lysis reagent kit (Qiagen). RNA was quantified on a nanodrop and the quality and integrity determined on a 1.2 % agarose gel containing 10ug/µl ethidium bromide run in 0.5X TBE.

4.4.7.1 Transgene expression

To determine transgene expression 1µg from the total RNA isolated was retreated with DNase I (Fermentas). The DNase I treated RNA was then used for cDNA synthesis using random hexamers following the RevertAid First Strand cDNA Synthesis Kit (Fermentas) protocol. First Strand cDNA Synthesis products were then used directly in PCR amplification reaction of Hyg, GUS and both arms of the inverted repeat (hairpin). PCR amplification reaction conditions used to screen MM2 and MM4 transgenic lines for transgene expression were the same as those described in **2.4.2.14**. MM6 and MM8 transgenic lines were screened for transgene expression following PCR reaction conditions described in **2.4.3.7**. PCR amplicons were visualised on a 1 % agarose gel containing 10ug/µl ethidium bromide run in 1X TAE.

4.4.7.2 Northern blots

Probes targeting ACMV AC1/4: AC2/3 and SACMV BC1 regions used to make the IR were PCR amplified and DNase I (Fermentas) to produce randomly sheared fragments of different sizes. This was followed by PCR purification using the PCR clean-up Gel extraction kit (Machery-Nagel). Purified fragments derived from the ACMV AC1/4: AC2/3 and SACMV BC1 sequences were then end labelled with radioactive 32^{P}- isotope (BLU502H250UC EASYTIDES ATP,[g-32P]- 250uCi, Perkin Elmer). Labelling reaction was performed using PNK (Fermentas). Probes were then purified and unbound isotope removed using the illustra™ MicroSpin™ G-25 Columns (Amersham GE healthcare). The same 32^{P}-isotope labelling and purification steps were followed to synthesise Arabidopsis miRNA167 loading control probe.

Total RNA (20µg) was denatured in 2X RNA loading dye (Fermentas) at 80 ºC for 5 min and then loaded and separated on a 15% polyacrylamide gel in 0.5% TBE. Total RNA was then transferred to Hybond-N+ membrane (Amersham GE Healthcare) using a semi-dry electro

blotter (Sigma Aldrich, SV20-SDB, UK). RNA was mobilised on the nylon membrane using the UV cross-linker CL-508 (Uvitec Cambridge) twice on the RNA side at 0.120J/cm^2. Membrane was pre-hybridised in Rapid-hyb buffer (Amersham GE Healthcare) at 42 ºC in a rotating oven. The synthesised probe was heated at 100 ºC for 5 min, cooled on ice and then added to the hybridisation buffer with the blot. This was allowed to hybridise overnight in the rotating oven at 42 ºC. The following day the hybridisation-probe solution was harvested and the membrane washed of unbound probe in 2X (SSC + 0.1 w/v SDS) solution at 42 ºC, this was step was repeated. The membrane was sealed and placed in an X-ray cassette and exposed to a sheet of Hyperfilm™MP (Amersham GE Healthcare) at 70 ºC for 2 days and developed. The membrane was then stripped in 1 % w/v SDS at 80 ºC for 30 min. Membrane was then re-probed with miRNA167 probe and the above hybridisation, washing, exposure and development steps performed.

4.5 Results

4.5.1 Standard curves for absolute viral load determinations

ACMV and SACMV standard curves were generated from crossing points (read off the exponential phase of the amplification curves) vs. the logged concentration virus DNA-A concentration. Each reaction was performed in duplicate. An efficiency of 1.970 and an acceptable error rate of 0.00695 were obtained for the ACMV standard curve. SACMV standard curve efficiency was 1.909 with an acceptable error rate of 0.00181.

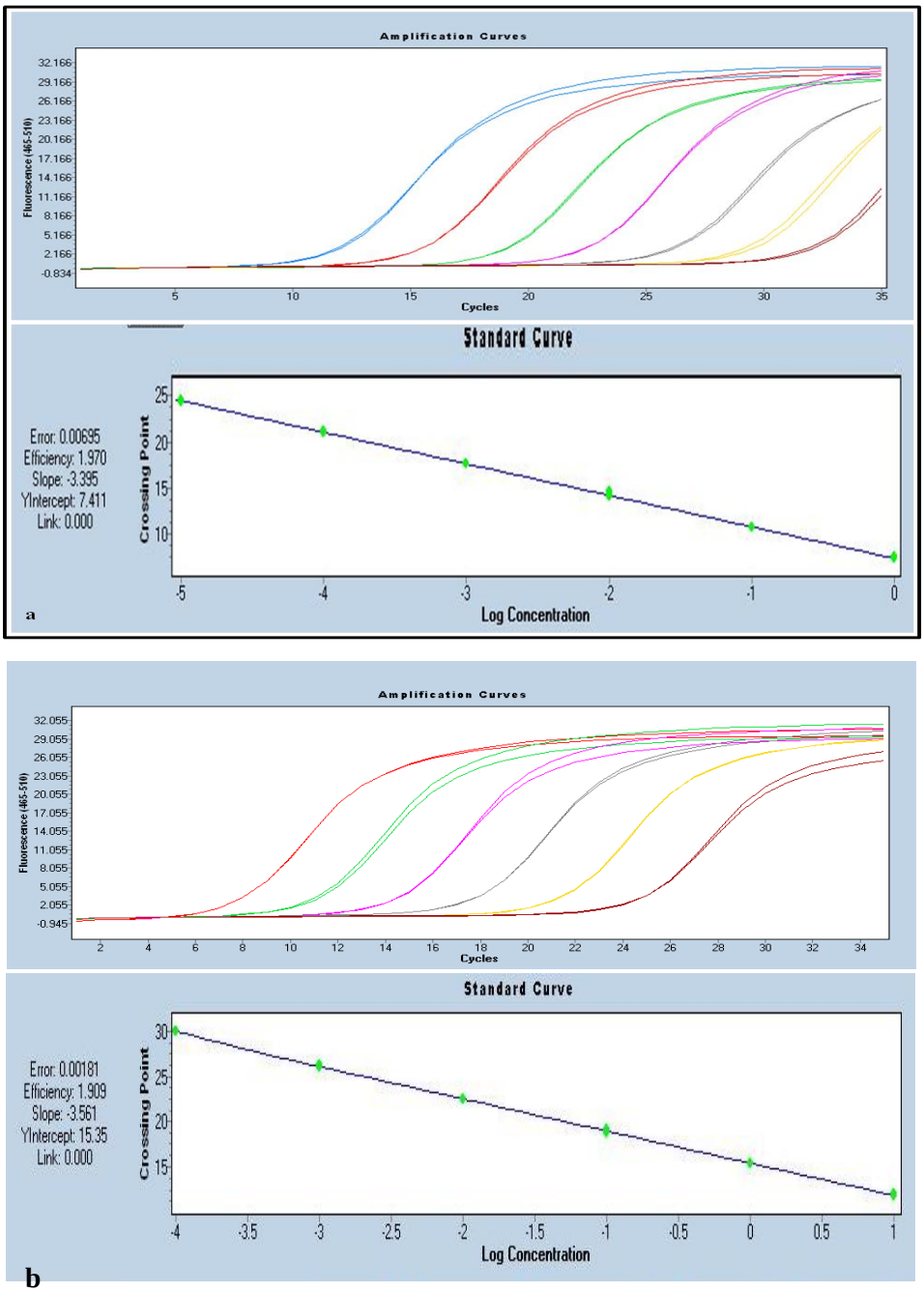


Figure 4. 2 Amplification curves from real-time qPCR of 5 serial (10-fold) dilutions of 10 ng of (a) ACMV-[NG-Ogo] DNA-A in linearised pCambia 1305.1(above). ACMV standard curve was generated from crossing points (read off the exponential phase of the amplification curves) plotted against log ACMV virus concentration (below). (b) Amplification curves from real-time PCR of 5 serial (10-fold) dilutions of 10 ng of SACMV DNA-A in linearised pBS (above).

SACMV standard curve generated from crossing points points (read off the exponential phase of the amplification curves) plotted against log SACMV virus concentration (below).

4.5.2 Screening of transgenic lines for virus resistance levels

Cassava cv.60444 transgenic lines from each transformation event were selected and challenged with infectious begomovirus clones and monitored for virus resistance levels. Plants were monitored and evaluated for virus symptom severity, plant height and viral load accumulation. Transgenic lines, from each transformation event, showing reduced symptoms as compared to wild-type infected cv.60444, and/or lines with delayed symptoms or a recovery phenotype at 67 dpi were selected for repeat virus resistance screening trials. A symptom severity score (sss) index (**fig.4.3**) was used to evaluate severity based on a scale of 0-5 (Fauquet & Fargette, 1990). The images were obtained from the virus challenge experiments performed in this study. In total 9 virus challenge trial experiments were performed however data from the preliminary screening trials is not shown. Only data from the final 4 trials was reported (**table 4.1**). Differences in symptom scores between controls and transgenic lines were considered significant at $p < 0.05$. Values less than this confidence interval were considered insignificant. P values for the t-tests are in (**appendix A-F**)

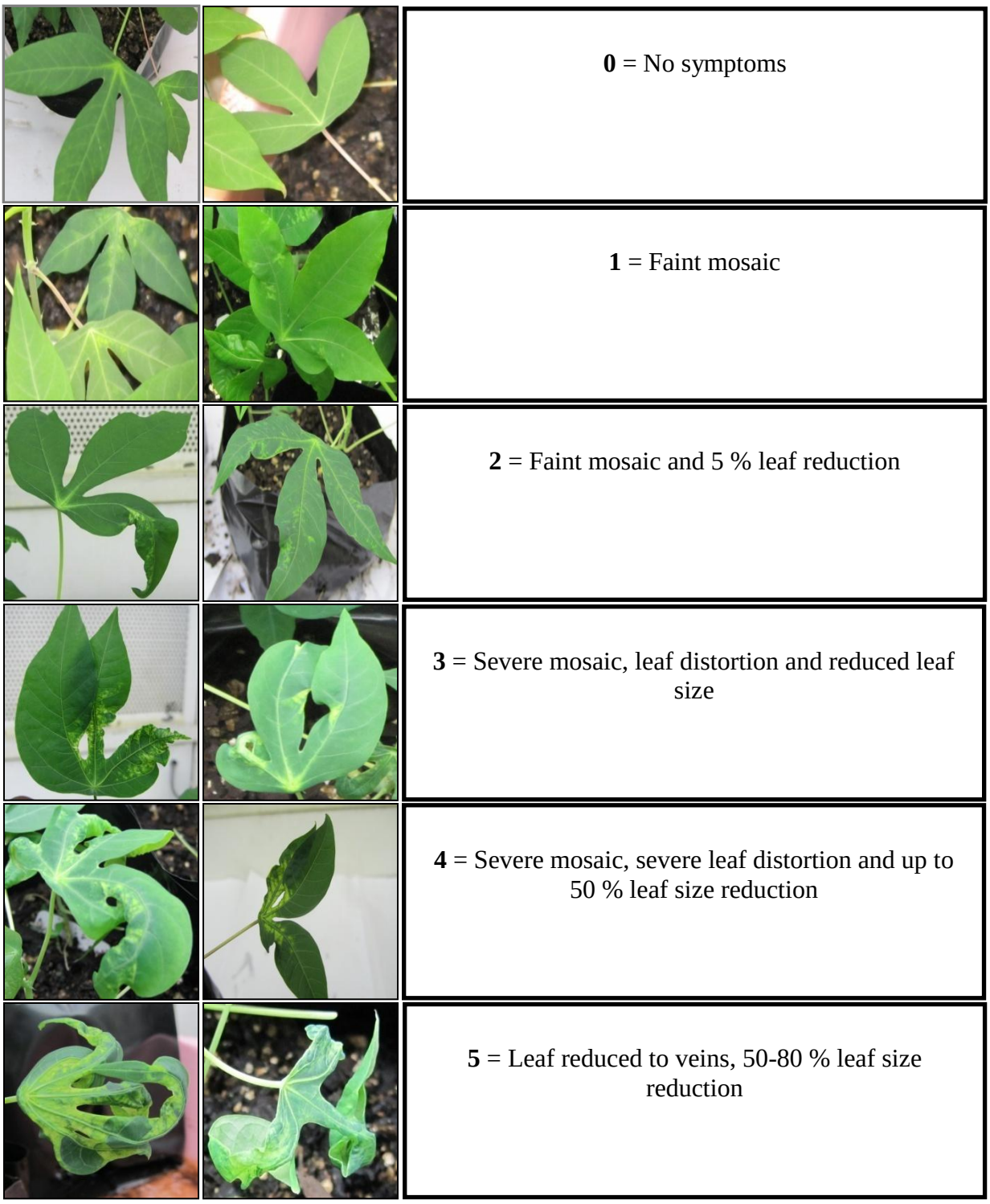


Figure 4. 3 Images of cassava mosaic disease symptomatic leaves. Leaves scored according to symptom severity scale by Fauquet & Fargette (1990). Two images representing each level of the 0-5 scale (0 being asymptomatic and 5 being fully symptomatic). Images complied from trials performed in this study.

4.5.2.1 A-MM2 resistance screening

Severity scores are depicted in **fig. 4.4a**. Overall, what was most noticeable is that symptom severity in the transgenic lines never exceeded a score of 2.0, and was always lower than the susceptible cv.60444 control. At 12 dpi, mean sss was lower than 1 for all wild-type infected susceptible cv.60444 and all transgenic lines. No symptoms were visible in A-MM2 54 and tolerant TME3 landrace control. At 32 dpi, an increase in sss was recorded for all transgenic lines and both susceptible and tolerant controls, however susceptible cv.60444 had the highest average sss (2.3) followed by transgenic line A-MM2 45 (2.2). Lines A-MM2 44, A-MM2 30, A-MM2 54 and A-MM2 52 sss were significantly lower than cv.60444, while A-MM2 54 and A-MM2 44 sss were comparable to TME3. At 67 dpi, sss for all transgenic lines, except A-MM2 44, was significantly lower than cv.60444. An increase in sss was only observed in cv.60444 and A-MM2 44. A-MM2 45 had the lowest sss and this greatest decrease; the sss was also significantly (**appendix A**) lower than TME3 sss.

Transgenic lines were on average 8.5 cm, 16 cm and 35 cm at 12, 32 and 67 dpi, respectively, while control infected lines were on average 7.9 cm, 13 and 33.1 cm at 12, 32 and 67 dpi, respectively (**fig.4b**). At 12 dpi, overall no significant difference in transgenic plant height and control plant height was observed, however A-MM2 54 was significantly more stunted than cv.60444. At 32 dpi, an increase in height was observed for all infected lines however a significant increase was observed for A-MM2 41, A-MM2 44 and A-MM2 45 height was significantly. These lines grew significantly taller than both cv.60444 and TME3. At 67 dpi, only A-MM2 52 was significantly taller than cv.60444 ($p= 0.02$) (**appendix A**).

In all infected transgenic lines viral load was unexpectedly high at 12 dpi (**fig.4.4c**). Viral load in A-MM2 41, 54, 52 and 53 was lower than in cv.60444 however only A-MM2 54 was considered significant ($p< 0,05$). Viral load measured in A-MM2 54 was 190-fold lower than cv.60444 viral load. The viral load was more comparable to TME3 viral load. At 32 dpi, the viral load decreased for all infected plants except A-MM2 54 and TME3. Transgenic line A-MM2 30 had the largest decrease in viral load. However the amount of viral load was still higher than cv.60444 viral load. At 32 dpi, viral load quantified in both A-MM2 45 and 30 was 52 and 53-fold lower, respectively, than at 12 dpi. What was noticeable was that at 67 dpi lines A-MM 45,

41, 52 and 30 lines had viral loads lower than cv.60444 and more comparable to tolerant TME3. However p-values were not significant (between 0.09 and 0.42) (**appendix A**).

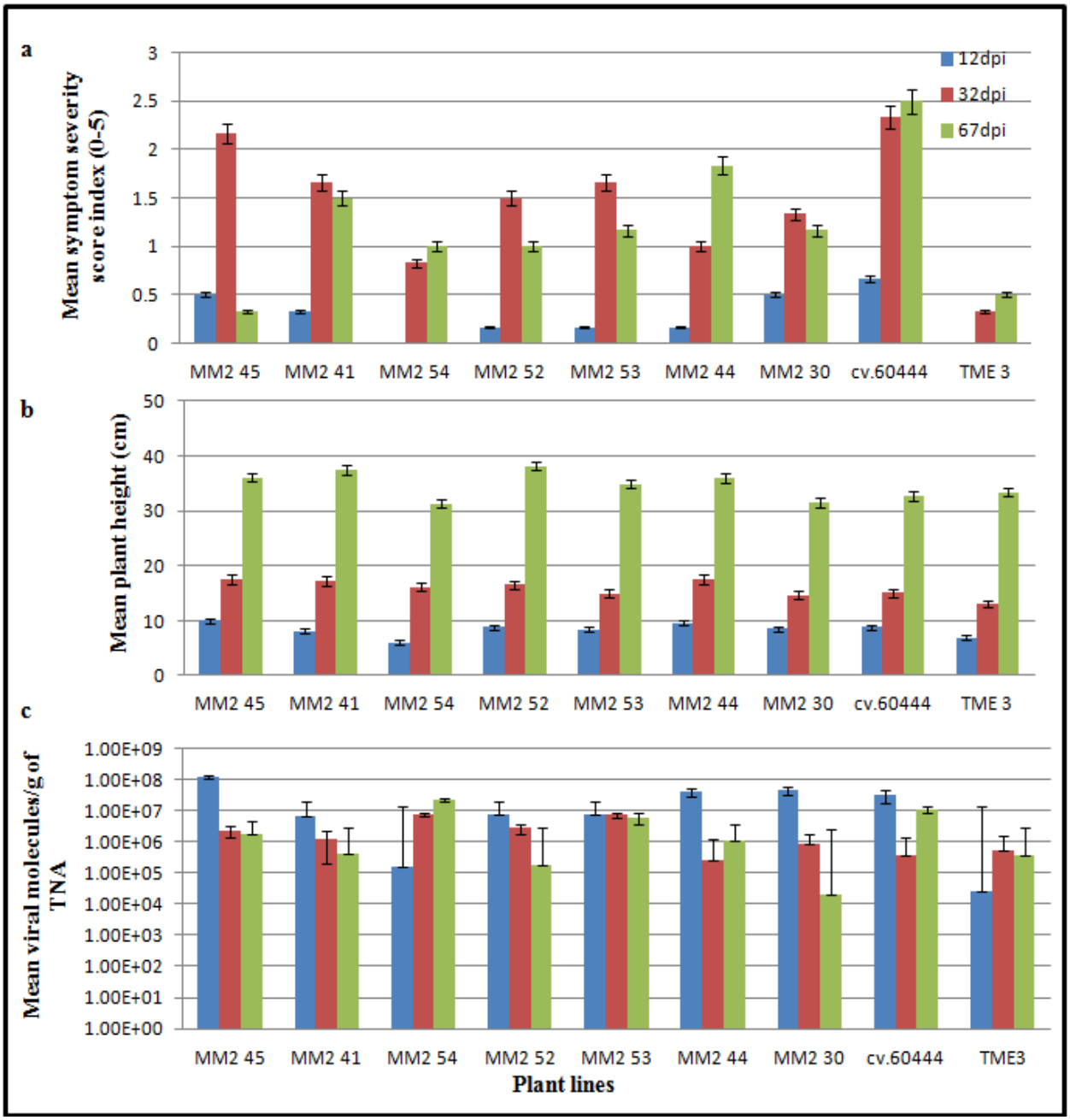


Figure 4. 4 A-MM2 transgenic lines and control plants agroinoculated with infectious ACMV-[NG-Ogo] clones. Plants were evaluated at 12dpi (blue), 32dpi (red) and 67dpi (green) for **(a)** Mean symptom severity scores, **(b)** Mean plant growth height and **(c)** Mean absolute viral load quantification (virus molecules/g of TNA).

4.5.2.2 A-MM4 resistance screening

At 12 dpi, all transgenic and cv.60444 plants presented with very mild symptoms, the mean sss were below 1(**fig. 4.5a**). Tolerant TME3 only became mildly symptomatic from 18 dpi. At 32 dpi, sss of all infected transgenic lines and control plants increased. A-MM4 59 sss was 3 fold lower than cv.60444 ($p<0.05$). Both A-MM4 11 and A-MM4 79 lines presented with a 2.4 fold lower sss than cv.60444 and a 1.7 fold lower sss was seen for both A-MM4 33 and A-MM4 46, and the observed differences were considered statistically significant (**appendix B**). At 67 dpi, an increase in sss was seen for all plants infected except TME3, A-MM4 34 and A-MM4 68. Average sss for A-MM4 34 and A-MM4 68 decreased to 1 and 1.3, respectively What was notable was that the sss were significantly lower in all transgenic lines compared with the susceptible non-transgenic cv.60444 control. A constant average sss below 1 was maintained for TME3 (**fig. 4.5a**).

At 12 dpi, no significant difference in plant height was seen for all transgenic lines and cv.60444 and TME3 controls. At 32 dpi the only notable and significant difference in plant height was measured for A-MM4 46, this transgenic line appeared more stunted than cv.60444 and the other transgenic lines. At 67 dpi, the measured plant height for cv.60444 was on average 30 % lower than all transgenic lines and control TME3 observed differences were considered statistically significant (**fig.4.5b**) (**appendix B**).

A similar trend to A-MM2 was observed, at 12 dpi the viral load in cv.60444 and transgenic lines, except A-MM4 11, was higher compared with 32 and 67 dpi (**fig. 4.5c**). The lowest viral load was recorded in A-MM4 46; between 12 and 32 dpi the viral load decreased 1159-fold, this was 552-fold and 4.4 fold lower than cv.60444 and TME3 viral load, respectively. Viral load recorded in A-MM4 33 was 225-fold lower at 32dpi than 12dpi. A-MM4 46 and A-MM4 11 viral load was significantly lower than cv.60444. At 32 dpi, a decrease in viral load was recorded in all transgenic lines, except in TME3 and A-MM4 11. As with A-MM2 transgenic lines, all A-MM4 lines had lower virus titers compared with the non-transgenic susceptible cv.60444 control at 67 dpi. Viral loads in tolerant TME3 were generally lower than cv.60444 and transgenic lines at all time points. At 67dpi, viral load was 61.5-fold lower than cv.60444 viral load. Transgenic

lines viral load was comparable to TME3. Statistical analyses (**appendix B**) indicated that the differences between TME3 control and transgenic lines were not highly significant.

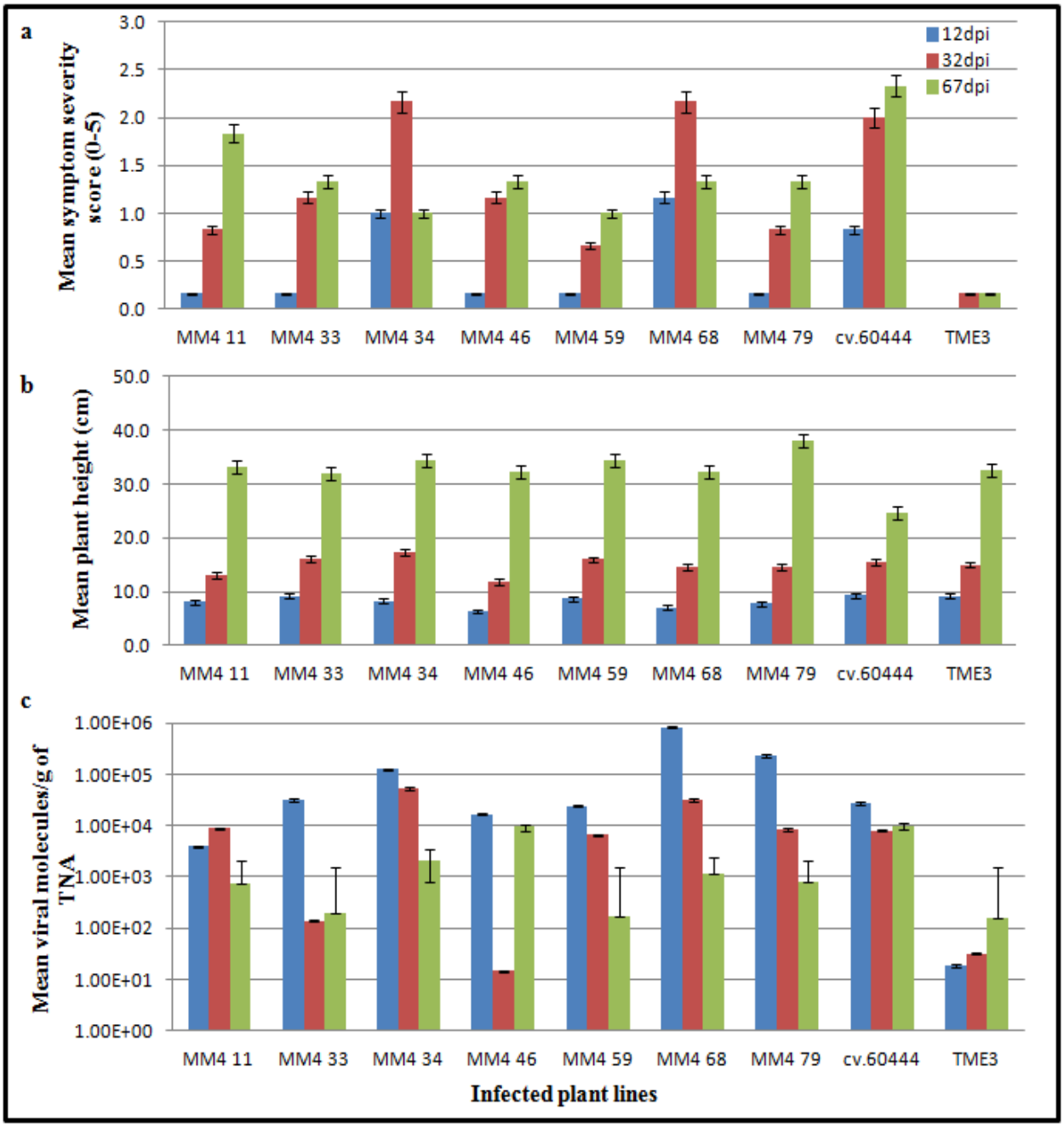


Figure 4. 5 A-MM4 transgenic lines and control plants agroinoculated with infectious SACMV clones. Plants were evaluated at 12dpi (blue), 32dpi (red) and 67dpi (green) for **(a)** Mean symptom severity scores, **(b)** Mean plant growth height and **(c)** Mean absolute viral load quantification (mean viral molecules/g TNA).

4.5.2.3 C-MM6 resistance screening

Notably, at all 3 time points post-ACMV challenge, transgenic lines and wild-type tolerant TME3 had lower severity scores (<2.0) than susceptible non-transgenic cv.60444 (**fig.4.6a**). Transgenic lines presented with a mean sss between 0 and 1.5. At 12 dpi, C-MM6 1 was the only asymptomatic line. The other transgenic lines had severity scores lower than cv.60444. Severity scores recorded for all transgenic lines, except C-MM8 8 and C-MM8 1, were significant. Transgenic line C-MM6 1 becoming symptomatic from 20 dpi and at 32 dpi a mean sss of 1.5 was recorded and a similar sss was recorded at 67 dpi. At 32 dpi, C-MM6 11 and C-MM6 10 had a 4-fold and 3-fold lower sss than cv.60444, respectively ($p<0.05$). At 67 dpi, all transgenic lines had sss lower than cv.60444 however only C-MM6 10 and 11 sss were statistically significant ($p<0.001$ and $p<0.007$, respectively) (**appendix C**).

At all 3 time points, no significant increase in transgenic plant height as compared to cv.60444 was observed. Only C-MM6 10 was considered significantly higher than cv.60444 at 67 dpi ($p=0.02$). C-MM6 2 was however significantly shorter than cv.60444 at 67 dpi. TME3 did not grow significantly taller than the transgenic lines at all 3 time points (**fig. 4.6b**) (**appendix C**).

While, at all 3 time points, viral load in susceptible cv.60444 was higher than the viral load recorded in all the transgenic lines and TME3 (**fig.4.6c**), the overall p-values were >0.05. The viral load considered significantly lower than cv.60444 was measured in C-MM6 1 and C-MM6 19 at 12 dpi. All the other viral loads were marginally high. At 12 dpi, C-MM6 1 had the lowest viral load and this was 220.3-fold lower than cv.60444. Tolerant TME3 had the lowest viral load and this was 109.6-fold lower than cv.60444 recorded viral load. At 32 dpi, viral load decreased in TME3 and transgenic lines except C-MM6 1. In C-MM6 1 the viral load increased 1.7-fold.
Viral load in cv.60444 decreased 15.9-fold at 32 dpi; however this was still the highest recorded viral load at 32dpi. At 67 dpi, cv.60444 viral load was higher than all transgenic lines. TME3 viral load increased 98.2-fold, this was the highest viral load increase at 67 dpi. At 67 dpi, the viral load in C-MM6 19, C-MM6 2, C-MM6 11, C-MM6 8, C-MM6 1 and C-MM6 10 were 73.9-fold, 64.9-fold, 19.9-fold, 9.6-fold, 8.3-fold and 3.3-fold lower than cv.60444 viral load, respectively. Statistical analyses (**appendix C**) indicated that the differences between cv.60444 control and transgenics were not highly significant.

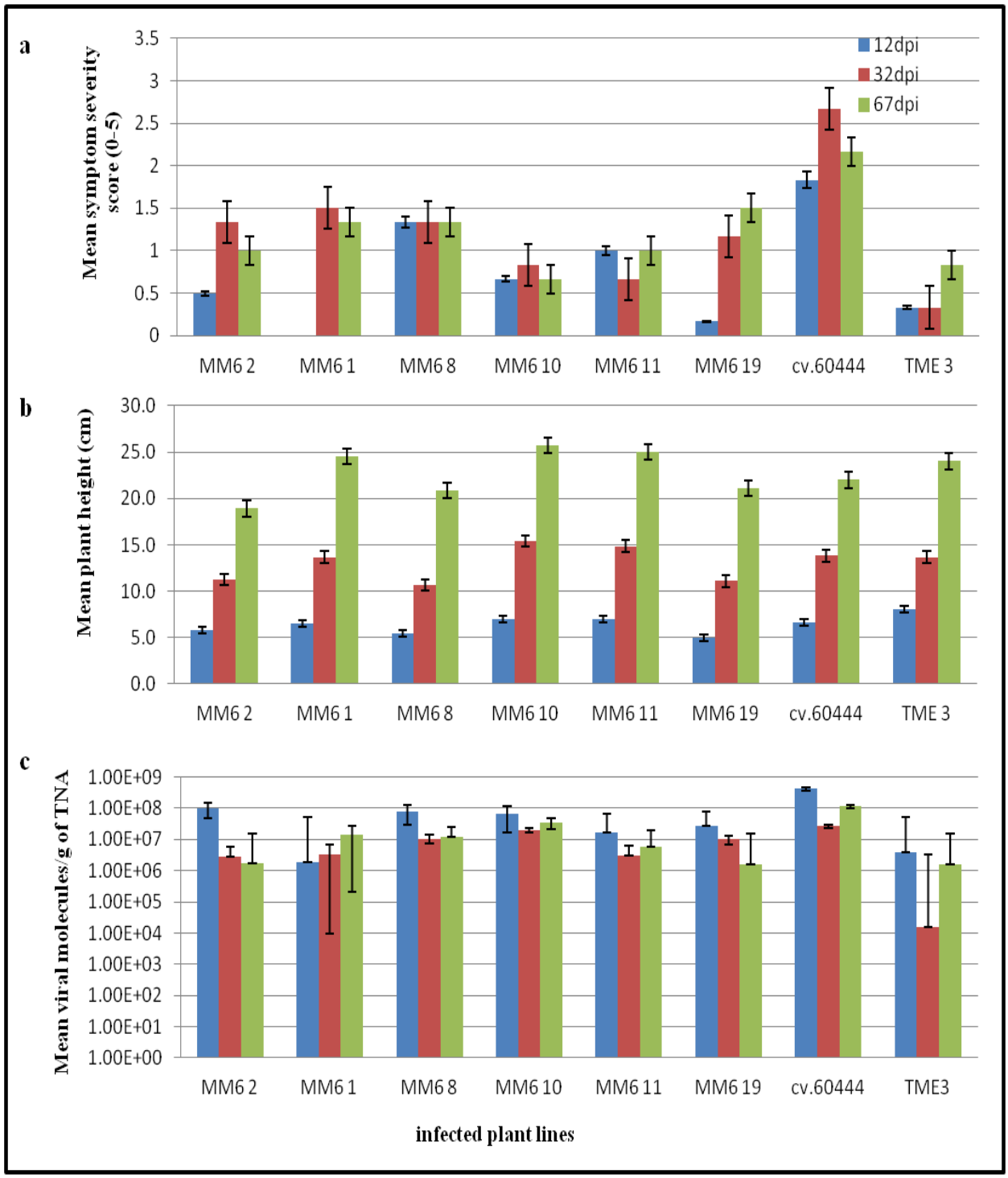


Figure 4. 6 C-MM6 transgenic lines and control plants infected with infectious ACMV-[NG-Ogo] clones. Plants were evaluated at 12dpi (blue), 32dpi (red) and 67dpi (green) for **(a)** Mean symptom severity scores, **(b)** Mean plant growth height and **(c)** Mean absolute viral load quantification (mean viral molecules/g TNA).

4.5.2.4 C-MM8 resistance screening

At 12 dpi, cv.60444 viral load was higher than all transgenic lines, however statistical analyses (**appendix D**) indicated that the differences between control and transgenic were not highly significant (**fig. 4.7a**). TME3 was remained asymptomatic until 21 dpi. At 32 dpi, cv.60444 had the sss highest increase; a 2.5-fold increase was seen. C-MM8 25 mean sss was 2.1-fold lower than cv.60444 sss ($p=0.007$). C-MM8 27 sss was 1.5 and this was significantly lower than cv.60444 ($p= 0.04$). At 67 dpi, a decrease in sss was seen for all transgenic lines. With the exception of C-MM8 3, sss for all transgenic lines were significantly lower than cv.60444. Mean sss for C-MM8 27 decreased by 2.3-fold and this represented the highest decrease and it was significantly lower than cv.60444 sss ($p=0.003$).

Overall at 12dpi, 32 dpi and 67 dpi no significant difference in mean plant height was recorded for all plants, except for C-MM8 25 which was slightly more stunted than the other transgenic lines and cv.60444 at 32 and 67 dpi (**fig. 4.7b**). Line C-MM8 1 was also significantly more stunted than cv.60444 at 67 dpi (**appendix D**).

At all 3 time points the viral load in cv.60444 was higher than all transgenic lines and TME3. However statistical analyses (**appendix D**) indicated that the differences between control and transgenic were not highly significant with the exception of C-MM8 23 at 32 dpi (**fig. 4.7c**). At 32 dpi, C-MM8 23 viral load was 7.5-fold lower than cv.60444 ($p< 0.02$). At 32 and 67dpi, the highest viral was recorded in cv.60444 and the lowest was recorded in TME3. TME3 viral load was 1077.5-fold lower than cv.60444 viral load.

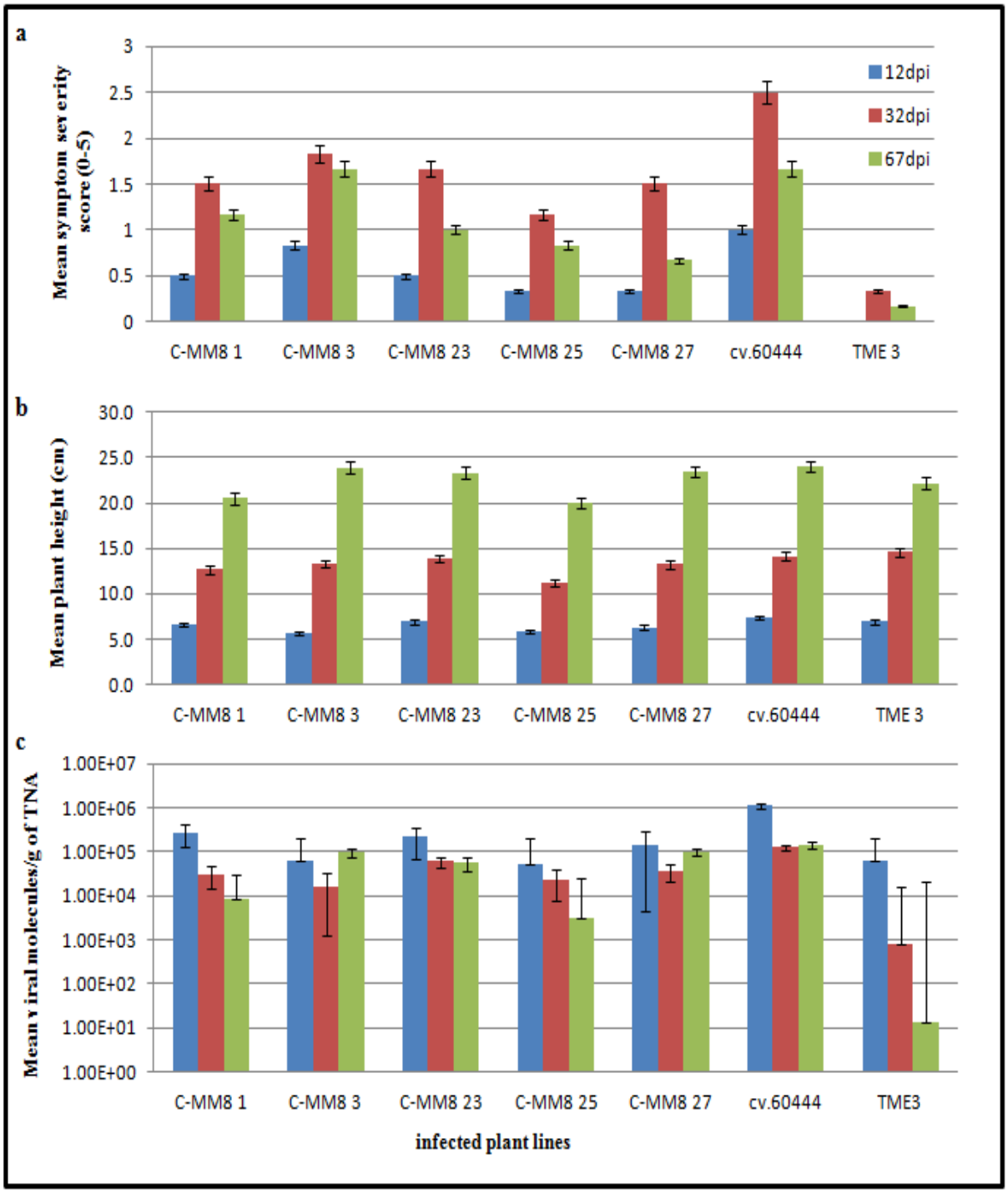


Figure 4. 7 C-MM8 transgenic lines and control plants infected with infectious SACMV clones. Plants were evaluated at 12dpi (blue), 32dpi (red) and 67dpi (green) for (a) Mean symptom severity scores, (b) Mean plant growth height and (c) Mean absolute viral load quantification (viral molecules/g TNA).

4.5.2.5 Evaluation of A-MM2 and A-MM4 transgenic lines at 365 dpi

At 365 dpi, ACMV infected transgenic lines A-MM2 30, A-MM2 52, A-MM2 53, A-MM2 41 and A-MM2 45 and tolerant TME3 appeared asymptomatic. AMM2 54 presented with very faint mosaic (sss=1). The sss for cv.60444 WT infected plants remained similar (**fig.4.8**) to sss recorded at 67 dpi (sss= 2-3) (**fig 4.4a**). ACMV virus replication was detected in all 7 transgenic lines and WT infected cv.60444 and TME3, despite recovery from symptoms. However ACMV titers in all the transgenic lines, except A-MM2 30, were significantly lower (3500-fold, 2884-fold, 2310-fold, 2320-fold and 41-fold for A-MM2 41, AMM2 54, A-MM2 52, A-MM2 53 and A-MM2 41, respectively) to susceptible non-transgenic cv.60444. Viral load in TME3 was 152-fold lower than cv.60444. In transgenic lines A-MM2 41, A-MM2 54, A-MM2 52 and A-MM2 53, ACMV viral load was 23-fold, 18-fold, 15.2-fold and 15.3-fold lower than in TME3. ACMV viral load in A-MM2 30 was similar to that in cv.60444. However this line was asymptomatic. At 365 dpi, an increase in viral load was quantified in A-MM2 30; this represented a 2.1-fold difference/increase at 67 dpi to 365 dpi. At 365 dpi, a 768-fold, 35399-fold, 230-fold and 7412-fold decreased in ACMV viral load was recorded in A-MM2 41, A-MM2 45, A-MM2 52 and A-MM2 53, respectively, at 67 dpi. A 31.2-fold viral load decrease was recorded in TME3 at 365 dpi (**fig 4.9 a**).

Similar to the MM2 lines, SACMV-challenged A-MM4 59, A-MM4 46 and A-MM4 68 were asymptomatic at 365 dpi, mild symptoms were observed for A-MM4 34, A-MM4 11 (**fig 4.8 e and f**). Wild-type cv.60444 infected plants presented with yellow mosaic speckles throughout the leaf surface but no leaf curling. At 365 dpi, no virus was detected in A-MM4 33, A-MM 46, A-MM4 59, A-MM4 68, A-MM4 79 and TME3. SACMV was detected in A-MM4 34 and infected WT cv.60444; however this was 24-fold and 3.65-fold lower, respectively, than at 67 dpi. SACMV viral load quantified in A-MM4 34 was 31-fold lower than in cv.60444. Differences in viral loads between infected susceptible non-transgenic cv.60444 and transgenic lines, as well as between 67 and 365 dpi were statistically significant ($p<0.05$) (**fig 4.9 b**) (**appendix E**).

Table 4. 2 Symptom severity scores of A-MM2 transgenic lines at 365 dpi with ACMV

A-MM2 transgenic line	sss at 365 dpi
A-MM2 30	0
A-MM2 52	0
A-MM2 53	0
A-MM2 41	0
A-MM2 45	0
A-MM2 54	1
Untransformed cv.60444	3
Untransformed TME3	0

Table 4. 3 Symptom severity scores of A-MM4 transgenic lines at 365 dpi with SACMV

A-MM4 transgenic line	sss at 365 dpi
A-MM4 11	1
A-MM459	0
A-MM4 46	0
A-MM4 68	0
A-MM4 34	1
A-MM4 79	0
A-MM4 33	0
Untransformed cv.60444	2
Untransformed TME3	0

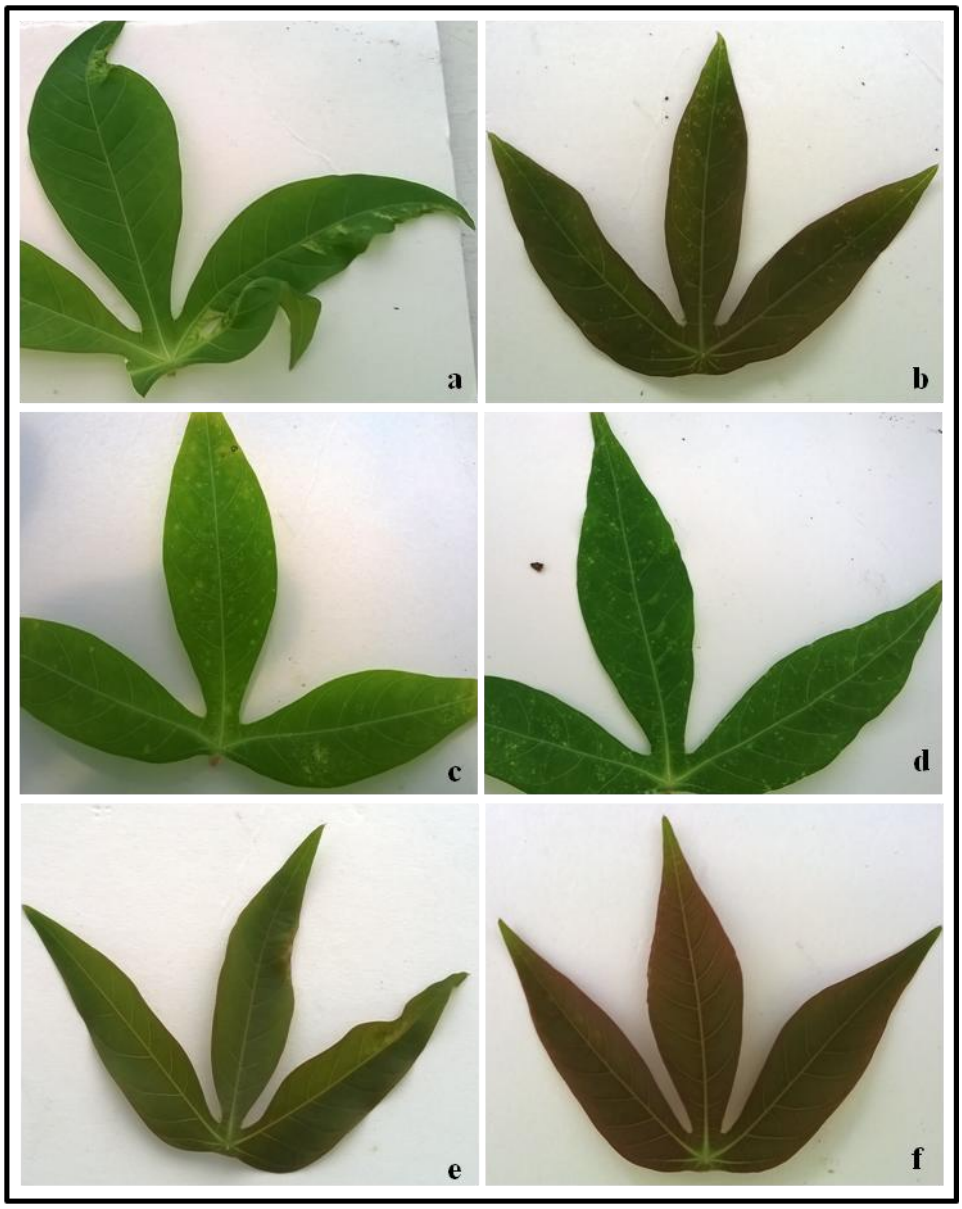


Figure 4. 8 CMD symptoms collected from ACMV and SACMV infected cassava plants at 365 dpi, **(a)** ACMV infected cv.60444, showing mosaic, leaf curl and size reduction, **(b)** ACMV infected A-MM2 54 leaf with faint yellow spots on entire leaf surface, **(c, d)** SACMV infected cv.60444 (WT) with yellow mosaic spotting on entire leaf surface, **(e)** SACMV infected A-MM4 11 leaf showing slight leaf curl and mosaic on leaf edge and **(f)** SACMV infected A-MM4 34 showing slight mosaic on the leaf margin and faint yellow spots on leaf surface.

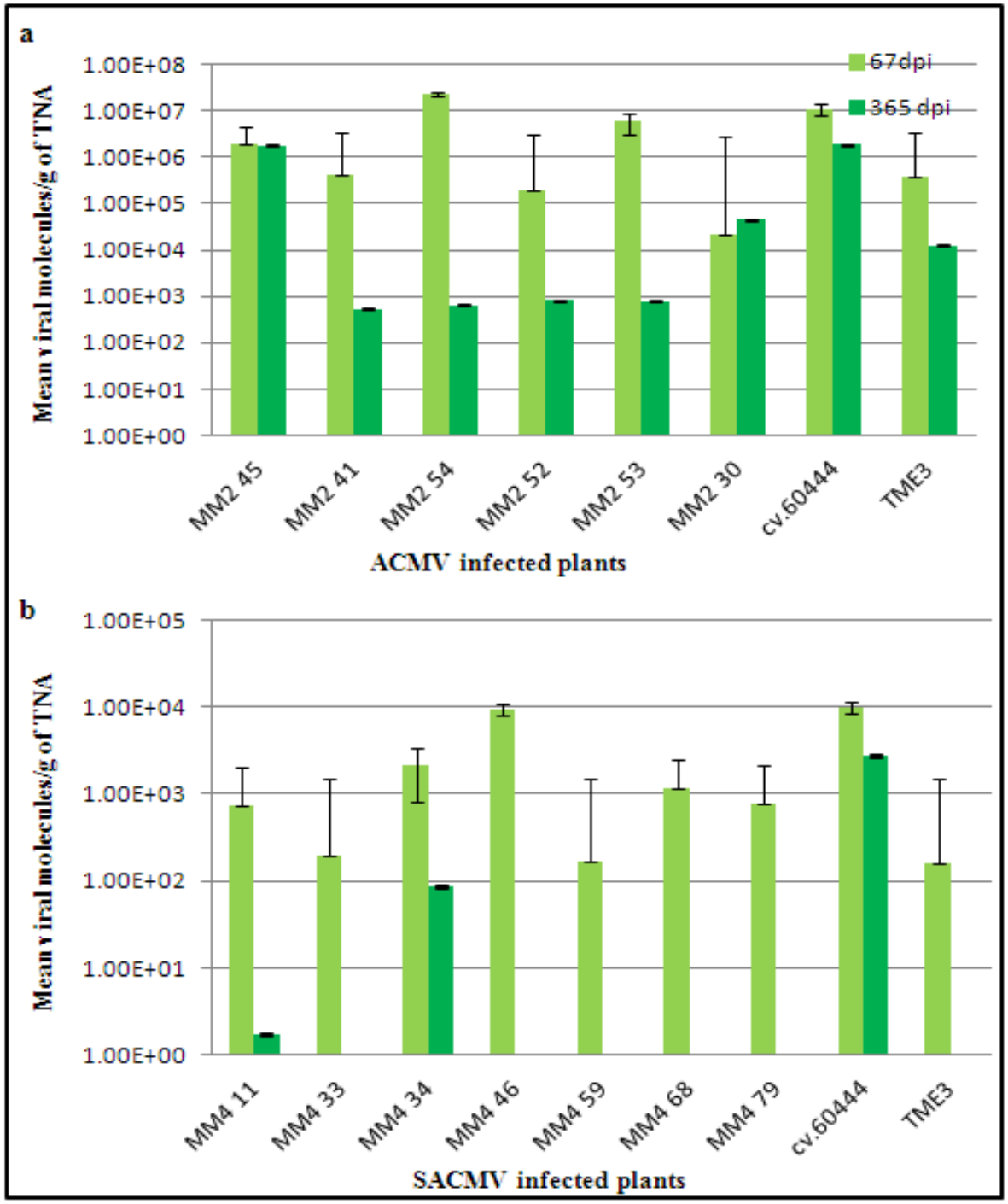


Figure 4. 9 Mean viral molecules/g of TNA at 365 dpi, quantified using qPCR, **(a)** ACMV infected A-MM2 transgenic lines and controls lines and **(b)** SACMV infected transgenic lines and control plants.

4.5.3 Transgene expression and siRNA detection

Only the lines selected in the final 4 trials were evaluated for transgene expression and siRNA detection

4.5.3.1 RNA extraction

High quality intact total RNA with very little residual DNA was successfully extracted from unchallenged tissue culture stocks of A-MM2, A-MM4, C-MM6 and C-MM8 transgenic lines screened above (**fig 4.10).** DNase I treatment step was performed to eliminate any remaining DNA following RNA extraction.

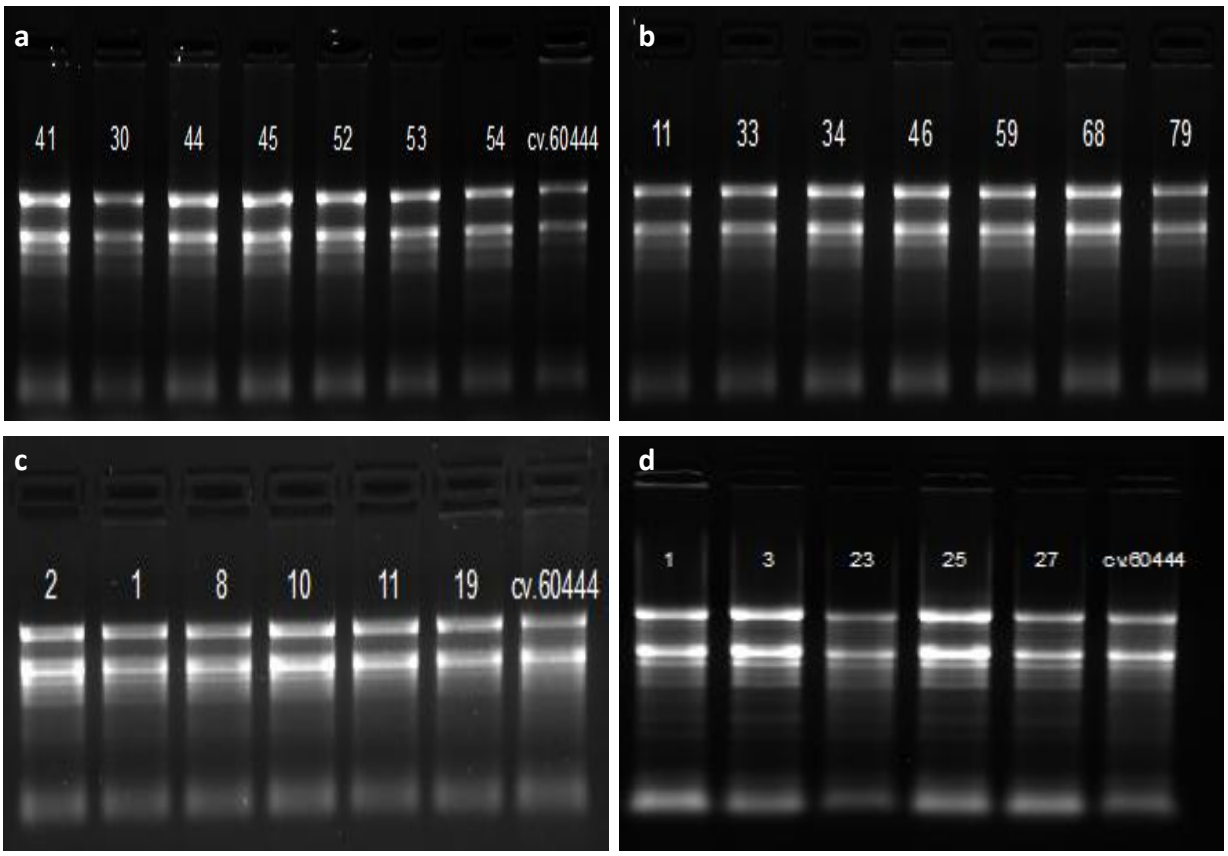


Figure 4. 10 1.2% agarose gel electrophoresis (10mg/ml EtBr) of total RNA extracted from **(a)** A-MM2 transgenic lines 41, 30, 44, 52, 53, 54 and non-transgenic cv.60444 WT, **(b)** A-MM4 transgenic lines 11, 33, 34, 46, 59, 68 and 79, **(c)** C-MM6 transgenic lines 2, 1, 8, 10, 11, 19 and non-transgenic cv.60444 and **(d)** C-MM8 transgenic lines 1, 3, 23, 25, 27 and non-transgenic cv.60444.

4.5.3.2 RT-PCR results

cDNA synthesis using Random hexamers and/or OligodT primers was used for RT-PCR amplification of *Hyg* (485 bp), *GUS* (181 bp) and transgene insert. In all seven A-MM2 selected lines, *GUS* and *Hyg* were successfully amplified and as expected no amplicons were detected in wildtype cv.60444, and the PCR amplification reaction controls were positive for both *GUS* and *Hyg* (**fig. 411a**). However in all seven A-MM2 lines, amplification of the RNAi hairpin was unsuccessful; amplification of the mutated sense-arm (319bp) fragment and non-mutated antisense arm (337bp) fragment of the MM2 hairpin construct from cDNA synthesised from random hexamers and oligodT primers yielded no amplicons (gel images not shown). In all seven A-MM4 transgenic lines both the 181bp *GUS* and 485 bp *Hyg* fragments were successfully amplified from cDNA synthesised using random hexamers. PCR amplification reaction controls for both *GUS* and *Hyg* were positive and no amplicons were amplified from cv.60444 synthesised cDNA. In all seven A-MM4 lines, the 221 bp MM4hp non-mutated strand was strongly amplified and the 239 bp MM4 hp mutated strand was weakly amplified. Amplicons were also generated for both MM4 *Xba*I and MM4 *Xho*I positive controls, while wild-type non-transgenic control cv.60444 was negative for MM4 *Xba*I and MM4 *Xho*I amplicons (**fig. 4.11b**). The 181bp *GUS* fragment, 485 bp *Hyg* fragment, the 319bp MM6 *Xba*I and 319 bp MM6 *Xho*I fragments were all successfully amplified from cDNA synthesised from C-MM6 transgenic lines. All PCR amplification positive controls produced expected amplicons while negative control reactions yielded no amplicons (**fig 4.11c**). RT-PCR was also performed using cDNA synthesised from RNA extracted from C-MM8 transgenic lines, and RT-PCR yielded the 181 bp *GUS*, 485 bp *Hyg*, 221 bp MM8 *Xba*I and 221 bp MM8 *Xho*I amplicons in all five C-MM8 transgenic lines. PCR amplification control and negative control produced expected results (**fig 4.11d**).

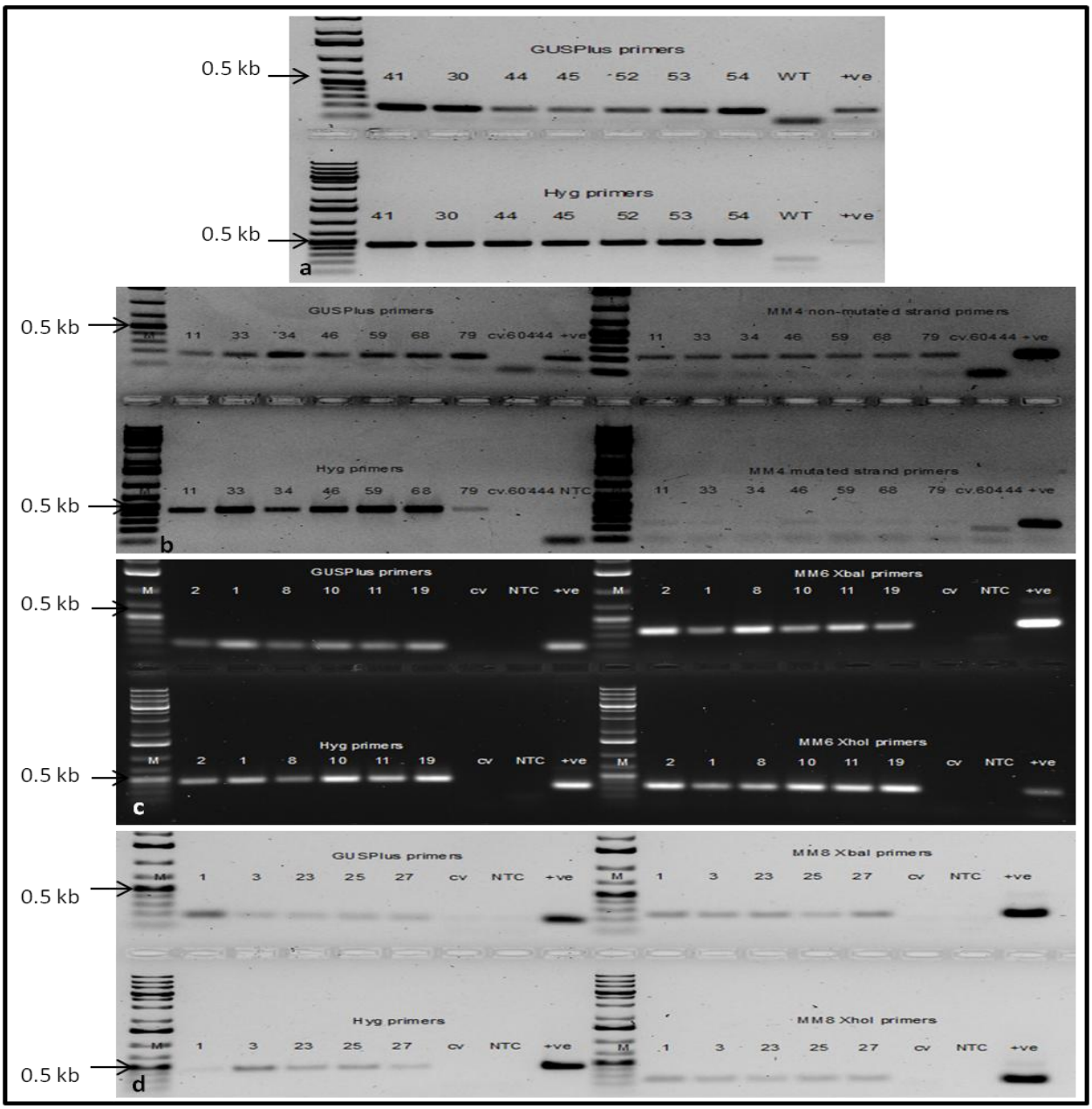


Figure 4. 11 RT-PCR amplification of transgne cDNA from (a) A-MM2 transgenic lines: 181 bp *GUS* (above) and 485 bp *Hyg* (below). M= O'GeneRuler 1kb Plus DNA ladder (Fermentas), (b) A-MM4 transgenic lines: 181 bp *GUS* (above, left) and 485 bp *Hyg* (below, left), 221 bp non-mutated anti-sense-arm (above, right); GU: 239 bp mutated sense-arm (below, right), (c) C-MM6 transgenic lines: 181 bp *GUS* (above, left) and 485 bp *Hyg* (below, left), 319 bp MM6 *Xba*I-arm (above, right) and 319 bp MM6 *Xho*I-arm (below, right) and (d) C-MM8 transgenic lines: 181 bp *GUS* (above, left) and 485 bp *Hyg* (below, left), 221 bp MM8 *Xba*I-arm and 221 bp MM8 *Xho*I-arm. cv is an untransformed uninfected control.

4.5.3.3 siRNA detection

ACMV AC1/4:AC2/3-derived siRNA molecules were detected at high levels in ACMV AC1/4:AC2/3 transgenic lines (A-MM2 and C-MM6) (**fig 4.12 a and c,** respectively) and in untransformed cv.60444. A dsAC1 transgenic line (known to be ACMV resistant (Vanderschuren *et al*., 2009) was used as a positive control. Accumulation of SACMV BC1-derived siRNA was detected at low levels in A-MM4 11, 33, 34 and 59 and weakly in A-MM4 48, 68 and 79 (**fig 4.12 b**). In C-MM8 transgenic lines, SACMV BC1 probe hybridised to higher molecular weight RNA (**fig 4.12 d**).

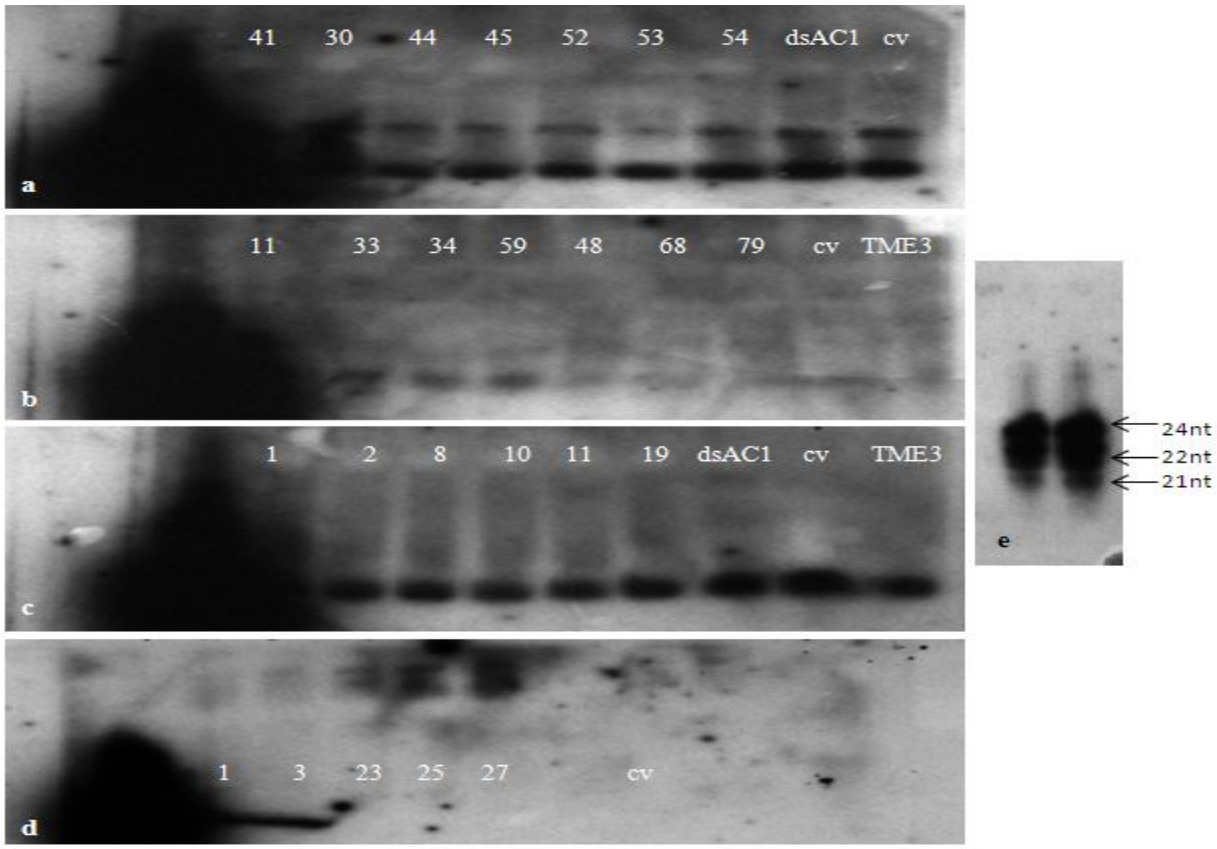


Figure 4. 12 siRNA detection in healthy transgenic lines and control lines. Probes were radioactively labelled with P^{32}, **(a)** A-MM2 transgenic lines and controls probes with ACMV AC1/4:AC2/3 generated probe, **(b)** SACMV BC1-derived probes used to probe A-MM4 transgenic lines, **(c)** C-MM6 transgenic lines probed with ACMV AC1/4:AC2/3-derived probe, **(d)** C-MM8 transgenic lines probed with SACMV BC1-derived probe and **(e)** radioactively labelled 21, 22 and 24 nt oligonucleotides used as markers.

Loading control miRNA 167 was detected in A-MM2, A-MM4 and C-MM6 transgenic lines and control lines (**fig 4.13 a-c**). In C-MM8 transgenic lines miRNA167 loading control probe detection was not as strong as in fig 4.13a-c.

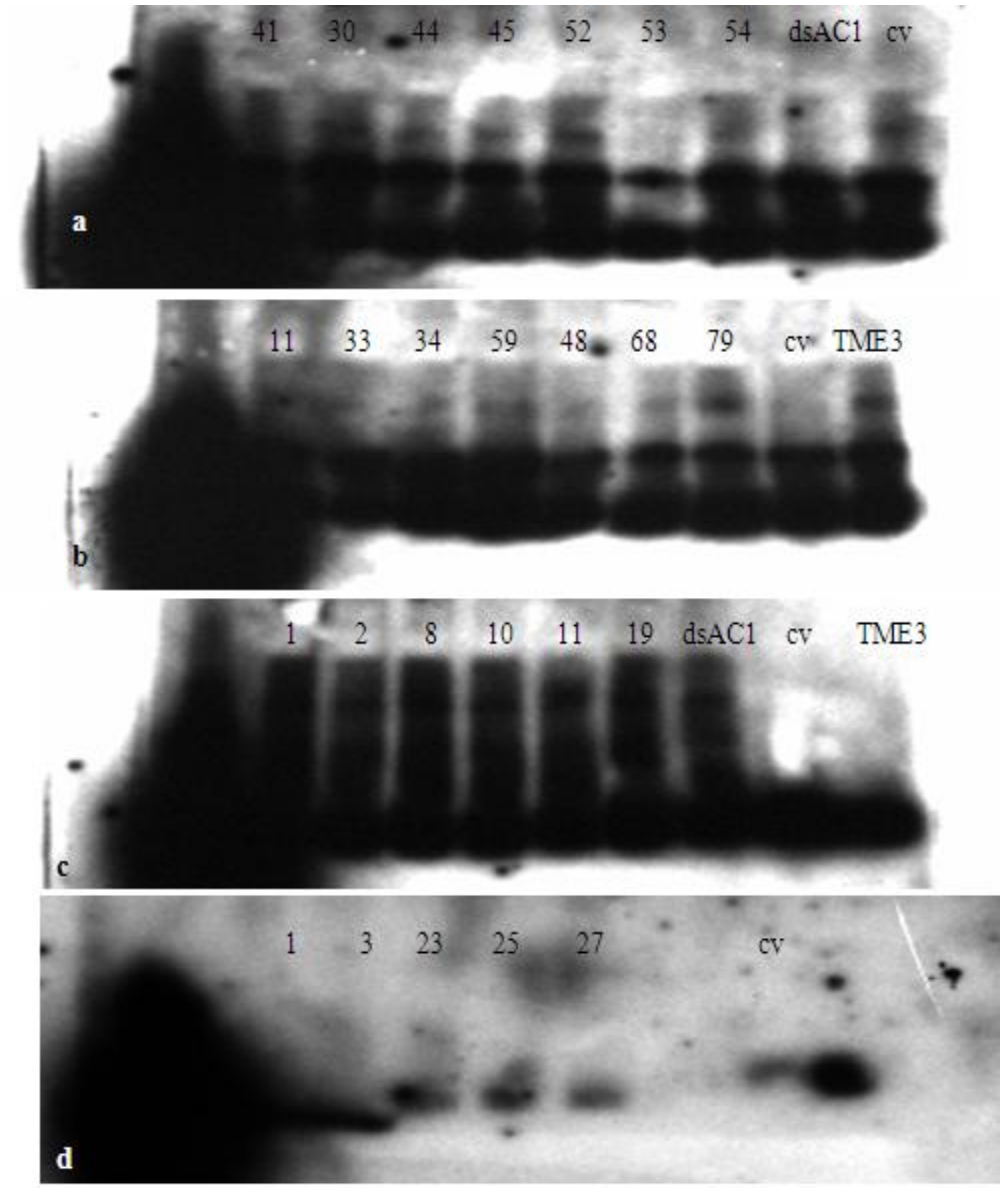


Figure 4. 13 Arabidopsis miRNA167 probe used for loading control in siRNA detection experiment to probe healthy control lines and transgenic **(a)** A-MM2 lines, **(b)** A-MM4 lines, **(c)** C-MM6 lines and **(d)** C-MM8 lines. Left lane is over loaded marker

4.6 Discussion

In the study cassava plants were successfully agro-inoculate with infectious geminivirus clones. SACMV or ACMV resistant transgenic plants were not identified in the screening process, however improved cv.60444 transgenic lines, expressing ACMV AC1/4: AC2/3 and SACMV BC1 ORF, showing ACMV and SACMV tolerance, respectively, were observed, where tolerance is described as plants having lower symptoms despite virus still being present (Fraile & García-Arenal, 2010; Oliver & Fuchs, 2011). Ideally, resistant plants would not show any symptoms, and no detectable viral titer (Oliver & Fuchs, 2011). Conversely, tolerance to virus infection leads to reduced crop damage or symptoms in the presence of the virus (Oliver & Fuchs, 2011). While none of the transgenic lines were symptom-free at 67 dpi, several transgenic lines presented mild tolerant phenotype, with either delayed symptoms or lower severity despite continuous virus replication, especially at 67 dpi, where these lines had significantly lower symptoms and viral loads compared to wild-type non-transgenic cv. 60444 control plants, but comparable with tolerant TME3. Notably, in transgenic lines, A-MM2 30, A-MM2 52, A-MM4 59, C-MM6 10, C-MM6 11 and C-MM8 25, lower CMD symptoms severity scores were observed, with no stunting, instead showing favourable growth while supporting relatively high virus multiplication. Significantly lower virus symptoms were recorded in these transgenic lines than in control infected wild-type cv.60444. In a study by Vanderschuren *et al*. (2007), ACMV resistant transgenic cassava was not engineered, however they were able to report attenuated CMD symptoms in two transgenic cassava lines expressing an ACMV bidirectional promoter hairpin construct. Virus resistance transient assays in leaf discs were performed, but unlike in our study they were able to report significant reduction in viral load correlating to lower symptom severity. Delayed symptom development was observed in transgenic lines A-MM2 54 and C-MM6 1. In these lines virus symptoms appeared between 18 and 21 dpi and not earlier stages between 10-12 dpi. Delays in symptom development were seen in transgenic tomato expressing *Tomato leaf curl virus* (TLCV) C*2* gene (Bian *et al*., 2006). Unexpectedly, a steady increase in TLCV viral load was observed even though siRNA accumulation was reported to be high. At 25 dpi, viral load accumulated at higher levels than in wild-type tomato plants. To try to understand the observed results, Bian and colleagues performed further experiments using a TLCV C*4* expressing RNA silencing marker tobacco plant. The tobacco plant was engineered to have distinct mosaic and leaf margin phenotype.

Upon infection with TLCV, plants lost the distinct phenotype and C*4* transcripts were undetectable. The constitutive 35S promoter, C4 ORF and TLCV genome were found to be highly methylated. These results suggested that geminiviruses are able to escape RNA silencing mechanism using 'geminivirus-induced transcriptional silencing'. This has been demonstrated in many other studies (Aregger *et al*., 2012; Paprotka *et al*., 2011; Pooggin, 2013; Raja *et al*., 2010; Wang *et al*., 2012).

Reduction in viral load in transgenic lines A-MM2 30, A-MM4 46, A-MM4 59, A-MM4 33 and C-MM8 25 as compared to control infected wild-type cv.60444 was also recorded, despite variations between plants within a selected line. Notably, in transgenic lines MM2 41, 52, 53 and 54, and A-MM4 transgenic lines (A-MM4 33, A-MM4 46, A-MM4 59, A-MM4 68 and A-MM4 79) a significant decrease in virus load was detected at 365 dpi which accompanied recovery from symptoms. Challenging of these promising lines will be repeated in a larger trial. Cassava geminivirus resistance engineering reports by Vanderschuren *et al.* and (2007) and Zhang *et al*. (2005) reported on transient ACMV replication assays in leaf discs. Virus in infected leaves was detected using DNA blotting and not qPCR. However while in this study we measured virus levels using qPCR, it is not possible to compare levels of virus replication between our study and theirs. Using semi-quantitative PCR, Vanderschuren *et al*. (2009) detected no virus in transgenic cassava expressing ACMV AC1 hairpin construct.

Transgenic line A-MM2 54 resembled cassava geminivirus tolerant TME3 landrace infection profile in terms delayed symptom development and viral load accumulation at both 12 and 32 dpi. A decrease in viral load similar to the tolerant TME3 control was observed at 67 dpi in A-MM4 33 and A-MM4 59. A decrease in viral load and reduction in symptoms was associated with the recovery phenotype in *Pepper gold mosaic virus* infected pepper plants (Carrillo-Tripp *et al*., 2007) and cassava (Vanitharani *et al*., 2003). The very mild symptoms recorded in C-MM6 10 and C-MM6 11 at all 3 dpi resembled symptoms recorded for TME3, however viral load result did not show a profile similar to TME3. These lines deviated from the generally accepted positive correlation that exists between symptoms and viral load (Chellappan, Vanitharani, *et al*., 2004; Elegba *et al*., 2013). Plants showing mildly infected shoots but with very high *Cassava brown streak virus* (CBSV) titers were reported in Uganda field evaluation

trials of cassava varieties (Kaweesi *et al*., 2014). Because of the negative correlation between symptoms and viral load observed in NASE 1, TZ/130, AR40-6 and NDL06/132 cassava varieties, it was suggested that virus multiplication restriction and restriction of symptom expression were controlled by different mechanisms.

A positive correlation between a high symptom severity score and high viral load was recorded for A-MM4, C-MM6 and C-MM8 at all 3 dpi (12, 32 and 67 dpi). (**appendix F**). This suggests that an increase in symptoms results in higher viral loads. In C-MM6 infected transgenic lines, the Pearson's correlation test performed on viral load and sss gave coefficients of 0.79, 0.65 and 0.70 at 12 dpi, 32 dpi and 67 dpi, respectively.In A-MM4 transgenc lines correlation coefficient for symptom severity and viral load were 0.65, 0.72 and 0.53 at 12, 32 and 67 dpi, respectively. In C-MM8 transgenic lines, coefficients of 0.67, 0.81 and 0.64 were obtained at 12, 32 and 67 dpi, respectively. In A-MM2, a very weak correlation efficient of 0.38, 0.03 and 0.22 at 12, 32 and 67 dpi was calculated, respectively. No significant level of viral knockdown was observed in most of virus challenged transgenic lines was observed at 12, 32 and 67 dpi Instead level of virus replication was generally variable and high between plants. Virus replication was also detectable in geminivirus-challenged tolerant TME3 controls. However, ACMV and SACMV tolerant A-MM2 and A-MM4 cassava plants showed a decrease or recovery from symptoms at 67 or 365 dpi, with a lower detectable virus replication compared to wild-type non-transgenic cv.60444 may be considered in further repeat greenhouse trials.

According to Koochakpour & Fakheri (2014) and Lin *et al*. (2007), RNAi-mediated resistance is less effective against DNA viruses than RNA viruses and engineering complete resistance against DNA viruses is rarely obtained. Engineering of CBV resistant transgenic cv.60444 cassava expressing sense, antisense or hairpin RNA silencing constructs has been reported by only a few research groups such as the Plant Biotechnology Group at ETH Zurich and the Donald Danforth Plant Centre (Chellappan *et al*., 2004; Taylor *et al*., 2012; Vanderschuren *et al*., 2007, 2009; Zhang *et al*., 2005). Several vectors have been developed for the efficient expression and processing of dsRNA hairpins in plants (Helliwell & Waterhouse, 2003; Wesley *et al*., 2001). Linking the sense and antisense arms by an intron has been shown to be the most efficient in plants (Smith *et al*., 2000; Wesley *et al.*, 2001), however, although intron-containing IR

constructs can stabilize some silencing constructs and efficiently induce RNA silencing, we found in early studies that the Pdk intron did not stabilize SACMV silencing constructs (unpublished data). In the construction of the mismatch contiguous IRs (MM2 and MM4 lines) tested in this study, the intention was to reduce the size of the transgene and create mismatch IRs without introns (Taylor *et al*., 2012b), and the two arms were joined by a small spacer loop which does stabilize the construct (Smith *et al*., 2000). Smith *et al*. showed that a 63 bp hpRNA with a spacer loop demonstrated 69% PTGS efficiency. We conclude that it is highly probable that our constructs were stable, as SACMV BC1 (MM4) was expressed in *N. benthamiana* (Taylor *et al*., 2012), but this may not hold true for cassava. In comparison with smaller hpRNAs (100-200 bp), our constructs were much longer, but did not detrimentally affect PTGS in *N. benthamiana*. Using hpRNA constructs containing sense/anti-sense arms ranging from 98 to 853 nt gave efficient silencing in a wide range of plant species (Wesley *et al*., 2001). The non-mismatch IR constructs (with an intron) (MM6 and MM8 lines), while demonstrating some level of tolerance compared to wild-type non-transgenic controls, also did not confer high levels of resistance, and therefore we cannot unequivocally attribute the lack of resistance to mismatches in the sense arm of the IRs.

The mismatch and non-mismatch ACMV constructs tested in this study comprised a contiguous set of four sequence stretches derived from regions of the AC1, AC2, AC3 and AC4 ORFs. It was expected that targeting these regions would deliver efficient silencing. However both constructs delivered only mild tolerance in some lines. In a transient study in *N. benthamiana*, three hairpin RNAi constructs were tested against *Cotton leaf curl Multan virus* (CLCuMV) (Mubin *et al*., 2011). However, only the construct targeting the overlapping Rep/AC1, TrAP /AC2 and Ren/AC3 was able to prevent systemic movement. The other two constructs, (i) targeting Rep and C4 genes and (ii) targeting the intergenic region, only managed to reduce viral replication. Based on the observed results they suggested that targeting the TrAP gene offers the most efficient resistance. They also concluded that that not all virus-derived sequences will result in efficient resistance against begomoviruses. In our study we targeted the 5'-terminal sequence of *Rep* and only the 3'-terminus of *TrAP*, unlike Mubin *et al*., (2011) who targeted the entire *TrAP* gene. Small interfering RNA studies have shown that siRNAs target several ORFs of geminviruses, and in *Arabidopsis* infected with *Cabbage leaf curl virus,* siRNAs covered the

entire viral genome sequence in both polarities (Aregger *et al*., 2012). In deep sequencing of the sRNAome cassava landraces T200 and TME3 (unpublished data), siRNAs were also shown to cover almost the entire genome of SACMV in both susceptible T200 and tolerant TME3 landraces, however siRNA populations derived from AC1/AC4 and AC2/AC3 were weakly represented in comparison siRNA derived from AC1, AC2 and AV1 regions. A study by Chellappan *et al*. (2004), siRNA derived from the *Rep* C-terminal, which overlaps with the 5'-terminal of *TrAP*, accumulated at high levels in ACMV-CM recovery *N. benthamiana* and cassava plants. In the same study, similar siRNA populations derived from the *Rep/TrAP* overlapping region were seen in *N. benthamiana* and cassava recovery plants infected with *Sri Lankan cassava mosaic virus* (SLCMV). While the natural accumulation of siRNAs derived from the *Rep* C-terminal/*TrAp* N-terminal overlap was found in ACMV-CM recovered plants (Chellappan *et al.*, 2004), plants infected with three distinct CBV species, EACMCV; isolate from Cameroon, EACMV-[UG] and *Indian cassava mosaic virus* (ICMV; isolate from India), did not result in a recovery phenotype or high accumulation of *Rep/TrAP*-derived siRNA. Instead in EACMCV infected plants, high siRNA populations were derived from the DNA-B component, especially off the C terminal of BC1 cell-to-cell movement protein (MP).

In our study, in addition to the DNA-A component-derived constructs, the 221 bp region within BC1 movement protein (MP) (in the middle of the C and N terminus) of SACMV was targeted as this has not been evaluated widely as a target gene in GM crops, including in a natural host such as cassava. We also speculated that a *Rep* transgene, such an essential multifunctional geminivirus protein (Hanley-Bowdoin *et al*., 2013), could be under great silencing or suppression pressure from incoming virus, and BC1, under less constraints, may offer tolerance rather than complete resistance. The geminivirus *Tomato golden mosaic virus* MP has been shown to have a deleterious effect on systemic infection of ACMV DNA in *Nicotiana benthamiana* plants (Von Arnim and Stanley, 1992). Furthermore, SACMV BC1 (MM4) mismatch IR constructs were expressed in the model test plant *N. benthamiana* and shown to produce siRNAs which resulted in a reduction in viral BC1 transcript levels and reduced symptoms upon SACMV infection (Taylor *et al.*, 2012). However no significant decrease in viral load was observed in cassava in this study up to 67 dpi. Chellappan *et al*. (2004) suggested that efficiency of PTGS may be dependent on geminivirus-cassava variety/landrace interactions.

Whether the siRNAs from the mismatch sense arm had any specific role in interfering with the SACMV or ACMV silencing specifically in the natural host cassava at 365 dpi needs to be explored further.

Only seven lines were screened in this study, and more lines need to be evaluated. However, most unexpectedly, some of the BC1 MM4 lines that were transferred to the greenhouse recovered from symptoms and had no detectable virus titers (**fig4.9b**). Whether the higher temperatures and light intensity in the greenhouse contributed to more efficient movement of the systemic silencing siRNAs is not clear, but this recovery was also observed in some MM2 lines. High light intensity and temperature showed the opposite effect in *N. benthamiana* plants in transient agroinfiltration experiments with several cassava begomoviruses (Patil & Fauquet, 2014). However this study was conducted in a highly susceptible experimental host, and in transient assays, which may not reflect the situation *in planta* or in the natural perennial host cassava over long periods of time (Romon *et al*., 2013). The observation of recovery of transgenics has been observed in several studies (Carrillo-Tripp *et al*., 2007; Ingelbrecht *et al*., 1999; Jovel & Walker, 2007) as well as in some non-transgenic cassava varieties in the field (Gasura *et al*., 2008; Gasura & Mukasa, 2010). However, since infected non-transgenic TME3 and cv.60444 did not recover at high temperatures and light intensity, we can probably rule out endogenous RNA silencing (Patil & Fauquet, 2014) as a possible cause, and conclude that the expression of the transgene is likely playing a role in recovery.

Interestingly, in a small RNA deep sequencing (Illumina Platform) experiment carried out in our laboratory (unpublished), siRNAs (21-24 nt) in both polarity were found to target SACMV, in infected T200 non-transgenic cassava, along the length of DNA A and B components, and in the intergenic region, but the 3'AC1/5' *TrAP* ORF regions had the highest hits. Our *Rep* targets were focused at the 5'AC1/AC4 and 3'AC2/5'AC3 overlapping DNA sequences, while in the Vanderschuren *et al*. (2009) study, a short 3'end (1690-1844) AC1 155 bp hairpin was used for transformation. Nonetheless, it is not possible to predict for certainty, without testing with site-targeted probes for our specific transgenic constructs, which populations of siRNAs will be generated, and at what level.

The lack of efficient silencing in MM4 (mismatch SACMV-transgenic cv.60444) at 12, 32 and 67 dpi was unexpected. A mismatch IR construct derived from SACMV AC1 alone induced PTGS more efficiently compared to a non-mismatch IR construct in a *N. benthamiana* callus system (Taylor, 2009). In A-MM2 transgenic lines, ACMV AC1/4:AC2/3 RNAi region was undetectable using RT-PCR even though integration of this region had been previously confirmed by PCR and Southern blot. Results observed suggest weak expression of the ACMV AC1/4:AC2/3 derived sequence or even low transcript accumulation levels due to rapid processing of dsRNA into siRNA molecules leading to transcript decay. Dalakouras & Tzanopoulou (2011) used a cytoplasmic reoviral dsRNA binding protein to identify possible transcript decay in *Cucumber mosaic virus* (CMV) CP expressing *N. benthamiana* lines. The protein prevented Dicer-mediated processing of dsRNA in CMV susceptible lines previously identified as hairpin RNA transcription deficient. It is unlikely that the lack of transcript amplification is a result of transcriptional inactivation triggered by multiple transgene copies (Schubert *et al*., 2004). All seven A-MM2 lines had a single RNAi copy, except A-MM2 33 which had a single copy and additional a truncated copy. In transgenic lines A-MM4 and C-MM6 and C-MM8 virus-derived transcripts were detected by RT-PCR, however lines showed only mild virus tolerantce. In other CMV CP expressing *N. Benthamiana*, high transcript and siRNA accumulation was observed (Dalakouras & Tzanopoulou, 2011). However these lines were still presented with a CMV susceptible phenotype. They concluded that transcription of hairpin derived sequences does not always lead to efficient RNA silencing; production of high quality effective siRNA is more important than siRNA quantity (Dalakouras & Tzanopoulou, 2011).

Other factors can influence the expression level of hairpins such as promoter strength, hairpin length and structure, introns and their distance to the promoter (Rose, 2004). Low transcripts levels can also occur due to "transcriptional interference" by an upstream promoter on a downstream promoter leading to a decreased promoter activity and hence low transcript levels (Bhullar *et al.*, 2009). The 35S promoters used in the vectors in this study are widely used and are thought not to play a factor herein. Low RT-PCR detection of the BC1 mutated-arm of MM4hp was seen in A-MM4 transgenic lines. The position of the target gene within the T-DNA could possibly explain the observed RT-PCR results. Gene position effects on transcript

detection levels was reported by Breyne *et al.* (1992). By inserting *gusA* reporter gene in the middle of the T-DNA, Breyne *et al.*, (1992) found that it was expressed in very low levels unlike when placing it towards the right border which resulted in four times higher expression levels. This could explain the lower RT-PCR detection of the mutated BC1 hairpin arm.

While transcription of the SACMV and ACMV transgenes was detected by RT-PCR, it is possible that the mismatch transcripts were not processed efficiently due to mismatches in the sense arm, and further processed by the RISC complex. However this would not explain why the non-mismatch constructs would not have been efficiently processed. Again, it is possible that temperature and light intensity in the growth chamber (60 000-80 000 lux) might have been too low for optimal spread of the silencing signal, if indeed recovery (mentioned earlier) was a result of higher temperatures and light intensity in the greenhouse after the plants were moved. It is becoming evident from several recent studies (Chellappan, Vanitharani, Ogbe, *et al.*, 2005; Ghoshal & Sanfaçon, 2014; Patil & Fauquet, 2014; Szittya *et al*., 2003) that environmental factors can play a critical role in RNA silencing expression.

Another consideration is the dosage of geminivirus administered in the resistance trials. Previous work by Zhang *et al*. (2005) showed that geminivirus resistance can be broken in transgenic cassava when the ACMV load (bombardment) is increased. In a later study by Vanderschuren *et al*. (2009), they demonstrated that increasing the viral pressure from 350ng to 700 ng increased the infection rate of line dsAC1-105 from 22.2 to 90%. This infection rate was similar to wild type cv.60444 infection rate (84%). In our study, we used agro-inoculation of SACMV or ACMV to challenge transgenic lines, wild type cv.60444 and wild type TME3, and average infection rates of between 90-100 % were achieved. Agro-infection with ACMV of resistant cassava lines performed the same as with biolistic bombardment, but the infection rate of transgenics remained significantly lower compared with wild-type. While in our study we use *Agrobacterium* containing the infectious DNA A and B clones at an OD of ~1.8-2, as this proved effective in our hands (Pierce, 2013), it is possible that this represents a high dosage which was sufficient, along with other factors, to break the RNAi effect.

Agro-inoculation of plants with infectious virus clones introduces higher virus pressure and is more infection efficient than bombardment and possibly natural infection (Ariyo *et al.*, 2006; Bi, *et al*., 2010; Kheyr-Pour *et al*., 1994). The lack of attenuated symptoms and viral load at the earlier time points (12, 32 and 67 dpi) post agroinoculation, in this study, could be due to a high initial virus inoculum pressure, which in some lines was overcome leading to tolerance later on.Kheyr-Pour *et al*. (1994) observed that, under natural field conditions, using natural vector-mediated virus transmission, wild *Lycopersicon* species are usually resistant to T*omato yellow leaf curl virus* (TYLCV). However this resistant phenotype was lost following agro-inoculation with TYLCV. It was believed that the high virus pressure presented by agro-inoculation was the main contributor for the break in resistance. These findings suggest that under field trials, transgenic lines showing tolerance could present with a more improved tolerance or resistance phenotype. Dosage responses in transgenic lines are also not uniform, as in the ACMV-cassava study Vanderschuren *et al*. (2009) three lines (dsAC1-2; dsAC1-101 and dsAC1-152) showed no infectivity by agro-inoculation and biolistics. Together with several other geminivirus studies, such as TYLCV resistance in tomato (Fuentes *et al*., 2006), high loads of hairpin-derived small RNAs correlated to high resistance. Contrary to this, in other studies a negative correlation between siRNA accumulation and resistance has also been shown to exist (Carrillo-Tripp *et al.*, 2007; Gómez *et al*., 2009; Lucioli *et al*., 2003). In some lines in the ACMV-cassava dosage experiment (Vanderschuren *et al*., 2009) gave low (almost undetectable) to medium accumulation of siRNAs. TME3 has to date been considered a CMD resistant landrace (Bi *et al*., 2010), however in our laboratory, infectivity studies showed clearly that this is a tolerant landrace (Allie *et al.*, 2014). In this study, TME3 was used as a virus-infection control, and was confirmed as being CMD tolerant, due to lower symptom severity while supporting virus replication. In our study we could successfully infect TME3 using agro-inoculation with infectious virus clones and symptoms were seen in up to 70% of infected TME3 plants. Real time qPCR results also confirmed that virus replication was supported in TME3 which demonstrated similar virus titers to some transgenic lines. We were able to report faint mosaic symptoms as well as stunted growth for TME3 in some of the virus challenge trials.

In our study, 5-6 week old transgenic plantlets were agro-inoculated with virus this was based on the idea that farmers transplant 2-3 node cassava stem cuttings at a very early developmental

stage. Vanderschuren *et al.* (2009) performed green-house resistance screening experiments on 12 week old ACMV AC1 expressing cassava plantlets, and demonstrated resistance. Plant developmental stage has been shown to direct affect resistance or susceptible phenotype displayed in transgenic plant studies (Jan *et al*., 2000; Law *et al*., 1989; Tenllado & Diaz-Ruiz, 1999; Tennant *et al.*, 2001; Vassilakos *et al*., 2008). In transgenic squash lines expressing CP of *Squash mosaic virus* (SqMV) the resistance phenotype was only observed in when lines were inoculated with SqMV at a later developmental stage (31-45 days post germination) (Jan *et al*., 2000). Lines were susceptible to SqMV when inoculated at early developmental stage (17 days post germination). Transgenic papaya line expressing CP of *Papaya ringspot virus* (PRSV) was susceptible to PRSV when inoculated at 6 weeks after germination however when inoculated at 16 weeks after germination transgenic line showed resistance to PSRV (Tennant *et al*., 2001). Jan *et al*. (2000) suggested that PTGS induction is timing dependent and more active at later developmental stages. Kalantidis *et al*. (2002) not only investigated the effects that temperature has on resistance but also the influence the plant developmental stage has on siRNA mediated. They reported that at 30 days post germination (dpg) tobacco transgenic plants expressing a 883bp *Cucumber mosaic virus* (CMV) gene fragment accumulated siRNA at higher levels than at 20dpg. This positive correlation between increase in resistance and increase in plant age was also demonstrated in transgenic papaya expressing coat protein of papaya ringspot virus (PRSV) HA from Hawaii (Tennant *et al.*, 2001). Resistance to PRSV HA was observed at older developmental stages. Resistance to other PRSV isolates was also seen at older developmental stages. Similar results were reported in tobacco plant expressing a replicase gene of *Tobacco rattle virus* (TRV). Elevated TRV tolerance levels were observed in older (4-5 leaf stage) transgenic tobacco plants expressing TRV *replicase* gene than in younger (2-leaf stage) transgenic plants (Vassilakos *et al*., 2008). In experiments involving transgenic tobacco expressing *Pepper mild mottle virus* (PMMoV), resistance against PMMoV was achieved in older plants (30-35 dpg) than in younger plants (15-20 dpg) (Tenllado & Diaz-Ruiz, 1999).

To establish the relationship between resistance and transgene-siRNA production levels, Northern blots for siRNA detection were performed. However unlike in Chellappan et al. (2004) and Patil & Fauquet (2014) no positive correlation in siRNA accumulation levels and resistance was observed. This was clearly demonstrated in A-MM2 and C-MM6 lines, which accumulated

high levels of ACMV AC1/4:AC2/3-derived siRNA fragments. Low levels of SACMV BC1-derived siRNA molecules were detected in SACMV BC1 transgenic lines (A-MM4 and C-MM8). Surprisingly, ACMV AC1/4:AC2/3-derived siRNA fragments were detected in untransformed cv.60444 and TME3 also. In a NGS small RNA study in our laboratory, in mock-inoculated T200. Low number of CBV-derived siRNA molecules were identified (unpublished), and this was attributed to possible integration of small viral fragments in the cassava genome. It is not unknown to find integrated or non-integrated viral-derived sequences from plant EST libraries or more recently virus metagenomics studies. However band intensities shown in **fig.4.12** demonstrate a high number of siRNAs and the reason for this is unknown. The probes used in this study were specific to SACMV and ACMV, but it is possible that shearing of the transgene-derived probes may have led to non-specific RNAs. However, CBSV-derived siRNA probes were derived from chemical random shearing of the transgene and did not give false positives in cassava (Ogwok *et al*., 2012). According to López *et al*. (2010) and Dalakouras & Tzanopoulou (2011) high transcription and siRNA accumulation does not necessarily lead to efficient silencing and resistance. Detection of ACMV AC1/AC4:AC2/3-derived siRNA molecules in untransformed healthy cv.60444 also suggest integrated ACMV DNA-A sequences in the cv.60444 genome (Harper *et al.*, 2002; Hull *et al*., 2000). The tolerant phenotype observed at 67 dpi in most transgenic lines could be due to primary siRNA biogenesis as a result of efficient processing of constitutive/early transgene-derived dsRNA expression (Aregger *et al*., 2012). This tolerant phenotype at 67 dpi may be more time induction dependant rather than level of accumulation dependent. The recovery phenotype observed in A-MM2 and A-MM4 at 365 dpi could be due to efficient late developmental stage transgene-derived siRNA biogenesis of production (discussed above). siRNA detection was however not performed at 365 dpi. In C-MM8 transgenic lines transgene-derived siRNA were not detected instead the SACMV-BC1-derived probe hybridized to higher molecular weight RNA. C-MM8 siRNA detection blots suggest low MM8 RNAi transcript levels, which is consistent with **fig 4.11d,** MM8 RNAi RT-PCR results. Low transcript levels generally results in low siRNA molecule accumulation (Dalakouras & Tzanopoulou, 2011). Alternatively, low siRNA molecule detection could be due to sequestering and trapping of siRNA molecules by the higher molecular weight RNA.

As previously mentioned, temperature-dependent effects on virus resistance levels have been demonstrated in transgenic plants studies (Bonfim *et al*., 2007; Chellappan *et al*., 2005; Ntui *et al*., 2014; Romon *et al*., 2013; Szittya *et al*., 2003; Vassilakos, 2012). Temperature is therefore an important factor to consider in future resistance screening trials. Chellappan *et al*. (2005) challenged tobacco plants with ACMV-[CM] and observed symptom severity at three temperatures. Symptoms of tobacco plants infected with ACMV-[CM] were found to be greater at 25°C than at 30°C. And at temperatures between 25°C and 30°C, they also reported moderate symptoms. Chellappan *et al*. (2005) infected cassava with ACMV-[CM] and monitored siRNA accumulation at 25°C, between 25-30°C and at 30°C. They observed a rise in siRNA accumulation with an increase in temperature. Work by Kalantidis *et al*. (2002) and Szittya *et al*. (2003) confirmed this positive correlation. Chellappan *et al*. (2005) concluded that slight changes in temperature can have an effect on PTGS. They suggested that this effect was as result of higher siRNA-derived plant defense activity or reduced PTGS suppressor activity at higher temperatures. However according to Schwind *et al*. (2009) at 21°C and 31°C there is no difference in siRNA accumulation levels. Differential siRNA accumulation was only observed at 15°C and 24°C. Further testing of transgenic lines at a range of temperatures may provide different, but while improved virus resistance may be obtained, this has serious implications for field implementation of the RNA silencing strategy and transgenic crops.

In conclusion, a large number of transgenic lines screened presented mild ACMV or SACMV tolerance at 67 dpi, with viral load and symptom phenotype more similar to non-transgenic tolerant landrace TME3, but with clearly lower than susceptible non-transgenic cv.60444. Some of the CMM6 and CMM8 lines that showed reduced virus load and symptom delay or reduction have been selected for further screening, but we could not establish a positive correlation between virus load and symptoms in many of the lines, and more in depth siRNA and transgene expression studies are required, as well as the relationship between endogenous gene silencing, transgene silencing and environmental factors. What was of considerable interest was the recovery of some A-MM2 and A-MM4 lines after several months in the greenhouse at higher temperature and light intensities. At 365 dpi, a reduction in ACMV viral load was recorded in four A-MM2 infected transgenic lines. These lines presented with lower symptoms and reduced viral load relative to susceptible cv.60444. No virus was detected in five A-MM4 transgenic lines

at 365 dpi. These five A-MM4 transgenic lines presented a full recovery phenotype, and repeat trials are planned in future. Tolerance and recovery may be desirable or useful in come field cultivation situations, but often can be unpredictable and can be overcome in mixed infections. Further transgenic lines need to be screened for resistance under different light and temperature regimes. While CMD-transgenic cassava expressing virus-targeted RNA silencing has been achieved in some studies under laboratory and greenhouse conditions, and is highly desirable, there remains many conflicting reports in the literature on the stability and efficacy of RNA silencing, and more research is needed if this technology is to be adopted, not only for cassava, but for other field crops.

CHAPTER 5: SUMMARY AND CONCLUSIONS

In the current study, four mismatched (mutated sense-arm) RNA silencing hairpin constructs and four non-mismatched (Gateway technology) RNA silencing hairpin constructs were created. These were designed to target SACMV BC1 and several ACMV genome regions simultaneously, namely the Rep (AC1), Ren (AC3) and the host gene silencing suppressor AC4 and AC2 (TrAP). Both design methods targeting the selected regions required numerous digest, ligation and cloning steps, however lower construction costs were associated with mutated sense-arm constructs compared with Gateway technology constructs as the conventional *E.coli* DH5α strainand standard plant transformation pCAMBIA 1305.1 vector, available in the lab, were used. Gateway constructs required the less conventional *ccdB* tolerant *E.coli* strain, *DB3.1*. pHellsgate 8 vector and *DB3.1* cells had to be sourced. The reduced costs associated with mutated sense-arm construct technology makes this method favourable especially for research occurring in developing countries. Another limitation to the Gateway technology was the lengthy screening of clones for correct IR fragment orientation.

Cassava cv.60444 and T200 FEC were successfully transformed using *Agrobacterium*-mediated transformation. High FEC transformation efficiencies in these processes, comparable with those reported by Taylor *et al*. (2012) and Bull *et al*. (2009) were obtained. Transformation and regeneration of cassava is genotype dependent and few cultivars or landraces have been successfully transformed and even far less have been transformed with virus-derived sequences (Hankoua *et al*., 2005; Nyaboga *et al*., 2013; Raemakers *et al*., 2001; Zainuddin *et al*., 2012). In a study by Nyaboga *et al*. (2013) three local farmer-preferred cultivars (Serere, Kibandameno and Ebwanateraka) were successfully transformed and regenerated, although not all somatic embryos produced plantlets, and L-tyrosine was required to generate FEC. In this study, unexpected high transformation and regeneration results were obtained for the SA landrace T200. Successfully transformed cv.60444 and T200 were achieved for subsequent virus challenging.

In order to further understand the molecular processes in our transgenic lines, further studies investigating the processing and action of the transgene-derived siRNAs are required.

Information on transgene insertion sites would also prove informative. Levels of resistance to geminivirus diseases in crop plants must be durable under agronomic growth conditions in the field. Although the transformation efficiency in cassava has improved (Bull *et al*., 2009), it is still estimated that at least 100 transformation events need to be established, and from that an estimated 30 independent transgenic lines have to be evaluated. Cassava transformation is a labour intensive process however platforms established by Bull *et al*. (2009) and Taylor *et al.* (2012) are aimed at high-throughput production and screening of transgenic lines. ACMV and SACMV transgenic lines showing milder symptoms and relatively reduced viral load compared to control infected wild-type cv.60444, but similar to tolerant TME3. An enhanced recovery phenotype was observed in certain A-MM2 and A-MM4 transgenic lines than control infected wild-type cv.60444. Currently more lines are being evaluated in our laboratory, under greenhouse controlled growth conditions, and new constructs are being developed, but even if these yield promising results, extensive natural field conditions need to be stringently tested over several generations before improved lines can be released for cultivation. In the framework of the recovery of MM2 and MM4 cassava lines in the greenhouse over longer periods of fluctuating temperature and light effects, factors such as plant developmental age, temperature and infectivity method could potentially have effects on the behaviour of resistant plants in the field.While tuber yields were not measured in these trials as these were restricted pot studies, this should also be performed in future experiments. Furthermore, more in depth molecular characterization of siRNA production, transgene expression and natural RNA silencing interactions in the mismatched hpRNA transformed transgenic plants needs to be performed. As a novel approach, more information needs to be gathered in regard to potential off targets of this mutation technology, and more in depth comparisons with analogous non-mismatched counterparts,

Implementation of the by Bull *et al*. (2009) cassava FEC induction and transformation protocol enabled successful transformation of model cassava cultivar cv.60444 and South African landrace T200 with virus-derived sequences. The objective of the Bull *et al.* research was to distribute detailed cassava transformation information to allow establishment and implementation of cassava genetic engineering technology in developing countries. Currently, few cassava virus resistance transformation reports have emerged directly from the African

continent. The Virus Resistant Cassava for Africa (VIRCA) initiative established in Kenya in collaboration with several institutions is such an example (Taylor *et al*., 2012). In the last 5 years preliminary cassava transformation research on the African continent was with empty plant transformation vectors. Not only do we report successful high transformation efficienies, we report successful cassava transformation with virus-derived sequences.

Transgenic lines showing higher SACMV and ACMV tolerance compared with wild-type cv.60444 have been identified. Some of these lines further showed a recovery phenotype, associated with reduced CMD symptoms and in certain transgenic lines absence of virus titre, compared to wild type cv.60444 plants when evaluated a year after infection. While these transgenic lines displayed resistance, it is not really understood why this was not evident in the earlier sample period (up to 67 dpi). Also the failure to achieve complete resistance at least in some lines needs to be investigated. Unexpectedly, in some of our data, no positive correlation was observed between symptom expression and viral load. This suggests an existing underlying mechanism that supports some virus replication while simultaneously reducing symptom expression. Tolerance and recovery in non-transgenic plants is not well understood, but has been reported to be, in part, associated with RNA silencing and high production of siRNAs targeting the virus (Chellappan *et al*., 2004; Ntui *et al*., 2015; Ogwok *et al*., 2012). Plant recovery from viral induced symptoms is phenotypically manifested by a progressive reduction in symptoms severity or appearance of symptomless leaves at the apices, and in some cases, a key genotypic indicator of tolerance is the RNA silencing defense mechanism (Rodríguez-Negrete *et al*., 2009). Tolerance to a virus is the ability to minimize viral-induced disease severity, while resistance is the ability to limit the parasite burden to non-detectable levels of virus replication. TME3 is a known tolerant cassava landrace (Allie *et al*., 2014) also displaying persistent ACMV and SACMV replication in this study, but demonstrating lower symptoms and viral loads, comparable to some transgenic lines in this study. More recently, high throughput profiling of transcriptomes either covering partial or complete recovery processes in DNA and RNA-viruses (Allie *et al*., 2014; Góngora-Castillo *et al*., 2012) are available, providing new insights on the molecular interconnections between tolerance and recovery.

Currently, available research has revealed complexities that were previously not known to exist in the field of RNA silencing. A large majority of available data on the use of RNA silencing technology in cassava for virus resistance report difference resistance levels and tolerance, complete resistance has been reported by the ETH research group. Substantial research on host endogenous mechanisms and pathways that regulate RNA silencing, virus encoded RNA silencing suppressors and abiotic factors are still required in the field of RNA silencing and genetics involved in resistance, especially against DNA viruses. This will then advance research in the field of the cassava genetic engineering for resistance against cassava infecting geminiviruses.

REFERENCES

Abel, P. P., Nelson, R. S., De, B., Hoffmann, N., Rogers, S. G., Fraley, R. T., & Beachy, R. N. (1986). Delay of disease development in transgenic plants that express the tobacco mosaic virus coat protein gene. *Science (New York, N.Y.)*, *232*(4751), 738–743.

Adams, M. J., King, a M. Q., & Carstens, E. B. (2013). Ratification vote on taxonomic proposals to the International Committee on Taxonomy of Viruses (2013). *Archives of Virology*, *158*(9), 2023–30. http://doi.org/10.1007/s00705-013-1688-5

Adenle, A. a, Aworh, O. C., Akromah, R., & Parayil, G. (2012). Developing GM super cassava for improved health and food security: future challenges in Africa. *Agriculture & Food Security*, *1*(11), 2–15. http://doi.org/10.1186/2048-7010-1-11

Agrawal, N., Dasaradhi, P., Mohmmed, A., Malhotra, P., Bhatnagar, R. K., & Mukherjee, S. K. (2003). RNA interference: biology, mechanism, and applications. *Microbiology and Molecular Biology Reviews*, *67*(4), 657. http://doi.org/10.1128/MMBR.67.4.657

Akbergenov, R., Si-Ammour, A., Blevins, T., Amin, I., Kutter, C., Vanderschuren, H., … Pooggin, M. M. (2006). Molecular characterization of geminivirus-derived small RNAs in different plant species. *Nucleic Acids Research*, *34*(2), 462–71. http://doi.org/10.1093/nar/gkj447

Ali, I., Amin, I., Briddon, R. W., & Mansoor, S. (2013). Artificial microRNA-mediated resistance against the monopartite begomovirus Cotton leaf curl Burewala virus. *Virology Journal*, *10*(1), 231. http://doi.org/10.1186/1743-422X-10-231

Allie, F., Pierce, E. J., Okoniewski, M. J., & Rey, C. (2014). Transcriptional analysis of South African cassava mosaic virus -infected susceptible and tolerant landraces of cassava highlights differences in resistance , basal defense and cell wall associated genes during infection. *BMC Genomics*, *15*, 1–30.

Amin, I., Hussain, K., Akbergenov, R., Yadav, J. S., Qazi, J., Mansoor, S., … Briddon, R. W. (2011). Suppressors of RNA Silencing Encoded by the Components of the Cotton Leaf Curl Begomovirus-BetaSatellite Complex. *Molecular Plant-Microbe Interactions : MPMI*, *24*(8), 973–983.

Anand, A., Zhou, T., Trick, H. N., Gill, B. S., Bockus, W. W., & Muthukrishnan, S. (2003). Greenhouse and field testing of transgenic wheat plants stably expressing genes for thaumatin-like protein, chitinase and glucanase against Fusarium graminearum. *Journal of Experimental Botany*, *54*(384), 1101–1111. http://doi.org/10.1093/jxb/erg110

Anandalakshmi, R. (2000). A Calmodulin-Related Protein That Suppresses Posttranscriptional Gene Silencing in Plants. *Science*, *290*(5489), 142–144. http://doi.org/10.1126/science.290.5489.142

Anandalakshmi, R., Pruss, G. J., Ge, X., Marathe, R., Mallory, a C., Smith, T. H., & Vance, V. B. (1998). A viral suppressor of gene silencing in plants. *Proceedings of the National Academy of Sciences of the United States of America*, *95*(22), 13079–13084. http://doi.org/10.1073/pnas.95.22.13079

Arbuthnot, P., Weinberg, M. S., Rey, M. E. C., Harmse, J., & Taylor, S. H. (2010). Use of double stranded RNA hairpin duplexes in gene silencing.

Aregger, M., Borah, B. K., Seguin, J., Rajeswaran, R., Gubaeva, E. G., Zvereva, A. S., … Pooggin, M. M. (2012). Primary and secondary siRNAs in geminivirus-induced gene silencing. *PLoS Pathogens*, *8*(9), e1002941. http://doi.org/10.1371/journal.ppat.1002941

Ariyo, O. a, Atiri, G. I., Dixon, a G. O., & Winter, S. (2006). The use of biolistic inoculation of cassava mosaic begomoviruses in screening cassava for resistance to cassava mosaic disease. *Journal of Virological Methods*, *137*(1), 43–50. http://doi.org/10.1016/j.jviromet.2006.05.031

Bai, S., Kasai, A., Yamada, K., Li, T., & Harada, T. (2011). A mobile signal transported over a long distance induces systemic transcriptional gene silencing in a grafted partner. *Journal of Experimental Botany*, *62*, 4561–4570. http://doi.org/10.1093/jxb/err163

Bailey, R., Willoughby, R., & Grzywacz, D. (2014). On Trial : Agricultural Biotechnology in Africa. *Energy, Environment and Resources*, (July), 1–26.

Bao, S., & Cagan, R. (2006). Fast cloning inverted repeats for RNA interference. *Method*, *12*, 2020–2024. http://doi.org/10.1261/rna.258406.in

Barrangou, R., Fremaux, C., Deveau, H., Richards, M., Boyaval, P., Moineau, S., … Horvath, P. (2007). CRISPR provides acquired resistance against viruses in prokaryotes. *Science (New York, N.Y.)*, *315*(5819), 1709–1712. http://doi.org/10.1126/science.1138140

Bartel, D. P., Lee, R., & Feinbaum, R. (2004). MicroRNAs : Genomics , Biogenesis , Mechanism , and Function Genomics : The miRNA Genes. *Cell*, *116*, 281–297.

Bartlett, J. G., Smedley, M. a, & Harwood, W. a. (2014). Analysis of T-DNA/Host-Plant DNA Junction Sequences in Single-Copy Transgenic Barley Lines. *Biology*, *3*, 39–55. http://doi.org/10.3390/biology3010039

Beachy, R. N., Loesch-fries, S., & Turner, N. E. (1990). Coat protein-mediated resistance against virus infection. *Annu. Rev. Phytopathol.*, *28*, 451–74.

Bernstein, E., Caudy, A. A., Hammond, S. M., & Hannon, G. J. (2001). Role for a bidentate ribonuclease in the initiation step of RNA interference. *Nature*, *409*(6818), 363–6. http://doi.org/10.1038/35053110

Berrie, L. C., Rey, M. E. C., Palmer, K. E., & Rybicki, E. P. (1998). Molecular characterisation of a distinct South African cassava infecting geminivirus. *Archives of Virology*, *143*(11), 2253–2260. Retrieved from http://www.springerlink.com/openurl.asp?genre=article&id=doi:10.1007/s007050050457

Berrie, L., Palmer, K., Rybicki, E., Hiyadat, S., Maxwell, D., & Rey, M. (1997). A new isolate of African cassava mosaic virus in South Africa. *African Journal of Root and Tuber Crops*, *2*, 49–52.

Berry, S. D., Fondong, V. N., Rey, C., Rogan, D., Fauquet, C. M., & Brown, J. K. (2004). (Homoptera: Aleyrodidae) Geographic Haplotypes Associated with Cassava Plants in Sub-Saharan Africa. *Annals of the Entomological Society of America*, *97*(4), 852–859. http://doi.org/10.1603/0013-8746(2004)097[0852:MEFFDB]2.0.CO;2

Berry, S., & Rey, M. E. C. (2001). Molecular evidence for diverse populations of cassava-infecting begomoviruses in southern Africa. *Archives of Virology*, *146*(9), 1795–1802. Retrieved from http://www.springerlink.com/openurl.asp?genre=article&id=doi:10.1007/s007050170065

Bhullar, S., Chakravarthy, S., Pental, D., & Burma, P. K. (2009). Analysis of promoter activity in transgenic plants by normalizing expression with a reference gene: Anomalies due to the influence of the test promoter on the reference promoter. *Journal of Biosciences*, *34*(6), 953–962. http://doi.org/10.1007/s12038-009-0109-0

Bi, H., Aileni, M., & Zhang, P. (2010). Evaluation of cassava varieties for cassava mosaic disease resistance jointly by agro-inoculation screening and molecular markers. *African Journal of Plant Science*, *4*(9), 330–338.

Bian, X.-Y., Rasheed, M. S., Seemanpillai, M. J., & Ali Rezaian, M. (2006). Analysis of silencing escape of tomato leaf curl virus: an evaluation of the role of DNA methylation. *Molecular Plant-Microbe Interactions : MPMI*, *19*(6), 614–24. http://doi.org/10.1094/MPMI-19-0614

Binns, A. N., & Thomashaw, M. F. (1988). Cell biology of AGROBACTERIUM infection and transformation of plants. *Annual Review of Microbiology*, *42*, 575–606.

Bisaro, D. M. (2006). Silencing suppression by geminivirus proteins. *Virology*, *344*(1), 158–68. http://doi.org/10.1016/j.virol.2005.09.041

Biswas, K. K., & Varma, a. (2001). Agroinoculation: a method of screening germplasm resistance to mungbean yellow mosaic geminivirus. *Indian Phytopathology. 2001;*, *54*(2), 240–245. Retrieved from <img src=http://library.wur.nl/pics/sfx_button.gif> http://sfx.library.wur.nl:9003/sfx_local?sid=SP:CABI&id=pmid:&id=&issn=0367-973X&isbn=&volume=54&issue=2&spage=240&pages=240-245&date=2001&title=&atitle=&aulast=Biswas&pid=<AN>20013126019</AN><AU>Biswas,

Blechl, A. E., Le, H. Q., & Anderson, O. D. (1998). Engineering changes in wheat flour by genetic transformation. *Journal of Plant Physiology*, *152*(6), 703–707. http://doi.org/10.1016/S0176-1617(98)80033-3

Blevins, T., Rajeswaran, R., Aregger, M., Borah, B. K., Schepetilnikov, M., Baerlocher, L., … Pooggin, M. M. (2011). Massive production of small RNAs from a non-coding region of Cauliflower mosaic virus in plant defense and viral counter-defense. *Nucleic Acids Research*, *39*, 5003–5014. http://doi.org/10.1093/nar/gkr119

Blevins, T., Rajeswaran, R., Shivaprasad, P. V., Beknazariants, D., Si-Ammour, A., Park, H. S., … Pooggin, M. M. (2006). Four plant Dicers mediate viral small RNA biogenesis and DNA virus induced silencing. *Nucleic Acids Research*, *34*(21), 6233–6246. http://doi.org/10.1093/nar/gkl886

Bock, K. R., Guthrie, E. J., & Meredith, G. (1978). Distribution, host range, properties and purification of cassava latent virus, a geminivirus. *Annals of Applied Biology*, *90*(3), 361–367. http://doi.org/10.1111/j.1744-7348.1978.tb02644.x

Bock, K. R., & Harrison, B. D. (1985). African cassava mosaic virus. *Electronic Journal of Enviromental, Agricultural and Food Chemistry*, *297*, 6.

Bonfim, K., Faria, J. C., Nogueira, E. O. P. L., Mendes, E. a, & Aragão, F. J. L. (2007). RNAi-mediated resistance to Bean golden mosaic virus in genetically engineered common bean (Phaseolus vulgaris). *Molecular Plant-Microbe Interactions : MPMI*, *20*(6), 717–726. http://doi.org/10.1094/MPMI-20-6-0717

Brencic, A., & Winans, S. C. (2005). Detection of and Response to Signals Involved in Host-Microbe Interactions by Plant-Associated Bacteria. *Microbiology and Molecular Biology Reviews*, *69*(1), 155–194. http://doi.org/10.1128/MMBR.69.1.155

Breyne, P., Gheysen, G., Jacobs, A., Montagu, M. Van, Depicker, A., Genetica, L., … Gent, B.-. (1992). Effect of T-DNA configuration on transgene expression. *Molecular And General Genetics*, *235*, 389–396.

Brigneti, G., Voinnet, O., Li, W. X., Ji, L. H., Ding, S. W., & Baulcombe, D. C. (1998). Viral pathogenicity determinants are suppressors of transgene silencing in Nicotiana benthamiana. *The EMBO Journal*, *17*(22), 6739–46. http://doi.org/10.1093/emboj/17.22.6739

Brodersen, P., & Voinnet, O. (2006). The diversity of RNA silencing pathways in plants. *TRENDS in Genetics*, *22*(5), 268–80. http://doi.org/10.1016/j.tig.2006.03.003

Brouns, S. J. J., Jore, M. M., Lundgren, M., Westra, E. R., Slijkhuis, R. J. H., Snijders, A. P. L., … van der Oost, J. (2008). Small CRISPR RNAs guide antiviral defense in prokaryotes. *Science (New York, N.Y.)*, *321*(5891), 960–964. http://doi.org/10.1126/science.1159689

Bull, S. E., Ndunguru, J., Gruissem, W., Beeching, J. R., & Vanderschuren, H. (2011). Cassava: constraints to production and the transfer of biotechnology to African laboratories. *Plant Cell Reports*. http://doi.org/10.1007/s00299-010-0986-6

Bull, S. E., Owiti, J. a, Niklaus, M., Beeching, J. R., Gruissem, W., & Vanderschuren, H. (2009). Agrobacterium-mediated transformation of friable embryogenic calli and regeneration of transgenic cassava. *Nature Protocols*, *4*(12), 1845–54. http://doi.org/10.1038/nprot.2009.208

Burgyán, J., & Havelda, Z. (2011). Viral suppressors of RNA silencing. *Trends in Plant Science*, *16*(5), 265–272. http://doi.org/10.1016/j.tplants.2011.02.010

Calvert, L. a, & Thresh, J. M. (2002). The Viruses and Virus diseases of Cassava. In *Cassava: biology, production and utilization* (pp. 237–260). http://doi.org/10.1079/9780851995243.0000

Carr, J. P., Marsh, L. E., Lomonossoff, G. P., E, S. M., & Zaitlin, M. (1992). Resistance to Tobacco mosaic virus induced by the 54kDa gene sequence requires expression of the 54kDa protein. *MOLECULAR PLANT-MICROBE INTERACTIONS*, *5*(5), 397–404.

Carrillo-Tripp, J., Lozoya-Gloria, E., & Rivera-Bustamante, R. F. (2007). Symptom Remission and Specific Resistance of Pepper Plants After Infection by Pepper golden mosaic virus. *Phytopathology*, *97*(1), 51–59. http://doi.org/10.1094/PHYTO-97-0051

Casali, N. (2003). Escherichia coli host strains. *Methods in Molecular Biology*, *235*(4), 27–48. http://doi.org/10.1385/1-59259-409-3:27

Cerutti, H., Ma, X., Msanne, J., & Repas, T. (2011). RNA-mediated silencing in Algae: biological roles and tools for analysis of gene function. *Eukaryotic Cell*, *10*(9), 1164–72. http://doi.org/10.1128/EC.05106-11

Chapman, E. J., Prokhnevsky, A. I., Gopinath, K., Dolja, V. V, & Carrington, J. C. (2004). Viral RNA silencing suppressors inhibit the microRNA pathway at an intermediate step. *Genes & Development*, *18*(10), 1179–86. http://doi.org/10.1101/gad.1201204

Chellappan, P., Masona, M. V, Vanitharani, R., Taylor, N. J., & Fauquet, C. M. (2004). Broad spectrum resistance to ssDNA viruses associated with transgene-induced gene silencing in cassava. *Plant Molecular Biology*, *56*(4), 601–11. http://doi.org/10.1007/s11103-004-0147-9

Chellappan, P., Vanitharani, R., & Fauquet, C. M. (2004). Short Interfering RNA Accumulation Correlates with Host Recovery in DNA Virus-Infected Hosts , and Gene Silencing Targets Specific Viral Sequences. *Journal of Virology*, *78*(14), 7465–7477. http://doi.org/10.1128/JVI.78.14.7465

Chellappan, P., Vanitharani, R., & Fauquet, C. M. (2005). MicroRNA-binding viral protein interferes with Arabidopsis development. *PNAS*, *102*(29), 10381–10386.

Chellappan, P., Vanitharani, R., Ogbe, F., Fauquet, C. M., Danforth, D., & Science, P. (2005). Effect of Temperature on Geminivirus-Induced RNA Silencing in Plants. *Plant Physiology*, *138*, 1828–1841.

Chen, L., Cong, Y., He, H., & Yu, Y. (2014). Maize (Zea mays L.) transformation by Agrobacterium tumefaciens infection of pollinated ovules. *Journal of Biotechnology*, *171*, 8–16. http://doi.org/10.1016/j.jbiotec.2013.11.019

Chetty, C. C., Rossin, C. B., Gruissem, W., Vanderschuren, H., & Rey, M. E. C. (2013). Empowering biotechnology in southern Africa: establishment of a robust transformation platform for the production of transgenic industry-preferred cassava. *New Biotechnology*, *30*(2), 136–43. http://doi.org/10.1016/j.nbt.2012.04.006

Chilton, M., Drummond, M. H., Merlo, J., Montoya, A. L., Gordont, M. P., & Nester, E. W. (1977). Stable incorporation of Plasmid DNA into Higher Plant Cells : the Molecular Basis of Crown Gall Tumorigenesis. *Cell*, *11*(June), 263–271.

Christou, P. (1992). Genetic transformation of crop plants using microprojectile bombardment. *The Plant Journal*, *2*(3), 275–281.

Chuang, C. F., & Meyerowitz, E. M. (2000). Specific and heritable genetic interference by double-stranded RNA in Arabidopsis thaliana. *Proceedings of the National Academy of Sciences of the United States of America*, *97*(9), 4985–90. http://doi.org/10.1073/pnas.060034297

Cleene, M., & Ley, J. (1976). The host range of crown gall. *The Botanical Review*, *42*(4), 389–466. http://doi.org/10.1007/BF02860827

Clemens, J. C., Worby, C. A., Simonson-Leff, N., Muda, M., Maehama, T., Hemmings, B. A., & Dixon, J. E. (2000). Use of double-stranded RNA interference in Drosophila cell lines to dissect signal transduction pathways. *Proceedings of the National Academy of Sciences of the United States of America*, *97*(12), 6499–503. http://doi.org/10.1073/pnas.110149597

Cooper, B., Lapidot, M., Heick, J. a., Dodds, J. A., Beachyi-, R. N., & Beachy, R. N. (1995). A defective movement protein of TMV in transgenic plants confers resistance to multiple viruses whereas the functional analog increases susceptibility. *Virology*, *206*(1), 307–313. http://doi.org/10.1016/S0042-6822(95)80046-8

Cuperus, J. T., Carbonell, A., Fahlgren, N., Garcia-ruiz, H., Burke, R. T., Takeda, A., … Carrington, J. C. (2011). Unique functionality of 22nt miRNAs in triggering RDR6-dependent siRNA biogenesis from target transcripts in Arabidopsis. *Molecular Cell*, *17*(8), 997–1003. http://doi.org/10.1038/nsmb.1866.

Dai, S., Zheng, P., Marmey, P., Zhang, S., Tian, W., Chen, S., … Fauquet, C. (2001). Comparative analysis of transgenic rice plants obtained by Agrobacterium-mediated transformation and particle bombardment. *Molecular Breeding*, *7*, 25–33.

Dalakouras, A., & Tzanopoulou, M. (2011). Hairpin transcription does not necessarily lead to efficient triggering of the RNAi pathway. *Transgenic Research*, *20*, 293–304. http://doi.org/10.1007/s11248-010-9416-3

Daphne. (1980). Cassava, a South African venture. *JOURNAL OF VIROLOGY*, *1*, 61–68. http://doi.org/10.1128/JVI.00537-09

De Felippes, F. F., Wang, J. W., & Weigel, D. (2012). MIGS: MiRNA-induced gene silencing. *Plant Journal*, *70*(3), 541–547. http://doi.org/10.1111/j.1365-313X.2011.04896.x

De Vetten, N., Wolters, A.-M., Raemakers, K., van der Meer, I., ter Stege, R., Heeres, E., … Visser, R. (2003). A transformation method for obtaining marker-free plants of a cross-pollinating and vegetatively propagated crop. *Nature Biotechnology*, *21*(4), 439–42. http://doi.org/10.1038/nbt801

De Vos, G., & Zambryski, P. (1989). Expression of Agrobacterium Nopaline-specific VirD1, VirD2, and Vir C1 proteind and their requirement for T-strand production in E.coli. *MOLECULAR PLANT-MICROBE INTERACTIONS*, *2*(2), 43–52.

Dessaux, Y., Guyon, P., Petit, A., Tempé, J., Demarez, M., Legrain, C., … Farrand, S. K. (1988). Opine utilization by Agrobacterium spp.: octopine-type Ti plasmids encode two pathways for mannopinic acid degradation. *JOURNAL OF BACTERIOLOGY*, *170*(7), 2939–46. Retrieved from http://www.pubmedcentral.nih.gov/articlerender.fcgi?artid=211232&tool=pmcentrez&rendertype=abstract

Ditt, R. F., Nester, E. W., & Comai, L. (2001). Plant gene expression response to Agrobacterium tumefaciens. *Proceedings of the National Academy of Sciences of the United States of America*, *98*(19), 10954–9. http://doi.org/10.1073/pnas.191383498

Douglas, C. J., Halperin, W., & Nester, E. W. (1982). Agrobacterium tumefaciens mutants affected in attachment to plant cells. *Journal of Bacteriology*, *152*(3), 1265–75. Retrieved from http://www.pubmedcentral.nih.gov/articlerender.fcgi?artid=221638&tool=pmcentrez&rendertype=abstract

Doyle, J., & Doyle JL. (1987). A rapid DNA isolation procedure for small quantities of fresh leaf tissue. *Phytochemistry Bulletin*, *19*, 11–15. http://doi.org/10.1631/jzus.B1100194

Dry, I. B., Krake, L. R., Rigden, J. E., & Rezaian, M. a. (1997). A novel subviral agent associated with a geminivirus: the first report of a DNA satellite. *Proceedings of the*

National Academy of Sciences of the United States of America, *94*(13), 7088–93. http://doi.org/10.1073/pnas.94.13.7088

Dry, I. B., Rigden, J. E., Krake, L. R., Mullineaux, P. M., & Rezaian, M. a. (1993). Nucleotide sequence and genome organization of tomato leaf curl geminivirus. *The Journal of General Virology*, *74 (Pt 1)*, 147–51. Retrieved from http://www.ncbi.nlm.nih.gov/pubmed/8423446

Duan, C.-G., Wang, C.-H., & Guo, H.-S. (2012). Application of RNA silencing to plant disease resistance. *Silence*, *3*(1), 5. http://doi.org/10.1186/1758-907X-3-5

Duckett, D. R., Murchie, a I., Diekmann, S., von Kitzing, E., Kemper, B., & Lilley, D. M. (1988). The structure of the Holliday junction, and its resolution. *Cell*, *55*(1), 79–89. Retrieved from http://www.ncbi.nlm.nih.gov/pubmed/17027027

Eagle, P. a, Orozco, B. M., & Hanley-Bowdoin, L. (1994). A DNA sequence required for geminivirus replication also mediates transcriptional regulation. *The Plant Cell*, *6*(8), 1157–70. http://doi.org/10.1105/tpc.6.8.1157

Eamens, A., Wang, M.-B., Smith, N. a, & Waterhouse, P. M. (2008). RNA silencing in plants: yesterday, today, and tomorrow. *Plant Physiology*, *147*(2), 456–468. http://doi.org/10.1104/pp.108.117275

Ecker, J. R., & Davis, R. W. (1986). Inhibition of gene expression in plant cells by expression of antisense RNA. *Proceedings of the National Academy of Sciences of the United States of America*, *83*(August), 5372–5376.

Ehrich, M., Zoll, S., Sur, S., & van den Boom, D. (2007). A new method for accurate assessment of DNA quality after bisulfite treatment. *Nucleic Acids Research*, *35*(5), 1–8. http://doi.org/10.1093/nar/gkl1134

Eichman, B. F., Vargason, J. M., Mooers, B. H., & Ho, P. S. (2000). The Holliday junction in an inverted repeat DNA sequence: sequence effects on the structure of four-way junctions. *Proceedings of the National Academy of Sciences of the United States of America*, *97*(8), 3971–6. Retrieved from http://www.pubmedcentral.nih.gov/articlerender.fcgi?artid=18126&tool=pmcentrez&rendertype=abstract

Eini, O., Dogra, S. C., Dry, I. B., & Randles, J. W. (2012). Silencing suppressor activity of a begomovirus DNA β encoded protein and its effect on heterologous helper virus replication. *Virus Research*, *167*(1), 97–101. http://doi.org/10.1016/j.virusres.2012.03.012

Elbashir, S. M., Martinez, J., Patkaniowska, a., Lendeckel, W., & Tuschl, T. (2001). Functional anatomy of siRNAs for mediating efficient RNAi in Drosophila melanogaster embryo lysate. *The EMBO Journal*, *20*(23), 6877–88. http://doi.org/10.1093/emboj/20.23.6877

Eleazu, C. O., Amajor, j U., Ikpeama, A. I., & Awa, E. (2011). Studies on the nutrient composition, antioxidant activities, functional properties and microbial load of flours of 10 elite cassava (Manihot esculenta) varieties. *Asian Journal of Clinical Nutrition*, *3*(1), 33–39.

Elegba, W., Appiah, A. S., Azu, E., Afful, N., Agbemavor, W. K. S., Agyei-amponsah, J., … Danso, K. E. (2013). Effect of mosaic virus diseases on dry matter content and starch yield of five cassava (Manihot esculenta Crantz) accessions in Ghana. *Africa Journal of Biotechnology*, *12*(27), 4310–4316. http://doi.org/10.5897/AJB12.2958

Elmer, J. S., Brand, L., Sunter, G., Gardiner, W. E., Bisaro, D. M., & Rogers, S. G. (1988). Genetic analysis of the tomato golden mosaic virus II. The product of the AL1 coding sequence is required for replication. *Nucleic Acids Research*, *16*(14), 7043–7060.

Ermak, G., Paszkowski, U., Wohlmuth, M., Mittelsten Scheid, O., & Paszkowski, J. (1993). Cytosine methylation inhibits replication of African cassava mosaic virus by two distinct mechanisms. *Nucleic Acids Research*, *21*(15), 3445–50. Retrieved from http://www.pubmedcentral.nih.gov/articlerender.fcgi?artid=331443&tool=pmcentrez&rendertype=abstract

Esterhuizen, L. L., Mabasa, K. G., Van Heerden, S. W., Czosnek, H., Brown, J. K., Van Heerden, H., & Rey, M. E. C. (2013). Genetic identification of members of the Bemisia tabaci cryptic species complex from South Africa reveals native and introduced haplotypes. *Journal of Applied Entomology*, *137*, 122–135. http://doi.org/10.1111/j.1439-0418.2012.01720.x

Fargette, D., Colon, L. T., Bouveau, R., & Fauquet, C. (1996). Components of resistance of cassava to African cassava mosaic virus. *European Journal of Plant Pathology*, *102*(7), 645–654. http://doi.org/10.1007/BF01877245

Fauquet, C., & Fargette, D. (1990). African Cassava Mosaic Virus : Etiology , Epidemiology , and Control. *Plant Disease*, *74*(6), 404–411.

Fauquet, C. M., Briddon, R. W., Brown, J. K., Moriones, E., Stanley, J., Zerbini, M., & Zhou, X. (2008). Geminivirus strain demarcation and nomenclature. *Archives of Virology*, *153*(4), 783–821. http://doi.org/10.1007/s00705-008-0037-6

Fire, A., Albertson, D., & Harrison, S. W. (1991). Production of antisense RNA leads to effective and specific inhibition of gene expression in C . elegans muscle. *Development*, *514*, 503–514.

Fire, A., Xu, S., Montgomery, M. K., Kostas, S. A., Driver, S. E., & C, M. C. (1998). Potent and specific genetic interference by double-stranded RNA in Caenorhabditis elegans. *Nature*, *391*(February), 806–811.

Fondong, V. N., Pita, J. S., Rey, M. E. C., Kochko, A. De, Beachy, R. N., & Fauquet, C. M. (2000). Evidence of synergism between African cassava mosaic virus and a new double-

recombinant geminivirus infecting cassava in Cameroon. *Journal of General Virology, 81*, 287–297.

Fraile, A., & García-Arenal, F. (2010). The coevolution of plants and viruses: resistance and pathogenicity. *Advances in Virus Research, 76*, 1–32. http://doi.org/10.1016/S0065-3527(10)76001-2

Fromm, M., Taylor, L. P., & Walbot, V. (1985). Expression of genes transferred into monocot and dicot plant cells by electroporation. *Proceedings of the National Academy of Sciences of the United States of America*, *82*(17), 5824–8. Retrieved from http://www.pubmedcentral.nih.gov/articlerender.fcgi?artid=390645&tool=pmcentrez&rendertype=abstract

Fuentes, A., Ramos, P. L., Fiallo, E., Callard, D., Sánchez, Y., Peral, R., … Pujol, M. (2006). Intron-hairpin RNA derived from replication associated protein C1 gene confers immunity to tomato yellow leaf curl virus infection in transgenic tomato plants. *Transgenic Research*, *15*(3), 291–304. http://doi.org/10.1007/s11248-005-5238-0

Galun, E. (2005). RNA silencing in plants. *In Vitro Cellular & Developmental Biology - Plant*, *41*(2), 113–123. http://doi.org/10.1079/IVP2004619

Gasura, E., Mashingaidze, a B., & Mukasa, S. B. (2008). GENETIC VARIABILITY FOR TUBER YIELD , QUALITY , AND VIRUS DISEASE COMPLEX TRAITS IN UGANDA SWEETPOTATO GERMPLASM Sweetpotato (Ipomoea batatas) is an important food crop in many areas of sub-Saharan Africa , where the crop is grown on about 2 . 1 million. *African Crop Science Journal*, *16*(2), 147–160.

Gasura, E., & Mukasa, S. B. (2010). PREVALENCE AND IMPLICATIONS OF SWEETPOTATO RECOVERY FROM SWEET POTATO VIRUS DISEASE IN UGANDA In Uganda , sweetpotato production is greatly constrained by the sweet potato virus disease (SPVD) that is caused by dual infection and synergistic interaction. *African Crop Science Journal*, *18*(4), 195–205.

Gelvin, S. B. (2003a). Agrobacterium -Mediated Plant Transformation : the Biology behind the Agrobacterium -Mediated Plant Transformation : the Biology behind the " Gene-Jockeying " Tool. *Microbiology and Molecular Biology Reviews*, *67*(1), 16–37. http://doi.org/10.1128/MMBR.67.1.16

Gelvin, S. B. (2003b). Agrobacterium-Mediated Plant Transformation : the Biology behind the " Gene-Jockeying " Tool. *MICROBIOLOGY AND MOLECULAR BIOLOGY REVIEWS*, *67*(1), 16–37. http://doi.org/10.1128/MMBR.67.1.16

Gelvin, S. B. (2003c). Improving plant genetic engineering by manipulating the host. *TRENDS in Biotechnology*, *21*(3), 95–8. Retrieved from http://www.ncbi.nlm.nih.gov/pubmed/12628361

Ghoshal, B., & Sanfaçon, H. (2014). Temperature-dependent symptom recovery in Nicotiana benthamiana plants infected with tomato ringspot virus is associated with reduced translation of viral RNA2 and requires ARGONAUTE 1. *Virology*, *456-457*(1), 188–197. http://doi.org/10.1016/j.virol.2014.03.026

Glick, E., Zrachya, A., Levy, Y., Mett, A., Gidoni, D., Belausov, E., … Gafni, Y. (2008). Interaction with host SGS3 is required for suppression of RNA silencing by tomato yellow leaf curl virus V2 protein. *Proceedings of the National Academy of Sciences of the United States of America*, *105*(1), 157–161. http://doi.org/10.1073/pnas.0709036105

Golemboski, D. B., Lomonossoff, G. P., & Zaitlin, M. (1990). Plants transformed with a tobacco mosaic virus nonstructural gene sequence are resistant to the virus. *Proceedings of the National Academy of Sciences of the United States of America*, *87*(16), 6311–5. Retrieved from http://www.pubmedcentral.nih.gov/articlerender.fcgi?artid=54523&tool=pmcentrez&rendertype=abstract

Gómez, P., Sempere, R. N., Elena, S. F., & Aranda, M. a. (2009). Mixed infections of Pepino mosaic virus strains modulate the evolutionary dynamics of this emergent virus. *Journal of Virology*, *83*(23), 12378–12387. http://doi.org/10.1128/JVI.01486-09

Góngora-Castillo, E., Ibarra-Laclette, E., Trejo-Saavedra, D. L., & Rivera-Bustamante, R. F. (2012). Transcriptome analysis of symptomatic and recovered leaves of geminivirus-infected pepper (Capsicum annuum). *Virology Journal*, *9*, 295. http://doi.org/10.1186/1743-422X-9-295

Gonzalez, A. ., Schopke, C., Taylor, N. J., Beachy, R. N., & Fauquet, C. M. (1998). Regeneration of transgenic cassava plants (Manihot esculenta Crantz) through Agrobacterium-mediated transformation of embryogenic suspension cultures. *Plant Cell Reports*, *17*, 827–831.

González, I., Martínez, L., Rakitina, D. V, Lewsey, M. G., Atencio, F. A., Llave, C., … Canto, T. (2010). Cucumber Mosaic Virus 2b Protein Subcellular Targets and Interactions : Their Significance to RNA Silencing Suppressor Activity. *Molecular Plant-Microbe Interactions : MPMI*, *23*(3), 294–303.

Goto, K., Kobori, T., Kosaka, Y., Natsuaki, T., & Masuta, C. (2007). Characterization of silencing suppressor 2b of cucumber mosaic virus based on examination of its small RNA-binding abilities. *Plant and Cell Physiology*, *48*(7), 1050–1060. http://doi.org/10.1093/pcp/pcm074

Gutierrez, C. (2000). DNA replication and cell cycle in plants : learning from geminiviruses. *Electronic Journal of Biotechnology*, *19*(5), 792–799.

Gutierrez, C. (2002). Strategies for geminivirus DNA replication and cell cycle interference. *Physiological and Molecular Plant Pathology*, *60*(5), 219–230. http://doi.org/10.1006/pmpp.2002.0401

Hagen, C., Rojas, M. R., Kon, T., & Gilbertson, R. L. (2008). Recovery from Cucurbit leaf crumple virus (family Geminiviridae, genus Begomovirus) infection is an adaptive antiviral response associated with changes in viral small RNAs. *Phytopathology*, *98*(9), 1029–1037. http://doi.org/10.1094/PHYTO-98-9-1029

Hahn, S. K., Terry, E. R., & Leuschner, K. (1980). Cassava for Cassava Resistance Disease. *Euphytica*, *29*, 673–683.

Hajdukiewicz, P., Svab, Z., & Maliga, P. (1994). The small, versatile pPZP family of Agrobacterium binary vectors for plant transformation. *Plant Molecular Biology*, *25*(6), 989–94. Retrieved from http://www.ncbi.nlm.nih.gov/pubmed/7919218

Halder, V., & Kombrink, E. (2015). Facile high-throughput forward chemical genetic screening by in situ monitoring of glucuronidase-based reporter gene expression in Arabidopsis thaliana. *Frontiers in Plant Science*, *6*(January), 1–12. http://doi.org/10.3389/fpls.2015.00013

Hamilton, A. J. (1999). A Species of Small Antisense RNA in Posttranscriptional Gene Silencing in Plants. *SCIENCE*, *286*(5441), 950–952. http://doi.org/10.1126/science.286.5441.950

Hamilton, A., Voinnet, O., Chappell, L., & Baulcombe, D. (2002). Two classes of short interfering RNA in RNA silencing. *The EMBO Journal*, *21*(17), 4671–9. Retrieved from http://www.pubmedcentral.nih.gov/articlerender.fcgi?artid=125409&tool=pmcentrez&rendertype=abstract

Hamilton, C. M., Frary, a, Lewis, C., & Tanksley, S. D. (1996). Stable transfer of intact high molecular weight DNA into plant chromosomes. *Proceedings of the National Academy of Sciences of the United States of America*, *93*(18), 9975–9. Retrieved from http://www.pubmedcentral.nih.gov/articlerender.fcgi?artid=38540&tool=pmcentrez&rendertype=abstract

Hammond, S. M., Bernstein, E., Beach, D., & Hannon, G. J. (2000). An RNA-directed nuclease mediates post-transcriptional gene silencing in Drosophila cells. *Nature*, *404*, 293–296.

Han, J., Lee, Y., Yeom, K., Kim, Y., Jin, H., & Kim, V. N. (2004). The Drosha – DGCR8 complex in primary microRNA processing. *Genes & Development*, *18*, 3016–3027. http://doi.org/10.1101/gad.1262504.mic

Hankoua, B., Ng, S. Y. ., Fawole, I., Puonti-Kaerlas, J., Pillay, M., & Dixon, A. G. O. (2005). Regeneration of a wide range of African cassava genotypes via shoot organogenesis from cotyledons of maturing somatic embryos and conformity of the field-established

regenerants. *Plant Cell, Tissue and Organ Culture*, *82*, 221–231. http://doi.org/10.1007/s11240-005-0514-5

Hankoua, B., Taylor, N. J., Ng, S. Y. C., Fawole, I., Puonti-Kaerlas, J., Padmanabhan, C., … Fondong, V. N. (2006). Production of the first transgenic cassava in Africa via direct shoot organogenesis from friable embryogenic calli and germination of maturing somatic embryos. *African Journal of Biotechnology*, *5*(19), 1700–1712.

Hanley-Bowdoin, L., Bejarano, E. R., Robertson, D., & Mansoor, S. (2013). Geminiviruses: masters at redirecting and reprogramming plant processes. *Nature Reviews. Microbiology*, *11*(11), 777–88. http://doi.org/10.1038/nrmicro3117

Harmse, J. (2007). *Engineering virus resistant transgenic cassava: the design of long hairpin RNA constructs against South African cassava mosaic virus*.

Harper, G., Hull, R., Lockhart, B., & Olszewski, N. (2002). Viral sequences integrated into the plant genomes. *Annual Review of Phytopathology*, *40*(1), 119–136. http://doi.org/10.1146/annurev.phyto.40.120301.105642

Harrison, B. D., & Robinson, D. J. (1999). Natural genomic and antigenic variation in whitefly-transmitted geminiviruses (begomoviruses). *Annual Review of Phytopathology*, *37*, 369–398.

Harrison, B. D., Zhou, X., Liu, Y., & Robinson, D. J. (1997). Role of a novel type of double infection in the geminivirus-induced epidemic of severe cassava mosaic in Uganda. *Annals of Applied Biology*, *131*, 437–448.

Harrison, S. F., H, B., Guthrie, E. J., Meredith, G., & Atkinson, M. (1977). Plant viruses with circular single stranded DNA. *Nature*, *270*, 760–762.

Hauge, B., Oggero, C., Nguyen, N., Fu, C., & Dong, F. (2009). Single tube, high throughput cloning of inverted repeat constructs for double-stranded RNA expression. *PLoS ONE*, *4*(9). http://doi.org/10.1371/journal.pone.0007205

He, Z., Zhu, Q., Dabi, T., Li, D., Weigel, D., & Lamb, C. (2000). Transformation of rice with the Arabidopsis floral regulator LEAFY causes early heading. *Transgenic Research*, *9*(3), 223–7. Retrieved from http://www.ncbi.nlm.nih.gov/pubmed/11032371

Heberlein, G. T., De Ley, J., & Tijtgat, R. (1967). Deoxyribonucleic acid homology and taxonomy of Agrobacterium, Rhizobium, and Chromobacterium. *Journal of Bacteriology*, *94*(1), 116–24. Retrieved from http://www.pubmedcentral.nih.gov/articlerender.fcgi?artid=251879&tool=pmcentrez&rendertype=abstract

Hehnle, S., Wege, C., & Jeske, H. (2004). Interaction of DNA with the Movement Proteins of Geminiviruses Revisited. *JOURNAL OF VIROLOGY*, *78*(14), 7698–7706. http://doi.org/10.1128/JVI.78.14.7698

Heilersig, B. H. J. B., Loonen, A. E. H. M., Wolters, A. A., & Visser, R. G. F. (2006). Presence of an intron in inverted repeat constructs does not necessarily have an effect on efficiency of post-transcriptional gene silencing. *Molecular Breeding*, *17*(4), 307–316. http://doi.org/10.1007/s11032-006-9001-x

Helliwell, C., & Waterhouse, P. (2003). Constructs and methods for high-throughput gene silencing in plants. *Methods*, *30*(4), 289–295. http://doi.org/10.1016/S1046-2023(03)00036-7

Herrera-Estrella, L., Block, M. D., Messens, E., Hernalsteens, J. P., Montagu, M. V, & Schell, J. (1983). Chimeric genes as dominant selectable markers in plant cells. *The EMBO Journal*, *2*(6), 987–995.

Hiei, Y., Ohta, S., Komari, T., & Kumashiro, T. (1994). Efficient transformation of rice (Oryza sativa L.) mediated by Agrobacterium and sequence analysis of the boundaries of the T-DNA. *The Plant Journal : For Cell and Molecular Biology*, *6*(2), 271–82. Retrieved from http://www.ncbi.nlm.nih.gov/pubmed/7920717

Holen, T., Amarzguioui, M., Wiiger, M. T., Babaie, E., & Prydz, H. (2002). Positional effects of short interfering RNAs targeting the human coagulation trigger Tissue Factor. *Nucleic Acids Research*, *30*(8), 1757–66. Retrieved from http://www.pubmedcentral.nih.gov/articlerender.fcgi?artid=113209&tool=pmcentrez&rendertype=abstract

Holliday, R., Ridgeway, T., & Hill, M. (1985). This Week's Citation Classic®. *Genet Res*, *5*, 282–304.

Holsters, M., de Waele, D., Depicker, a., Messens, E., van Montagu, M., & Schell, J. (1978). Transfection and transformation of Agrobacterium tumefaciens. *MGG Molecular & General Genetics*, *163*(2), 181–187. http://doi.org/10.1007/BF00267408

Hommelsheim, C. M., Frantzeskakis, L., Huang, M., & Ülker, B. (2014). PCR amplification of repetitive DNA: a limitation to genome editing technologies and many other applications. *Scientific Reports*, *4*, 5052. http://doi.org/10.1038/srep05052

Honda, M., Muramoto, Y., Kuzuguchi, T., Sawano, S., Machida, M., & Koyama, H. (2002). Determination of gene copy number and genotype of transgenic Arabidopsis thaliana by competitive PCR. *Journal of Experimental Botany*, *53*(373), 1515–20. Retrieved from http://www.ncbi.nlm.nih.gov/pubmed/12021299

Hong, Y. G., Robinson, D. J., & Harrison, B. D. (1993). Nucleotide sequence evidence for the occurrence of three distinct whitefly-transmitted geminiviruses in cassava. *The Journal of*

General Virology, *74 (Pt 11*, 2437–43. Retrieved from http://www.ncbi.nlm.nih.gov/pubmed/8245859

Hong, Y., Saunders, K., & Stanley, J. (1997). Transactivation of dianthin transgene expression by African cassava mosaic virus AC2. *Virology*, *228*(228), 337–383. http://doi.org/10.1006/viro.1996.8403

Hossbach, M., Gruber, J., Osborn, M., Weber, K., & Tuschl, T. (2006). Gene silencing with siRNA duplexes composed of target-mRNA-complementary and partially palindromic or partially complementary single-stranded siRNAs. *RNA Biology*, *3*(2), 82–89. http://doi.org/10.4161/rna.3.2.3110

Huang, Y., & Liu, Z.-R. (2002). The ATPase, RNA unwinding, and RNA binding activities of recombinant p68 RNA helicase. *The Journal of Biological Chemistry*, *277*(15), 12810–5. http://doi.org/10.1074/jbc.M200182200

Huesken, D., Lange, J., Mickanin, C., Weiler, J., Asselbergs, F., Warner, J., … Hall, J. (2005). Design of a genome-wide siRNA library using an artificial neural network. *Nature Biotechnology*, *23*(8), 995–1001. http://doi.org/10.1038/nbt1118

Hull, R., Harper, G., & Lockhart, B. (2000). Viral sequences integrated into plant genomes. *Trends in Plant Science*, *5*(9), 362–365. http://doi.org/10.1016/S1360-1385(00)01723-4

Incarbone, M., & Dunoyer, P. (2013). RNA silencing and its suppression: Novel insights from in planta analyses. *Trends in Plant Science*, *18*(7), 382–392. http://doi.org/10.1016/j.tplants.2013.04.001

Ingelbrecht, I. L., Irvine, J. E., & Mirkov, T. E. (1999). Posttranscriptional Gene Silencing in Transgenic Sugarcane . Dissection of Homology-Dependent Virus Resistance in a Monocot That Has a Complex Polyploid Genome 1. *Plant Physiology*, *119*(April), 1187–1197.

Ingram, D., Pascal, E., & Lazarowitz, S. G. (1995). Both bipartite geminivirus movement proteins define host range, but only BC1 determines viral pathogenicity. *Virology*, *207*, 191–204.

Jan, F. J., Pang, S. Z., Tricoli, D. M., & Gonsalves, D. (2000). Evidence that resistance in squash mosaic comovirus coat protein-transgenic plants is affected by plant developmental stage and enhanced by combination of transgenes from different lines. *The Journal of General Virology*, *81*(Pt 9), 2299–306. Retrieved from http://www.ncbi.nlm.nih.gov/pubmed/10950989

Jauvion, V., Elmayan, T., & Vaucheret, H. (2010). The conserved RNA trafficking proteins HPR1 and TEX1 are involved in the production of endogenous and exogenous small interfering RNA in Arabidopsis. *The Plant Cell*, *22*(8), 2697–2709. http://doi.org/10.1105/tpc.110.076638

Jefferson, R. a, Kavanagh, T. a, & Bevan, M. W. (1987). GUS fusions: beta-glucuronidase as a sensitive and versatile gene fusion marker in higher plants. *The EMBO Journal*, *6*(13), 3901–3907.

Jovel, J., & Walker, M. (2007). Recovery of Nicotiana benthamiana Plants from a Necrotic Response Induced by a Nepovirus Is Associated with RNA Silencing but Not with Reduced Virus Titer □. *Journal of Virology*, *81*(22), 12285–12297. http://doi.org/10.1128/JVI.01192-07

Kalantidis, K., Psaradakis, S., Tabler, M., & Tsagris, M. (2002). The occurrence of CMV-specific short Rnas in transgenic tobacco expressing virus-derived double-stranded RNA is indicative of resistance to the virus. *Molecular Plant-Microbe Interactions : MPMI*, *15*(8), 826–833. http://doi.org/10.1094/MPMI.2002.15.8.826

Kanno, T., & Habu, Y. (2011). SiRNA-mediated chromatin maintenance and its function in Arabidopsis thaliana. *Biochimica et Biophysica Acta - Gene Regulatory Mechanisms*, *1809*(8), 444–451. http://doi.org/10.1016/j.bbagrm.2011.05.002

Kaweesi, T., Kawuki, R., Kyaligonza, V., Baguma, Y., Tusiime, G., & Ferguson, M. E. (2014). Field evaluation of selected cassava genotypes for cassava brown streak disease based on symptom expression and virus load. *Virology Journal*, *11*(1). http://doi.org/10.1186/s12985-014-0216-x

Ketting, R. F., Fischer, S. E., Bernstein, E., Sijen, T., Hannon, G. J., & Plasterk, R. H. (2001). Dicer functions in RNA interference and in synthesis of small RNA involved in developmental timing in C. elegans. *Genes & Development*, *15*(20), 2654–9. http://doi.org/10.1101/gad.927801

Kheyr Pour, A., Gronenborn, B., & Czosnek, H. (1994). Agroinoculation of tomato yellow leaf curl virus (TYLCV) overcomes the virus resistance of wild Lycopersicon species. *Plant Breeding*, *112*(3), 228–233. Retrieved from <img src=http://library.wur.nl/pics/sfx_button.gif> http://sfx.library.wur.nl:9003/sfx_local?sid=SP:BX&id=pmid:&id=&issn=0179-9541&isbn=&volume=112&issue=3&spage=228&pages=228-233&date=1994&title=Plant Breeding&atitle=Agroinoculation of tomato yellow leaf

Kheyr-Pour, A., Gronenborn, B., & Czosnek, H. (1994). Agroinoculation of Tomato Yellow Leaf Curl Virus (TYLCV) Overcomes the Virus Resistance of Wild Lycopersicon Species. *Plant Breeding*, *112*, 228–233.

Khraiwesh, B., Arif, M. A., Seumel, G. I., Ossowski, S., Weigel, D., Reski, R., & Frank, W. (2010). Transcriptional control of gene expression by microRNAs. *Cell*, *140*(1), 111–22. http://doi.org/10.1016/j.cell.2009.12.023

Khvorova, A., Reynolds, A., & Jayasena, S. D. (2003). Functional siRNAs and miRNAs exhibit strand bias. *Cell*, *115*(2), 209–16. Retrieved from http://www.ncbi.nlm.nih.gov/pubmed/14567918

Kini, H. K., & Walton, S. P. (2009). Effect of siRNA terminal mismatches on TRBP and Dicer binding and silencing efficacy. *The FEBS Journal*, *276*(22), 6576–85. http://doi.org/10.1111/j.1742-4658.2009.07364.x

Kohli, A., Griffiths, S., Palacios, N., Twyman, R. M., Vain, P., Laurie, D. a, & Christou, P. (1999). Molecular characterization of transforming plasmid rearrangements in transgenic rice reveals a recombination hotspot in the CaMV 35S promoter and confirms the predominance of microhomology mediated recombination. *The Plant Journal : For Cell and Molecular Biology*, *17*(6), 591–601. Retrieved from http://www.ncbi.nlm.nih.gov/pubmed/10230059

Kolawole, P. O., Agbetoye, L., & Ogunlowo, S. a. (2010). Sustaining World Food Security with Improved Cassava Processing Technology: The Nigeria Experience. *Sustainability*, *2*(12), 3681–3694. http://doi.org/10.3390/su2123681

Kononov, M. E., Bassuner, B., & Gelvin, S. B. (1997). Integration of T-DNA binary vector "backbone" sequences into the tobacco genome: evidence for multiple complex patterns of integration. *The Plant Journal : For Cell and Molecular Biology*, *11*(5), 945–57.

Kotakis, C., Vrettos, N., Kotsis, D., Tsagris, M., Kotzabasis, K., & Kalantidis, K. (2010). Light intensity affects RNA silencing of a transgene in Nicotiana benthamiana plants. *BMC Plant Biology*, *10*(1), 1–11. http://doi.org/10.1186/1471-2229-10-220

Koukolíková-Nicola, Z., Raineri, D., Stephens, K., Ramos, C., Tinland, B., Nester, E. W., & Hohn, B. (1993). Genetic analysis of the virD operon of Agrobacterium tumefaciens: a search for functions involved in transport of T-DNA into the plant cell nucleus and in T-DNA integration. *Journal of Bacteriology*, *175*(3), 723–31. Retrieved from http://www.pubmedcentral.nih.gov/articlerender.fcgi?artid=196211&tool=pmcentrez&rendertype=abstract

Lal, A., Pant, M., & Rani, A. (2015). THE WHO ' S WHO OF PLANT VIRUSES : A COGNITIVE APPROACH. *Asian Journal of Pharmaceutical and Clinical Research*, *8*(1), 60–68.

Lapidot, M., & Friedmann, M. (2002). Breeding for resistance to whitefly-transmitted geminiviruses. *Annals of Applied Biology*, *140*(2), 109–127. http://doi.org/10.1111/j.1744-7348.2002.tb00163.x

Lapidot, M., Weil, G., Cohen, L., Segev, L., & Gaba, V. (2007). Biolistic inoculation of plants with tomato yellow leaf curl virus DNA. *Journal of Virological Methods*, *144*(1-2), 143–8. http://doi.org/10.1016/j.jviromet.2007.04.011

Latham, J. R., Wilson, A. K., & Steinbrecher, R. a. (2006). The mutational consequences of plant transformation. *Journal of Biomedicine and Biotechnology*, *2006*, 1–7. http://doi.org/10.1155/JBB/2006/25376

Laufs, J., Traut, W., Heyraud, F., Matzeit, V., Rogers, S. G., Schell, J., & Gronenborn, B. (1995). In vitro cleavage and joining at the viral origin of replication by the replication initiator protein of tomato yellow leaf curl virus. *Proceedings of the National Academy of Sciences of the United States of America*, *92*(9), 3879–83. Retrieved from http://www.pubmedcentral.nih.gov/articlerender.fcgi?artid=42065&tool=pmcentrez&rendertype=abstract

Law, M., Moyer, J., & Payne, G. (1989). Effects of host resistance on pathogenesis of Maize dwarf mosaic virus. *The American Phytopathological Society*, *79*(7), 757–761.

Lee, R. C., Feinbaum, R. L., & Ambros, V. (1993). The C. elegans heterochronic gene lin-4 encodes small RNAs with antisense complementarity to lin-14. *Cell*, *75*(5), 843–54. Retrieved from http://www.ncbi.nlm.nih.gov/pubmed/8252621

Legg, J. P., & Fauquet, C. M. (2004). Cassava mosaic geminiviruses in Africa. *Plant Molecular Biology*, *56*(4), 585–99. http://doi.org/10.1007/s11103-004-1651-7

Legg, J. P., Jeremiah, S. C., Obiero, H. M., Maruthi, M. N., Ndyetabula, I., Okao-Okuja, G., … Lava Kumar, P. (2011). Comparing the regional epidemiology of the cassava mosaic and cassava brown streak virus pandemics in Africa. *Virus Research*, *159*(2), 161–170. http://doi.org/10.1016/j.virusres.2011.04.018

Lessl, M., & Lanka, E. (1994). Common mechanisms in bacterial conjugation and Ti-mediated transfer to plant cells. *Cell*, *77*, 321–324.

Li, F., Huang, C., Li, Z., & Zhou, X. (2014). Suppression of RNA Silencing by a Plant DNA Virus Satellite Requires a Host Calmodulin-Like Protein to Repress RDR6 Expression. *PLoS Pathogens*, *10*(2), e1003921. http://doi.org/10.1371/journal.ppat.1003921

Li, H. Q., Sautter, C., Potrykus, I., & Puonti-Kaerlas, J. (1996). Genetic transformation of cassava (Manihot esculenta Crantz). *Nature Biotechnology*, *14*, 736 – 739.

Li, H.-Q., Guo, J.-Y., Huang, Y.-W., Liang, C.-Y., Liu, H.-X., Potrykus, I., & Puonti-Kaerlas, J. (1998). Regeneration of cassava plants via shoot organogenesis. *Plant Cell Reports*, *17*(5), 410–414. http://doi.org/10.1007/s002990050416

Li, Y., Rosso, M. G., Ülker, B., & Weisshaar, B. (2006). Analysis of T-DNA insertion site distribution patterns in Arabidopsis thaliana reveals special features of genes without insertions. *Genomics*, *87*, 645–652. http://doi.org/10.1016/j.ygeno.2005.12.010

Lilley, D. M., & Norman, D. G. (1999). The Holliday junction is finally seen with crystal clarity. *Nature Structural Biology*, *6*(10), 897–9. http://doi.org/10.1038/13255

Lima, A. T. M., Sobrinho, R. R., González-Aguilera, J., Rocha, C. S., Silva, S. J. C., Xavier, C. a D., … Zerbini, F. M. (2013). Synonymous site variation due to recombination explains higher genetic variability in begomovirus populations infecting non-cultivated hosts. *The Journal of General Virology*, *94*, 418–31. http://doi.org/10.1099/vir.0.047241-0

Lin, S.-S., Henriques, R., Wu, H.-W., Niu, Q.-W., Yeh, S.-D., & Chua, N.-H. (2007). Strategies and mechanisms of plant virus resistance. *Plant Biotechnology Reports*, *1*(3), 125–134. http://doi.org/10.1007/s11816-007-0021-8

Lipardi, C., Wei, Q., & Paterson, B. M. (2001). RNAi as random degradative PCR: siRNA primers convert mRNA into dsRNAs that are degraded to generate new siRNAs. *Cell*, *107*(3), 297–307. Retrieved from http://www.ncbi.nlm.nih.gov/pubmed/11701121

Liu, J., Zheng, Q., Ma, Q., Gadidasu, K. K., & Zhang, P. (2011). *Cassava Genetic Transformation and Its Application in Breeding*. *Africa*.

Liu, Z., Gao, S., & Zhang, S. (2014). Complex structures of transgene rearrangement implicate novel mechanisms of RNA-directed DNA methylation and convergent transcription. *Genes Genom*, *36*, 95–103. http://doi.org/10.1007/s13258-013-0147-8

Lomonossoff, G. P. (1995). Pathogen-derived resistance to plant viruses. *Annual Review of Phytopathology*, *33*, 323–343.

López, C., Cervera, M., Fagoaga, C., Moreno, P., Navarro, L., Flores, R., & Peña, L. (2010). Accumulation of transgene-derived siRNAs is not sufficient for RNAi-mediated protection against Citrus tristeza virus in transgenic Mexican lime. *Molecular Plant Pathology*, *11*(1), 33–41. http://doi.org/10.1111/J.1364-3703.2009.00566.X

Lu, S., Shi, R., Tsao, C.-C., Yi, X., Li, L., & Chiang, V. L. (2004). RNA silencing in plants by the expression of siRNA duplexes. *Nucleic Acids Research*, *32*(21), e171. http://doi.org/10.1093/nar/gnh170

Lucioli, A., Noris, E., Brunetti, A., Tavazza, R., Ruzza, V., Castillo, A. G., … Tavazza, M. (2003). Tomato Yellow Leaf Curl Sardinia Virus Rep-Derived Resistance to Homologous and Heterologous Geminiviruses Occurs by Different Mechanisms and Is Overcome if Virus-Mediated Transgene Silencing Is Activated. *JOURNAL OF VIROLOGY*, *77*(12), 6785–6798. http://doi.org/10.1128/JVI.77.12.6785

Luong, H., Shewryb, P. R., & Lazzeri, P. (1995). Transient gene expression in cassava somatic embryos by tissue electroporation. *Plant Science*, *107*, 105–115.

Lyznik, L. A., Kamo, K. K., Grimes, H. D., Ryan, R., Chang, K., & Hodges, T. K. (1989). Stable transformation of maize: the impact of feeder cells on protoplast growth and transformation efficiency. *Plant Cell Reports*, *8*, 292–295.

Mabasa, K. (2007). *Epidemiology of cassava mosiac disease and molecular characterisation of cassava mosaic viruses and their associated Whitefly (Bemisia Tabaci) vector in South Africa*.

MacRae, I. J., Zhou, K., & Doudna, J. a. (2007). Structural determinants of RNA recognition and cleavage by Dicer. *Nature Structural & Molecular Biology*, *14*(10), 934–40. http://doi.org/10.1038/nsmb1293

Mallory, A. C., Reinhart, B. J., Jones-Rhoades, M. W., Tang, G., Zamore, P. D., Barton, M. K., & Bartel, D. P. (2004). MicroRNA control of PHABULOSA in leaf development: importance of pairing to the microRNA 5' region. *The EMBO Journal*, *23*(16), 3356–64. http://doi.org/10.1038/sj.emboj.7600340

Matveeva, O. V., Kang, Y., Spiridonov, A. N., Sætrom, P., Nemtsov, V. a., Ogurtsov, A. Y., … Shabalina, S. a. (2010). Optimization of duplex stability and terminal asymmetry for shRNA design. *PLoS ONE*, *5*(4). http://doi.org/10.1371/journal.pone.0010180

Mccormick, S., Niedermeyer, J., Fry, J., Barnason, A., Horsch, R., & Fraley, R. (1986). Leaf disc transformation of cultivated tomato (L . esculentum) using Agrobacterium tumefaciens. *Plant Cell Reports*, *5*, 81–84.

McRobert, L., & McConkey, G. a. (2002). RNA interference (RNAi) inhibits growth of Plasmodium falciparum. *Molecular and Biochemical Parasitology*, *119*(2), 273–8. Retrieved from http://www.ncbi.nlm.nih.gov/pubmed/11814579

Medina-Hernández, D., Rivera-Bustamante, R. F., Tenllado, F., & Holguín-Peña, R. J. (2013). Effects and effectiveness of two RNAi constructs for resistance to pepper golden mosaic virus in Nicotiana benthamiana plants. *Viruses*, *5*, 2931–2945. http://doi.org/10.3390/v5122931

Meister, G., Landthaler, M., Patkaniowska, A., Dorsett, Y., Teng, G., & Tuschl, T. (2004). Human Argonaute2 Mediates RNA Cleavage Targeted by miRNAs and siRNAs. *Molecular Cell*, *15*, 185–197.

Meister, G., Landthaler, M., Peters, L., Chen, P. Y., Urlaub, H., Lührmann, R., & Tuschl, T. (2005). Identification of novel argonaute-associated proteins. *Current Biology : CB*, *15*(23), 2149–55. http://doi.org/10.1016/j.cub.2005.10.048

Melnyk, C. W., Molnar, A., & Baulcombe, D. C. (2011). Intercellular and systemic movement of RNA silencing signals. *The EMBO Journal*, *30*(17), 3553–3563. http://doi.org/10.1038/emboj.2011.274

Mohammed, I. U., Abarshi, M. M., Muli, B., Hillocks, R. J., & Maruthi, M. N. (2012). The symptom and genetic diversity of cassava brown streak viruses infecting cassava in east africa. *Advances in Virology*, *2012*. http://doi.org/10.1155/2012/795697

Montanucci, L., Fariselli, P., Martelli, P. L., Rossi, I., & Casadio, R. (2008). In Silico Evidence of the Relationship Between miRNAs and siRNAs. *The 0pen Applied Informatics Journal*, *2*, 9–13.

Montgomery, M. K., & Fire, a. (1998). Double-stranded RNA as a mediator in sequence-specific genetic silencing and co-suppression. *Trends in Genetics*, *14*(7), 255–258. http://doi.org/10.1016/S0168-9525(98)01510-8

Moreno, I., Gruissem, W., & Vanderschuren, H. (2011). Reference genes for reliable potyvirus quantitation in cassava and analysis of Cassava brown streak virus load in host varieties. *Journal of Virological Methods*, *177*(1), 49–54. http://doi.org/10.1016/j.jviromet.2011.06.013

Mourrain, P., Béclin, C., Elmayan, T., Feuerbach, F., Godon, C., Morel, J. B., … Vaucheret, H. (2000). Arabidopsis SGS2 and SGS3 genes are required for posttranscriptional gene silencing and natural virus resistance. *Cell*, *101*(5), 533–542. http://doi.org/10.1016/S0092-8674(00)80863-6

Mubin, M., Hussain, M., Briddon, R. W., & Mansoor, S. (2011). Selection of target sequences as well as sequence identity determine the outcome of RNAi approach for resistance against cotton leaf curl geminivirus complex. *Virology Journal*, *8*(1), 122. http://doi.org/10.1186/1743-422X-8-122

Mueller, E., Gilbert, J., Davenport, G., Brigneti, G., & Baulcombe, D. C. (1995). Homology dependent resistance: transgenic virus resistance in plants related to homology-dependent gene silencing. *The Plant Journal*, *7*(6), 1001–1013.

Müller, a E., Kamisugi, Y., Grüneberg, R., Niedenhof, I., Hörold, R. J., & Meyer, P. (1999). Palindromic sequences and A+T-rich DNA elements promote illegitimate recombination in Nicotiana tabacum. *Journal of Molecular Biology*, *291*(1), 29–46. http://doi.org/10.1006/jmbi.1999.2957

Munyikwa, R. I., Raemakers, K., Schreuder, M. M., Kok, R., Schippers, M., Jacobsen, E., & Visser, R. G. F. (1998). Pinpointing towards improved transformation and regeneration of cassava (Manihot esculenta Crantz). *Plant Science*, *135*(1), 87–101. http://doi.org/10.1016/S0168-9452(98)00074-0

Neumann, E., Schaefer-Ridder, M., Wang, Y., & Hofschneider, P. (1982). Gene transfer into mouse lyoma cells by electroporation in high electric fields. *EMBO Journal*, *1*(7), 841–845.

Newell, C. A., Brown, N. J., Liu, Z., Pflug, A., Gowik, U., Westhoff, P., & Hibberd, M. (2010). Agrobacterium tumefaciens -mediated transformation of Cleome gynandra L ., a C 4 dicotyledon that is closely related to Arabidopsis thaliana. *Journal of Experimental Botany*, *61*(5), 1311–1319. http://doi.org/10.1093/jxb/erq009

Njock, T. E. (2014). Evaluation of the infection of cassava and Nicotiana benthamiana with cassava mosaic geminiviruses and their combinations for potential synergism. *Global Advanced Research Journal of Agricultural Science*, *3*(10), 310–316.

Nomura, K., Ohshima, K., Anai, T., Uekusa, H., & Kita, N. (2004). RNA Silencing of the Introduced Coat Protein Gene of Turnip mosaic virus Confers Broad-Spectrum Resistance in Transgenic Arabidopsis. *Phytopathology*, *94*(7), 730–6. http://doi.org/10.1094/PHYTO.2004.94.7.730

Ntui, V. O., Kong, K., Azadi, P., Khan, R. S., Chin, D. P., Igawa, T., … Nakamura, I. (2014). RNAi-Mediated Resistance to Cucumber Mosaic Virus (CMV) in Genetically Engineered Tomato. *American Journal of Plant Sciences*, *5*, 554–572.

Ntui, V. O., Kong, K., Khan, R. S., Igawa, T., Janavi, G. J., Rabindran, R., … Mii, M. (2015). Resistance to Sri Lankan Cassava Mosaic Virus (SLCMV) in Genetically Engineered Cassava cv. KU50 through RNA Silencing. *Plos One*, *10*(4), e0120551. http://doi.org/10.1371/journal.pone.0120551

Nyaboga, E., Njiru, J., Nguu, E., Gruissem, W., Vanderschuren, H., & Tripathi, L. (2013). Unlocking the potential of tropical root crop biotechnology in east Africa by establishing a genetic transformation platform for local farmer-preferred cassava cultivars. *Frontiers in Plant Science*, *4*(December), 526. http://doi.org/10.3389/fpls.2013.00526

Obbard, D. J., Gordon, K. H. J., Buck, A. H., & Jiggins, F. M. (2009). The evolution of RNAi as a defence against viruses and transposable elements. *Philosophical Transactions of the Royal Society of London. Series B, Biological Sciences*, *364*(October 2008), 99–115. http://doi.org/10.1098/rstb.2008.0168

Ogwok, E., Odipio, J., Halsey, M., Gaitán-Solís, E., Bua, A., Taylor, N. J., … Alicai, T. (2012). Transgenic RNA interference (RNAi)-derived field resistance to cassava brown streak disease. *Molecular Plant Pathology*, *13*, 1019–1031. http://doi.org/10.1111/j.1364-3703.2012.00812.x

Oliver, J. E., & Fuchs, M. (2011). Tolerance and resistance to viruses and their vectors in vitis sp.: A virologist's perspective of the literature. *American Journal of Enology and Viticulture*, *62*(4), 438–451. http://doi.org/10.5344/ajev.2011.11036

Orozco, B. M., Miller, a B., Settlage, S. B., & Hanley-Bowdoin, L. (1997a). Functional domains of a geminivirus replication protein. *The JOURNAL OF BIOLOGICAL CHEMISTRY*, *272*(15), 9840–6.

Orozco, B. M., Miller, A. B., Settlage, S. B., & Hanley-Bowdoin, L. (1997b). Functional Domains of a Geminivirus Replication Protein. *Journal of Biological Chemistry*, *272*(15), 9840–9846. http://doi.org/10.1074/jbc.272.15.9840

Pang, S. Z., Jan, F. J., & Gonsalves, D. (1997). Nontarget DNA sequences reduce the transgene length necessary for RNA-mediated tospovirus resistance in transgenic plants. *Proceedings of the National Academy of Sciences of the United States of America*, *94*(15), 8261–6. Retrieved from http://www.pubmedcentral.nih.gov/articlerender.fcgi?artid=21591&tool=pmcentrez&rendertype=abstract

Paprotka, T., Deuschle, K., Metzler, V., & Jeske, H. (2011). Conformation-Selective Methylation of Geminivirus DNA. *Journal of Virology*, *85*(22), 12001–12012. http://doi.org/10.1128/JVI.05567-11

Parisi, O., Lepoivre, P., & Jijakli, M. H. (2009). Plant-RNA viroid relationship : a complex host pathogen interaction. *Biotechnology, Agronomy, Society and Environment*, *14*(3), 461–470.

Parizotto, E. A., Dunoyer, P., Rahm, N., Himber, C., & Voinnet, O. (2004). In vivo investigation of the transcription , processing , endonucleolytic activity , and functional relevance of the spatial distribution of a plant miRNA. *Genes & Development*, *18*(2237-2242), 2237–2242. http://doi.org/10.1101/gad.307804.by

Paszkowski, J., Shillito, R. D., Saul, M., Mandák, V., Hohn, T., Hohn, B., & Potrykus, I. (1984). Direct gene transfer to plants. *The EMBO Journal*, *3*(12), 2717–22. Retrieved from http://www.pubmedcentral.nih.gov/articlerender.fcgi?artid=557758&tool=pmcentrez&rendertype=abstract

Patil, B. L., Dutt, N., Briddon, R. W., Bull, S. E., Rothenstein, D., Borah, B. K., … Jeske, H. (2007). Deletion and recombination events between the DNA-A and DNA-B components of Indian cassava-infecting geminiviruses generate defective molecules in Nicotiana benthamiana. *Virus Research*, *124*(1-2), 59–67. http://doi.org/10.1016/j.virusres.2006.10.003

Patil, B. L., & Fauquet, C. M. (2009). Cassava mosaic geminiviruses: actual knowledge and perspectives. *Molecular Plant Pathology*, *10*(5), 685–701. http://doi.org/10.1111/j.1364-3703.2009.00559.x

Patil, B. L., & Fauquet, C. M. (2014). Light intensity and temperature affect systemic spread of silencing signal in transient agroinfiltration studies. *Molecular Plant Pathology*, n/a–n/a. http://doi.org/10.1111/mpp.12205

Piccin, A., Salameh, A., Benna, C., Sandrelli, F., Mazzotta, G., Zordan, M., … Costa, R. (2001). Efficient and heritable functional knock-out of an adult phenotype in Drosophila using a GAL4-driven hairpin RNA incorporating a heterologous spacer. *Nucleic Acids Research*, *29*(12), 2–5. Retrieved from http://www.pubmedcentral.nih.gov/articlerender.fcgi?artid=55754&tool=pmcentrez&rendertype=abstract

Pierce, E. (2013). *Transcriptome profiling of susceptible model and natural host systems in response to South African cassava mosaic virus*.

Pita, J. S., Fondong, V. N., Sangar, A., Kokora, R. N. N., & Fauquet, C. M. (2001). Genomic and biological diversity of the African cassava geminiviruses. *Euphytica*, *2*(1997), 115–125.

Pita, J. S., Fondong, V. N., Sangaré, A., Otim-Nape, G. W., Ogwal, S., & Fauquet, C. M. (2001). Recombination, pseudorecombination and synergism of geminiviruses are determinant keys to the epidemic of severe cassava mosaic disease in Uganda. *Journal of General Virology*, *82*(Pt 3), 655–65. Retrieved from http://www.ncbi.nlm.nih.gov/pubmed/11172108

Pitzschke, A., & Hirt, H. (2010). New insights into an old story: Agrobacterium- induced tumour formation in plants by plant transformation. *EMBO Journal*, *29*(6), 1021–1032. http://doi.org/10.1038/emboj.2010.8

Pooggin, M. M. (2013). How can plant DNA viruses evade siRNA-directed DNA methylation and silencing? *International Journal of Molecular Sciences*, *14*(8), 15233–59. http://doi.org/10.3390/ijms140815233

Pruss, G., Ge, X., Shi, X. M., Carrington, J. C., & Bowman Vance, V. (1997). Plant viral synergism: the potyviral genome encodes a broad-range pathogenicity enhancer that transactivates replication of heterologous viruses. *The Plant Cell*, *9*(6), 859–868. http://doi.org/10.1105/tpc.9.6.859

Pumplin, N., & Voinnet, O. (2013). RNA silencing suppression by plant pathogens: defence, counter-defence and counter-counter-defence. *Nature Reviews. Microbiology*, *11*(11), 745–60. http://doi.org/10.1038/nrmicro3120

Rabbi, I. Y., Hamblin, M. T., Kumar, P. L., Gedil, M. a, Ikpan, A. S., Jannink, J.-L., & Kulakow, P. a. (2014). High-resolution mapping of resistance to cassava mosaic geminiviruses in cassava using genotyping-by-sequencing and its implications for breeding. *Virus Research*, *186*, 87–96. http://doi.org/10.1016/j.virusres.2013.12.028

Raemakers, C. J. J. M., Sofiari, E., Jacobsen, E., & Visser, R. G. F. (1997). Regeneration and transformation of cassava. *Euphytica*, *96*, 153–161.

Raemakers, C. J. J. M., Tayloti, E. S. N., Henshaw, G., Jacobsen, E., & Visser, R. G. F. (1996). Production of transgenic cassava (Manihot esczdenta Crantz) plants by particle bombardment using luciferase activity as selection marker. *Molecular Breeding*, *2*, 339–349.

Raemakers, K., Schreuder, M., Pereira, I., Munyikwa, T., Jacobsen, E., & Visser, R. (2001). Progress made in FEC transformation of cassava. *Euphytica*, *120*(1995), 15–24.

Raizis, A., F, S., & Jost, J. (1995). A bisulfite method of 5-methylcytosine mapping that minimizes template degradation. *Analytical Biochemistry*, *226*, 161–166.

Raja, P., Wolf, J. N., & Bisaro, D. M. (2010). RNA silencing directed against geminiviruses: post-transcriptional and epigenetic components. *Biochimica et Biophysica Acta*, *1799*(3-4), 337–51. http://doi.org/10.1016/j.bbagrm.2010.01.004

Rajeswaran, R., & Pooggin, M. M. (2012). RDR6-mediated synthesis of complementary RNA is terminated by miRNA stably bound to template RNA. *Nucleic Acids Research*, *40*(2), 594–599. http://doi.org/10.1093/nar/gkr760

Rattray, A. J. (2004). A method for cloning and sequencing long palindromic DNA junctions. *Nucleic Acids Research*, *32*(19), 1–8. http://doi.org/10.1093/nar/gnh143

Rentería-Canett, I., Xoconostle-Cázares, B., Ruiz-Medrano, R., & Rivera-Bustamante, R. F. (2011). Geminivirus mixed infection on pepper plants: synergistic interaction between PHYVV and PepGMV. *Virology Journal*, *8*(1), 104. http://doi.org/10.1186/1743-422X-8-104

Rey, M. E. C., Ndunguru, J., Berrie, L. C., Paximadis, M., Berry, S., Cossa, N., … Esterhuizen, L. L. (2012). Diversity of dicotyledenous-infecting geminiviruses and their associated DNA molecules in southern Africa, including the South-west Indian ocean islands. *Viruses*, *4*(9), 1753–91. http://doi.org/10.3390/v4091753

Ribeiro, S. G., Lohuis, H., Goldbach, R., & Prins, M. (2007). Tomato chlorotic mottle virus is a target of RNA silencing but the presence of specific short interfering RNAs does not guarantee resistance in transgenic plants. *Journal of Virology*, *81*(4), 1563–73. http://doi.org/10.1128/JVI.01238-06

Rigden, J. E., Dry, I. B., Krake, L. R., & Rezaian, M. a. (1996). Plant virus DNA replication processes in Agrobacterium: insight into the origins of geminiviruses? *Proceedings of the National Academy of Sciences of the United States of America*, *93*(September), 10280–10284. http://doi.org/10.1073/pnas.93.19.10280

Riva, G. A. De, González-cabrera, J., & Vázquez-padrón, R. (1998). Agrobacterium tumefaciens : a natural tool for plant transformation. *Electronic Journal of Biotechnology*, *1*(3), 1–16.

Rodríguez-Negrete, E. a, Carrillo-Tripp, J., & Rivera-Bustamante, R. F. (2009). RNA silencing against geminivirus: complementary action of posttranscriptional gene silencing and transcriptional gene silencing in host recovery. *Journal of Virology*, *83*(3), 1332–1340. http://doi.org/10.1128/JVI.01474-08

Romon, M., Soustre-Gacougnolle, I., Schmitt, C., Perrin, M., Burdloff, Y., Chevalier, E., … Masson, J. E. (2013). RNA silencing is resistant to low-temperature in grapevine. *PLoS ONE*, *8*(12), 1–7. http://doi.org/10.1371/journal.pone.0082652

Roossinck, M. J., Sleat, D., & Palukaitis, P. (1992). Satellite RNAs of Plant Viruses : Structures and Biological Effects I- ’ CA-. *MICROBIOLOGICAL REVIEWS*, *56*(2), 265–279.

Rose, A. B. (2004). The effect of intron location on intron-mediated enhancement of gene expression in Arabidopsis. *Plant Journal*, *40*, 744–751. http://doi.org/10.1111/j.1365-313X.2004.02247.x

Rudi, N., Norton, G. W., Alwang, J., & Asumugha, G. (2010). Economic impact analysis of marker-assisted breeding for resistance to pests and post- harvest deterioration in cassava. *African Journal of Agricultural and Resource Economics*, *4*(2), 110–122.

Saeed, M. (2008). Limitations observed in the use of agroinoculation for geminivirus research. *Virus Genes*, *37*, 434–435. http://doi.org/10.1023/A

Saeed, M., Zafar, Y., Randles, J. W., & Rezaian, M. A. (2007). A monopartite begomovirus-associated DNA beta satellite substitutes for the DNA B of a bipartite begomovirus to permit systemic infection. *The Journal of General Virology*, *88*, 2881–9. http://doi.org/10.1099/vir.0.83049-0

Salvo-Garrido, H., Travella, S., Billiam, L. J., Harwood, W. a., & Snape, J. W. (2004). The distribution of transgene insertion sites in barley determined by physical and genetic mapping. *Genetics*, *167*(July), 1371–1379. http://doi.org/10.1534/genetics.103.023747

Sanz, a I., Fraile, a, García-Arenal, F., Zhou, X., Robinson, D. J., Khalid, S., … Harrison, B. D. (2000). Multiple infection, recombination and genome relationships among begomovirus isolates found in cotton and other plants in Pakistan. *The Journal of General Virology*, *81*(Pt 7), 1839–49. Retrieved from http://www.ncbi.nlm.nih.gov/pubmed/10859391

Sarria, R., Torres, E., Angel, F., Chavarriaga, P., & Roca, W. M. (2000). Transgenic plants of cassava (Manihot esculenta) with resistance to Basta obtained by Agrobacterium - mediated transformation. *Plant Cell Reports*, *19*(4), 339–344. http://doi.org/10.1007/s002990050737

Savenkov, E. I., & Valkonen, J. P. (2001). Potyviral helper-component proteinase expressed in transgenic plants enhances titers of Potato leaf roll virus but does not alleviate its phloem limitation. *Virology*, *283*(2), 285–93. http://doi.org/10.1006/viro.2000.0838

Sayre, R., Beeching, J. R., Cahoon, E. B., Egesi, C., Fauquet, C., Fellman, J., … Zhang, P. (2011). The BioCassava plus program: biofortification of cassava for sub-Saharan Africa. *Annual Review of Plant Biology*, *62*, 251–272. http://doi.org/10.1146/annurev-arplant-042110-103751

Saze, H., Tsugane, K., Kanno, T., & Nishimura, T. (2012). DNA methylation in plants: Relationship to small rnas and histone modifications, and functions in transposon inactivation. *Plant and Cell Physiology*, *53*(5), 766–784. http://doi.org/10.1093/pcp/pcs008

Schopke, C., Taylor, N., Carcamo, R., Gonzalez De Schopke, A. ., Konan, N. K., Marmey, P., … Fauquet, C. (1997). Stable transformation of cassava (Manihot esculenta Crantz) by particle

bombardment and by Agrobacterium. *African Journal of Root and Tuber Crops*, *2*, 187–193.

Schreuder, M. M., Raemakers, C. J. J. M., Jacobsen, E., & Visser, R. G. F. (2001). Effcient production of transgenic plants by Agrobacterium-mediated transformation of cassava (Manihot esculenta Crantz). *Euphytica*, *120*, 35–42.

Schubert, D., Lechtenberg, B., Forsbach, A., Gils, M., Bahadur, S., & Schmidt, R. (2004). Silencing in Arabidopsis T-DNA transformants: the predominant role of a gene-specific RNA sensing mechanism versus position effects. *The Plant Cell*, *16*(10), 2561–2572. http://doi.org/10.1105/tpc.104.024547

Schuck, J., Gursinsky, T., Pantaleo, V., Burgyán, J., & Behrens, S. E. (2013). AGO/RISC-mediated antiviral RNA silencing in a plant in vitro system. *Nucleic Acids Research*, *41*, 5090–5103. http://doi.org/10.1093/nar/gkt193

Schwab, R., Ossowski, S., Riester, M., Warthmann, N., & Weigel, D. (2006). Highly Specific Gene Silencing by Artificial MicroRNAs in Arabidopsis. *The Plant Cell*, *18*(May), 1121–1133. http://doi.org/10.1105/tpc.105.039834.1

Schwarz, D. S., Hutvágner, G., Du, T., Xu, Z., Aronin, N., & Zamore, P. D. (2003). Asymmetry in the assembly of the RNAi enzyme complex. *Cell*, *115*(2), 199–208. Retrieved from http://www.ncbi.nlm.nih.gov/pubmed/14567917

Schwind, N., Zwiebel, M., Itaya, A., Ding, B., Wang, M. B., Krczal, G., & Wassenegger, M. (2009). RNAi-mediated resistance to Potato spindle tuber viroid in transgenic tomato expressing a viroid hairpin RNA construct. *Molecular Plant Pathology*, *10*(4), 459–469. http://doi.org/10.1111/j.1364-3703.2009.00546.x

Semizarov, D., Frost, L., Sarthy, A., Kroeger, P., Halbert, D. N., & Fesik, S. W. (2003). Specificity of short interfering RNA determined through gene expression signatures. *Proceedings of the National Academy of Sciences of the United States of America*, *100*(11), 6347–52. http://doi.org/10.1073/pnas.1131959100

Senshu, H., Yamaji, Y., Minato, N., Shiraishi, T., Maejima, K., Hashimoto, M., … Namba, S. (2011). A dual strategy for the suppression of host antiviral silencing: two distinct suppressors for viral replication and viral movement encoded by potato virus m. *Journal of Virology*, *85*(19), 10269–10278. http://doi.org/10.1128/JVI.05273-11

Seppänen, P., Puska, R., Honkanen, J., Tyulkina, L. G., Fedorkin, O., Morozov, S. Y., & Atabekov, J. G. (1997). Movement protein-derived resistance to triple gene block-containing plant viruses. *Journal of General Virology*, *78*(6), 1241–1246.

Settlage, S. B., See, R. G., & Hanley-Bowdoin, L. (2005). Geminivirus C3 protein: replication enhancement and protein interactions. *Journal of Virology*, *79*(15), 9885–9895. http://doi.org/10.1128/JVI.79.15.9885-9895.2005

Shao, Y., Chan, C. Y., Maliyekkel, A., Lawrence, C. E., Roninson, I. B., & Ding, Y. (2007). Effect of target secondary structure on RNAi efficiency. *RNA (New York, N.Y.)*, *13*, 1631–1640. http://doi.org/10.1261/rna.546207

Shapiro, R and Weisgras, J. (1970). Bisulfite-catalyzed transamination of cytosine and cytidine. *Biochemical and Biophysical Research Communications*, *40*(4), 839–843.

Sharma, P., Ikegami, M., & Kon, T. (2010). Identification of the virulence factors and suppressors of posttranscriptional gene silencing encoded by Ageratum yellow vein virus, a monopartite begomovirus. *Virus Research*, *149*(1), 19–27. http://doi.org/10.1016/j.virusres.2009.12.008

Shepherd, D. N., Mangwende, T., Martin, D. P., Bezuidenhout, M., Kloppers, F. J., Carolissen, C. H., … Thomson, J. a. (2007). Maize streak virus-resistant transgenic maize: a first for Africa. *Plant Biotechnology Journal*, *5*(6), 759–767. http://doi.org/10.1111/j.1467-7652.2007.00279.x

Shepherd, D. N., Martin, D. P., & Thomson, J. A. (2009). Transgenic strategies for developing crops resistant to geminiviruses. *Plant Science*, *176*, 1–11.

Shimura, H., & Pantaleo, V. (2011). Viral induction and suppression of RNA silencing in plants. *Biochimica et Biophysica Acta - Gene Regulatory Mechanisms*, *1809*(11-12), 601–612. http://doi.org/10.1016/j.bbagrm.2011.04.005

Siddiqui, S. A., Sarmiento, C., Truve, E., Lehto, H., & Lehto, K. (2008). Phenotypes and functional effects caused by various viral RNA silencing suppressors in transgenic Nicotiana benthamiana and N. tabacum. *Molecular Plant-Microbe Interactions : MPMI*, *21*(2), 178–87. http://doi.org/10.1094/MPMI-21-2-0178

Sijen, T., Wellink, J., Hiriart, J., & Van Kammen, a. (1996). RNA-Mediated Virus Resistance: Role of Repeated Transgenes and Delineation of Targeted Regions. *The Plant Cell*, *8*(12), 2277–2294. http://doi.org/10.1105/tpc.8.12.2277

Smardon, a, Spoerke, J. M., Stacey, S. C., Klein, M. E., Mackin, N., & Maine, E. M. (2000). EGO-1 is related to RNA-directed RNA polymerase and functions in germ-line development and RNA interference in C. elegans. *Current Biology : CB*, *10*(4), 169–78. Retrieved from http://www.ncbi.nlm.nih.gov/pubmed/10704412

Smith, C. J. S., Watson, C. F., Bird, C. R., Ray, J., Schuch, W., & Grierson, D. (1990). Expression of a truncated tomato polygalacturonase gene inhibits expression of the endogenous gene in transgenic plants. *Molecular And General Genetics*, *224*, 477–481.

Smith, E. F., & Townsend, C. O. (1907). A plant tumour of bacterial origin. *SCIENCE*, *25*, 671–673.

Smith, N. A., Singh, S. P., Wang, M.-B., Stoutjesdijk, P. A., Green, A. G., & Waterhouse, P. M. (2000). Total silencing by intron-spliced hairpin RNAs. *Nature*, *407*, 319–320. http://doi.org/10.1016/j.echo.2007.08.009

Soifer, H. S., Sano, M., Sakurai, K., Chomchan, P., Sætrom, P., Sherman, M. a., … Rossi, J. J. (2008). A role for the Dicer helicase domain in the processing of thermodynamically unstable hairpin RNAs. *Nucleic Acids Research*, *36*(20), 6511–6522. http://doi.org/10.1093/nar/gkn687

Solomon-Blackburn, R. M., & Barker, H. (2001). Breeding virus resistant potatoes (Solanum tuberosum): a review of traditional and molecular approaches. *Heredity*, *86*(Pt 1), 17–35. Retrieved from http://www.ncbi.nlm.nih.gov/pubmed/11298812

Southgate, E., Davey, M., Power, J., & Westcott, R. (1998). A comparison of methos for direct gene transfer into maize (Zea Mays L.). *In Vitro Cellular & Developmental Biology - Plant*, *34*, 218–224.

Sserubombwe, W. S., Briddon, R. W., Baguma, Y. K., Ssemakula, G. N., Bull, S. E., Bua, a., … Stanley, J. (2008). Diversity of begonmoviruses associated with mosaic disease of cultivated cassava (Manihot esculenta Crantz) and its wild relative (Manihot glaziovii Müll. Arg.) in Uganda. *Journal of General Virology*, *89*, 1759–1769. http://doi.org/10.1099/vir.0.83637-0

Sseruwagi, P., Sserubombwe, W. S., Legg, J. P., Ndunguru, J., & Thresh, J. M. (2004). Methods of surveying the incidence and severity of cassava mosaic disease and whitefly vector populations on cassava in Africa: A review. *Virus Research*, *100*, 129–142. http://doi.org/10.1016/j.virusres.2003.12.021

Stanley, J. (1995). Analysis of African cassava mosaic virus recombinants suggests strand nicking occurs within the conserved nonanucleotide motif during the initiation of rolling circle DNA replication. *Virology*, *206*(1), 707–712. http://doi.org/10.1016/S0042-6822(95)80093-X

Stanley, J., & Frischmuth, T. (1990). Defective viral DNA ameliorates symptoms of geminivirus infection in transgenic plants. *Proceedings of the National Academy of Sciences*, *87*, 6291–6295.

Stanley, J., Saunders, K., Pinner, M. S., & Wong, S. M. (1997). Novel Defective Interfering DNAs Associated with Ageratum Yellow Vein Geminivirus Infection of Ageratum conyzoides 1. *Virology*, *239*, 87–96.

Stanley, J., & Townsend, R. (1985). Characterisation of DNA forms associated with cassava latent virus infection. *Nucleic Acids Research*, *13*(7), 2189–2206.

Sukharev, S. I., Klenchin, V. a, Serov, S. M., Chernomordik, L. V, & Chizmadzhev YuA. (1992). Electroporation and electrophoretic DNA transfer into cells. The effect of DNA

interaction with electropores. *Biophysical Journal*, *63*(5), 1320–1327. http://doi.org/10.1016/S0006-3495(92)81709-5

Szittya, G., Silhavy, D., Molnár, A., Havelda, Z., Lovas, A., Lakatos, L., … Burgyán, J. (2003). Low temperature inhibits RNA silencing-mediated defence by the control of siRNA generation. *The EMBO Journal*, *22*(3), 633–40. http://doi.org/10.1093/emboj/cdg74

Takayama, K. M. (1990). Antisense RNA. *Biochemistry and Molecular Biology*, *25*(3), 155–184.

Tang, K., Tinjuangjun, P., Xu, Y., Sun, X., Gatehouse, J. A., Ronald, P. C., … Kohli, A. (1999). Particle-bombardment-mediated co-transformation of elite Chinese rice cultivars with genes conferring resistance to bacterial blight and sap-sucking insect pests. *Planta*, *21*, 552–563.

Tao, Q., & Zhang, H. B. (1998). Cloning and stable maintenance of DNA fragments over 300 kb in Escherichia coli with conventional plasmid-based vectors. *Nucleic Acids Research*, *26*(21), 4901–9. Retrieved from http://www.pubmedcentral.nih.gov/articlerender.fcgi?artid=147936&tool=pmcentrez&rendertype=abstract

Taylor, N., Chavarriaga, P., Raemakers, K., Siritunga, D., & Zhang, P. (2004). Development and application of transgenic technologies in cassava. *Plant Molecular Biology*, *56*(4), 671–88. http://doi.org/10.1007/s11103-004-4872-x

Taylor, N., Gaitán-Solís, E., Moll, T., Trauterman, B., Jones, T., Pranjal, A., … Fauquet, C. M. (2012a). A High-throughput Platform for the Production and Analysis of Transgenic Cassava (Manihot esculenta) Plants. *Tropical Plant Biology*, *5*, 127–139. http://doi.org/10.1007/s12042-012-9099-4

Taylor, N., Halsey, M., Gaitán-Solís, E., Anderson, P., Gichuki, S., Miano, D., … Fauquet, C. M. (2012b). The VIRCA Project: Virus resistant cassava for Africa. *GM Crops & Food*, *3*(2), 0–10. http://doi.org/10.4161/gmcr.19144

Taylor, N. J., Masona, M. V, Carcamo, R., Ho, T., Schöpke, C., & Fauquet, C. M. (2001). Production of embryogenic tissues and regeneration of transgenic plants in cassava (Manihot esculenta Crantz). *Euphytica*, *120*, 25–34.

Taylor, S. H. (2009). *THE DEVELOPMENT OF SACMV - RESISTANT CASSAVA USING PATHOGEN - DERIVED RESISTANCE STRATEGIES , TARGETING THE DNA - A COMPONENT*. *Doctor*. University of the Witwatersrand.

Taylor, S. H., Harmse, J., Arbuthnot, P., Van Den Berg, F., Weinberg, M. S., & Rey, M. E. C. (2012c). Construction of effective inverted repeat silencing constructs using sodium bisulfite treatment coupled with strand-specific PCR. *BioTechniques*, *52*(4), 254–62. http://doi.org/10.2144/0000113839

Tenllado, F., & Di, J. R. (2001). Double-Stranded RNA-Mediated Interference with Plant Virus Infection. *Journal of Virology*, *75*(24), 12288–12297. http://doi.org/10.1128/JVI.75.24.12288

Tenllado, F., & Diaz-Ruiz, J. (1999). Complete resistance to pepper mild mottle tobamovirus mediated by viral replicase sequences partially depends on transgene homozygosity and is based on a gene silencing mechanism. *Transgenic Research*, *8*, 83–93.

Tenllado, F., Garcia-Luque, I., Serra, M., & Diaz-Ruiz, J. (1995). Nicotiana benthamiana plants transformed with the 54-kDa region of the Pepper mild mottle tobamovirus replicase gene exhibit two types of resistance responses against viral infection. *Virology*, *211*, 170–183.

Tennant, P., Fermin, G., Fitch, M. M., Manshardt, R. M., Slightom, J. L., & Gonsalves, D. (2001). Papaya ringspot virus resistance of transgenic Rainbow and SunUp is affected by gene dosage , plant development , and coat protein homology. *European Journal of Plant Pathology*, *107*, 645–653.

Thomas, C. L., Jones, L., Baulcombe, D. C., & Maule, a J. (2001). Size constraints for targeting post-transcriptional gene silencing and for RNA-directed methylation in Nicotiana benthamiana using a potato virus X vector. *The Plant Journal*, *25*(4), 417–25. Retrieved from http://www.ncbi.nlm.nih.gov/pubmed/11260498

Thresh, J. . . (2003). Control of Plant Virus Diseases in Sub-Saharan Africa: the Possibility and Feasibility of an Integrated Approach. *African Crop Science Journal*, *11*(3), 199–223.

Thresh, J. M., Fargette, D., & Otim-Nape, G. W. (1994). The viruses and virus diseases of cassava in Africa. *African Crop Science Journal*, *2*(4), 459–478.

Thresh, J. M., Otim-nape, G. W., Thankappan, M., & Muniyappa, V. (1998). The mosaic disease of cassava in Africa and India caused by whitefly-borne geminiviruses. *Plant Pathology*, *77*, 935–945.

Tomari, Y., Matranga, C., Haley, B., Martinez, N., & Zamore, P. D. (2004). A protein sensor for siRNA asymmetry. *Science (New York, N.Y.)*, *306*(5700), 1377–80. http://doi.org/10.1126/science.1102755

Tomoyasu, Y., Miller, S. C., Tomita, S., Schoppmeier, M., Grossmann, D., & Bucher, G. (2008). Exploring systemic RNA interference in insects: a genome-wide survey for RNAi genes in Tribolium. *Genome Biology*, *9*(1), R10. http://doi.org/10.1186/gb-2008-9-1-r10

Trench, T. N., Martin, M. M., & Hemmes, E. a. (1985). An assessment of cassava African mosaic disease in South Africa and Swaziland. *S Afr J Plant Soil*, *2*(September 2014), 169–170. http://doi.org/10.1080/02571862.1985.10634163

Trinks, D., Rajeswaran, R., Shivaprasad, P. V, Oakeley, E. J., Veluthambi, K., Pooggin, M. M., … Hohn, T. (2005). Suppression of RNA Silencing by a Geminivirus Nuclear Protein , AC2

, Correlates with Transactivation of Host Genes. *Journal of Virology*, *79*(4), 2517–2527. http://doi.org/10.1128/JVI.79.4.2517

Tuschl, T., Zamore, P. D., Lehmann, R., Bartel, D. P., & Sharp, P. a. (1999). Targeted mRNA degradation by double-stranded RNA in vitro. *Genes & Development*, *13*(24), 3191–7. Retrieved from http://www.pubmedcentral.nih.gov/articlerender.fcgi?artid=317199&tool=pmcentrez&rendertype=abstract

Tusnády, G. E., Simon, I., Váradi, A., & Arányi, T. (2005). BiSearch: primer-design and search tool for PCR on bisulfite-treated genomes. *Nucleic Acids Research*, *33*(1), e9. http://doi.org/10.1093/nar/gni012

Ui-Tei, K., Naito, Y., Takahashi, F., Haraguchi, T., Ohki-Hamazaki, H., Juni, A., … Saigo, K. (2004). Guidelines for the selection of highly effective siRNA sequences for mammalian and chick RNA interference. *Nucleic Acids Research*, *32*(3), 936–48. http://doi.org/10.1093/nar/gkh247

Ui-Tei, K., Nishi, K., Takahashi, T., & Nagasawa, T. (2012). Thermodynamic control of small RNA-mediated gene silencing. *Frontiers in Genetics*, *3*(June), 1–12. http://doi.org/10.3389/fgene.2012.00101

Vaistij, F. E., Jones, L., & Baulcombe, D. C. (2002). Spreading of RNA Targeting and DNA Methylation in RNA Silencing Requires Transcription of the Target Gene and a Putative RNA-Dependent RNA Polymerase. *The Plant Cell*, *14*(April), 857–867. http://doi.org/10.1105/tpc.010480.radation

Vanderschuren, H., Akbergenov, R., Pooggin, M. M., Hohn, T., Gruissem, W., & Zhang, P. (2007). Transgenic cassava resistance to African cassava mosaic virus is enhanced by viral DNA-A bidirectional promoter-derived siRNAs. *Plant Molecular Biology*, *64*(5), 549–57. Retrieved from http://www.ncbi.nlm.nih.gov/pubmed/17492253

Vanderschuren, H., Alder, A., Zhang, P., & Gruissem, W. (2009). Dose-dependent RNAi-mediated geminivirus resistance in the tropical root crop cassava. *Plant Molecular Biology*, *70*(3), 265–72. http://doi.org/10.1007/s11103-009-9472-3

Vanderschuren, H., Moreno, I., Anjanappa, R. B., Zainuddin, I. M., & Gruissem, W. (2012). Exploiting the combination of natural and genetically engineered resistance to cassava mosaic and cassava brown streak viruses impacting cassava production in Africa. *PloS One*, *7*(9), e45277. http://doi.org/10.1371/journal.pone.0045277

Vanderschuren, H., Stupak, M., Fütterer, J., Gruissem, W., & Zhang, P. (2007). Engineering resistance to geminiviruses--review and perspectives. *Plant Biotechnology Journal*, *5*(2), 207–20. http://doi.org/10.1111/j.1467-7652.2006.00217.x

Vanitharani, R., Chellappan, P., & Fauquet, C. M. (2003). Short interfering RNA-mediated interference of gene expression and viral DNA accumulation in cultured plant cells. *Proceedings of the National Academy of Sciences*, *100*(16), 9632–9636. http://doi.org/10.1073/pnas.1733874100

Vanitharani, R., Chellappan, P., & Fauquet, C. M. (2005). Geminiviruses and RNA silencing. *TRENDS in Plant Science*, *10*(3), 144–51. http://doi.org/10.1016/j.tplants.2005.01.005

Vanitharani, R., Chellappan, P., Pita, J. S., & Fauquet, C. M. (2004). Differential Roles of AC2 and AC4 of Cassava Geminiviruses in Mediating Synergism and Suppression of Posttranscriptional Gene Silencing. *Journal of Virology*, *78*(17), 9487–9498. http://doi.org/10.1128/JVI.78.17.9487

Varma, A., & Malathi, V. G. (2003). Emerging geminivirus problems: A serious threat to crop production. *Annals of Applied Biology*, *142*(2), 145–164. http://doi.org/10.1111/j.1744-7348.2003.tb00240.x

Vassilakos, N. (2012). Stability of Transgenic Resistance Against Plant Viruses. In Y. O. Çiftç (Ed.), *Trangenic plants-Advances and limitations* (pp. 219–236). In Tech. Retrieved from http://www.intechopen.com/books/transgenic-plants-advances-and-limitations/stability-of-transgenic- resistance-against-plant-viruses\nInTech

Vassilakos, N., Bem, F., Tzima, A., Barker, H., Reavy, B., Karanastasi, E., & Robinson, D. J. (2008). Resistance of transgenic tobacco plants incorporating the putative 57-kDa polymerase read-through gene of Tobacco rattle virus against rub-inoculated and nematode-transmitted virus. *Transgenic Research*, *17*(5), 929–41. http://doi.org/10.1007/s11248-008-9176-5

Vaucheret, H., & Fagard, M. (2001). Transcriptional gene silencing in plants: Targets, inducers and regulators. *Trends in Genetics*, *17*(1), 29–35. http://doi.org/10.1016/S0168-9525(00)02166-1

Verdel, A., Jia, S., Gerber, S., Sugiyama, T., Gygi, S., Grewal, S. I. S., & Moazed, D. (2004). RNAi-mediated targeting of heterochromatin by the RITS complex. *Science*, *303*(5658), 672–6. http://doi.org/10.1126/science.1093686

Viswanath, V., Ma, C., Etherington, E., Dharmawardhana, P., Pearce, D. W., Rood, S. B., … Strauss, S. H. (2011). Greenhouse and field evaluation of transgenic poplars with modified gibberellin metabolism and signaling genes. *BMC Proceedings*, *5*(Suppl 7), O22. http://doi.org/10.1186/1753-6561-5-S7-O22

Voinnet, O., Pinto, Y. M., & Baulcombe, D. C. (1999). Suppression of gene silencing: a general strategy used by diverse DNA and RNA viruses of plants. *Proceedings of the National Academy of Sciences of the United States of America*, *96*(24), 14147–52. Retrieved from http://www.pubmedcentral.nih.gov/articlerender.fcgi?artid=24205&tool=pmcentrez&rendertype=abstract

Von Arnim, A., & Stanley, J. (1992). Determinants of Tomato Golden Mosaic Virus Symptom Development Located on DNA B. *Virology*, *293*, 286–293.

Vu, T. Van, Choudhury, N. R., & Mukherjee, S. K. (2013). Transgenic tomato plants expressing artificial microRNAs for silencing the pre-coat and coat proteins of a begomovirus , Tomato leaf curl New Delhi virus , show tolerance to virus infection. *Virus Research*, *172*, 35–45. http://doi.org/10.1016/j.virusres.2012.12.008

Wagaba, H., Beyene, G., Trembley, C., Alicai, T., Fauquet, C. M., & Taylor, N. J. (2013). Efficient transmission of cassava brown streak disease viral pathogens by chip bud grafting. *BMC Research Notes*, *6*, 516. http://doi.org/10.1186/1756-0500-6-516

Wan, Y., & Lemaux, P. G. (1994). Generation of Large Numbers of Independently Transformed Fertile Barley Plants. *Plant Physiology*, *104*(1), 37–48. Retrieved from http://www.pubmedcentral.nih.gov/articlerender.fcgi?artid=159160&tool=pmcentrez&rendertype=abstract

Wang, B., Li, F., Huang, C., Yang, X., Qian, Y., Xie, Y., & Zhou, X. (2014). V2 of tomato yellow leaf curl virus can suppress methylation-mediated transcriptional gene silencing in plants. *The Journal of General Virology*, *95*(Pt 1), 225–30. http://doi.org/10.1099/vir.0.055798-0

Wang, H., Buckley, K. J., Yang, X., Cody, R., Bisaro, D. M., & Buchmann, R. C. (2005). Adenosine Kinase Inhibition and Suppression of RNA Silencing by Geminivirus AL2 and L2 Proteins Adenosine Kinase Inhibition and Suppression of RNA Silencing by Geminivirus AL2 and L2 Proteins. *Journal of Virology*, *79*(12), 7410–7418. http://doi.org/10.1128/JVI.79.12.7410

Wang, K., Herrera-Estrella, L., Van Montagu, M., & Zambryski, P. (1984). Right 25 bp terminus sequence of the nopaline T-DNA is essential for and determines direction of DNA transfer from agrobacterium to the plant genome. *Cell*, *38*(2), 455–62. Retrieved from http://www.ncbi.nlm.nih.gov/pubmed/6467373

Wang, L., Luo, Y.-Z., Zhang, L., Jiao, X.-M., Wang, M.-B., & Fan, Y.-L. (2008). Rolling circle amplification-mediated hairpin RNA (RMHR) library construction in plants. *Nucleic Acids Research*, *36*(22), e149. http://doi.org/10.1093/nar/gkn715

Wang, M.-B., Masuta, C., Smith, N. a., & Shimura, H. (2012). RNA Silencing and Plant Viral Diseases. *Molecular Plant-Microbe Interactions*, *25*(10), 1275–1285. http://doi.org/10.1094/MPMI-04-12-0093-CR

Wang, Q., Han, Y., Qiu, Y., Zhang, S., Tang, F., Wang, Y., … Zhou, X. (2012). Identification and characterization of RNA duplex unwinding and ATPase activities of an alphatetravirus superfamily 1 helicase. *Virology*, *433*(2), 440–8. http://doi.org/10.1016/j.virol.2012.08.045

Ward, B. M., Medville, R., Lazarowitz, S. G., & Turgeon, R. (1997). The geminivirus BL1 movement protein is associated with endoplasmic reticulum-derived tubules in developing phloem cells. *JOURNAL OF VIROLOGY*, *71*(5), 3726–33. Retrieved from http://www.pubmedcentral.nih.gov/articlerender.fcgi?artid=191522&tool=pmcentrez&rendertype=abstract

Wassenegger, M., Heimes, S., Riedel, L., & Sänger, H. L. (1994). RNA-directed de novo methylation of genomic sequences in plants. *Cell*, *76*(3), 567–76. Retrieved from http://www.ncbi.nlm.nih.gov/pubmed/8313476

Waterhouse, P. M., Graham, M. W., & Wang, M. B. (1998). Virus resistance and gene silencing in plants can be induced by simultaneous expression of sense and antisense RNA. *Proceedings of the National Academy of Sciences of the United States of America*, *95*(23), 13959–64. Retrieved from http://www.pubmedcentral.nih.gov/articlerender.fcgi?artid=24986&tool=pmcentrez&rendertype=abstract

Weinheimer, I., Boonrod, K., Moser, M., Wassenegger, M., Krczal, G., Butcher, S. J., & Valkonen, J. P. T. (2014). Binding and processing of small dsRNA molecules by the class 1 RNase III protein encoded by sweet potato chlorotic stunt virus. *Journal of General Virology*, *95*, 486–495. http://doi.org/10.1099/vir.0.058693-0

Wesley, S. V., Helliwell, C. A., Smith, N. A., Wang, M., Rouse, D. T., Liu, Q., … Waterhouse, P. M. (2001). Construct design for effcient , effective and high- throughput gene silencing in plants. *The Plant Journal*, *27*(6), 581–590.

Wesley, S. V, Helliwell, C. a, Smith, N. a, Wang, M. B., Rouse, D. T., Liu, Q., … Waterhouse, P. M. (2001). Construct design for efficient, effective and high-throughput gene silencing in plants. *The Plant Journal*, *27*(6), 581–90.

White, P. R., & Braun, A. C. (1942). A Cancerous Neoplasm of Plants . Autonomous Bacteria-Free Crown-Gall Tissue A Cancerous Neoplasm of Plants A u t o n o m o u s Bacteria-Free Crown-Gall Tissue. *Cancer Research*, *2*, 597–617.

Wilson, R. C., & Doudna, J. a. (2013). Molecular mechanisms of RNA interference. *Annual Review of Biophysics*, *42*, 217–39. http://doi.org/10.1146/annurev-biophys-083012-130404

Wu, L., Zhou, H., Zhang, Q., Zhang, J., Ni, F., Liu, C., & Qi, Y. (2010). DNA Methylation Mediated by a MicroRNA Pathway. *Molecular Cell*, *38*(3), 465–475. http://doi.org/10.1016/j.molcel.2010.03.008

Wu-Scharf, D., Jeong, B., Zhang, C., & Cerutti, H. (2000). Transgene and transposon silencing in Chlamydomonas reinhardtii by a DEAH-box RNA helicase. *SCIENCE*, *290*(5494), 1159–62. Retrieved from http://www.ncbi.nlm.nih.gov/pubmed/11073454

Wyman, a R., Wolfe, L. B., & Botstein, D. (1985). Propagation of some human DNA sequences in bacteriophage lambda vectors requires mutant Escherichia coli hosts. *Proceedings of the National Academy of Sciences of the United States of America*, *82*(May), 2880–2884. http://doi.org/10.1073/pnas.82.9.2880

Xie, Z., Fan, B., Chen, C., & Chen, Z. (2001). An important role of an inducible RNA-dependent RNA polymerase in plant antiviral defense. *Proceedings of the National Academy of Sciences of the United States of America*, *98*(11), 6516–6521. http://doi.org/10.1073/pnas.111440998

Xie, Z., Johansen, L. K., Gustafson, A. M., Kasschau, K. D., Lellis, A. D., Zilberman, D., … Carrington, J. C. (2004). Genetic and functional diversification of small RNA pathways in plants. *PLoS Biology*, *2*(5), E104. http://doi.org/10.1371/journal.pbio.0020104

Xu, P., Zhang, Y., Kang, L., Roossinck, M. J., & Mysore, K. S. (2006). Computational estimation and experimental verification of off-target silencing during posttranscriptional gene silencing in plants. *Plant Physiology*, *142*(2), 429–40. http://doi.org/10.1104/pp.106.083295

Yang, H., Volfovsky, N., Rattray, A., Chen, X., Tanaka, H., & Strathern, J. (2014). GAP-Seq: a method for identification of DNA palindromes. *BMC Genomics*, *15*, 394. http://doi.org/10.1186/1471-2164-15-394

Yang, X., Baliji, S., Buchmann, R. C., Wang, H., Lindbo, J. a, Sunter, G., & Bisaro, D. M. (2007). Functional modulation of the geminivirus AL2 transcription factor and silencing suppressor by self-interaction. *Journal of Virology*, *81*(21), 11972–11981. http://doi.org/10.1128/JVI.00617-07

Yang, Y., Sherwood, T. a, Patte, C. P., Hiebert, E., & Polston, J. E. (2004). Use of Tomato yellow leaf curl virus (TYLCV) Rep Gene Sequences to Engineer TYLCV Resistance in Tomato. *Phytopathology*, *94*(5), 490–6. http://doi.org/10.1094/PHYTO.2004.94.5.490

Ye, J., Qu, J., Mao, H., Ma, Z., Estya, N., Rahman, B., … Jiang, S. (2014). Engineering geminivirus resistance in Jatropha curcus. *Biotechnology for Biofuels*, *7*(149), 1–11. http://doi.org/10.1186/s13068-014-0149-z

Yu, B., Yang, Z., Li, J., Minakhina, S., Yang, M., Padgett, R. W., … Chen, X. (2005). Methylation as a crucial step in plant microRNA biogenesis. *Science (New York, N.Y.)*, *307*(5711), 932–935. http://doi.org/10.1126/science.1107130

Zaenen, I., Van Larebeke, N., Van Montagu, M., & Schell, J. (1974). Supercoiled circular DNA in crown-gall inducing Agrobacterium strains. *Journal of Molecular Biology*, *86*(1), 109–27. Retrieved from http://www.ncbi.nlm.nih.gov/pubmed/4854526

Zainuddin, I. M., Schlegel, K., Gruissem, W., & Vanderschuren, H. (2012). Robust transformation procedure for the production of transgenic farmer-preferred cassava landraces. *Plant Methods*, *8*(24), 1–8. http://doi.org/10.1186/1746-4811-8-24

Zeng, F., Zhan, Y., Nan, N., Xin, Y., Qi, F., & Yang, C. (2009). Expression of bgt gene in transgenic birch (Betula platyphylla Suk.). *African Journal of Biotechnology*, *8*(15), 3392–3398.

Zeng, Y., Wagner, E. J., Cullen, B. R., & Carolina, N. (2002). Both Natural and Designed Micro RNAs Can Inhibit the Expression of Cognate mRNAs When Expressed in Human Cells Technique. *Molecular Cell*, *9*, 1327–1333.

Zhang, J., Dong, J., Xu, Y., & Wu, J. (2012). V2 protein encoded by Tomato yellow leaf curl China virus is an RNA silencing suppressor. *Virus Research*, *163*(1), 51–58. http://doi.org/10.1016/j.virusres.2011.08.009

Zhang, P., Legris, G., Coulin, P., & Puonti-Kaerlas, J. (2000). Production of stably transformed cassava plants via particle bombardment. *Plant Cell Reports*, *19*(10), 939–945. http://doi.org/10.1007/s002990000224

Zhang, P., Vanderschuren, H., Fütterer, J., & Gruissem, W. (2005). Resistance to cassava mosaic disease in transgenic cassava expressing antisense RNAs targeting virus replication genes. *Plant Biotechnology Journal*, *3*(4), 385–97. http://doi.org/10.1111/j.1467-7652.2005.00132.x

Zhang, X., & Rossi, J. J. (2011). Phylogenetic comparison of small RNA-triggered transcriptional gene silencing. *Journal of Biological Chemistry*, *286*(34), 29443–29448. http://doi.org/10.1074/jbc.R111.276378

Zhang, X., Yuan, Y. R., Pei, Y., Lin, S. S., Tuschl, T., Patel, D. J., & Chua, N. H. (2006). Cucumber mosaic virus-encoded 2b suppressor inhibits Arabidopsis Argonaute1 cleavage activity to counter plant defense. *Genes and Development*, *20*(23), 3255–3268. http://doi.org/10.1101/gad.1495506

Zheng, H., Dai, S., He, S., Tian, W., & Li, L. (1996). Genetic transfor- mation of indica rice using the biolistic method. *Chinese Journal of Genetics*, *23*, 201–208. http://doi.org/10.1007/BF02773396

Zhou, X., Liu, Y., Calvert, L., Munoz, C., Otim-nape, G. W., Robinson, D. J., & Harrison, B. D. (1997). Evidence that DNA-A of a geminivirus associated with severe cassava mosaic disease in Uganda has arisen by interspecific recombination. *Journal of General Virology*, *78*, 2101–2111.

Zrachya, A., Glick, E., Levy, Y., Arazi, T., Citovsky, V., & Gafni, Y. (2007). Suppressor of RNA silencing encoded by Tomato yellow leaf curl virus-Israel. *Virology*, *358*(1), 159–165. http://doi.org/10.1016/j.virol.2006.08.016

Zvereva, A. S., & Pooggin, M. M. (2012). Silencing and innate immunity in plant defense against viral and non-viral pathogens. *Viruses*, *4*(11), 2578–97. http://doi.org/10.3390/v4112578

APPENDICES

Appendix A Student's t-test accessing the mean statistical difference between A-MM2transgenic line and cv.60444symptom severity score index, plant height and ACMV viral load, at 12, 32 and 67dpi.

	Symptom severity score			Plant height			ACMV viral load		
Line ID	**12 dpi**	**32 dpi**	**67 dpi**	**12 dpi**	**32 dpi**	**67 dpi**	**12 dpi**	**32dpi**	**67dpi**
A-MM2 45	0.36	0.36	0.00015	0.11	0.03	0.15	0.09	0.17	0.25
A-MM2 41	0.2	0.005	0.01	0.27	0.01	0.07	0.19	0.16	0.14
A-MM2 53	0.1	0.06	0.01	0.37	0.47	0.21	0.13	0.06	0.15
A-MM2 52	0.03	0.03	0.002	0.5	0.2	0.02	0.15	0.2	0.16
A-MM2 30	0.3	0.01	0.007	0.34	0.33	0.29	0.5	0.23	0.34
A-MM2 54	0.03	0.0027	0.00031	0.01	0.23	0.29	0.05	0.19	0.09
A-MM2 44	0.1	0.09	0.08	0.18	0.05	0.08	0.18	0.37	0.42

Appendix B Student's t-test accessing the mean statistical difference between A-MM4transgenic line and cv.60444symptom severity score index, plant height and SACMV viral load, at 12, 32 and 67dpi.

	Symptom severity score			Plant height			SACMV viral load		
	12 dpi	**32 dpi**	**67 dpi**	**12 dpi**	**32 dpi**	**67 dpi**	**12 dpi**	**32 dpi**	**67 dpi**
A-MM4 11	0.1	0.001	0.2	0.14	0.08	0.009	0.18	0.44	0.13
A-MM4 33	0.04	0.05	0.02	0.45	0.37	0.003	0.44	0.05	0.12
A-MM4 34	0.4	0.34	0.001	0.16	0.17	0.003	0.16	0.1	0.16
A-MM4 46	0.04	0.01	0.02	0.003	0.02	0.05	0.3	0.05	0.48
A-MM4 59	0.04	0.001	0.0001	0.32	0.41	0.004	0.45	0.42	0.12
A-MM4 68	0.5	0.34	0.001	0.01	0.29	0.004	0.08	0.06	0.14
A-MM4 79	0.04	0.007	0.003	0.08	0.26	0.001	0.11	0.47	0.13

Appendix C Student's t-test accessing the mean statistical difference between C-MM6 transgenic line and cv.60444symptom severity score index, plant height and ACMV viral load, at 12, 32 and 67dpi.

	Symptom severity score			**Plant height**			**ACMV viral load**		
	12 dpi	**32 dpi**	**67 dpi**	**12 dpi**	**32 dpi**	**67 dpi**	**12 dpi**	**32 dpi**	**67 dpi**
MM6 2	0.01	0.01	0.06	0.15	0.01	0.05	0.1	0.15	0.16
MM6 1	0.001	0.08	0.07	0.38	0.4	0.08	0.04	0.16	0.45
MM6 8	0.25	0.003	0.07	0.01	0.002	0.31	0.08	0.24	0.16
MM6 10	0.03	0.0003	0.001	0.27	0.07	0.02	0.07	0.39	0.17
MM6 11	0.07	0.0002	0.007	0.35	0.2	0.06	0.05	0.16	0.09
MM6 19	0.004	0.001	0.08	0.01	0.01	0.34	0.1	0.25	0.11

Appendix D Student's t-test accessing the mean statistical difference between A-MM2transgenic line and cv.60444symptom severity score index, plant height and ACMV viral load, at 12, 32 and 67dpi.

	Symptom severity score			**Plant height**			**SACMV viral load**		
	12 dpi	**32 dpi**	**67 dpi**	**12 dpi**	**32 dpi**	**67 dpi**	**12 dpi**	**32 dpi**	**67 dpi**
MM8 1	0.13	0.04	0.04	0.173	0.068	0.007	0.17	0.3	0.11
MM8 3	0.36	0.14	0.5	0.036	0.230	0.484	0.12	0.13	0.01
MM8 23	0.13	0.07	0.03	0.291	0.411	0.328	0.15	0.02	0.17
MM8 25	0.07	0.007	0.02	0.032	0.003	0.008	0.11	0.28	0.14
MM8 27	0.07	0.04	0.003	0.148	0.183	0.361	0.13	0.25	0.07

Appendix E Student's t-test accessing the mean statistical difference between transgenic lines, A-MM2 and AMM4, and cv.60444 viral load at 365 dpi.

	356 dpi
MM2 30	0.01
MM2 41	0.01
MM2 45	0.47
MM2 52	0.01
MM2 53	0.01
MM2 54	0.01
MM4 11	0.06
MM4 33	0.051
MM4 34	0.056
MM4 46	0.051
MM4 59	0.051
MM4 68	0.051
MM4 79	0.051

Appendix F Pearson's correlation coefficient measuring the relationship (correlation) between symptom severity score (sss) and plant height, correlation between viral load and symptom severity score and the correlation between viral load and plant height for A-MM2, A-MM4, C-MM6 and C-MM8, at 12, 32 and 67 dpi.

A-MM2 lines	**12 dpi**	**32 dpi**	**67 dpi**
sss and plant height	0.610447	0.492424	-0.08328
viral load and sss	0.384241	0.036675	0.221859
viral load and height	0.332099	0.127402	-0.46538
A-MM4 lines	**12 dpi**	**32 dpi**	**67 dpi**
sss and plant height	-0.1357	0.287488	-0.49311
viral load and sss	0.653513	0.719185	0.53428
viral load and height	-0.45104	0.472436	-0.65425
C-MM6 lines	**12 dpi**	**32 dpi**	**67 dpi**
sss and plant height	0.000803	-0.17019	-0.37778
viral load and sss	0.785741	0.651456	0.700429
viral load and height	-0.02671	0.212623	0.033412
C-MM8 lines	**12dpi**	**32 dpi**	**67 dpi**
sss and height	0.056928	0.037954	0.377394
viral load and sss	0.676871	0.814072	0.643269
viral load and height	0.669174	0.279488	0.852673